CRISPR-based genome editing tools for virus resistance in grapevine

by

Katarina Paula Spencer

Thesis presented in partial fulfilment of the requirements for the degree of Master of Science in the Faculty of Science at Stellenbosch University

Supervisor: Prof. J. T. Burger

Co-supervisor: Dr. M. Campa

December 2022

DECLARATION

By submitting this thesis electronically, I declare that the entirety of the work contained therein is my own, original work, that I am the sole author thereof (save to the extent explicitly otherwise stated), that reproduction and publication thereof by Stellenbosch University will not infringe any third-party rights and that I have not previously in its entirety or in part submitted it for obtaining any qualification.

Katarina Paula Spencer

December 2022

ABSTRACT

Grapevine (*Vitis vinifera*) is an important fruit crop which contributes significantly to the South African agricultural sector, and is a major produce crop worldwide. Grapevine viruses are widespread and cause serious diseases which impact the quality and quantity of crop yields. More than 80 viruses plague grapevine, with RNA viruses constituting the largest of virus pathogens. Clustered regularly interspaced, short palindromic repeat (CRISPR), along with its CRISPR-associated (Cas) proteins, is a system which has been harnessed from the prokaryotic immune system and adapted for genome editing technologies. The first CRISPR system to be adapted for genome editing was CRISPR/Cas9, which is characterised by its ability to target double-strand DNA. A recent extension to the CRISPR armoury is the Cas13 effector, which exclusively targets single-strand RNA. CRISPR/Cas has been implemented as a defence mechanism in plants, against both DNA and RNA viruses, by being programmed to directly target and cleave the viral genomes. The efficacy of the CRISPR/Cas tool in plants is dependent on efficient delivery of its components into plant cells. Geminiviruses, a group of small DNA viruses with a useful replication mechanism, have been reconstructed into efficient expression vectors and used for the delivery of genome editing components. By harnessing the CRISPR/Cas tool, and implementing the use of a viral vector for the expression thereof, a robust approach to induce virus resistance in plants can be achieved. To this end, the first aim of this study was to use CRISPR/CasRx to target an infectious clone of the RNA virus, grapevine virus A (GVA). GVA naturally infects *V. vinifera*, but can infect the model plant *Nicotiana benthamiana*, making it a helpful model to study virus infection in grapevine. The second aim of this study sought to use a geminivirus vector based on the bean yellow dwarf virus (BeYDV) to deliver and express CRISPR/Cas9 components in *N. benthamiana*. Firstly, constructs harbouring CasRx and a guide RNA (gRNA) targeting the replicase gene of GVA were assembled, and used for *Agrobacterium*-mediated transformation of *N. benthamiana*. Transgenic lines were infiltrated with the GVA infectious clone, but no consistent GVA interference was observed. To improve virus targeting, gRNAs were designed against the coat protein (*CP*) gene of GVA. *N. benthamiana* plants expressing CasRx were co-infiltrated with the infectious clone, and with a tobacco rattle virus (TRV)-gRNA expression vector, harbouring a CP gRNA. Results indicated more consistent GVA reductions, specifically CP gRNA 2, which demonstrated a significant negative correlation with GVA accumulation, as well as multiple gRNA co-infiltrations which similarly showed reduced GVA titre. When the pRIC BeYDV vector was used

for gene targeting with CRISPR/Cas9, exogenously-delivered enhanced green fluorescence protein (eGFP), as well as endogenous *N. benthamiana* genes phytoene desaturase (*PDS*), and green fluorescence protein (*GFP*), from the transgenic *N. benthamiana* 16c line, were successfully cleaved and edited. By establishing a virus-targeting defence system in plants, and utilising a high-expressing geminivirus vector for the delivery of genome editing components, efficient virus interference mechanisms can be established and applied to major crops, such as grapevine.

ACKNOWLEDGEMENTS

I would like to acknowledge and express my sincere gratitude towards the following individuals and institutions:

The **Wine Industry Network of Expertise and Technology (Winetech)** and the **National Research Foundation (NRF)**, for research funding and financial support.

To a remarkable supervisor, **Prof Johan Burger**, for your guidance and belief in me, throughout the course of my MSc.

Dr Manuela Campa, the best mentor any student could ask for. Thank you for your constant mentorship and support, which helped me to grow during my studies. Your passion for science inspired me daily, and your guidance was always appreciated.

Dr Justin Lashbrooke, for your enthusiasm to help me grasp certain concepts, and for your assistance with the facilities needed for my analyses. And to the **South African Grape and Wine Research Institute (SAGWRI)**, for lending space in the growth room for my plant material.

The **Vitis lab**, for providing an enjoyable and stimulating work environment.

To my Crispy Crew comrades, **Gaëlle Robertson and Alex Dijkerman**, who took me under their wing. And to the fellow **Crispy Crew members** who joined us along the way, bringing with them joy and friendship.

To my **friends** and **family**, who cheered me on throughout the course of my MSc, never faltering their confidence in me. Thank you for your support and encouragement, from near and far.

Finally, **Thomas**, having you by my side was the best support I could have asked for. Your willingness to help and motivation were inspiring. And to your family, for always providing a warm and kind home whenever I missed my own.

All figures included in this thesis were created with **BioRender.com**.

TABLE OF CONTENTS

LIST OF FIGURES

LIST OF TABLES

LIST OF ABBREVIATIONS

aa	amino acid
Ago2	argonaute 2 protein
BAP	6-benzylaminopurine
BeYDV	bean yellow dwarf virus
bp	base pair
BSCTV	beet severe curly top virus
CAF	central analytical facility
CaLCuV	cabbage leaf curl virus
CaMV	cauliflower mosaic virus
Cas	CRISPR-associated proteins
cDNA	complementary DNA
CMV	cucumber mosaic virus
CP	coat protein
CRISPR	clustered regularly interspaced shot palindromic repeat
crRNA	CRISPR RNA
CTAB	cetyltrimethylammonium bromide
DNA	deoxyribonucleic acid
DNase	deoxyribonuclease
dpi	days-post infiltration
DR	direct repeat
DSB	double strand break
dsDNA	double-strand DNA
dsRNA	double-strand RNA
eGFP	enhanced green fluorescence protein
GFP	green fluorescence protein
GIGS	guide-induced gene silencing
GLD	grapevine leafroll disease
GLRaV	grapevine leafroll-associated virus
GMO	genetically modified organism
gRNA	guide RNA

GVA	grapevine virus A
GVR	geminivirus-based replicon
HDR	homology-directed repair
HEPN	higher eukaryotic and prokaryotic nucleotide binding domains
ICE	Inference of CRISPR Edits
IR	intergenic region
kb	kilobases
kDa	kilodalton
LB	Luria-Bertani
LIR	long intergenic region
MP	movement protein
mRNA	messenger RNA
NES	nuclear export signal
NGS	next generation sequencing
NHEJ	non-homologous end joining
NLS	nuclear localisation signal
ns	non-specific
nt	nucleotide
NUC	nuclease lobe
OD	optical density
ORF	open reading frame
PAM	protospacer-adjacent motif
PCR	polymerase chain reaction
PEBV	pea early browning virus
PEG	polyethylene glycol
PFS	protospacer flanking sequence
PI	PAM-interacting domain
RdRp	RNA dependent RNA polymerase
REC	recognition lobe
RISC	RNA-induced silencing complex
RNA	ribonucleic acid
RNAi	RNA interference

RNase	ribonuclease
RNP	ribonucleoprotein
rpm	revolutions per minute
RT-qPCR	reverse-transcription quantitative-PCR
SEM	standard error mean
sgRNA	single-guide RNA
shRNA	small hairpin RNA
SIR	short intergenic region
siRNA	short interfering RNA
SPLCV	sweet potato leaf curl virus
SPVD	sweet potato virus disease
sRNA	small RNA
ssDNA	single-strand DNA
SSN	sequence-specific nuclease
ssRNA	single-strand RNA
TALE	transcription activator-like effector
TALEN	transcription activator-like effector nuclease
TbCSV	tobacco curly shoot virus
TBSV	tomato bushy stunt virus
TMV	tobacco mosaic virus
tracrRNA	trans-activating CRISPR RNA
TRBO-G	TMV-RNA-based overexpressing GFP system
TRV	tobacco rattle virus
TYLCCV	tomato yellow leaf curl china virus
w/v	weight/volume
WDV	wheat dwarf virus
WT	wild-type
YEP	yeast extract peptone
ZFN	zinc finger nuclease

CHAPTER 1: Introduction

1.1 BACKGROUND INFORMATION

The grapevine industry is a major contributor to the economic sector in South Africa, as well as an important produce crop globally (Goszczynski, du Preez and Burger, 2008; Coetzee *et al.*, 2010). Viruses and viral diseases plague grapevine crops, hindering the quality and yield of the crop and impacting the productive life of vineyards (Fargette *et al.*, 2006; Coetzee *et al.*, 2010; Nicaise, 2014). Grapevine cultivars are vulnerable to over 80 different viruses, while RNA viruses constitute the largest group of these viruses (Chaudhary, 2018; Zherdev *et al.*, 2018; Cao *et al.*, 2021). Currently, no agrochemicals exist which have proven efficacy against viruses (Zhao *et al.*, 2020). Moreover, the rapid evolution of viruses has allowed for them to avoid natural antiviral mechanisms which exist within plants, such as RNA interference (RNAi) (Li and Wang, 2019). As a result, the development of long-term disease management strategies is hindered, and a sustainable method for controlling viruses is of urgent importance for the protection of grapevine cultivars.

The Clustered Regularly Interspaced Short Palindromic Repeat (CRISPR) locus, and its CRISPR-associated (Cas) proteins, is an adaptive immune system possessed by most archaea and many bacteria, which functions to protect these prokaryotes against invading nucleic acids (Makarova *et al.*, 2015; Abudayyeh *et al.*, 2016). The CRISPR/Cas system has been harnessed and adapted as a genome editing tool which allows the precise introduction of mutations at desired sites within a genome (Jinek *et al.*, 2012; Schindele, Wolter and Puchta, 2018). CRISPR-Cas9, a Class 2 Type II system, was the first of the CRISPR systems to be adapted for genome editing, and is characterised by its ability to target double-stranded DNA, when guided by a guide RNA (gRNA) (Wolter and Puchta, 2018; Mahas, Aman and Mahfouz, 2019). A recent extension to the CRISPR toolbox is the Class 2 Type VI CRISPR-Cas13 system, where the Cas13 nuclease is the first effector to exclusively target single-stranded RNA (Koonin, Makarova and Zhang, 2017; Yan *et al.*, 2018). Since most plant viruses have RNA genomes, the CRISPR-Cas13 system can be a helpful tool in controlling grapevine viruses and viral infection (Chaudhary, 2018; Cao *et al.*, 2021).

The efficient delivery of CRISPR/Cas components into plants has proved to be a bottleneck. An approach to overcome this bottleneck is to deliver genome editing components using modified

plant viruses (Kalinina *et al.*, 2020). The use of both DNA geminiviruses, such as bean yellow dwarf virus (BeYDV), and RNA viruses, such as tobacco rattle virus (TRV), are being exploited as CRISPR/Cas reagent vehicles (Baltes *et al.*, 2014; Yin *et al.*, 2015; Gil-Humanes *et al.*, 2017; Shan-E-Ali Zaidi and Mansoor, 2017). The deconstruction of BeYDV into an efficient expression vector has allowed for the convenient delivery of genome editing components in plant cells, due to its rolling-circle replication mechanism which results in high copy numbers and efficient expression of the transgene (Kalinina *et al.*, 2020). The ability of geminiviruses to infect a number of plant species, including major crops, makes it an attractive vehicle for the delivery of genome editing components (Rey *et al.*, 2012; Sun *et al.*, 2020).

1.2 AIMS AND OBJECTIVES

Chapter 3: To investigate the ability of a CRISPR/CasRx system to confer virus resistance against grapevine virus A (GVA) in *Nicotiana benthamiana*.

To achieve this aim, the following objectives were formulated:

i. Design gRNA(s) targeting the replicase and coat protein (*CP*) genes of a GVA infectious clone.
ii. Assemble the construct(s) for CRISPR/CasRx-targeting and gRNA delivery using Gibson assembly, Golden Gate assembly, and restriction enzyme-based cloning techniques.
iii. Perform *Agrobacterium*-mediated transformation of *N. benthamiana* and produce regenerated transgenic plant lines.
iv. Use quantitative molecular analysis to evaluate the virus titre of GVA following Agro-infiltration into transgenic *N. benthamiana*.

Chapter 4: To investigate the use of a BeYDV-based vector, pRIC, to express and deliver CRISPR/Cas9 components in *N. benthamiana*.

To achieve this aim, the following objectives were formulated:

i. Design gRNA(s) targeting the *N. benthamiana* phytoene desaturase (*NbPDS*) gene and transgenic *N. benthamiana* 16c-*GFP* gene.
ii. Assemble the pRIC vector(s) harbouring the specific gRNA.
iii. Perform transient *Agrobacterium*-mediated transformation of *N. benthamiana.*
iv. Evaluate CRISPR/Cas9 targeting and editing with molecular analyses.

1.3 OVERVIEW OF CHAPTERS

Chapter 2 reviews the functioning of various CRISPR/Cas systems, and highlights existing literature on genome editing applications in plants to induce virus resistance, as well as the delivery methods of specific genome editing components. The use of geminivirus-based constructs as vectors for the delivery of genome editing components is also reviewed.

In **Chapter 3**, CRISPR/CasRx construct(s) harbouring components targeting an infectious clone of GVA are assembled and introduced into *N. benthamiana* by *Agrobacterium*-mediated transformation. The GVA titre in transformed plants is molecularly quantified to assess successful virus interference.

Chapter 4 demonstrates transient experiment(s) where pRIC vector(s) harbouring CRISPR/Cas9 components were assembled and co-infiltrated into *N. benthamiana*. Thereafter, target loci were molecularly and bioinformatically analysed to assess cleavage and editing of the target gene(s).

Finally, the major findings of each research chapter are summarised in **Chapter 5**, and considerations for future studies are suggested.

1.4 RESEARCH OUTPUTS

Conference Attendance: Poster Presentations

Spencer KP, Robertson GM, Campa M, Burger JT. CRISPR-Cas13a-mediated virus resistance induction in *Nicotiana benthamiana*. Virology Africa, 10-14 February 2020. Cape Town, South Africa.

Spencer KP, Campa M, Burger JT. CRISPR-based genome editing tools for virus resistance in grapevine XIth International Symposium on Grapevine Physiology and Biotechnology, 31 October - 5 November 2021. Stellenbosch, South Africa

CHAPTER 2: Literature Review

2.1 GENERAL INTRODUCTION

Plant selection has played a pivotal role in food production for humans for over 10,000 years, and has been fundamental in food security and safety since the 1900s (Ahmar *et al.*, 2020). For thousands of years, traditional breeding techniques, such as genetic selection, mutagenic breeding and somaclonal variation, have been used for the domestication of plants (Mao *et al.*, 2019). These historical methods of breeding are uncontrollable and inefficient, and may take up to two decades to complete (Mao *et al.*, 2019; Ahmar *et al.*, 2020). Recently, plant science and agriculture are being revolutionised by genome editing, a rapidly evolving and emerging field that aims to develop methods for efficient and targeted modifications to plant genomes for crop improvement (Čermák *et al.*, 2017; Schmidt, Belisle and Frommer, 2020).

Over the last few decades, in-depth knowledge and understanding has been accumulated regarding molecular genetics and the biochemistry of bacteria and viruses (Kamburova *et al.*, 2017). This information has sequentially allowed the development of novel methods to manipulate DNA, by creating various tools and vector systems which allow delivery of this machinery into cells (Kamburova *et al.*, 2017). With the emergence of genome editing tools, such as the Clustered Regularly Interspaced Short Palindromic Repeat (CRISPR), and the CRISPR-associated (Cas) proteins, plant science has been transformed, allowing the establishment of crops which are resistant to abiotic and biotic stresses (Kamburova *et al.*, 2017). This literature review aims to elucidate the CRISPR/Cas technology as an immune system against RNA viruses in plants, as well as to discuss the applications of viral vectors for the delivery of genome editing constructs *in planta*.

2.2 VIRUS PATHOGENS AFFECTING PLANTS

Plant diseases are estimated to cause reductions of 10 to 15% in global crop yields annually (Anderson *et al.*, 2004; Boualem, Dogimont and Bendahmane, 2016). Plant viruses, which infect many agricultural systems, are responsible for 47% of this yield loss (Zaidi *et al.*, 2016; Chaudhary, 2018; Varanda *et al.*, 2021). Viruses are obligate, intracellular parasites which exist in an inactive state until entry of the host, where they then depend on the host's machinery to replicate themselves (Nicaise, 2014; Marwal and Gaur, 2020). Viruses contain DNA or RNA genomes, which

encode only a few genes, such as the genes responsible for replication, movement, transmission and pathogenesis (Hanley-Bowdoin *et al.*, 2013). Viral diseases are specifically difficult to control, and the emergence of viruses is mainly driven by four factors: i) monocrop agricultural systems with low genetic diversity and high plant density; ii) virus spread by global trade of plant material, hosts, and vectors; iii) climate change resulting in the distribution area of vectors and hosts being altered; and iv) the rapid evolution and adaptation of viruses (Anderson *et al.*, 2004; Jones, 2009; Elena, Fraile and García-Arenal, 2014).

For agronomic use, there are no chemical products which target the virus directly, and due to their intracellular nature, there are no treatments for plants already infected with a virus (Varanda *et al.*, 2021). Therefore, disease management has to rely on preventing viruses from entering plants or having plants which are resistant to viral infection (Rubio, Galipienso and Ferriol, 2020; Varanda *et al.*, 2021). Some sanitary measures are in place for the prevention of virus infection and spread, such as the rapid removal and destruction of infected plants, virus vector population control, and legislative measures for commercialisation and trade of plant material which is virus free (Boualem, Dogimont and Bendahmane, 2016). Although these measures may hamper infection slightly, some are unsustainable for the environment and are still not enough to halt viral infection, steering the development for more efficient and long-term approaches. The development and implementation of virus resistant plant varieties would be a robust and sustainable solution to control plant virus diseases and viral infections (Varanda *et al.*, 2021).

2.2.1 Grapevine viruses

Grapevine (*Vitis vinifera* L.) is a major perennial fruit crop that is clonally propagated and provides a large contribution to many regions' economic sectors through wine and table grape production (Moriondo *et al.*, 2011). The yield and quality of this globally cultivated crop are important, as grape production is involved in making jams, juice, jellies and wine (Alabi *et al.*, 2016). Eighty-six grapevine viruses have been isolated worldwide, making grapevine a crop which is able to be infected with the most viruses (Fuchs, 2020). Grapevine viruses belong to the families *Betaflexiviridae*, *Caulimoviridae*, *Closteroviridae*, *Secoviridae* and *Geminiviridae* (Fuchs, 2020). The different vectors which transmit grapevine viruses are; mealybugs, soft scale insects, aphids, dagger nematodes, treehoppers and eriophyid mites (Fuchs, 2020). These viruses cause

economically detrimental diseases such as leafroll, leaf mottling, rugose wood and fleck. Grapevine leafroll disease (GLD) is a complex viral disease, which poses a serious threat to wine grapes across many regions, and causes significant reductions in the quality and yield of the fruit, with up to 30-68% in yield losses (Naidu *et al.*, 2014; Jiao *et al.*, 2022).

Grapevine leafroll-associated viruses (GLRaVs) have been implicated in GLD, with grapevine leafroll-associated virus 3 (GLRaV-3) being viewed as the "main etiological agent" as it is the most prevalent strain in grape-growing regions worldwide (Maree *et al.*, 2013). GLRaV-3, from the family *Closteroviridae*, is a monopartite, positive-strand RNA virus which is transmitted by vegetative propagation, and in a semi-persistent manner by mealybugs and scale insects (Tsai *et al.*, 2010; Le Maguet *et al.*, 2012; Jiao *et al.*, 2022). Antiviral strategies such as conventional breeding with the goal of combining antiviral traits with other superior traits is time-consuming and costly, and limited molecular antiviral research has been performed in grapevine, especially pertaining to GLRaV-3 (Jiao *et al.*, 2022).

Grapevine virus A (GVA) is a member of the genus *Vitivirus*, and within the *Flexiviridae* family (Martelli *et al.*, 2007). It is a phloem-associated virus, which replicates in the cytoplasm of the plant cell (Minafra, Saldarelli and Martelli, 1997; Rampersad and Tennant, 2018). It has a filamentous structure about 800 nm long (Muruganantham *et al.*, 2009). This single-stranded positive-sense RNA (ssRNA) virus possesses a 7.4 kilobase (kb) genome, consisting of five open reading frames (ORFs) capped at the 5'-terminus and polyadenylated at the 3'-end (Fig. 2.1) (Saldarelli, Dell'Orco and Minafra, 2000; N. Galiakparov *et al.*, 2003; Muruganantham *et al.*, 2009).

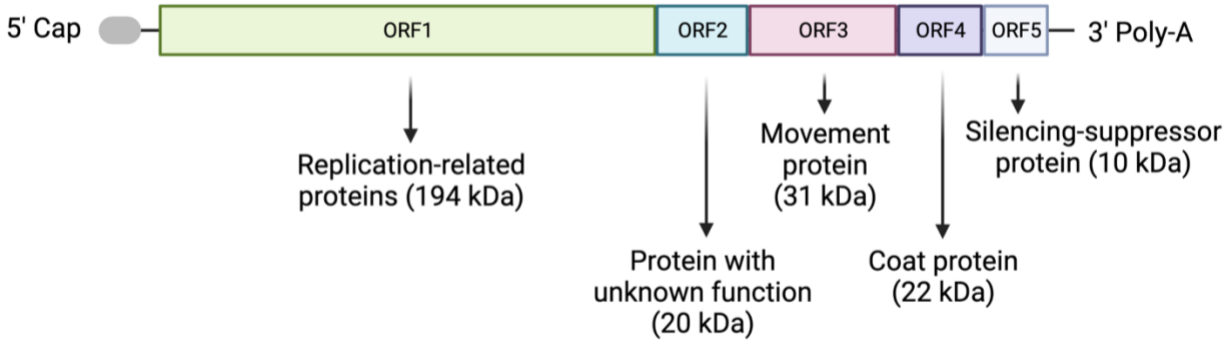

Figure 2.1. The grapevine virus A (GVA) genome organisation, consisting of five open reading frames and their related encoded proteins.

Located at the 5'-terminus, the first ORF (ORF1) encodes a 194-kilodalton (kDa) polypeptide containing conserved motifs of RNA virus replication-associated proteins; helicase and the RNA dependent RNA polymerase (RdRp) (Saldarelli, Dell'Orco and Minafra, 2000; N. Galiakparov *et al.*, 2003; Goszczynski, du Preez and Burger, 2008; Muruganantham *et al.*, 2009). A 20-kDa protein with unknown function is encoded by ORF2, while ORF3 is the gene responsible for encoding a 31-kDa movement protein (MP). ORF4 encodes the coat protein (CP), and ORF5 encodes a small protein (10-kDa) with two distinct domains, presenting sequence similarities to small RNA binding proteins of various plant viruses and exhibiting RNA-silencing suppression activity (Nurbol Galiakparov *et al.*, 2003; Chiba *et al.*, 2006; Zhou *et al.*, 2006; Goszczynski, du Preez and Burger, 2008; Haviv *et al.*, 2012).

A powerful tool for the functional analysis of RNA virus genomes is the use of infectious clones (Naidu *et al.*, 2014). Infectious clones are double-stranded DNA copies of a viral genome, which upon delivery into a cell, produces an infectious virus (Saldarelli, Dell'Orco and Minafra, 2000). Infectious clones of GVA have been constructed previously, which allow for the study of genome expression and pathogenesis of these viruses (Saldarelli, Dell'Orco and Minafra, 2000). The natural host of GVA is grapevine, nevertheless, GVA can also infect the model plant *Nicotiana benthamiana* (Goszczynski and Jooste, 2003). This makes GVA a helpful model for the study of viruses in herbaceous plants, allowing GVA to act as a proxy for GLRaV-3, and for a method to be established in *N. benthamiana* which can be transferred to grapevine.

2.3 EARLIER METHODS TO CONTROL PLANT VIRUSES

2.3.1 RNA interference for virus resistance

Previously, transgenic plant approaches encoded virus proteins to interfere with viral function upon infection, but this method was overcome with the observation that virus resistance was predominantly RNA-mediated (Taliansky *et al.*, 2021). RNA silencing or RNA interference (RNAi) is a eukaryotic immune response mechanism which is driven by sequence similarity, in order to control endogenous gene expression and destroy invading nucleic acids (Taliansky *et al.*, 2021). RNAi is triggered by the occurrence of double strand RNA (dsRNA) precursors. The enzyme Dicer is responsible for the initial cleavage of dsRNA or small hairpin RNA (shRNA), resulting in the generation of double-stranded short interfering RNA (siRNA) (Bernstein *et al.*, 2001). The RNA-induced silencing complex (RISC) processes the resulting siRNA by degrading the sense strand

while loading the anti-sense strand into RISC (Elbashir, Lendeckel and Tuschl, 2001). Using complementary base-pairing, RISC recognises the target RNA and the Argonaute 2 (Ago2) nuclease cleaves it nonspecifically (Martinez *et al.*, 2002; Liu *et al.*, 2004). Through the use of siRNA or shRNA, the sequence-specific targeting of RNA can be achieved, and has thus become a widely used RNA silencing method, and RNAi as an antiviral strategy in plants has been implemented (Bernstein *et al.*, 2001; Konermann *et al.*, 2018; Loriato *et al.*, 2020; Smargon, Shi and Yeo, 2020; Akbar, Wei and Zhang, 2022).

The low cost and robust silencing of target RNA makes RNAi a powerful tool (Wang *et al.*, 2019). However, a major implication with RNAi is the high number of off-target effects which have been observed throughout the transcriptome (Jackson *et al.*, 2003; Cox *et al.*, 2017). Although the average knockdown efficiency of RNAi is relatively high (~65%), its limited specificity may cause knockdown of unintended transcripts and consequently result in false-positive outcomes (Wang *et al.*, 2019). Not only is RNAi associated with a high number of off-targets, but plant viruses have evolved counter-defensive measures against RNAi, one being suppressor proteins that can inhibit specific steps in the silencing pathway (Voinnet, 2005; Burgyán and Havelda, 2011).

2.3.2 Plant genome editing technologies

The classical plant breeding and transgenic (genetically modified organism - GMO) methods which have been adopted for sustainable food production and improvement of crop plants have been surpassed by precise and efficient targeted genome editing (Belhaj *et al.*, 2013). Earlier tools used for genome editing, such as the programmable meganucleases, zinc finger nucleases (ZFNs), and transcription activator-like effector nucleases (TALENs), have been adapted with the purpose of introducing a double strand break (DSB) in DNA. In eukaryotic cells, DSBs are repaired by two mechanisms, either by non-homologous end joining (NHEJ) or by homology-directed repair (HDR) (Fig. 2.2) (Belhaj *et al.*, 2013; Gaj, Gersbach and Barbas, 2013; Nemudryi *et al.*, 2014; Weeks, Spalding and Yang, 2016; Mao *et al.*, 2019).

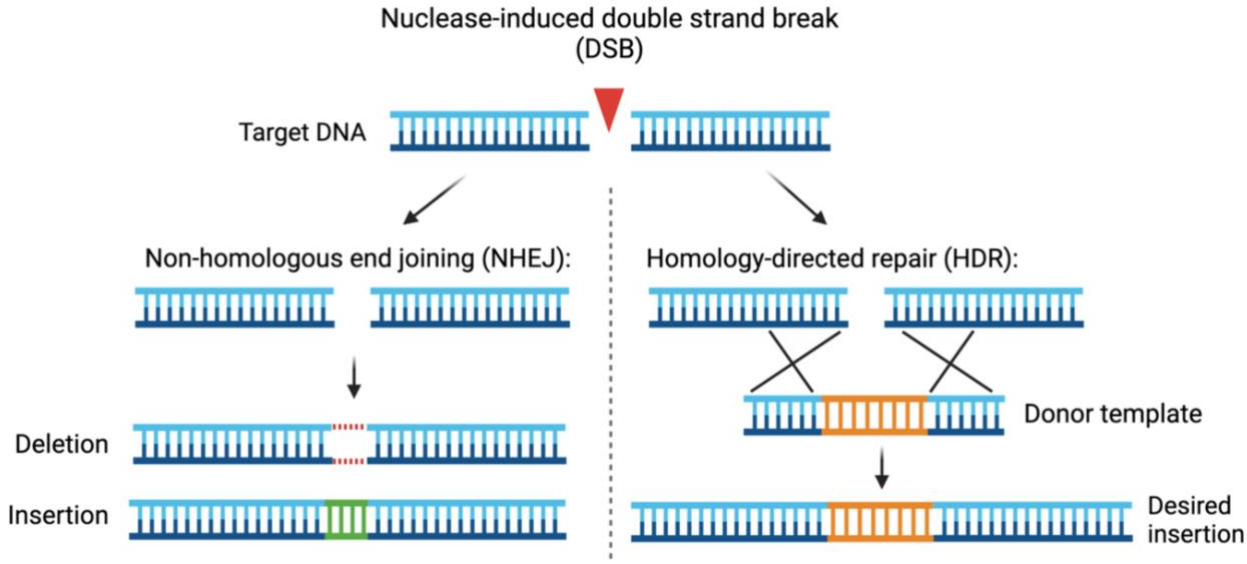

Figure 2.2. Eukaryotic repair mechanisms following induction of a double-strand break (DSB) in DNA. Following the nuclease-induced DSB, non-homologous end joining (NHEJ) leads to the error-prone repair resulting in random insertions or deletions (indels). Repair with homology-directed repair (HDR) results in more precise desired sequence insertions through recombination with the donor template.

NHEJ is most common in plants, and has been shown to be error-prone, usually resulting in insertions or deletions (indels) of nucleotide(s) (nt) at the cut site (Petolino, 2015). These mutations result in gene knockout or gene inactivation due to the disruption of the reading frame (Weeks, Spalding and Yang, 2016). HDR can result in gene replacement or gene insertions, by introducing an exogenous DNA fragment harbouring a sequence variation, followed by recombination with the donor template (Voytas, 2013; Weeks, Spalding and Yang, 2016). Therefore, by introducing DSBs into a plant's genome using programmable nucleases, specific alterations at target loci can be achieved.

Meganucleases, low frequency cutters which recognise 12-24 bp DNA sequences, were discovered in yeast in 1985 (Jacquier and Dujon, 1985). Meganucleases were the first sequence specific nucleases employed for double stranded DNA breaks (Silva *et al.*, 2011). The high specificity of meganucleases limits targetable loci, and re-engineering their DNA recognition sites increased the flexibility and applications of meganucleases. However, reconstruction of the protein for each new target is cumbersome and time-consuming (Tröder and Zevnik, 2022). In 1996, ZFNs were harnessed for genome editing by coupling the FokI endonuclease domain to their C-terminus, engineering a nuclease which could induce a DSB at the specified site when flanking a sequence of interest (Belhaj *et al.*, 2013). This mechanism functioned by binding to a recognition site on each DNA strand, and creating a DSB between the two ZNFs (Gaj, Gersbach

and Barbas, 2013; Weeks, Spalding and Yang, 2016; Kamburova *et al.*, 2017). One study effectively targeted both tomato yellow leaf curl China virus (TYLCCV) and tobacco curly shoot virus (TbCSV) using a programmed ZFN in plants (Chen *et al.*, 2014). Subsequent developments of genome editing tools led to the discovery of TALENs in 2009, after the identification of transcription activator-like effector (TALE) proteins (Boch *et al.*, 2009; Moscou and Bogdanove, 2009; Kamburova *et al.*, 2017; Malzahn, Lowder and Qi, 2017). When this TALE protein is fused with the FokI nuclease, now a chimeric TALEN, a pair of these chimeras can introduce a DSB into the genome (Nemudryi *et al.*, 2014). One study showed partial resistance to three begomoviruses in transgenic *N. benthamiana* with the use of an artificial TALEN (Cheng *et al.*, 2015).

2.4 THE NEW ERA OF VIRUS CONTROL: CRISPR/Cas TECHNOLOGY

Both ZFNs and TALENs were the dominant sequence-specific nuclease (SSN) gene editing tools until 2013, when they were taken over by the ground-breaking CRISPR RNA-guided nuclease (Belhaj *et al.*, 2013; Bortesi and Fischer, 2015). The CRISPR/Cas system is less complicated and inexpensive, when compared to previous genome editing tools. The Cas9/guide RNA (gRNA) complex was used for genome editing in plants, displaying high efficiency and adaptability (Li *et al.*, 2013; Nekrasov *et al.*, 2013; Shan *et al.*, 2013; Bortesi and Fischer, 2015). Subsequent to this, an eruption of plant-based genome engineering research followed, where both NHEJ and HDR repair pathways were reported to have introduced mutations (Belhaj *et al.*, 2013; Feng *et al.*, 2013; Mao *et al.*, 2013; Miao *et al.*, 2013; Xie and Yang, 2013). The CRISPR technology was adapted from the bacterial and archaeal immune system, which these prokaryotes use to protect themselves from invading nucleic acids, such as bacteriophages (Fig. 2.3) (Bhaya, Davison and Barrangou, 2011; Terns and Terns, 2011; Wiedenheft, Sternberg and Doudna, 2012; Bortesi and Fischer, 2015).

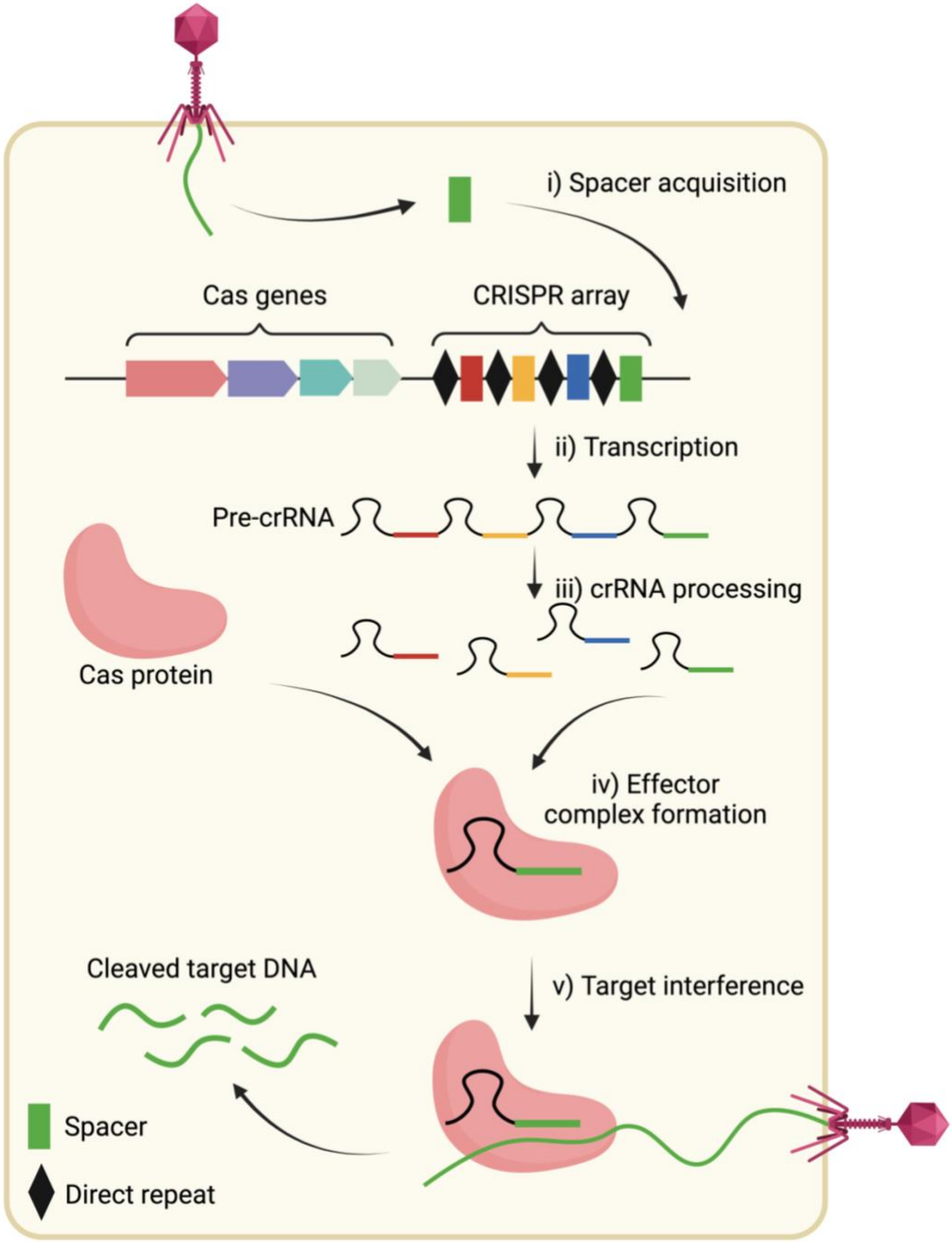

Figure 2.3. The stages and mechanism of CRISPR/Cas immunity in a bacterial cell. **i**) Spacer acquisition where a portion of the invading nucleic acid is integrated into the CRISPR array. **ii**) The CRISPR locus is transcribed into pre-CRISPR RNA (crRNA) and the Cas proteins. **iii**) The transcribed pre-crRNA is processed into mature crRNAs. **iv**) Formation of the effector complex. **v**) The crRNA guides the Cas protein to the target DNA, followed by interference of the target DNA and immunity against the invading nucleic acid.

The fundamental aspect of the CRISPR immune system is for the host to integrate a short fragment of foreign sequence (protospacer) into the CRISPR array of its genome (Fig. 2.3i), where each protospacer is separated by a spacer of identical direct repeats (DRs) (CRISPR array) (Bhaya, Davison and Barrangou, 2011; Terns and Terns, 2011; Wiedenheft, Sternberg and Doudna, 2012;

Cong *et al.*, 2013). After expression and maturation of the integrated protospacer (Fig. 2.3ii and iii), now a short crRNA, the complex between the crRNA and Cas protein will form (Fig. 2.3iv) (Haurwitz *et al.*, 2010; Deltcheva *et al.*, 2011). Then, the complex can recognise subsequent invasions of that foreign nucleic acid, and silence it by cleaving the nucleic acid (Fig. 2.3v) (Brouns *et al.*, 2008; Bortesi and Fischer, 2015). The discovery of this CRISPR/Cas immune system has been harnessed and adapted as a genome editing tool, allowing for the precise introduction of mutations at desired sites within the genome, and is a desirable system to use for genome editing because of its specificity, versatility, easily programmable nature and reduced off-target effects (Jinek *et al.*, 2012; Schindele, Wolter and Puchta, 2018).

2.4.1 The classes of CRISPR/Cas systems

Two classes of CRISPR/Cas systems have been classified and subdivided into six types: Class 1 subtypes are Type I, III and IV, while Class 2 subtypes are Type II, V and VI (Makarova *et al.*, 2015; Mohanraju *et al.*, 2016). The distinction between the two classes is that Class 1 employs multi-subunits, while Class 2 employs a ribonucleoprotein (RNP) complex composed of a single nuclease and a crRNA to mediate interference (Makarova *et al.*, 2011; Shmakov *et al.*, 2017). The specific nucleases of the Class 2 systems are; type II (Cas9), type V (Cas12) and type VI (Cas13) (Fig. 2.4) (Shmakov *et al.*, 2017; Chaudhary, 2018; Xu *et al.*, 2021).

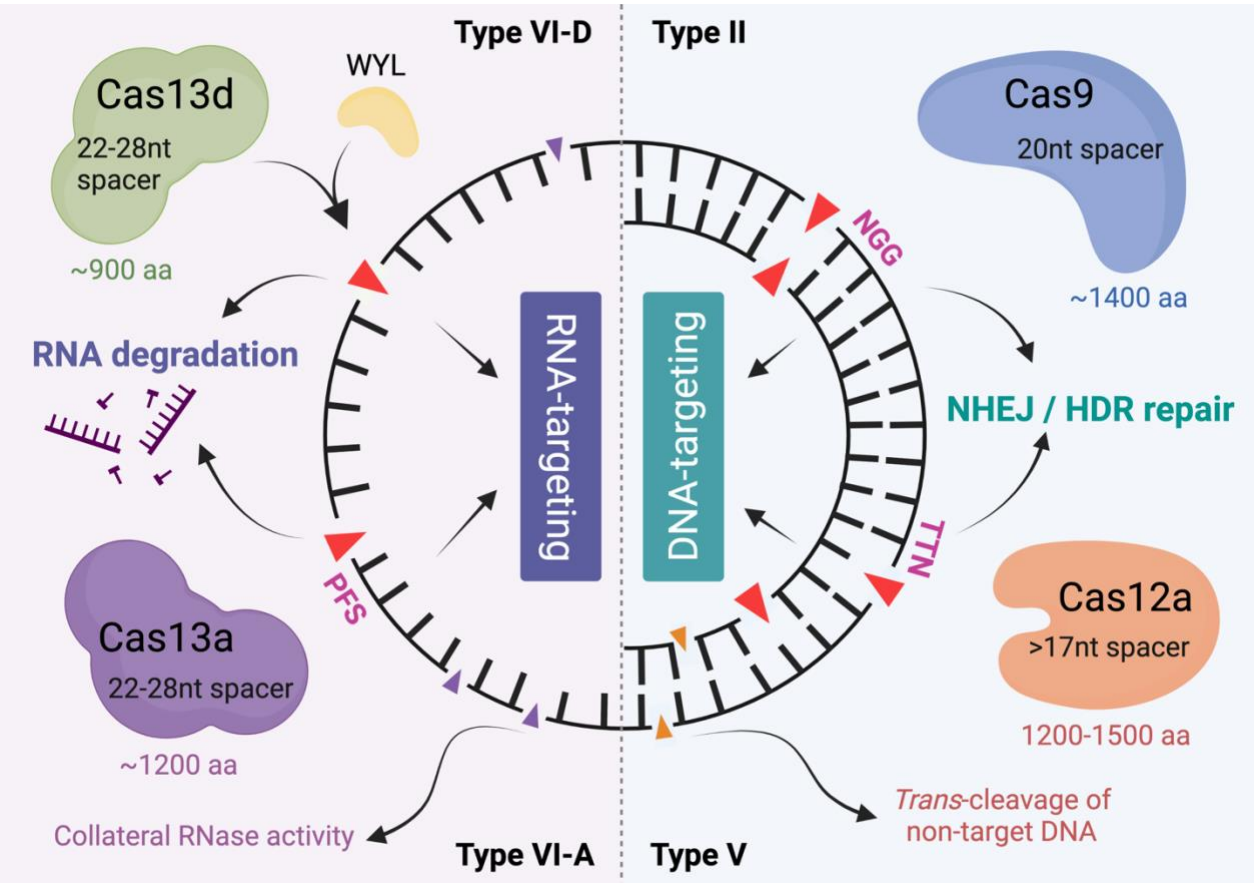

Figure 2.4. A schematic representing the Class 2 CRISPR systems, with their target nucleic acid, cleavage pattern (red arrows), protospacer-adjacent motif (PAM) or protospacer flanking sequence (PFS) (pink), and the respective spacer length.

The simple architecture of these Class 2 effector proteins is the reason Class 2 CRISPR systems have been intensively researched and are widely adopted for genome and transcriptome editing technology (Jinek *et al.*, 2012; Cong *et al.*, 2013; Mahas, Aman and Mahfouz, 2019). Types II and V target double-strand DNA (dsDNA), whereas type VI CRISPR systems, such as Cas13a and Cas13d, are characterised for exclusively targeting ssRNA (Abudayyeh *et al.*, 2016; Jiang, Samai and Marraffini, 2016; Mahas, Aman and Mahfouz, 2019).

2.4.1.1 Type II CRISPR/Cas9 systems

The type II CRISPR/Cas9 system functions through a single effector – Cas9, a crRNA and a trans-activating crRNA (tracrRNA) (Doudna and Charpentier, 2014). The crRNA is made up of two components; at the 5'- end is a 20nt guide-sequence complimentary to the target DNA, and at the 3'-end is a DR sequence of 19-22nt, which is hybridised to the tracrRNA via complementarity (Deltcheva *et al.*, 2011). The 20nt spacer sequence is responsible for the target specificity, while the tracrRNA is involved in the recruitment of the Cas9 protein (Doudna and Charpentier, 2014).

To make the CRISPR/Cas9 genome editing system more convenient, scientists engineered a single RNA chimera which mimics the crRNA:tracrRNA structure and function, named the single guide RNA (sgRNA) or gRNA (Fig. 2.5) (Jinek *et al.*, 2012).

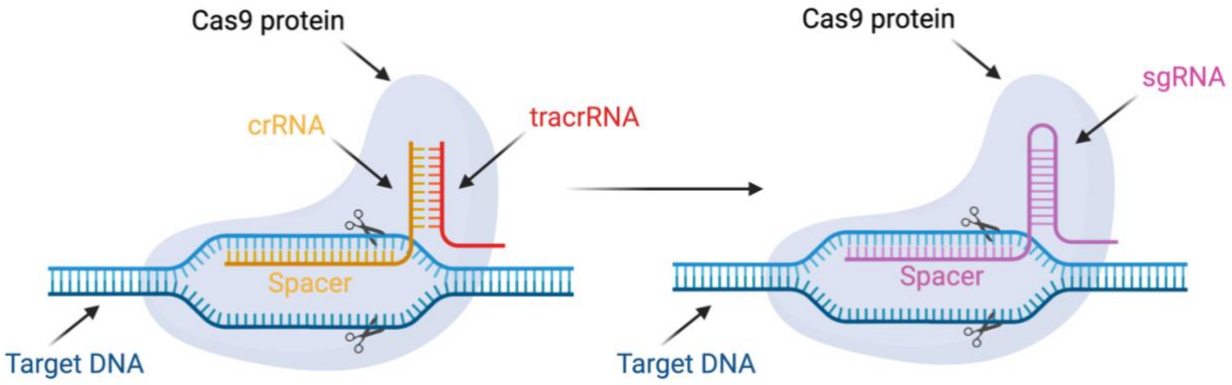

Figure 2.5. The Cas9 protein complexed with the crRNA and tracrRNA, followed by the complex of the Cas9 protein with the convenient single-guide RNA (sgRNA). Subsequent to complex formation, the respective sgRNAs direct the Cas protein to the target DNA, complementary to the spacer sequence, and cleave the target DNA.

The CRISPR array located in the host's genome encodes the crRNAs, which are initially transcribed as long pre-crRNAs (Fig. 2.3), followed by hybridisation with the multiple tracrRNAs, when finally, RNase III processes the complexes into single crRNA-tracrRNA structures. The Cas9 protein complexes with the crRNA-tracrRNA, which ultimately guides the Cas9 protein to any homologous target sites in the invader's genome (Deltcheva *et al.*, 2011; Jiang and Doudna, 2017). A short sequence located downstream of the target, known as the protospacer-adjacent motif (PAM), is responsible for the base-pairing of the complex and target sequence (Mojica *et al.*, 2009). The PAM-interacting (PI) domain of the complexed Cas9 protein(s) recognises the PAM sequence, causing base-pairing between the crRNA and the target sequence, and results in the DNA melting process of the adjacent regions (Sternberg *et al.*, 2014). Each Cas9 system from a different species recognises a distinct PAM sequence, which are often 3' GC-rich (Nishimasu *et al.*, 2014; Koonin, Makarova and Zhang, 2017). A seed region within the spacer sequence of the crRNA plays a vital role in the specificity of the system, and mismatches within this region radically impair or abolish DNA binding (Semenova *et al.*, 2011; Pattanayak *et al.*, 2013). For the type II systems, the 10-12 nts in the 3' end of the spacer sequence are the nts denoting the seed region (Jinek *et al.*, 2012; Cong *et al.*, 2013). Most Cas9 effectors have a bi-lobed architecture, comprising of the recognition (REC) and nuclease (NUC) lobes; where the NUC lobe is comprised of the PI domain, along with

the RuvC and HNH domains responsible for cleaving the non-target and target DNA strands, respectively (Nishimasu *et al.*, 2014; Tang and Fu, 2018). The REC and NUC lobes form a positively charged groove, ultimately attracting and accommodating the negatively charged gRNA:target DNA heteroduplex (Nishimasu *et al.*, 2014, 2015; Yamada *et al.*, 2017). Once the gRNA directs the Cas9 protein to the target DNA, the RuvC and HNH domains catalyse DNA cleavage 3 base pairs (bp) upstream of the PAM sequence, resulting in a staggered end DNA cut (Molla and Yang, 2020).

The first and most widely used CRISPR/Cas9 system harnessed for genome editing is the Cas9 from *Streptococcus pyogenes* (SpCas9) (Fig. 2.4) (Cong *et al.*, 2013). The PAM sequence of the SpCas9 protein is 5' NGG, while the protein size is 1368 amino acids (aa) (Nishimasu *et al.*, 2014). Another widely used and studied CRISPR/Cas9 system is the *Staphylococcus aureus* (SaCas9) (Nishimasu *et al.*, 2015). When compared to SpCas9, SaCas9 is much smaller (1053 aa, ~3.2 kb), but shares the bi-lobed structure (Nishimasu *et al.*, 2015). The PAM sequence of SaCas9 is a 5' NNGRRT, which increases the specificity by reducing the probability of off-targets, but simultaneously reduces the potential target sites (Wang, Zhang and Feng, 2020). One of the largest Cas9 variants is the *Francisella novicida* Cas9 (FnCas9; ~4.9 kb), which belongs to the type II-B system, and exhibits high targeting-specificity with negligible off-target binding. FnCas9 mostly interacts with a 5'-NGG-3' PAM sequence in DNA, and does not possess the bilobed structure of Cas9. Notably, FnCas9 also exhibits RNA targeting activity (Price *et al.*, 2015; Hirano *et al.*, 2016).

2.4.1.2 Type V CRISPR/Cas12 systems

Identification of other Class 2 CRISPR/Cas systems besides type II systems has expanded the CRISPR toolbox for genome editing (Lewis and Ke, 2017). The earliest Cas nuclease from the type V system to be characterised was Cas12a (Fig. 2.4), followed by Cas12b (Shmakov *et al.*, 2015; Zetsche *et al.*, 2015). Although there is large diversity between the type V systems, some common characteristics are shared which distinguish them from the type II systems (Wang, Zhang and Feng, 2020). The Cas12 systems lack the HNH nuclease domain, and only possess one RuvC domain, unlike Cas9 which possesses both. The recognised PAM sequence is T-rich and located 5' upstream to the target region on the non-target strand (Zetsche *et al.*, 2015). After the Cas12-crRNA complex binds the target DNA, each DNA strand is nicked to yield a sticky-end-like 4 or 5 nt overhang, followed by *trans*-cleavage of non-target DNAs (Fig. 2.4) (Zetsche *et al.*, 2015). Upon

binding to target DNA, certain orthologs also possess collateral single-stranded DNase activity (Swarts and Jinek, 2019). The protein sizes of Cas12a variants range from 1200 aa (3.6 kb) to 1500 aa (4.5 kb) (Zetsche *et al.*, 2015). The bi-lobed architecture of Cas9 is mimicked in Cas12a, consisting of a REC and NUC lobe (Dong *et al.*, 2016). Additionally, the crRNA of Cas12a can mediate robust DNA cleavage, and a tracrRNA is not needed for crRNA maturation (Zetsche *et al.*, 2015). Cas12b requires both the tracrRNA and crRNA for complexing with the effector and DNA cleavage, while the cleavage pattern of Cas12b is a staggered DSB with seven-nt overhangs (Koonin, Makarova and Zhang, 2017; Li and Peng, 2019). Cas12b systems possess high sensitivity when binding to target DNA, resulting in minimal off-target activity (Liu, Chen, *et al.*, 2017; Chen *et al.*, 2018).

2.4.1.3 Type VI CRISPR/Cas13 systems

There are six subtypes of Cas13 effectors, formerly known as C2c2; VI-A (Cas13a), VI-B (Cas13b), VI-C (Cas13c), VI-D (Cas13d), and the most recently characterised VI-X (Cas13X) and VI-Y (Cas13Y) (Makarova *et al.*, 2020; Xu *et al.*, 2021). Unlike the DNA targeting Cas9 and Cas12 effectors, Cas13 exclusively targets and cleaves ssRNA (Fig. 2.4) (Abudayyeh *et al.*, 2016; Kordyś, Sen and Warkocki, 2022). The Cas13 systems possess two distinct RNase abilities; i) target degradation provided by the two conserved higher eukaryotic and prokaryotic nt binding domains (HEPN) – each containing an RNA cleavage site, and ii) processing and maturation of the pre-crRNA into mature crRNA (East-Seletsky *et al.*, 2016; Liu, Li, Wang, *et al.*, 2017). Only the crRNA complexes with the Cas13 effector, lacking the need for a tracrRNA (Liu, Li, Ma, *et al.*, 2017). Comparable to the PAM sequence of Cas9 and Cas12, Cas13 requires a protospacer-flanking site (PFS), which is downstream of the target site and essential for RNA targeting (Abudayyeh *et al.*, 2016). Some Cas13 effectors lack the requirement of a PFS, such as Cas13d and some Cas13a systems (Abudayyeh *et al.*, 2017; Yan *et al.*, 2018). The presence of a central seed region within the middle of the crRNA has been discovered, where mismatches are not tolerated between the crRNA spacer – protospacer base-pairing (Aman, Ali, *et al.*, 2018). A distinguishing characteristic of Cas13 is the haphazard cleaving of non-target RNA, termed collateral activity (Wang, Zhang and Feng, 2020). The two HEPN domains are activated upon binding to the target RNA, subjecting any other exposed RNAs to indiscriminate cleavage by the active HEPN catalytic pocket, inducing cell death to prevent viral spread (Abudayyeh *et al.*, 2016; Makarova *et al.*, 2020).

Cas13a (C2c2)

CRISPR/Cas13a was the first subtype to be characterised, with the well-characterised variants being *Leptotrichis shahii* (LshCas13a), *Leptotrichia wadei* (LwaCas13a), *Leptotrichia buccalis* (LbuCas13a) and *Lachnospiraceae bacterium* (LbaCas13a) (Abudayyeh *et al.*, 2016, 2017; East-Seletsky *et al.*, 2016; Knott *et al.*, 2017; Kordyś, Sen and Warkocki, 2022). Two additional adaptive proteins are present with the Cas13a system; Cas1 – new protospacer acquisition, and Cas2 – the adaptation complex scaffold (Amitai and Sorek, 2016). Programmable RNA-targeting was initially demonstrated using the LshCas13a ortholog (~4.2 kb) (Abudayyeh *et al.*, 2016). The crRNA, which contains a 28-nt spacer sequence, guides the Cas13a nuclease to the target ssRNA with a PFS of either A, U or C. Secondary structures within the target sequence have an effect on Cas13a's catalytic activity, and uracil residues within secondary structures of the target site are the preferential cleavage sites for Cas13a (Aman, Ali, *et al.*, 2018).

Cas13b

The Cas13b locus codes for the Cas13b effector (1100 aa, ~3.3 kb) and a small accessory protein (200 aa) (Smargon *et al.*, 2017). There are two variant systems of Cas13b; i) VI-B1 from *Bergeyella zoohelcum* Cas13b (Bzcas13b, accessory protein Csx27), and ii) VI-B2 from *Prevotella buccae* Cas13b (PbCas13b, accessory protein Csx28) (Smargon *et al.*, 2017). The roles of the accessory proteins have been found to be antagonistic, where Cas13b activity is repressed by Csx27, while Csx28 enhances Cas13b activity (Smargon *et al.*, 2017). A double PFS is required for Cas13b; the 5'-end needs a 5' D and the 3'-end needs 5' NAN/NNA (Smargon *et al.*, 2017). Taken together, the accessory proteins and the double PFS expand the opportunities of the Cas13b system (Wang, Zhang and Feng, 2020).

Cas13d

A recent addition to the Cas13 subtypes, Cas13d, is smaller (less than 1000 aa, ~3 kb) and portrays minimal sequence identify to previous Cas13 effectors (Fig. 2.4) (Mahas, Aman and Mahfouz, 2019). Cas13d possess two HEPN domains, similarly to other Cas13 variants, which are responsible for the processing of pre-crRNA (B. Zhang *et al.*, 2019). Four characteristics of Cas13d make it attractive for RNA targeting: i) the small size allows for easy delivery, ii) target selection is not limited by a PFS requirement, iii) RNA interference is increased due to their strong co-occurrence with WYL-domain-containing accessory proteins, which positively stimulate RNA

cleavage, and iv) cleavage of target RNA is highly specific (Konermann *et al.*, 2018; Yan *et al.*, 2018; B. Zhang *et al.*, 2019). The seed regions of the Cas13d spacer are located internally and at the 3'-end of the spacer, and thus in order for target recognition, correct base pairing must occur in these regions (B. Zhang *et al.*, 2019). The Cas13d from *Ruminococcus flavefaciens* (CasRx) has been harnessed for programmable RNA-guided ssRNA-targeting, and has been shown to be effective against RNA virus interference (Mahas, Aman and Mahfouz, 2019; Cao *et al.*, 2021). Notably, a study found that CasRx does not exhibit collateral RNase activity *in planta* (Mahas, Aman and Mahfouz, 2019). Studies have also shown that CasRx activity in mammalian cells has consistently demonstrated efficient interference, when compared to previous Cas13 proteins, namely Lwacas13a and PspCas13b (Konermann *et al.*, 2018).

2.5 PLANT VIRUS INTERFERENCE USING THE CRISPR/Cas SYSTEM

CRISPR/Cas technology offers a powerful alternative to classical plant breeding for trait improvement, and is a popular toolkit for plant genome editing due to its easy design, high efficiency and great flexibility (Kalinina *et al.*, 2020; Sandhya *et al.*, 2020). Vast research has gone into the use of CRISPR/Cas to combat devastating viral pathogens for crop protection (Ali, Abulfaraj, *et al.*, 2015; Ji *et al.*, 2015; Chaudhary, 2018). Two main strategies are implemented to confer plant virus resistance using the CRISPR/Cas system. Firstly, gene targeting for mutation induction in host plant genes or susceptibility genes which play a role in the virus replication and spread. This strategy has been used to combat viral infections in plants, as extensively reviewed by the Hashimoto and Mäkinen groups (Hashimoto *et al.*, 2016; Mäkinen, 2020). Secondly, engineering the CRISPR/Cas system to function in plants to directly target viral genomes. For example, DNA-targeting CRISPR systems, like Cas9, have been programmed to target DNA viruses, while RNA-targeting systems, such as Cas13, have been deployed in cleaving RNA viral genomes (Fig. 2.6) (Zaidi *et al.*, 2016; Freije *et al.*, 2019; Kalinina *et al.*, 2020).

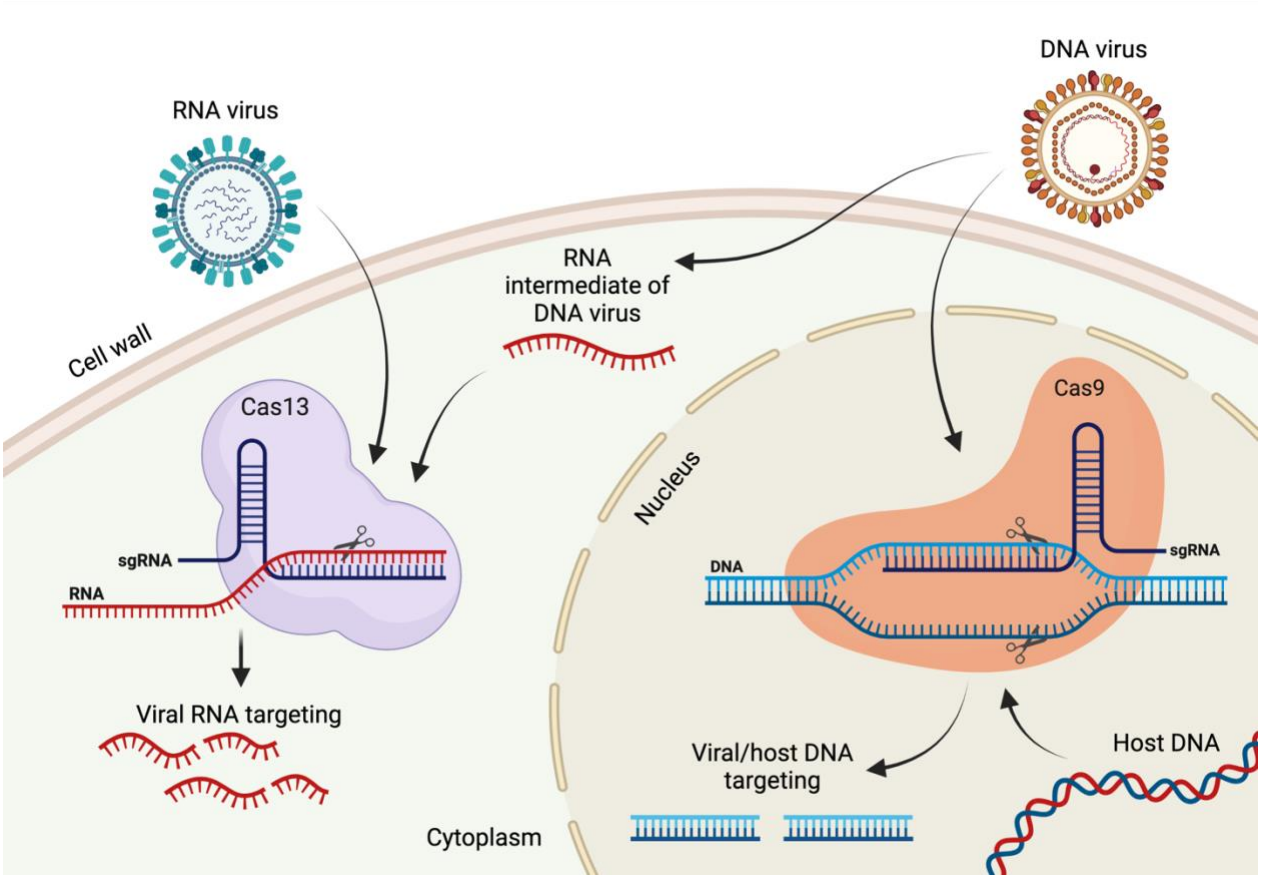

Figure 2.6. The CRISPR/Cas systems employed for DNA and RNA virus targeting. The CRISPR/Cas9 system is commonly used to target DNA viruses, while the CRISPR/Cas13 system is often used to target RNA viruses and the RNA intermediate stage of DNA viruses. Both systems directly target the viral genome and result in cleavage of the target nucleic acid.

2.5.1 DNA virus targeting

CRISPR/Cas9 has been harnessed and adapted for gene editing, and employed in plants for the interference of DNA viruses (Ali, Abulfaraj, *et al.*, 2015; Ali *et al.*, 2016; Zaidi *et al.*, 2016; Ji *et al.*, 2018). Geminiviruses are estimated to be responsible for the loss of billions of dollars in grain, vegetable and fruit crops annually (Ji *et al.*, 2018). To prevent such losses, the CRISPR/SpCas9 system is well studied and most commonly used as a means of developing crops with DNA virus tolerance (Kamburova *et al.*, 2017; Shmakov *et al.*, 2017).

In one study, when the geminivirus bean yellow dwarf virus (BeYDV) genome was targeted with Cas9, mutations within the virus genome were introduced, and decreased virus accumulation was observed in *N. benthamiana* in both transient and stable assays (Baltes *et al.*, 2015). In another study targeting geminiviruses, CRISPR/Cas9 was engineered to target tomato yellow leaf curl virus (TYLCV) (Ali, Abulfaraj, *et al.*, 2015). Stably transformed *N. benthamiana* constitutively expressing

the *Cas9* gene and a systemic gRNA targeting the intergenic region (IR), where the origin of replication and RNA polymerase II promoter are located, were challenged with TYLCV infection by Agro-infiltration (Yang *et al.*, 2014). Results showed that CRISPR/Cas9 targeting the IR of TYLCV resulted in reduction of virus titre and attenuation of viral symptoms, with mutations introduced at the target sequences (Ali, Abulfaraj, *et al.*, 2015). A similar study also targeted coding and non-coding regions of the TYLCV genome, and found that the replication of the virus was halted when the IR was targeted, and the CRISPR/Cas9 machinery had successfully provided virus interference against TYLCV strains in *N. benthamiana* overexpressing the *Cas9* gene (Ali *et al.*, 2016). Immunity against another geminivirus, beet severe curly top virus (BSCTV), was also achieved in *N. benthamiana* and *Arabidopsis thaliana* plants overexpressing both Cas9 and a gRNA (Ji *et al.*, 2015).

A number of studies have shown that CRISPR/Cas9 provides attenuation to DNA viruses *in planta* (Ali, Abulfaraj, *et al.*, 2015; Ji *et al.*, 2015, 2018; Ali *et al.*, 2016; Zaidi *et al.*, 2016). However, one study observed off-targets within the host genome caused by constitutively overexpressed CRISPR/Cas9 components (Ji *et al.*, 2018). The prevalence of off-targets caused by Cas9 in the host genome could limit the desirability of this system in conveying DNA virus resistance to various plant species. Thus, a method of decreasing the possibility of off-targets was developed by creating a virus-inducible CRISPR/Cas9 system (Ji *et al.*, 2018). CRISPR/Cas9 vectors driven by the BSCTV pV86 and pC86 promoters which were *trans*-activated by co-infecting BSCTV, efficiently inhibited BSCTV accumulation in transient assays with *N. benthamiana* and stably-transformed *A. thaliana* lines. Deep sequencing detected no off-target mutations from either virus-inducible system, demonstrating an alternative approach to virus targeting with no apparent off-target editing in the host genome (Ji *et al.*, 2018).

2.5.2 RNA virus targeting

It is evident that successful interference against DNA viruses has been achieved with CRISPR/Cas systems. Nevertheless, a method for interference against RNA viruses is indispensable, since the bulk of viruses have RNA genomes. The CRISPR/Cas13 systems have often been exploited in plants as antiviral strategies against RNA viruses (Zaidi *et al.*, 2016).

2.5.2.1 FnCas9 and Cas13a

The first study which harnessed the CRISPR/Cas immune system for direct genomic RNA virus cleavage utilised the CRISPR/FnCas9 system to confer immunity against the positive-sense RNA viruses – cucumber mosaic virus (CMV) and tobacco mosaic virus (TMV) – in *N. benthamiana* and *A. thaliana* (T. Zhang *et al.*, 2018). Viral symptoms and accumulation were both significantly reduced, while stably-transformed *A. thaliana* provided heritable virus resistance with progenies portraying significant virus interference. FnCas9 was localised to the cytosol with a nuclear export signal (NES) sequence, which was necessary for the virus interference, in contrast to Cas9 which requires a nuclear localisation signal (NLS) for DNA targeting. The study also concluded that endonuclease activity of FnCas9 was unnecessary for virus inhibition, and that RNA-binding activity was indispensable for RNA targeting. Thus, RNA-binding resulted in virus inhibition due to the lack of protein translation as the viral genome replication was blocked, and not due to genome cleavage (T. Zhang *et al.*, 2018). Although Fncas9 exhibited virus interference, the type VI CRISPR/Cas13 systems have also been employed to directly cleave RNA virus genomes for virus inhibition *in planta*.

The CRISPR/LshCas13a system was harnessed to mediate virus interference against the RNA turnip mosaic virus (TuMV) *in planta* (Aman, Ali, *et al.*, 2018). For convenient assessment of virus interference, a recombinant TuMV expressing the green fluorescence protein (*GFP*) reporter gene was used. In order to target TuMV-GFP, four gRNAs were designed which targeted two regions in *GFP* (GFP1 and GFP2), one in the helper component proteinase silencing suppressor (*HC-Pro*) gene and one in the coat protein (*CP*) gene. Expression of the gRNAs was achieved by engineering the RNA2 genome of tobacco rattle virus (TRV) to transiently and systemically express them under the pea early browning virus (PEBV) promoter. Transient assays in plants with gRNAs HC-Pro and GFP2 showed a 50% reduction in GFP signal levels in the systemic leaves, while the gRNAs targeting CP and GFP1 showed low but detectable reductions in GFP signal, compared to the control. *N. benthamiana* plants constitutively expressing the *Cas13a* gene exhibited results consistent with the transient assays, where a 50% reduction in GFP signal was observed with HC-Pro and GFP2, while CP and GFP1 exhibited only moderate reductions in GFP levels (Aman, Ali, *et al.*, 2018). Similarly, CRISPR/LshCas13a was used to assess RNA interference in the model plant *A. thaliana*, by providing durable and heritable virus interference against TuMV-GFP (Aman, Mahas, *et al.*, 2018). The same gRNAs; HC-Pro, CP, GFP1 and GFP2, were delivered and systemically

expressed via the TRV system. Congruently, HC-Pro and GFP2 resulted in the most efficient virus interference, compared to the non-specific (ns)-gRNA controls. These two studies demonstrate the potential of using CRISPR/Cas13a as an antiviral strategy to crop-threatening viruses (Aman, Mahas, *et al.*, 2018).

One study sought to develop resistance against GLRaV-3 using two CRISPR/Cas systems in grapevine (Jiao *et al.*, 2022). Using the Cas protein variants; namely FnCas9 and LshCas13a, efficient CRISPR-induced GLRaV-3 interference was obtained by *Agrobacterium*-mediated transient expression for *in vitro* grapevine plantlets. Expression levels of *FnCas9* and *LshCas13a* were positively correlated with GLRaV-3 inhibition, and LshCas13a virus interference was more efficient than FnCas9. CRISPR/FnCas9 targeting of the *Hsp90h* gene resulted in efficient virus inhibition, while CRISPR/LshCas13a targeting of *Hsp70h* and *CP* genes produced the highest virus inhibition, compared to the other gRNAs. Resultantly, the RNase activity of LshCas13a portrayed better virus targeting than FnCas9, which depended on RNA binding and not cleavage ability (Jiao *et al.*, 2022).

The introduction of a Cas13 nuclease and precise gRNA into plants can act as an antiviral immune response (Aman, Ali, *et al.*, 2018; Mahas, Aman and Mahfouz, 2019; T. Zhang *et al.*, 2019). Conversely, it has been reported that in the absence of Cas13, the gRNA alone can elicit reductions in viral and endogenous plant RNA (Sharma *et al.*, 2022). This guide-induced gene silencing (GIGS) was found to be dependent on sequence similarity of the crRNA and the target RNA, while the Argonaute protein(s) of the endogenous RNAi pathway control functionality. The discovery of GIGS provides a new avenue for targeted RNA reduction (Sharma *et al.*, 2022). The Cas13a variants, LbaCas13a and LbuCas13a, were used for TuMV-GFP targeting in *N. benthamiana*. When Cas13a was present, viral reduction of up to 90% was observed, with single or multi-guide crRNAs. Additionally, it was observed that in the absence of Cas13a, viral accumulation was still inhibited, specifically with the multi-guide (Sharma *et al.*, 2022). GIGS was found to function systemically, with the single-guide 2 and the multi-guide resulting in the highest viral interference (90%), while single-guide 1 and 3 caused only 30 to 40% reduction in TuMV levels. It was reasoned that GIGS functioned through components of RNAi, as there was an abundance of small RNAs (sRNAs) present, which had a corresponding sequence to the target RNA (Sharma *et al.*, 2022).

2.5.2.2 CasRx virus interference

To assess CasRx-mediated virus interference in *N. benthamiana* against TuMV-GFP, gRNAs targeting genes *HC-Pro* or *GFP* were employed (Cao *et al.*, 2021). gRNA expression was achieved using either the *A. thaliana* small nuclear RNA U6 (AtU6) promoter, or using the TRV delivery (Aman, Ali, *et al.*, 2018). Imaging and molecular analysis of GFP signals showed a significant decrease in TuMV-GFP RNA and proteins (Cao *et al.*, 2021). The CasRx-antiviral system was also tested on ssRNA plant viruses from different families, namely TMV and CMV. Consistently, as with TuMV-GFP, attenuation of both TMV-GFP and CMV-GFP infection was observed (Cao *et al.*, 2021). Thus, CasRx-mediated virus interference was achieved when targeting TuMV, TMV and CMV, establishing an efficient RNA virus interference system (Cao *et al.*, 2021).

In order to identify robust Cas13 RNA interference *in planta*, nine different variants were analysed (Mahas, Aman and Mahfouz, 2019). For optimum activity, either a stabiliser was fused to the Cas13 variant, or a subcellular localisation signal. Localisation was controlled by adding either an NLS or NES to the Cas13 protein. In transient assays, the TMV-RNA-based overexpressing GFP (TRBO-G) system was targeted, and the TRV-based expression system was employed to express the gRNAs targeting *GFP* or the replicase genes. The variants LwaCas13a-NLS, LwaCas13a-NES, and PspCas13b-NES exhibited efficient interference against the TRBO-GFP virus. However, the highest interference levels against TRBO-GFP was observed with CasRx, specifically CasRx-NES. Notably, when the protein levels of CasRx-NES and CasRx-NLS were compared, CasRx-NES levels were significantly lower than CasRx-NLS. However, the interference activity of CasRx-NES was still more robust than CasRx-NLS, demonstrating the importance of the localisation signal for Cas13 TuMV interference, as TuMV replicates in the cytoplasm (Mahas, Aman and Mahfouz, 2019). *N. benthamiana* plants stably-expressing the *Cas13* gene corroborated this data, where plants overexpressing the CasRx variant exhibited the highest virus interference, as well as high specificity to the targeted virus. When two non-competing RNA viruses were coinfected together, CasRx was also able to target both viruses simultaneously, indicating that CasRx activity is highly specific and does not possess collateral activity *in planta* (Mahas, Aman and Mahfouz, 2019).

Sweet potato virus disease (SPVD), which results from the synergistic co-infection of two RNA viruses, is a devastating disease affecting sweet potato, with yield loses of 80-90% observed in infected plants (Karyeija, Gibson and Valkonen, 1998; Bednarek *et al.*, 2021). A study was

conducted which aimed at establishing virus resistance in sweet potato using the CRISPR/Cas13 system (Yu *et al.*, 2022). Firstly, when the CmYLCV promoter replaced AtU6 for gRNA expression, CasRx showed the highest RNA interference activity, as opposed to when driven by the AtU6 promoter (Aman, Ali, *et al.*, 2018; Mahas, Aman and Mahfouz, 2019). This observation demonstrates that gRNA expression levels are correlated with RNA targeting efficiency in plants. LwaCas13a and CasRx were found to have the highest interference activity against TuMV-GFP, and both Cas13 variants exhibited multiple virus targeting abilities when also targeting CMV along with TuMV (Yu *et al.*, 2022). As SPCSV-RNase3 abolishes RNAi mechanisms in the host, rendering it unable to combat viral infection, the LwaCas13a system was used to target the SPCSV-*RNase3* gene. LwaCas13a activity successfully recovered the RNAi defense activity in host cells, and furthermore, transgenic *N. benthamiana* expressing an RNase3-targeted LwaCas13a system portrayed enhanced virus resistance against TuMV-GFP and CMV-RNase3 co-infection. Finally, transgenic sweet potato plants expressing the CasRx system targeting RNase3 exhibited substantial resistance to SPVD, demonstrating that CRISPR/Cas13 possesses the ability to develop SPVD-resistant crops (Yu *et al.*, 2022).

The CRISPR/CasRx system offers abundant potential for controlling plant viruses, but in order to achieve efficient and robust genome editing, the delivery and expression of the respective CRISPR components in plant cells is important (Kuluev *et al.*, 2019). This poses a significant bottleneck experienced among scientists, specifically for HDR events (Baltes *et al.*, 2014). In plant cells, homologous DNA templates are necessary for the HDR pathway to precisely and accurately repair DNA (Vu *et al.*, 2020). However, low amount of homologous template DNA at the DNA breakage site will result in low frequencies of HDR (Baltes *et al.*, 2014). Thus, the correct strategies for the delivery of CRISPR components and template DNA are important for achieving efficient genome editing.

2.6 DELIVERY SYSTEMS FOR CRISPR/Cas COMPONENTS

For the delivery of CRISPR/Cas cargo into plant cells, there are different forms of “packaging” which exist: i) DNA plasmids which encode the Cas protein and gRNA, ii) in vitro transcripts (IVTs) that upon delivery are expressed *in planta*, and iii) RNP complexes, which are composed of a Cas protein and gRNA (Ran, Liang and Gao, 2017; Liang *et al.*, 2018). There are two main groups of delivery methods: i) indirect delivery – the introduction of a plasmid-carrying gene construct by

bacteria (*Agrobacterium tumefaciens* or *Agrobacterium rhizogenes*) or viruses (TRV and geminiviruses), and ii) direct delivery – bypassing the use of other biological organisms as mediators for delivery, such as protoplast transfection or biological ballistics (biolistics) delivery (Ran, Liang and Gao, 2017). The common methods used for transformation are *Agrobacterium*-mediated, protoplast transfection, biolistic delivery and virus-based delivery (Fig. 2.7) (Ran, Liang and Gao, 2017).

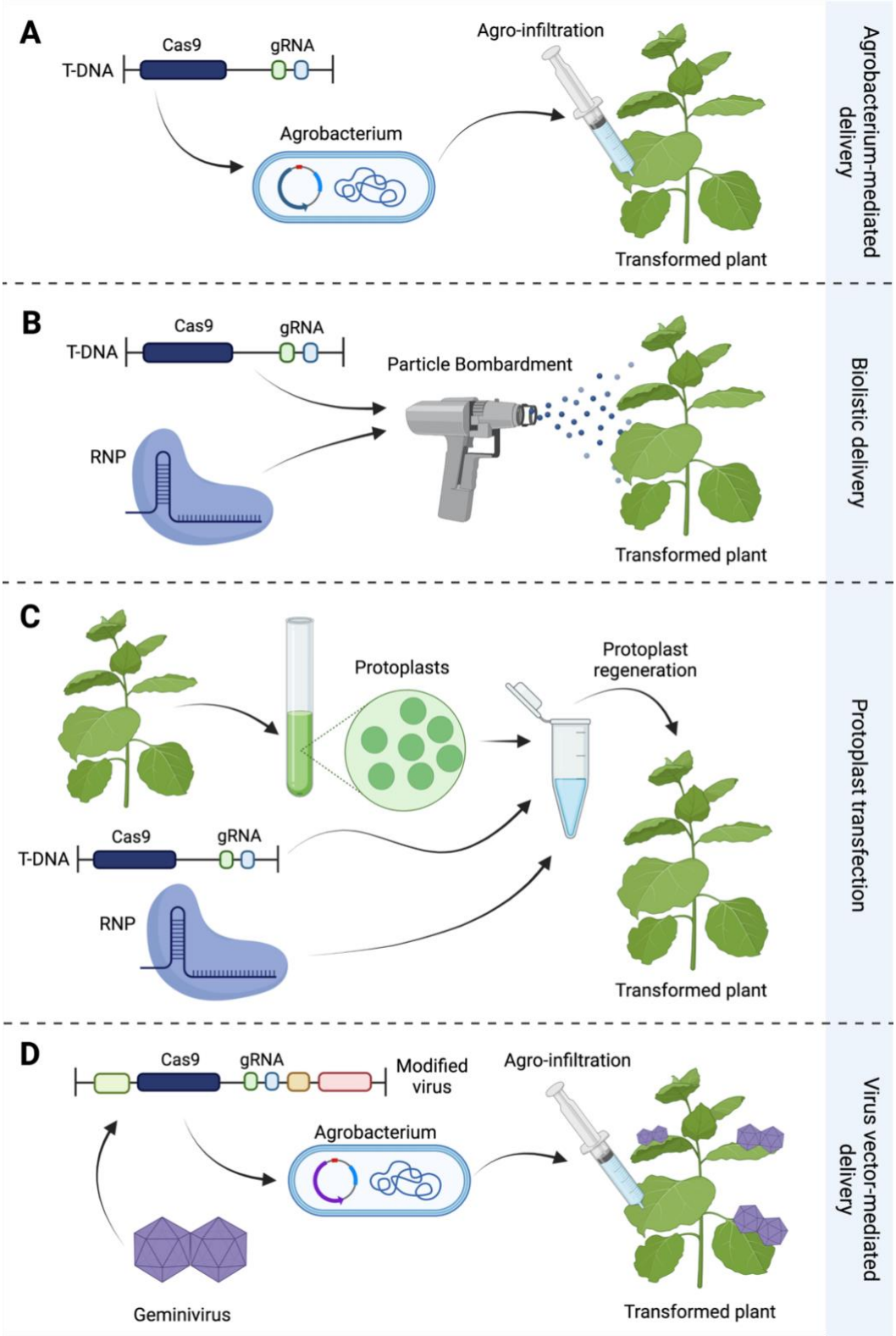

Figure 2.7. Delivery systems for CRISPR/Cas components. **A**) *Agrobacterium*-mediated delivery. The T-DNA is modified to contain *Cas9* and a gRNA. Agro-infiltration is performed to transform a model plant with *Agrobacterium* harbouring the modified CRISPR/Cas9 construct. **B**) Biolistic delivery. The plasmid containing the T-DNA sequence harbouring *Cas9* and a gRNA, or a ribonucleoprotein (RNP), are coated onto microprojectiles and bombarded onto the sample. **C**) Protoplast transfection. Protoplasts are prepared and incubated with polyethylene glycol (PEG), along with either the plasmid containing the T-DNA sequence harbouring *Cas9* and a gRNA, or an RNP, and then regenerated on selective media. **D**) Virus

vector-mediated delivery. A modified and reconstructed virus containing *Cas9* and a gRNA are Agro-infiltrated into a model plant, where the virus begins replicating and expressing the CRISPR components.

2.6.1 Agrobacterium-mediated delivery

Agrobacterium-mediated gene transfer (Fig. 2.7A) is used in both transient and stable expression approaches for gRNA and *cas* gene delivery, and is the most common method for delivery of genome editing constructs in a broad range of model plants as well as crops (Ran, Liang and Gao, 2017; Sandhya *et al.*, 2020). Transient *Agrobacterium*-mediated assays involve Agro-infiltration, where transgenes are expressed transiently *in planta*, from binary vectors without integration of T-DNA (Kuluev *et al.*, 2019). The stable expression of transgenes is achieved by *A. tumefaciens* inserting the T-DNA from the binary vector into the host genome, resulting in constitutive expression of the transgenes (Kuluev *et al.*, 2019). Some drawbacks exist with this *Agrobacterium*-mediated delivery: i) not all plant species can be transformed with *A. tumefaciens* – such as recalcitrant crops (monocots in particular and woody crops), ii) foreign DNA integration into the host genome (which may impede commercialisation), and iii) stable integration results in extended expression of the CRISPR constructs which may increase off-target frequency (Kalinina *et al.*, 2020). However, *Agrobacterium*-mediated delivery results in high efficiency transformation, is broadly applicable and easily available, while less costly than other methods (Sandhya *et al.*, 2020).

2.6.2 Biolistic delivery

Biological ballistics (biolistics) is the method of bombarding cells with microcarriers such as gold, silver or tungsten microprojectiles which have been coated with DNA or an RNP, using a “gene gun” or “biolistic gun” (Fig. 2.7B) (Ran, Liang and Gao, 2017; Sandhya *et al.*, 2020). A gene gun machine delivers the DNA into the cell by penetrating the cell wall, followed by regeneration of the treated tissue (Kalinina *et al.*, 2020). Successful biolistic bombardment of preformed Cas:gRNA RNP complexes into maize and wheat cells allowed for the regeneration of DNA-free genome edited plants (Svitashev *et al.*, 2016; Ran, Liang and Gao, 2017). Bombardment of RNP complexes is a popular method, as it does not result in insertions of foreign DNA (DNA-free), and the chance of off-targets is reduced because of the limited time the RNPs are active (Kalinina *et al.*, 2020; Sandhya *et al.*, 2020).

2.6.3 Protoplast transfection

Some plant systems have exhibited successful transformation with CRISPR/Cas reagents by protoplast transfection, such as tobacco, potato, and lettuce (Ran, Liang and Gao, 2017). Protoplast transformation is achievable with DNA, RNAs, or RNP complexes, allowing for DNA-free gene editing (Fig. 2.7C) (Kalinina *et al.*, 2020). A drawback of this method is the laborious regeneration of viable plants from transformed protoplasts, as protocol optimisation is often dependent on plant species and cultivar (Kalinina *et al.*, 2020). Protoplast transfection is attainable through polyethylene glycol (PEG)-mediated delivery (Sandhya *et al.*, 2020). The protoplasts, PEG solution at the required concentration, and either a plasmid containing the Cas9 and gRNA cassette, or an RNP, are incubated together, followed by protoplast regeneration on suitable media (Lowder *et al.*, 2015; Sandhya *et al.*, 2020).

2.6.4 Virus vector-mediated delivery

The exploitation of plant viruses as autonomous replicating vectors used for the expression of recombinant proteins has been done for more than 30 years (Cody and Scholthof, 2019). More recently, genome editing components are being delivered by modified plant viruses into plant cells, where both DNA and RNA viruses are being exploited as CRISPR/Cas reagent vehicles (Fig. 2.7D) (Baltes *et al.*, 2014; Yin *et al.*, 2015; Gil-Humanes *et al.*, 2017; Shan-E-Ali Zaidi and Mansoor, 2017; Kalinina *et al.*, 2020). TRV has been harnessed for the delivery of gRNAs alone, and not Cas proteins, due to their inability to express large proteins (Ali, Abul-Faraj, *et al.*, 2015). TRV has a bipartite genome, TRV-RNA1 and TRV-RNA2, where the latter is amenable to carry the gRNA, which is expressed under the strong viral promoter PEBV (Kuluev *et al.*, 2019). As the cargo capacity of geminiviruses is limited, conversion into non-infections systems (replicons) by removal of the CP and MP allows for increased capacity for foreign expression cassettes harbouring the *cas* gene and gRNA sequences (Čermák *et al.*, 2015). Geminivirus-based replicons (GVRs) are attractive vehicles for CRISPR/Cas reagent delivery due to their rolling-circle replication mechanism. This results in high copy numbers and ultimately high editing efficiency, though limited to the inoculated leaf area as replacement of the MP does not allow for systemic spread (Kalinina *et al.*, 2020).

2.7 GEMINIVIRUS-BASED DELIVERY OF CRISPR/Cas COMPONENTS

Geminiviruses, from the family *Geminiviridae*, have a small genome of roughly 2.8 kb (Shan-E-Ali Zaidi and Mansoor, 2017). These viruses are widespread and have the ability to infect a number of plant species, such as major crops as well as ornamental plants and common weeds (Rey *et al.*, 2012). There are four features of geminiviruses which make them attractive for genome editing: i) the ability to infect a number of plant species (monocotyledonous and dicotyledonous), ii) only the replication associated protein, Rep, is necessary to initiate replication in the host cell, expressed under either its natural promoter or constitutive/inducible promoters, iii) replicate within the host cell by rolling circle replication and homologous recombination-dependent replication, and iv) high amounts of replicons are produced due to efficient replication (Hanley-Bowdoin *et al.*, 2013; Baltes *et al.*, 2014; Richter *et al.*, 2016). Due to the small genome size, cargo capacity is limited in these viruses. To combat this, genes involved in cell-to-cell movement and infection can be replaced with the desired transgenes, resulting in the conversion of the vectors into non-infectious replicons (Shan-E-Ali Zaidi and Mansoor, 2017). By removing the CP and MP coding sequences, geminivirus vectors have been harnessed for the delivery of genome editing cassettes in plants (Shan-E-Ali Zaidi and Mansoor, 2017).

2.7.1 Geminivirus genome assembly and replication mechanism

BeYDV is a small ambisense single strand DNA (ssDNA) virus, belonging to the genus *Mastrevirus*, family *Geminiviridae* (Baltes *et al.*, 2014). In Fig. 2.8, the genome organisation and replication mechanism of a geminivirus vector is depicted.

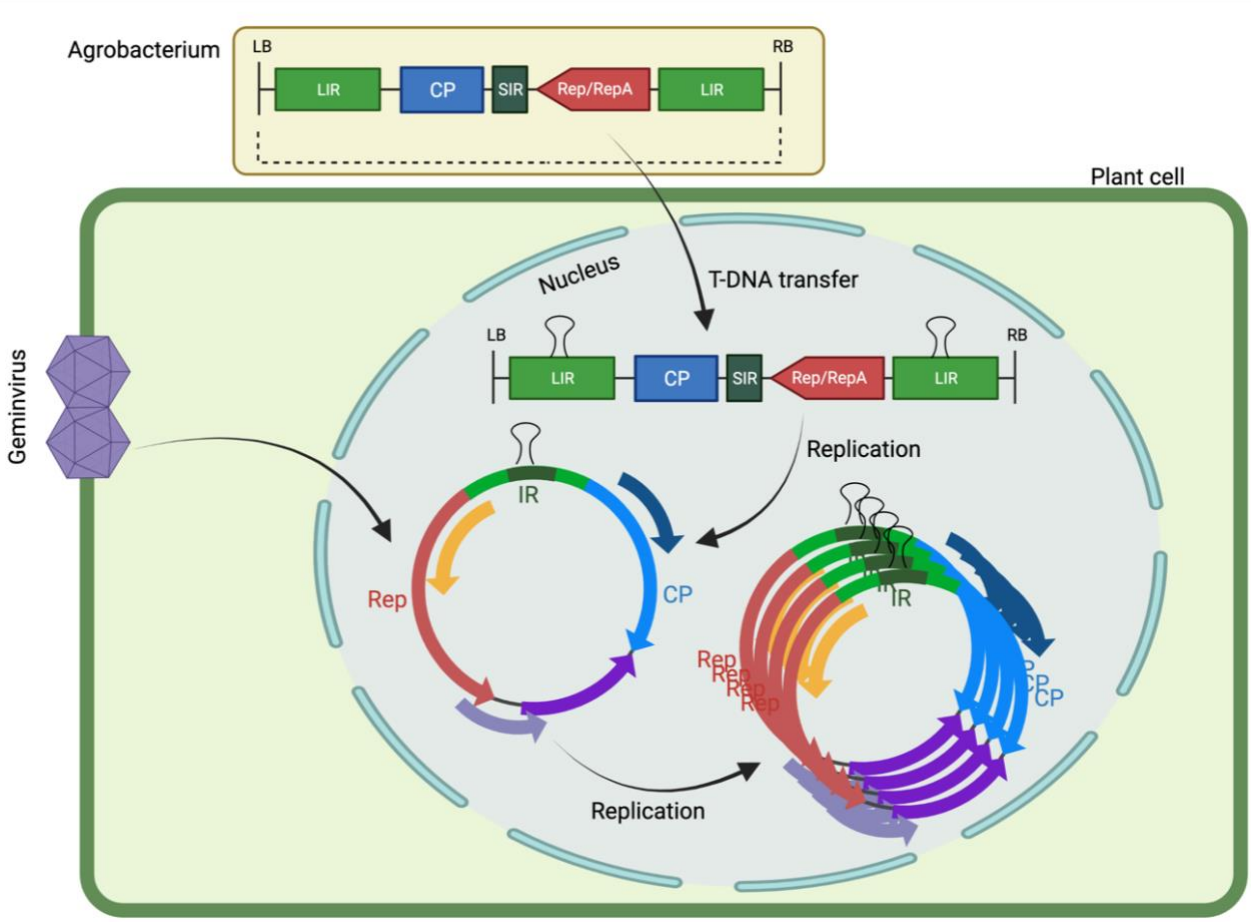

Figure 2.8. A schematic representing the simplified genome organisation of the wild-type geminivirus and the T-DNA assembly of a geminivirus replicon (GVR) vector from a binary plasmid. Upon entry into the nucleus of the plant cell, the rolling-circle replication mechanism of the virus results in high copy numbers.

Following entry into the host cell's nucleus, the host DNA polymerases converts the ssDNA virus into a double-stranded intermediate, which becomes the template for transcription of viral genes and rolling circle amplification (Baltes *et al.*, 2014). Rolling circle amplification is carried out by the Rep/RepA proteins, along with host-encoded proteins, yielding high amounts of expressed recombinant protein (Hefferon and Dugdale, 2003). There are three viral elements necessary for the replication of BeYDV; the long intergenic region (LIR) (*cis*-acting), the short intergenic region (SIR) and the replication-initiation protein (Rep) and replication-associated proteins (RepA) (Baltes *et al.*, 2014). Transcriptional promoters and the viral origin of replication are located in the LIR, while the SIR contains the binding site for complementary strand DNA synthesis as well as transcription termination signals. BeYDV has been 'deconstructed' into an expression vector by retaining genes necessary for virus replication only. All BeYDV vector constructs are designed to be bordered by duplicate copies of the LIR, subsequently when *A. tumefaciens* delivers the T-

DNA to the host cell's nucleus, this allows the replicational release and re-circularisation of the active BeYDV vector form (Regnard *et al.*, 2010).

2.7.2 Geminivirus-based replicons (GVRs) for genome editing

The readily available SSNs for genome editing in plants has revolutionised targeted modifications, such as gene knockout or gene knock-in (gene replacement or targeting) (Eini *et al.*, 2022). When CRISPR/Cas technology is applied for genome editing in plants, the two DNA repair mechanisms – NHEJ and HDR – are activated to repair the DSB (Fig. 2.2). However, there is a bias towards the NHEJ mechanism, as NHEJ is active throughout the cell cycle (except for during mitosis), whereas HDR is active only during the late S and G2 phases of the cell cycle (Orthwein *et al.*, 2015). Another limitation resulting in the low efficiency of HDR is due to the low copy number of template DNA delivered into the plant cells which is necessary for gene replacement to occur as the DSB is repaired (Baltes *et al.*, 2014). This limitation can be addressed with GVRs (Fig. 2.8) (Eini *et al.*, 2022).

GVRs have been successfully used to deliver genome editing constructs in model plants such as *N. benthamiana* and *Nicotiana tabacum* (Baltes *et al.*, 2014; Yu *et al.*, 2020; Eini *et al.*, 2022), and crop plants such as tomato, potato, wheat and cassava (Butler *et al.*, 2015, 2016; Čermák *et al.*, 2015; Gil-Humanes *et al.*, 2017; Hummel *et al.*, 2018; Vu *et al.*, 2020). The major studies which harnessed geminivirus vectors for genome editing are highlighted in Table 2.1.

Table 2.1. Geminivirus-replicon (GVR)-based delivery of genome editing components for gene targeting (knock-out) or gene transfer (knock-in) in plants.

Virus genus	Virus name	Plant species	Gene of interest	Type of genome editing	Replication-associated gene	Purpose	Reference
Mastrevirus	Bean yellow dwarf virus (BeYDV)	*N. tabacum*	Acetolactate synthase (*ALS*)	Gene mutation and gene transfer	*Trans*-acting	Using GVRs to deliver SSNs to generate DNA changes across plant species.	(Baltes *et al.*, 2014)
		Tomato (*S. lycopersicum*)	Anthocyanin mutant 1 (*ANT1*)	Gene transfer	*Cis*-acting	GVRs used to create heritable modifications to the tomato genome at high frequencies, using CRISPR/Cas9.	(Čermák *et al.*, 2015)
			Carotenoid isomerase (*CRTISO*) and phytoene synthase 1 (*PSY1*)	Gene mutation and gene transfer		CRISPR/Cas9 system, along with a GVR delivering template DNA, resulted in high frequencies of gene transfer in tomato plants.	(Dahan-Meir *et al.*, 2018)
			Anthocyanin mutant 1 (*ANT1*), High-affinity K^+ transporter 1;2 (*HKT1;2*)	Gene transfer		CRISPR/LbCas12a used with a multi-replicon system for knock-in gene transfer to target a salt-tolerance.	(Vu *et al.*, 2020)
		Potato (*Solanum tuberosum* L.)	Acetolactate synthase1 (*StALS1*)	Gene mutation	*Trans*-acting	SSNs for targeted mutagenesis in diploid and tetraploid potato plants.	(Butler *et al.*, 2015)
			Acetolactate synthase1 (*StALS1*)	Gene transfer	*Trans*-acting (Constitutively expressed)	GVR's ability to express SSNs and repair templates for gene targeting, to confer reduced herbicide susceptibility.	(Butler *et al.*, 2016)
		Cassava (*Manihot esculenta*)	5-enolpyruvylshikimate-3-phosphate synthase (*EPSPS*)	Gene mutation and gene transfer	*Cis*-acting	CRISPR/Cas9 editing and template delivery with GVR increased glyphosate tolerance, but GVR was found to be unfavourable in cassava and therefore T-DNA resulted in efficient editing events.	(Hummel *et al.*, 2018)

		Grapevine (*Vitis vinifera*)	Auxin induced in root culture 12 (*AIR12*), sugars will eventually be exported transporter (*SWEET4*), lesion initiation 2 (*LIN2*), dimerisation partner-e2f-like 1 (*DEL1*)	Gene transfer	*Cis*-acting and *Trans*-acting (Constitutively expressed)	CRISPR/Cas9 was used to target the grapevine fungal susceptibility genes by gene transfer, where one *VviDEL1* double-cut edited line exhibited efficient resistance to powdery mildew infection.	(Olivares *et al.*, 2021)
	Wheat dwarf virus (WDV)	Rice (*Oryza sativa*)	Actin-1 (*ACT1*), glutathione S-transferase (*GST*)	Gene transfer		GVRs were used for efficient and abundant deliver of template DNA into rice cells for gene targeting.	(Wang *et al.*, 2017)
		Wheat (*T. aestivum* cv. Bobwhite)	Ubiquitin (*Ubi1)*	Gene targeting and gene transfer	*Cis*-acting	Development of a GVR system for genome editing cereal crops. Gene-targeted integration in all three homoeoalleles (A, B and D) of the hexaploidy wheat genome was achieved at frequencies of ~1%.	(Gil-Humanes *et al.*, 2017)
Begomovirus	Cabbage Leaf Curl virus (CaLCuV)	*N. benthamiana* (overexpressing *Cas9*)	Phytoene desaturase (*NbPDS*), *NbIspH*	Gene targeting	*Cis*-acting (MP *trans*-acting)	Virus-based guide gRNA delivery into *N. benthamiana* overexpressing *Cas9*, and resulted in photo-bleached phenotype of newly developed leaves.	(Yin *et al.*, 2015)
	Sweet potato leaf curl virus (SPLCV)	*N. benthamiana*, 16c *N. benthamiana*	Phytoene desaturase (*NbPDS1*), Green fluorescence protein (*mGFP5*)	RNA targeting and gene targeting	*Cis*-acting	SPLCV-replicon system successfully delivered CRISPR components in model plants for both RNA targeting and gene editing.	(Yu *et al.*, 2020)
Curtovirus	Beet curly top virus (BCTV)	*N. benthamiana*, 16c *N. benthamiana*	Phytoene desaturase (*PDS*), Green fluorescence protein (*mGFP5*)	Gene targeting and gene transfer	*Trans*-acting	CRISPR/Cas12a delivered using the GVR for efficient gene mutation and gene transfer (*GFP* to *YFP*), when compared to conventional T-DNA agroinfiltration.	(Eini *et al.*, 2022)

Briefly highlighting some studies from Table 2.1; template DNA delivery has been achieved with BeYDV in tobacco and tomato plants, and with wheat dwarf virus (WDV) in wheat and rice (Baltes *et al.*, 2014; Čermák *et al.*, 2015; Gil-Humanes *et al.*, 2017; Wang *et al.*, 2017). Alternatively, one study used BeYDV to transiently deliver both SSNs (ZFNs, TALENs and CRISPR/Cas) and DNA repair templates for gene mutation (NHEJ) and gene transfer (HDR) in *N. tabacum*, and gene targeting frequencies were increased by one to two orders of magnitude when compared to conventional *A. tumefaciens* T-DNA (Baltes *et al.*, 2014). Another study showed tenfold higher targeting frequencies than regular T-DNA delivery, when a strong promoter was inserted upstream of a gene controlling anthocyanin biosynthesis, and these modifications proved to be precise and heritable (Čermák *et al.*, 2015). Heritable gene mutations were detected in callus and stable events when BeYDV delivered Cas9 and a gRNA into potato (*S. tuberosum*) (Butler *et al.*, 2015). In tomato (*S. lycopersicum*), a BeYDV GVR was used for efficient gene transfer, where it expressed TALEN and CRISPR/Cas9 editing systems, along with a *cis*-acting *REP* gene (Čermák *et al.*, 2015). A study by Olivares and colleagues employed BeYDV for the delivery of CRISPR/Cas9 machinery, along with a paired gRNA, to increase fungal tolerance in grapevine. Preliminary phytopathological behavior indicated one double-cut edited line, *VviDEL1*, which showed increased tolerance to mildew infection (Olivares *et al.*, 2021).

A vector based on the mild strain of BeYDV (BeYDV-m) was constructed as an expression shuttle vector, to allow for high yields of transiently expressed proteins (Regnard *et al.*, 2010). The distinguishing factor between the design of the vector, pRIC, and other common BeYDV vectors, is that the transgene does not replace the *REP* gene, but rather the *MP* and *CP* genes, rendering the vector unable to move systemically, but providing a *cis*-replicating gene expression shuttle vector (Halley-Stott *et al.*, 2007; Regnard *et al.*, 2010). Transient cytoplasmic expression of the transgene from the novel pRIC vector and the high-expressing non-replicating pTRac vector were compared in *N. benthamiana* to analyse the vector efficacy (Maclean *et al.*, 2007). There was an evident improvement of 1.5- to 7-fold increase in protein expression when pRIC was compared to the non-replicating pTRAc vector (Regnard *et al.*, 2010). The pRIC vector has expanded the possibilities of enhanced transgene expression, and also provided more opportunity for such expression in various plant types due to BeYDV's wide host range (Pietersen *et al.*, 1997; Halley-Stott *et al.*, 2007). Implementation of the pRIC vector for CRISPR/Cas strategies may pave the way for high efficiency genome editing in plants, due to the high expression of *Cas9* and the gRNA,

which have been found to be correlated with editing efficiency (Jiao *et al.*, 2022). Still, in order to quantify the editing efficiency of CRSPR/Cas studies, certain systems and methods are necessary to extrapolate meaningful results of successful editing events.

2.8 MUTATION PATTERNS AND EDITING INFERENCE

The action of modifying plant genomes is an ancient practice; where selective breeding was initially used, followed by mutagenesis and transgenesis, and subsequently the more recent genome editing practices (Weeks, Spalding and Yang, 2016). The latter method is favourable as random mutation events are avoided by the use of SSNs which introduce DSBs at the specific target site (Zhu *et al.*, 2017). The NHEJ repair system creates indels at the DSB site, while HDR requires a donor template with homologous ends to each border of the target site, resulting in more precise repair mechanisms (Fig. 2.2) (Zhu, Li and Gao, 2020). Mutation frequencies vary depending on nuclease-specific factors; such as the nuclease, target site sequence, and cleavage pattern, as well as target genome factors; such as size, GC content or repetitive DNA content (Zhu *et al.*, 2017).

2.8.1 Mutation patterns caused by CRISPR/Cas in plants

Previously, it was believed that Cas9 resulted in random repair outcomes following the induction of a DSB (Molla *et al.*, 2022). However, the emergence of multiple novel studies indicates that the repair mechanism following NHEJ can be predicted, and is dependent on the target DNA sequence (Chakrabarti *et al.*, 2019; Molla and Yang, 2020). Studies have found that Cas9 cleavage commonly results in short indel mutations (<10 bp), predominantly single nts, with A/T insertions being preferential (Zhang *et al.*, 2014; Zhu *et al.*, 2017). These observations, in *A. thaliana*, rice, barley and *Brassica napus* (an oilseed crop), for example, all found that 1 bp insertions or short deletions were the predominant mutation caused by CRISPR/Cas9 cleavage (Li *et al.*, 2012; Feng *et al.*, 2014; Zhang *et al.*, 2014; Lawrenson *et al.*, 2015; Ma *et al.*, 2015; Yang *et al.*, 2017). The position of the mutation usually occurs at the Cas9 cut site, 3 bp upstream of the PAM sequence, where one study found that 91.3% of mutations occurred at this site (Jinek *et al.*, 2012; Yang *et al.*, 2017).

While the DSB site created by the CRISPR/Cas system can be precisely controlled, the overall efficiency of editing (% non-wild type) and genotypes induced within one experiment are highly variable and heterogeneous across cells, with DNA editing precision varying dramatically between

different targets sites of the same genome (Chakrabarti *et al.*, 2019). Thus, in order to quantify post-editing outcomes with meaningful results, the development of specific mutation analysis techniques is necessary (Clement *et al.*, 2019).

2.8.2 Editing inference strategies

Determining editing events with next-generation sequencing (NGS) provides sequence-level resolution with extreme sensitivity (Sentmanat *et al.*, 2018). However, NGS is not widely available, comes at a higher cost and has a slower turnaround time (Conant *et al.*, 2022). The more accessible Sanger sequencing has the drawback that the results are a convolution of all genotypes in the sample, suggesting the need for a computational tool which can infer individual sequences within the sample and provide significant editing inference (Conant *et al.*, 2022). Previous tools such as TIDE (Tracking of Insertions and Deletions) (https://tide.nki.nl/) and DECODR (Deconvolution of Complex DNA Repair) (https://decodr.org/) were used to infer convoluted Sanger data, but both tools exhibit drawbacks, such as the requirement of a license for batch processing (Brinkman *et al.*, 2014; Bloh *et al.*, 2021; Conant *et al.*, 2022).

Conant *et al*. (2022) present a tool called ICE (Inference of CRISPR Edits) (https://ice.synthego.com/#/) with an improved algorithm for the CRISPR editing community, which allows low- and high-throughput genotyping for Sanger data (Conant *et al.*, 2022). This software analyses both knockout (NHEJ) editing and donor-mediated editing (HDR) events. Genotypes derived from NGS and ICE were compared and found to have a high correlation, indicating that the ICE tool is a reliable substitute for editing inference (Conant *et al.*, 2022). However, the ICE software exhibits limitations, like only insertions and deletions are detected without the possibility of understanding the composition of the inserted nts. The local DNA sequence near the predicted cut site allows for the prediction of mutation patterns in plant cells (Molla and Yang, 2020). A study that employed three models, inDelphi (https://indelphi.giffordlab.mit.edu/), FORECasT (https://partslab.sanger.ac.uk/FORECasT) and SPROUT (https://zou-group.github.io/SPROUT), to predict the NHEJ mutation outcome in rice cells (Molla *et al.*, 2022), corroborated the findings of previous studies, where the –4 nt is identical to the inserted nt (Lemos *et al.*, 2018; Chakrabarti *et al.*, 2019; Molla *et al.*, 2022). This occurrence can be explained by the sequential events following Cas9-induced staggered cleavage; where the 5’ single-base overhang is filled in by DNA polymerase, by using the noncomplementary strand as

a template (Fig. 2.9) (Zuo and Liu, 2016; Lemos *et al.*, 2018; Molla and Yang, 2020; Molla *et al.*, 2022).

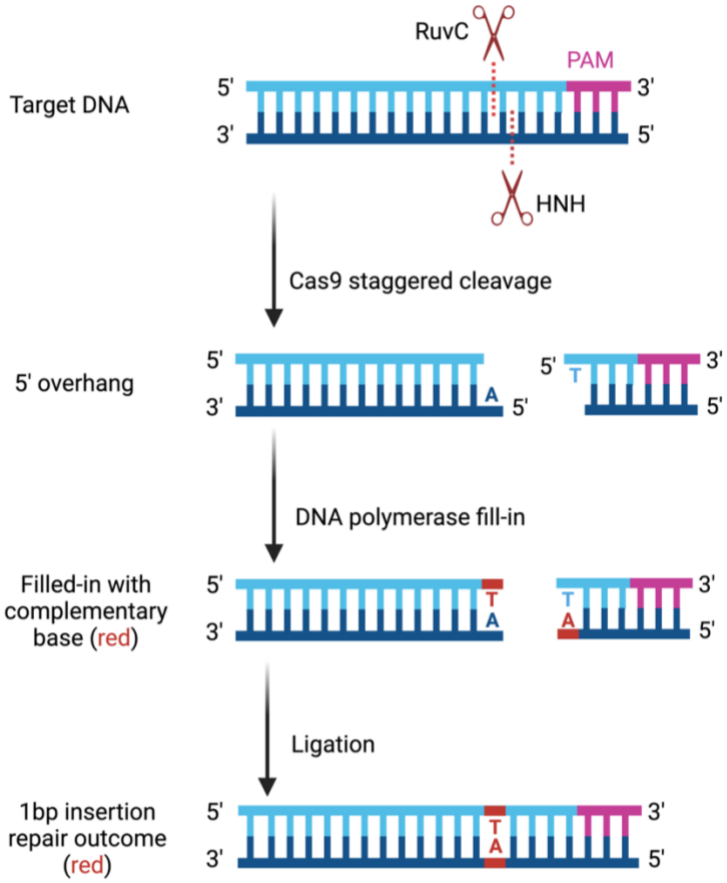

Figure 2.9. A schematic representing the sequence of events following Cas9 double strand break (DSB) cleavage in the target DNA. The RuvC and HNH nuclease domains of the Cas9 protein cleave the target DNA 3 base pairs (bps) upstream of the protospacer adjacent motif (PAM) sequence (pink), resulting in a in blunt and staggered cuts. The staggered cut is subsequently filled-in (red nt) with DNA polymerase and uses the non-complementary strand as a template (blue nt). Ligation with the ligase protein then joins the DNA, completing the repair process.

Through the development of software such as FORECasT and inDelphi, the predictability of NHEJ repair outcomes for precise indel generation in plants is greatly facilitated.

2.9 CONCLUSION

Productive and sustainable agriculture is constantly threatened by viral diseases worldwide (Rubio, Galipienso and Ferriol, 2020). Grapevine provides a large contribution to many regions' economic sectors, but is susceptible to over 80 viruses, with a majority being RNA viruses (Moriondo *et al.*, 2011). These viruses cause economically detrimental diseases, highlighting the

importance of a sustainable method to control them. The CRISPR/Cas technology offers a powerful alternative to classical plant breeding for trait improvement, and is a popular toolkit for plant genome editing due to its easy design, high efficiency and great flexibility (Kalinina *et al.*, 2020; Sandhya *et al.*, 2020). CRISPR/Cas13 systems exhibiting RNase activity have been exploited for the use of targeting RNA viruses *in planta.* Specifically, the CRISPR/CasRx system offers abundant potential for controlling plant viruses due to its efficiency and specificity as a nuclease. A major bottleneck in genome editing is the effective delivery and expression of CRISPR components in plant cells (Kuluev *et al.*, 2019). In order to overcome this bottleneck, viral vectors have been employed to act as vehicles for the efficient delivery of genome editing cassettes. Jointly, CRISPR/CasRx for virus interference *in planta* offers great potential for the control of RNA viruses, while the use of a geminivirus vector for the efficient delivery of genome editing components poses vast opportunities for targeted genome editing in plants.

CHAPTER 3: CRISPR/CasRx-mediated targeting of grapevine virus A

3.1 INTRODUCTION

Global agriculture is under constant threat by plant diseases, which result in decreased yields and reduced quality. Plant viruses are responsible for numerous plant diseases and cause around 50% of the observed yield losses (Anderson *et al.*, 2004; Boualem, Dogimont and Bendahmane, 2016). The development and implementation of virus-resistant plant varieties would be a robust and sustainable solution to control plant virus diseases and viral infections (Varanda *et al.*, 2021).

Grapevine is a major agricultural crop, which is cultivated globally and contributes to economic sectors worldwide, but is plagued by over 80 viruses (Fuchs, 2020). Grapevine virus A (GVA) is an RNA virus that replicates in the cytoplasm of the plant cell and is a member of the genus *Vitivirus* (Minafra, Saldarelli and Martelli, 1997; Martelli *et al.*, 2007; Rampersad and Tennant, 2018). GVA naturally infects grapevine, but is also able to infect the model plant *Nicotiana benthamiana*, making it a helpful model for the study of viruses in herbaceous plants (Goszczynski and Jooste, 2003). By utilising an infectious clone of GVA, which has been modified to contain a region of the endogenous *N. benthamiana* phytoene desaturase (*NbPDS*) gene (pBINSN_GVA118_NbPDS) (Du Preez, 2005), the establishment of an RNA virus-targeting system in *N. benthamiana* can be investigated.

CRISPR/Cas technology has provided a new approach to classical plant breeding approaches (Kalinina *et al.*, 2020). This technology has become popular within the scientific community due to its easy design, efficiency and flexibility, and has been harnessed to target both DNA and RNA viruses (Fig. 2.6) (Zaidi *et al.*, 2016; Freije *et al.*, 2019; Sandhya *et al.*, 2020). Virus interference with CRISPR can be achieved by directly targeting and cleaving the genome of the virus; where RNA-targeting CRISPR/Cas13 systems have become a popular technique for controlling RNA viruses in plants. A recent addition to the Cas13 subtypes, Cas13d, is smaller (less than 1000 aa, ~3 kb) than previous Cas13 effectors, while possessing efficient RNA interference abilities (Konermann *et al.*, 2018; Mahas, Aman and Mahfouz, 2019). The Cas13d variant from *Ruminococcus flavefaciens* (CasRx) has been harnessed for single-strand RNA (ssRNA)-targeting and is an effective approach for RNA virus interference *in planta* (Mahas, Aman and Mahfouz, 2019; Cao *et al.*, 2021). A study by Cao and colleagues used the CRISPR/CasRx system to

successfully target the coat protein (*CP*) gene of green fluorescent protein (GFP)-expressing RNA virus turnip mosaic virus (TuMV-GFP) *in planta* (Cao *et al.*, 2021). Similarly, one study found that when nine Cas13 variants were compared to determine their respective interference capabilities, the CasRx variant exhibited the most robust interference when the replicase gene of tobacco mosaic virus (TMV)-RNA-based overexpressing GFP (TRBO-G) system was targeted, as well as when various guide RNA (gRNA) targets of TuMV-GFP were targeted (Mahas, Aman and Mahfouz, 2019).

Effective delivery and expression of CRISPR components in plants is necessary to achieve efficient and robust genome editing (Kuluev *et al.*, 2019). Recently, the exploitation of plant viruses for the delivery of genome editing cassettes into plant cells has become popular, due to the easy manipulation of viral genomes and the ability of the virus to infect numerous plant species (Kalinina *et al.*, 2020). Specifically, the RNA virus tobacco rattle virus (TRV) has been modified for transient and systemic expression of gRNAs in plants, and is an efficient system as it allows for the empirical testing and validation of multiple gRNAs simultaneously (Ali, Abul-Faraj, *et al.*, 2015; Aman, Mahas, *et al.*, 2018).

A recent, novel discovery within the CRISPR/Cas13 system is that in the absence of Cas13, a gRNA alone can elicit reductions in viral and endogenous plant RNA (Sharma *et al.*, 2022). This mechanism, called guide-induced gene silencing (GIGS), was found to be dependent on sequence similarity of the gRNA and target RNA, and functions in a manner analogous to the endogenous RNA silencing or interference (RNAi) pathway. It was discovered that Argonaute protein(s) of the endogenous RNAi pathway control functionality of GIGS, and that an abundance of small RNAs (sRNAs) were present, which had corresponding sequence similarity to the target RNA (Sharma *et al.*, 2022). The discovery of GIGS provides a new avenue for targeted RNA reduction and virus interference methods in plants (Sharma *et al.*, 2022).

The aim of this chapter was to induce virus interference against GVA; by employing CRISPR/CasRx in *N. benthamiana*. Initially, the replicase gene of GVA was targeted, due to its essential role in virus replication and spread. *N. benthamiana* was stably transformed to express the replicase gRNA and *CasRx* gene. The regenerated transgenic plants were subsequently infected with pBINSN_GVA118_NbPDS. Relative quantification of GVA transcripts was assessed to establish

CRISPR/CasRx virus interference. Following unsuccessful virus interference when the replicase gene was targeted, new gRNA targets were designed against the *CP* gene of GVA. The CP gRNAs were assayed in two methods; namely transient and stable experiments. For transient experiments, wild-type *N. benthamiana* plants were co-infiltrated with a binary construct harbouring the *CasRx* gene and a gRNA (pCasRx:CP), and with pBINSN_GVA118_NbPDS. Transient experiments were performed as a preliminary test to validate gRNA efficiency. Stable experiments utilised transgenic *N. benthamiana* plants expressing the *CasRx* gene (hereafter referred to as CasRx-EMPTY plants), which were infiltrated with TRV-expression vectors harbouring a gRNA (pTRV2:CP), and with the GVA infectious clone. TRV was chosen as the delivery system for gRNAs in subsequent experiments because it allowed for multiple gRNAs to be assayed rapidly. Simultaneously, the occurrence of GIGS was assayed in the stable experiments. The first stable experiment was performed to assess RNA interference efficiency of individual CP gRNAs in CasRx-EMPTY plants. The second and third stable experiments were performed to assess CRISPR/CasRx virus interference when multiple gRNAs were present, as well as the effectiveness of GIGS at reducing GVA accumulation. Additionally, gRNA expression was quantified to compare expression levels from binary pCasRx:CP vectors and pTRV2:CP vectors.

3.2 MATERIAL AND METHODS

3.2.1 Design of gRNAs

To assess the capability of CasRx to successfully target viral RNA, three gRNAs were designed against the *CP* gene of GVA. The software cas13design (https://cas13design.nygenome.org/), which integrates the gRNA design rules stipulated in (Wessels *et al.*, 2020) and (Guo *et al.*, 2021), was used to design custom gRNAs. The input sequence for cas13design software was between 80-500 nucleotides (nts) in length, and putative gRNAs were selected based on their rank, guide score, quartile, and off-target hits. *N. benthamiana* off-targets were assessed against the *N. benthamiana* transcriptome (https://sefapps02.qut.edu.au/blast/blast_link2.cgi). The secondary structure of the CasRx scaffold sequence and gRNA [gaacccctaccaactggtcggggtttgaaacG(22-28nt target)] was assessed using the programs mFold (http://www.unafold.org/mfold/applications/rna-folding-form.php) and RNAfold (http://rna.tbi.univie.ac.at/cgi-bin/RNAWebSuite/RNAfold.cgi). The secondary structure of the target RNA was assessed with the same software, to ensure that the gRNA, specifically the seed region, were designed to target accessible (single-strand or looped) regions. The gRNAs were

designed to contain BbsI overhangs on their 5'-ends, for subsequent cloning with Golden Gate assembly. For cloning into the TRV2 vector, the gRNAs were designed to contain an XbaI overhang and CasRx scaffold sequence on their 5'-end and an XhoI overhang on their 3'-end (Supplementary Table 1).

3.2.2 Plasmids

Table 3.1. Plasmids confirmed with screening and used in subsequent experiments.

Plasmid name	Addgene plasmid #	Referred to as
pXR001:EF1a-CasRx-2A-EGFP	109049	pCasRx
pXR003:CasRx-gRNA-cloning-backbone	109053	pCasRx-backbone
pYL192	148968	pTRV1
SPDK3876 (TRV2-pPEBV-MCS)	149275	pTRV2

The plasmids mentioned in Table 3.1 were streaked-out onto solid Luria-Bertani (LB) medium containing the necessary selection (Bertani, 1951), and incubated at 37°C overnight. Single colonies were inoculated in 5mL liquid LB medium with selection, and incubated shaking at 37°C overnight. The following day, plasmid isolations were performed using a GeneJET Plasmid Miniprep Kit (Thermo Fisher Scientific, USA), following the manufacturer's instructions. The plasmid concentration was assessed using a Nanodrop 2000 spectrophotometer (Thermo Fisher Scientific, USA). The integrity of the plasmids pCasRx, pCasRx-backbone, pTRV1 and pTRV2 were confirmed by restriction enzyme digestion using the following NEB (USA) restriction enzymes; BamHI and PvuI, AseI, EcoRI-HF®, AseI and BamHI, respectively. Reactions were incubated at 37°C for 2 hrs, and visualised with agarose gel electrophoresis (1% w/v). The plasmid maps are available in Supplementary Figure 1.

3.2.3 Gibson assembly

Gibson Assembly (NEBuilder HiFi DNA Assembly Cloning Kit; NEB, USA) was used to modify the two intermediate vectors; pJJB308 (Addgene; plasmid #107699) and pJJB296 (Addgene; plasmid #107691,) following the manufacturer's protocol. The vectors pJJB308 and pJJB296 were digested in the following reactions: 1µg of DNA, 2µL 10x AarI Buffer (Thermo Fisher Scientific, USA), 0.4µL 50x AarI Oligos (Thermo Fisher Scientific, USA), 2U AarI (Thermo Fisher Scientific, USA), and dH_2O to a final volume of 50µL; and 1µg of DNA, 5µL 10X NEBuffer 3.1 (NEB, USA), 20U BamHI (NEB, USA), 10U HindIII (Thermo Fisher Scientific, USA), and dH_2O to a final volume of 50µL, respectively.

The reactions were incubated at 37°C overnight. A high-fidelity DNA polymerase (Phusion® High-Fidelity DNA Polymerase; NEB, USA) PCR was performed to amplify the desired fragments from gRNA backbone and CasRx using specific primers (Table 3.2).

Table 3.2. Primers used for cloning strategies, Sanger sequencing and RT-qPCR analysis.

Primer name	Sequence 5'-3'	Tm (°C)	Amplicon (bp)
gRNA_backbone_fwd	aagagcgcccacctgccaggggacGAGGGCCTATTTCCCATG	55.6*	302
gRNA_backbone_rev	gcttttcatcacctgcgtcaccggaaaAAAAAGGTCTTCTCGAAGAC	49.7*	
CasRx_fwd	acgggggactcccgacatggCCCAAGAAGAAGAGAAAG	46.2*	3000
CasRx_rev	aacacaaacttaagcacacaCACCTTCCTCTTTTTCTTAG	47.6*	
pJJB308-CasRx_F	GCTCACATGTTCTTTCCTGCG	56.7	510
pJJB308-CasRx_R	TCATCGCACATTTCCCCGAA	57.1	
CaMV-35S_F	ACGTAAGGGATGACGCACAA	56.1	3285
pJJB296-CasRx_R	GTCCGTCACCAGAGCTCTG	56.4	
CasRx_F	GGATTCAGCTCCGTCACCAA		N/A
CaMV-35S_F2	ACGTAAGGGATGACGCACAA	56.0	613
CasRx-screening_R1	CAGAGTTTCCTTCAGGCCGA	57.0	
TC430	GTTGGATCTCTTCTGCAGCA	55.0	820
M13F	GTAAAACGACGGCCAGT	51.7	
TRV2-confirm_F	CATAATTATACTGATTTGTCTCTCG	49.4	N/A
RTbent_actin_F	GTCCCTATACGCCAGT	50.3	216**
RTbent_actin_R	ACATCGCGGACAATTT	48.9	488***

*binding Tm
** cDNA
*** DNA
lower case nts: primer extension sequence

The PCR cycle conditions were set to: 98°C/30sec + 35 x (98°C/30sec + 60°C/30sec + 72°C/30sec) + 72°C/5min + 4°C hold, and 98°C/30sec + 35 x (98°C/30sec + 67°C/30sec + 72°C/30sec) + 72°C/5min + 4°C hold, respectively. The following bands were recovered after agarose gel electrophoresis; pJJB308 digestion (vector ~2017 bp) and pCasRx-backbone PCR (insert ~300 bp) (1% w/v); pJJB296 digestion (vector ~3.1kb) and pCasRx PCR (insert ~3kb) (0.5% w/v), using the ZymoClean Gel DNA Recovery Kit (Zymo Research, USA) following the manufacturer's instructions, and quantified as previously described. The purified insert and vector fragments were assembled using the NEBuilder HiFi DNA Assembly Cloning Kit (NEB, USA) according to the

manufacturer's instructions. Positive colonies were screened by end-point PCR with the primers pJJB308-CasRx_F/pJJB308-CasRx_R and CaMV-35S_F/pJJB296-CasRx_R respectively (Table 3.2), and the thermocycler conditions were set to: 95°C/2min + 25 x (95°C/30sec + 52°C/30sec + 72°C/1min) + 72°C/5mins + 4°C hold, for both reactions. The assembled vector pJJB308-CasRx-backbone was confirmed by Sanger sequencing at the Central Analytical Faculty (CAF; Stellenbosch University, SA) with the primers; pJJB308-CasRx_F/pJJB308-CasRx_R, and vector pJJB296-CasRx was confirmed with primers; CaMV-35S_F/CasRx-screening_R1 (~438 bp) and CasRx_F/pJJB296-CasRx-R (~891 bp) (Table 3.2).

3.2.4 gRNA cassette and intermediate vector assembly

The targets were ordered from IDT (Integrated DNA Technologies, USA) and synthesised as single strand DNA (ssDNA) oligonucleotides containing BbsI (NEB, USA) overhangs on the 5'-end. Adapter preparation consisted of annealing the ssDNA oligos in a reaction containing 1.5µL forward oligo (100µM), 1.5µL reverse oligo (100µM), 5µL 10X NEBuffer 2.1, and dH_2O to a final volume of 50µL. The forward and reverse oligo sequences can be found in Supplementary Table 1. The reactions were incubated at 95°C for 4 minutes, followed by 70°C for 10 minutes in a thermocycler. Reactions were then transferred to a beaker containing 1L of H_2O at 70°C and left to cool to room temperature. The pJJB308-CasRx-backbone was linearised with restriction enzyme BbsI (NEB, USA) in the following reaction: 1µg of DNA, 10U BbsI (NEB, USA), 5µL 10X NEBuffer 2.1, and dH2O to a final volume of 50µL. The digestion was incubated at 37°C overnight, and the linearised (~2.3kb) fragment was excised, purified, and quantified as previously described. A ligation reaction containing the annealed oligos (Supplementary Table 1) and linearised vector was set up using 1µL annealed oligos, 20ng linearised vector, 2µL 10X T4 DNA Ligase Buffer (Thermo Fisher Scientific, USA), 5U T4 DNA Ligase (Thermo Fisher Scientific, USA), and dH_2O to a final volume of 20µL. The ligation reaction was incubated at 4°C overnight, and 4µL of ligation reaction was used to transform DH5α chemically competent *E. coli* cells by heat-shock transformation. The cells were plated on selection plates containing 100µg/mL ampicillin, and incubated at 37°C overnight. Plasmid isolation performed as previously described, and assembled pJJB308-CasRx-gRNA intermediate vectors were confirmed with Sanger sequencing using the primers pJJB308-CasRx_F/pJJB308-CasRx_R (Table 3.2).

3.2.5 Golden Gate assembly of pCasRx constructs

A one-step Golden Gate assembly reaction was performed containing the assembled pJJB308-CasRx-gRNA vector, the assembled pJJB296-CasRx vector, intermediate module vector pMOD_C0000 (Addgene; plasmid #91081), and transformation backbone vector pTRANS_220d (Addgene; plasmid #91114). Additionally, for the assembly of the vector without a gRNA, the modified pJJB308-CasRx-backbone plasmid was used in the Golden Gate assembly reaction. The reaction was set up as stipulated in the paper by Čermák and colleagues (Čermák *et al.*, 2017). Briefly, the Golden Gate reaction was set up with pTRANS_220d (75ng), pJJB296-CasRx (150ng), pJJB308-CasRx-gRNA or pJJB308-CasRx-backbone (150ng), pMOD_C000 (150ng), 0.8µL AarI oligonucleotide (0.5µM) (Thermo Fisher Scientific, USA), 2U AarI (Thermo Fisher Scientific, USA), 5U T4 DNA Ligase (NEB), 2µL 10x T4 DNA ligase buffer, and dH_2O to a final volume of 20µL. The thermocycler conditions were set to: 10 x (37°C/5min + 16°C/10min) + 37°C/15min + 80°C/5min + 4°C hold. The reaction was transformed into NEB 5-α chemically competent *E. coli* cells using the High Efficiency Transformation Protocol (NEB, USA), with 5µL of the reaction. Selection plates containing 50µg/mL kanamycin were incubated at 37°C overnight. A colony PCR using the primers TC430/M13F (Table 3.2) screened for positive colonies with the following cycle parameters: 95°C/2min + 25 x (95°C/30sec + 52°C/30sec + 72°C/30sec) + 72°C/5mins + 4°C hold. Sanger sequencing with the primers TC430/M13F was used for confirmation of assembled vectors. The final plasmid maps are provided in Supplementary Figure 2.

3.2.6 pTRV2-gRNA vector assembly

The gRNAs for pTRV2 delivery were designed to contain the CasRx-scaffold sequence (5'-AACCCCTACCAACTGGTCGGGGTTTGAAACG-3') at the 5'-end, and gRNA sequence with poly-T-tail [5'-(gRNA sequence)TTTTTTTTT-3'] at the 3'-end, as well as XbaI and XhoI overhangs on the 5'- and 3'-end respectively (Supplementary Table 1). The targets were ordered and synthesised as ssDNA oligos, from IDT (Integrated DNA Technologies, USA). The oligos were phosphorylated using T4 Polynucleotide Kinase (Promega, USA), following the manufacturer's protocol. Briefly, the reaction contained 1µL of each oligo (100µM), 4µL of 10X Kinase Buffer (Promega, USA), 4µL ATP (1mM), 10U T4 Polynucleotide Kinase (Promega, USA), and dH_2O to a final volume of 40µL. The reaction was incubated in the thermocycler at 37°C for 30 minutes, followed by termination of the reaction at 70°C for 10 minutes. The phosphorylated oligos were annealed as previously described. The TRV2 vector was digested with XbaI and XhoI to allow for restriction-based cloning

of the annealed gRNAs. The vector was digested in the following reaction; 1µg of DNA, 5µL of 10X CutSmart Buffer (NEB, USA), 20U of XbaI (NEB, USA), 10U of XhoI (NEB, USA), and dH2O to a final volume of 50µL. The digestion reaction was incubated at 37°C overnight, and resolved on a 1% (w/v) agarose gel, then excised and purified as previously described. A ligation reaction containing the annealed gRNAs and linearised vector was prepared using 1µL of annealed gRNA, 20ng of linearised vector, 2µL 10X T4 Ligase Buffer (Thermo Fisher Scientific, USA), 10U T4 DNA Ligase (Thermo Fisher Scientific, USA), and dH_2O to a final volume of 20µL. The reaction was incubated at 4°C overnight. DH5α chemically competent *E. coli* cells were transformed with 3µL of ligation reaction by heat-shock transformation. The cells were plated on selection plates containing 50µg/mL kanamycin, and incubated at 37°C overnight. Plasmid isolation performed as previously described, and assembled pTRV2-gRNA vectors were confirmed with Sanger sequencing using the primer TRV2_gRNA_confirm_F (Table 3.2).

3.2.7 Stable plant transformation of *N. benthamiana*

The constructs assembled with Golden Gate cloning (pCasRx:Rep_T1, pCasRx:Rep_T2), were individually electroporated into electrocompetent *A. tumefaciens* strain EHA105. Single colonies were inoculated into 5mL liquid Yeast Extract Peptone (YEP) (5g/L yeast extract, 10g/L peptone and 5g/L NaCl) medium containing 50µg/mL kanamycin and 50µg/mL rifampicin selection. Inoculations were incubated at 28°C overnight shaking at 150 revolutions per minute (rpm). The next day, 1mL of the starter culture was inoculated into 50mL liquid YEP containing 50µg/mL kanamycin, 50µg/mL rifampicin and 100µg/mL acetosyringone, and incubated with agitation (150rpm) at 28°C overnight. Centrifugation of the culture was performed at 3000rpm for 15 minutes at room temperature, and resuspended in sterile MS3 broth (4.4g/L Murashige & Skoog (MS) medium, 30g/L sucrose, 100µg/mL acetosyringone, pH 5.8) to an optical density $(OD)_{600}$ of 0.8-1. Wild-type *in vitro N. benthamiana* leaves were dissected into approximately 50 leaf disc explants of $1cm^2$ each, and used for *Agrobacterium*-mediated stable transformation, as described (Clemente, 2006). Leaf disc explants were regenerated on selective medium (4.4g/L MS, 30g/L sucrose, 3.3g/L PhytoAgar, 1mL 6-Benzylaminopurine (BAP) (1µM), pH 5.8) containing 100µg/mL kanamycin and 400µg/mL carbenicillin. Selective plates were incubated at 25°C with a 16hr light/8hr dark photoperiod cycle, and explants were placed on fresh selective medium every 14 days. Regenerated shoots produced from calli were excised and placed on rooting medium (2.2g/L MS, 15g/L sucrose, 3.3g/L PhytoAgar, pH 5.8) containing 100µg/mL kanamycin and 400µg/mL

carbenicillin. Following the onset of root formation, regenerated plantlets were maintained on rooting medium containing selection in Magenta™ pots.

3.2.8 Confirmation of transgenic events

In vitro leaf material was harvested from the regenerated plantlets, and the 200mg aliquots were frozen in liquid nitrogen. The material was homogenised with Eppendorf grinders in 2mL Eppendorf tubes. The standard Cetyltrimethylammonium bromide (CTAB) method (Murray and Thompson, 1980) was used for genomic DNA extraction. Putative transgenic plants were screened with an end-point PCR, using the primers CaMV-35S_F2/CasRx-screening_R1 (Table 3.2), and the PCR cycle parameters were set to: 95°C/2min + 32 x (95°C/30sec + 56°C/30sec + 72°C/1min) + 72°C/5mins + 4°C hold. After screening of putative transgenics, positive events were propagated until the desired number of plants for that line was achieved.

3.2.9 Agro-infiltration of *N. benthamiana* plant material

The binary pCasRx vectors harbouring the respective CP gRNAs, named pCasRx:CP_T1, pCasRx:CP_T2, pCasRx:CP_T3, were individually electroporated into *A. tumefaciens* strain EHA105 with 100ng of plasmid DNA, using a MicroPulser™ Electroporator (Bio Rad, USA). Transformed cells were grown on selection plates containing 50µg/mL kanamycin and 50µg/mL rifampicin. Plates were incubated at 28°C for 48 hours. An end-point PCR with the primers TC430/M13F (Table3.1) were used to screen for positive colonies; and the thermocycler conditions were: 95°C/2min + 25 x (95°C/30sec + 52°C/30sec + 72°C/30sec) + 72°C/5mins + 4°C hold. The unmodified pTRV1 vector, as well as the modified pTRV2 vectors harbouring the CP gRNAs (pTRV2:CP_T1, pTRV2:CP_T2, pTRV2:CP_T3), were individually electroporated into *A. tumefaciens* strain GV3101, with 100ng of plasmid DNA, using a MicroPulser™ Electroporator (Bio Rad, USA). Transformed cells were grown on selection plates containing 50µg/mL kanamycin, 10µg/mL rifampicin and 30µg/mL gentamicin. Plates were incubated at 28°C for 48 hours. An end-point PCR with the primers TRV2-confirm_F/oligo-specific_R (Table 3.2 and Supplementary Table 1 respectively) were used to screen for positive colonies; and the thermocycler conditions were: 95°C/2min + 25 x (95°C/30sec + 55°C/30sec + 72°C/30sec) + 72°C/5mins + 4°C hold. Single colonies were grown in liquid LB cultures containing suitable antibiotics. Liquid cultures were incubated with agitation overnight (28°C, 150rmp). Overnight cultures were centrifuged at 4000rpm for 15 minutes at room temperature, and resuspended in infiltration buffer (10mM MES [pH 5.6], 10mM

$MgCl_2$, 200µM acetosyringone) to a final OD_{600} of 0.8-1.0. The resuspended cultures were incubated in the dark at ambient room temperature for 2 hours. The cultures containing pCasRx constructs were mixed in a 1:1 ratio with the culture of the infectious clone of GVA, and the desired mixtures were infiltrated by *Agrobacterium*-mediated infiltration. Mixed cultures were infiltrated into the underside of three fully expanded four-week old wild-type *N. benthamiana* leaves grown under long-day conditions (16-hour light, 8-hour dark at 25°C), using a needleless 2mL syringe.

3.2.10 RNA extraction and cDNA synthesis

Infiltrated wild-type *N. benthamiana* leaf material was harvested 5- or 14-days post-infiltration (dpi), and three infiltrated leaves per plant were pooled together and subsequently frozen in liquid nitrogen. The pooled material was then finely ground with liquid nitrogen in a mortar and pestle, and aliquots of 100mg were made in 2mL Eppendorf tubes. Total RNA was extracted from the 100mg aliquots using the Spectrum™ Plant Total RNA Kit (Sigma, USA) following the manufacturer's instructions. A DNase treatment was performed on the total RNA with the On-Column DNase I Digestion Set (Sigma, USA) following the manufacturer's instructions, and total RNA was eluted in 40µL nuclease-free dH_2O. The RNA quantification and purity were assessed using spectrophotometry (Nanodrop 2000; Thermo Fisher Scientific, USA) and RNA integrity was assessed using gel electrophoresis on a 2% agarose gel (w/v). First-strand complementary DNA (cDNA) synthesis was performed using 1µg of DNase-treated total RNA with Random Primers (Promega, USA) and Maxima Reverse Transcriptase (Thermo Fisher Scientific, USA), following the manufacturer's instructions. Successful cDNA synthesis was assessed with an end-point PCR using the primer set RTbent_actin_F/RTbent_actin_R (Table 3.2) to amplify the housekeeping gene *actin*. Thermocycler conditions were set to: 95°C/2min + 35 x (95°C/30sec + 54°C/30sec + 72°C/30sec) + 72°C/5mins + 4°C hold. Correct fragment amplification was confirmed with 1% (w/v) agarose gel electrophoresis.

3.2.11 Reverse-transcription quantitative-PCR (RT-qPCR) expression analysis

The cDNA samples were diluted 100-fold. A QuantStudio™ 3 Real-Time PCR System (Applied Biosystems, USA), along with the reporter PowerUp™ SYBR™ Green Master Mix (Applied Biosystems, USA) were used. Diluted cDNA (2µL) was loaded into a 96-well 0.2mL plate, with three technical replicates for each biological replicate, along with 400nM for each primer, 5µL of the 2X

master mix, and dH_2O to a final volume of 10µL. The housekeeping gene adenine phosphoribosyltransferase like (*APR*) (Liu *et al.*, 2012) was chosen as the internal control (Table 3.3), and the desired RT-qPCR primer sets for gene expression analysis are listed in Table 3.3.

Table 3.3. RT-qPCR primers used for gene expression analysis.

Primer name	Sequence 5'-3'	Tm (°C)	Amplicon (bp)
APR_F	CATCAGTGTCGTTGCAGGTATT	55.3	107
APR_R	GCAACTTCTTGGGTTTCCTCAT	55.6	
CasRx_gRNA-scaf_F	AACCCCTACCAACTGGTCGGG	59.9	~70
CP_T1_qPCR_R	TAGACCCGCGCGGAAAGTTG	59.6	
CP_T2_qPCR_R	CTGAGCTGGTGGGAAGGATGAGA	59.5	
CP_T3_qPCR_R	TAGCGAGGGACCCGTGAAAGG	60.1	
CasRx_qPCR_2F	TGTTTCCGCCTTCAGCAAAC	56.1	147
CasRx_qPCR_2R	TTAGCGTTGACTCCGATGAGAG	56.1	
GVA_qPCR Rep_F	ATCGCGAGCGCAAAAAGTAC	56.4	76
GVA_qPCR Rep_R	TGGCAACGATTTCAGAACGC	56.2	
GVA_qPCR CP_F1	TTGTATCTGAGCTGGTGGGAAG	55.8	87
GVA_qPCR CP_R1	ACATTTGCCTAAGCGTTGCC	56.2	
GVA_qPCR CP_F2	CGGTACTAGCAAAAAGGCGATC	55.9	139
GVA_qPCR CP_R2	AGCCACACTCAGAGTTCTCATC	55.9	

The comparative C_T ($\Delta\Delta C_T$) method was selected, the cycle parameters were set for Standard cycling mode (Primer $T_m \geq 60°C$): 50°C/2min + 95°C/2min + 40x (95°C/15sec + 60°C/1min), and the melt curve parameters were set as the default settings. The $2^{-\Delta\Delta CT}$ method was used to calculate the gene expression levels, relative to the reference sample, in the online Design and Analysis app (Thermo Fisher Scientific, USA). The error bars serve as an indication between the RQ minimum and RQ maximum for the sample. A confidence interval of 95% was used.

3.2.12 Statistical analysis

The relative gene expression of GVA was analysed statistically using a two-tailed unpaired Student's t-test. GraphPad Prism Version 9.1.1 (GraphPad Software, USA) software was used to compute the analysis, by comparing the sample-group to the control -group. Data represents the mean ± standard error of the mean (SEM), and the significance determination was set at $p \leq 0.05$.

The Pearson correlation coefficient (r) was used to calculate the correlation between the relative gene expression of the respective gRNA compared to the expression of the GVA *CP* gene.

3.3 RESULTS

3.3.1 Stable transformation of *N. benthamiana* plants with pCasRx constructs

The gRNAs targeting the replicase gene (ORF1) of pBINSN_GVA118_NbPDS were designed in a previous study (Spencer, 2019). The binary vectors harbouring these gRNAs (pCasRx:Rep-T1 and pCasRx:Rep-T2), as well as a binary vector not harbouring a gRNA (pCasRx-EMPTY), were used to transform *N. benthamiana* by *Agrobacterium*-mediated stable transformation. Fig. 3.1 depicts the stages of the transformation and the subsequent regeneration of the putatively transformed plantlets.

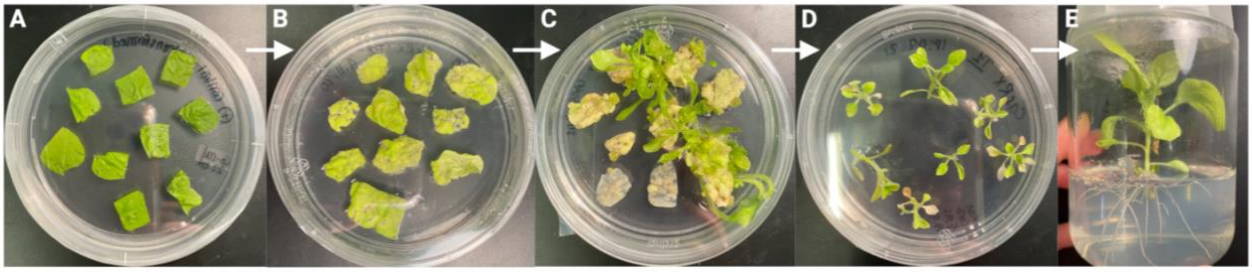

Figure 3.1. *Agrobacterium*-mediated stable transformation and regeneration, of the wild-type *N. benthamiana* leaf disc organogenesis process. **A**) Leaf discs on co-cultivation medium immediately after incubation with the *Agrobacterium* harbouring the respective constructs. **B**) leaf discs begin to form into calli, after some time on selective medium. **C**) Callus stage with shoots, on selective medium. **D**) isolated shoots on rooting medium containing selection. **E**) Fully regenerated putative transgenic plantlet on selective medium.

Subsequent to a well-developed root system, the regenerated plantlets were screened to identify successful transgenic events. Table 3.4 depicts the number of leaf discs transformed, the number of regenerated plants for each construct, and the number of transgenic events obtained and screened.

Table 3.4. Total numbers of the leaf discs transformed, the subsequent regenerated plantlets, and the total screened and confirmed transgenic plants for each construct.

Constructs transformed with *A. tumefaciens*	Total number of leaf discs	Total regenerated plantlets	Regenerated plantlets (%)	Total screened plants	Total confirmed transgenic plants	Transgenic events (%)
pCasRx:Rep-T1	50	16	**32**	9	8	**88**
pCasRx:Rep-T2	50	12	**24**	8	7	**87**
pCasRx-EMPTY	60	11	**18**	2	2	**100**

A total of 16 regenerated plantlets were obtained from 50 transformed leaf discs for the construct pCasRx:Rep-T1, 12 from 50 transformed leaf discs for pCasRx:Rep-T2, and 11 from 60 leaf discs for the pCasRx-EMPTY construct. Therefore, the percentage of regenerated plantlets, calculated by dividing the total number of regenerated plantlets by the total number of leaf discs, was 32, 24 and 18% respectively (Table 3.4). The regenerated plantlets were screened using end-point PCR, to identify transformation events (Supplementary Fig. 3). The percentage of transgenic events, calculated by dividing the total number of confirmed transgenic plants by the total number of screened plants, was 88, 87 and 100% respectively, for each construct (Table 3.4). All transgenic lines were propagated and hardened-off, once the desired number of plantlets was achieved.

3.3.2 Virus interference when targeting the replicase gene

The binary vectors harbouring the *CasRx* gene and replicase gene targets were introduced into *N. benthamiana*, to assess the ability of the CRISPR/CasRx system to induce virus resistance after being infected with the GVA clone. The constructs pCasRx:Rep-T1, pCasRx:Rep-T2 and pCasRx-EMPTY were used to transform *N. benthamiana* plants. Following the confirmation and subsequent propagation of transgenic events, five plants of each transgenic line were hardened-off. After the hardened-off plants had acclimatised, they were Agro-infiltrated with the GVA infectious clone. Total plant RNA was extracted 14 dpi, and cDNA was synthesised and confirmed with an end-point PCR (Supplementary Fig. 4). GVA accumulation and *CasRx* expression were assessed in parallel, using RT-qPCR. As negative controls, Cas13a-EMPTY plants – plants which had been transformed with a construct harbouring the *Cas13a* gene and no gRNA (Robertson,

2021), and wild-type plants, were infiltrated with the GVA clone since at the time, no stably-transformed CasRx-EMPTY plants had been regenerated. Samples were harvested 14 dpi, and three leaves per plant were pooled, prior to RNA extraction and cDNA synthesis. RT-qPCR analysis was performed to quantify GVA, with primer pair GVA_qPCR Rep_F/GVA_qPCR Rep_R (Table 3.3), and *CasRx* transcripts, with primer pair CasRx_qPCR_2F/CasRx_qPCR_2R (Table 3.3). One line of pCasRx:Rep-T1 was analysed (Line 1), while four lines of pCasRx:Rep-T2 were analysed (Line 1, 2, 5 and 7) for GVA interference (Fig. 3.2).

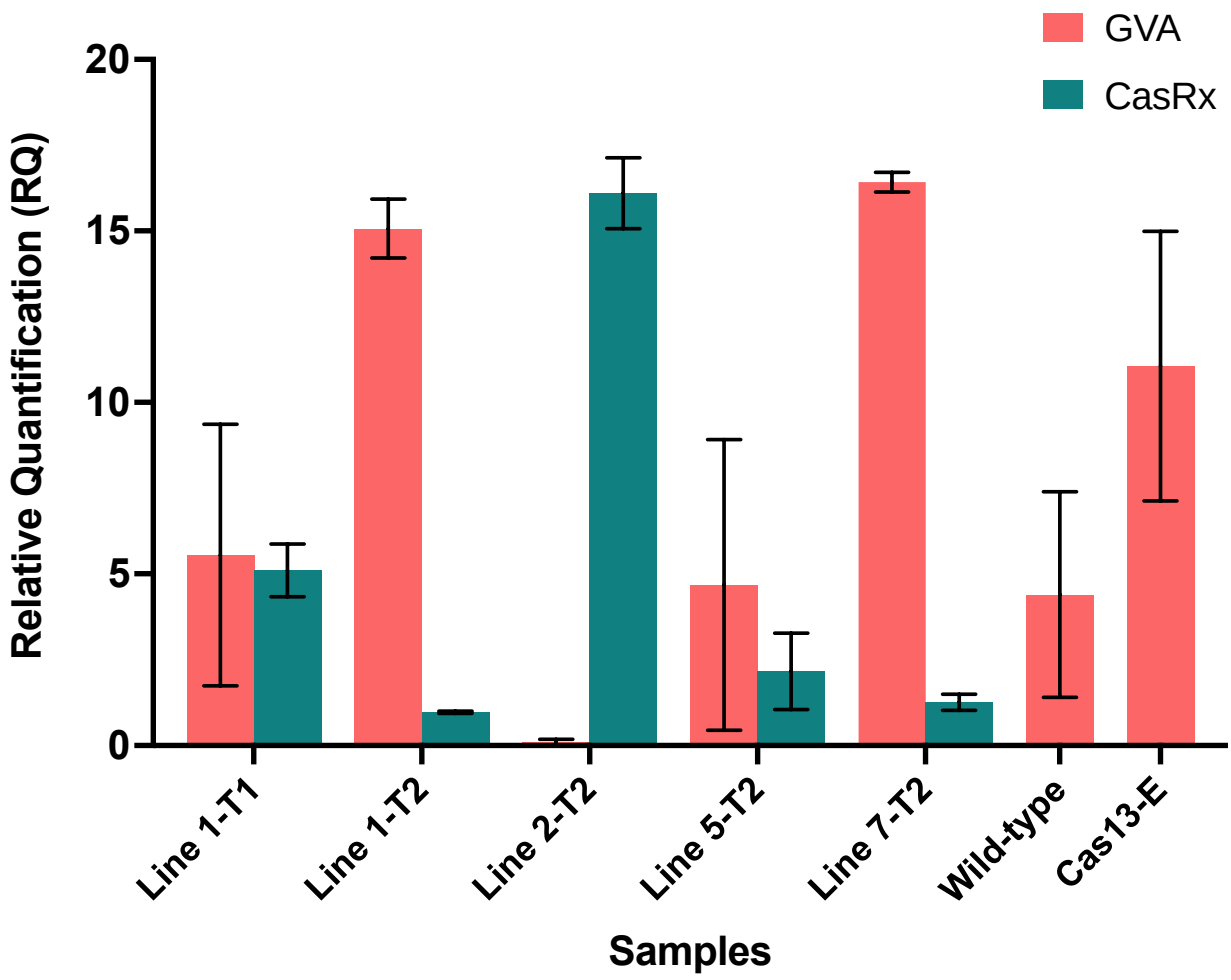

Figure 3.2. The gene expression analysis of stably-transformed CasRx:Rep plant lines, containing the integrated T-DNA region harbouring *CasRx* and the replicase gRNA. T1 refers to pCasRx:Rep-T1, T2 refers to pCasRx:Rep-T2, wild-type and Cas13a-EMPTY (Cas13-E) refer to the control samples. The lines represent different events, which were propagated until at least five plants were obtained, and then Agro-infiltrated with the GVA clone (OD_{600}=1). Each line represents n=5 plants, which were pooled due to the large variation observed following Agro-infiltration. The error bars represent the minimum and maximum values of n=5 biological replicates. The correlation analysis was performed using the Pearson correlation coefficient (r); with the correlation being significant at $p \leq 0.05$.

Due to the high amount of variation observed following Agro-infiltration, all plants from the same line were pooled together (n=5) (Fig. 3.2). Line 2-T2 seemed to result in the most robust virus

interference, with a ~4-fold reduction in GVA quantification, when compared to the wild-type control. Line 2-T2 additionally expressed the highest levels of the *CasRx* gene, roughly an ~8-fold increase of CasRx when compared to line 1-T2. However, Line 1-T2 and Line 7-T2 showed higher virus accumulation compared to the controls, while concurrently expressing the lowest *CasRx* levels. Additionally, Line 1-T1 and Line 5-T2 showed similar virus accumulation compared to the wild-type control, with moderate and low *CasRx* gene expression, respectively. No significant correlation was found when a correlation test between *CasRx* expression and GVA quantification was performed.

The respective replicase gRNAs were designed in a previous study (Spencer, 2019). Since then, new literature has emerged which highlights necessary factors pertaining to the design of a gRNA, such as the accessibility of target RNA, accessibility of the central seed region, and formation of secondary structures within the gRNA-scaffold sequence (Wessels *et al.*, 2020). Due to the ambiguous results obtained when the replicase gene of GVA was targeted, it was speculated that the ineffective GVA targeting was due to the replicase gRNAs. Thus, new gRNAs targeting the *CP* gene of GVA were designed, in order to improve the efficiency of CRISPR/CasRx virus targeting.

3.3.3 Coat protein gRNA design and vector construction

Open reading frame four (ORF4) of pBINSN_GVA118_NbPD encodes the *CP* gene, and was chosen as the target for CRISPR/CasRx virus interference, as previous literature had observed that targeting the CP resulted in decreased viral accumulation (Aman, Ali, *et al.*, 2018; Aman, Mahas, *et al.*, 2018). Three gRNAs were designed against the *CP* gene of GVA, in a region which revealed increased accessibility (Fig. 3.3A).

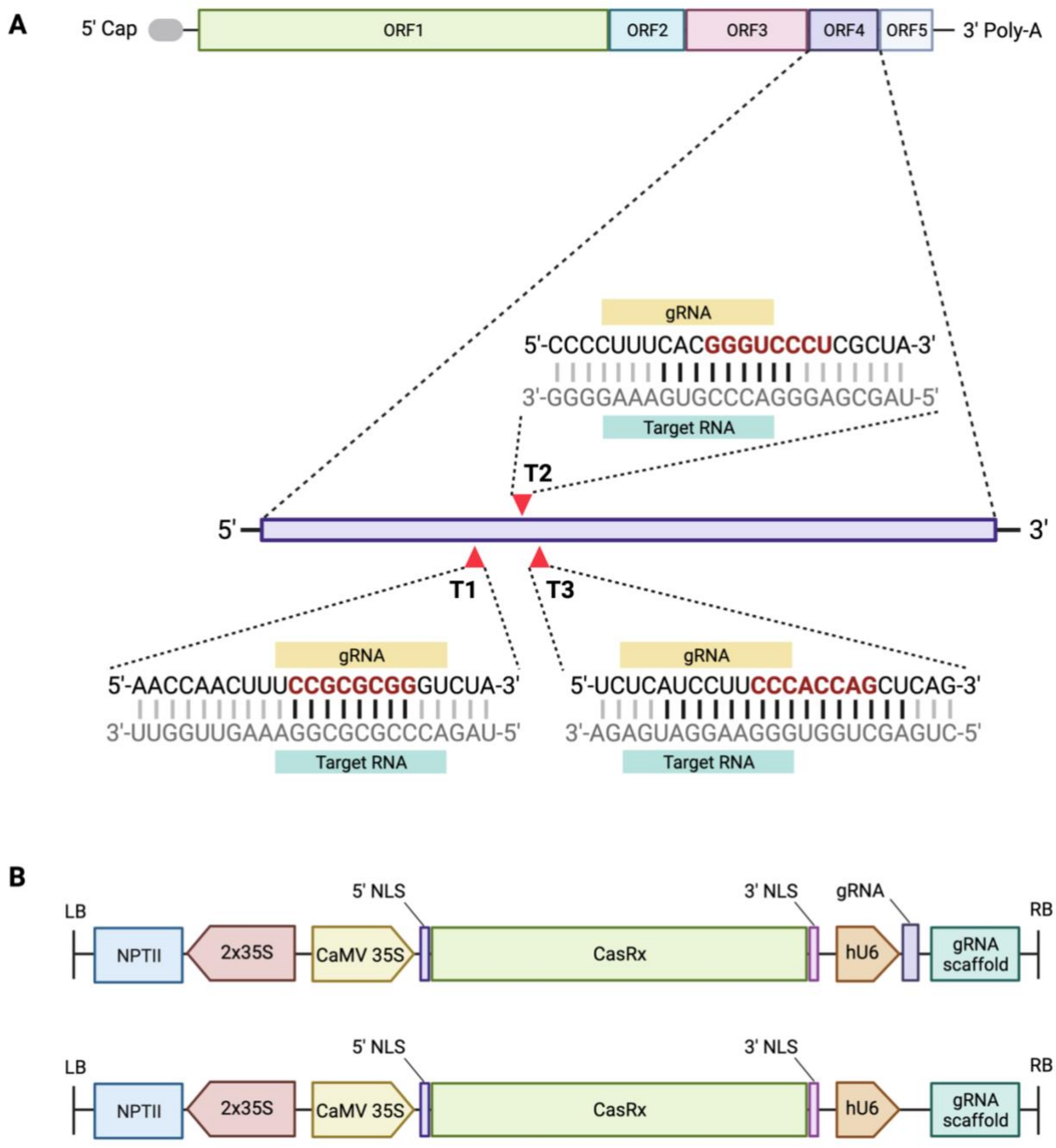

Figure 3.3. A schematic representing the GVA genome organisation and the gRNAs designed to target the open reading frame (ORF) four, which encodes the coat protein (CP), as well as the assembled constructs. **A**) GVA genome organisation, ORF1 encodes replication-related proteins; ORF2 encodes a protein with an unknown function; ORF3 encodes the movement protein (MP); ORF4 encodes the CP, and ORF5 encodes a silencing-suppressor protein. The three gRNAs were designed to target ORF4 of GVA. The seed region of the gRNA sequence is represented in red. The black horizontal lines between the gRNA and target RNA represent the nucleotides complementing single-stand RNA (ssRNA). **B**) Schematic representation of the T-DNA region of the pCasRx-gRNA or pCasRx-EMPTY constructs, assembled using Golden Gate cloning. The neomycin phosphotransferase type II gene (*NPTII*) is driven by 2x35S promoters. The cauliflower mosaic virus (CaMV) 35S promoter drives the *CasRx* expression, while the human U6 (hU6) promoter is responsible for expressing the respective gRNA and gRNA scaffold. NLS, nuclear localisation signal; LB, left border; RB, right border.

The gRNAs which were determined to lie in a more accessible region, specifically the seed region (position 11-18 nt), were selected as gRNAs. Off-targets against the *N. benthamiana* transcriptome were analysed, and gRNAs with the least off-targets were selected. The Cas13design software output ranks the gRNA in number and quartile, where quartile 4 (Q4) are the best scored and quartile 1 (Q1) are the worst scored gRNAs. The accessibility of the seed region was emphasised during the gRNA selection process, as well as the folding of the gRNA with the scaffold sequence (Supplementary Fig. 5). The CP gRNAs selected were: Target 1 (T1) (rank 90, Q3), Target 2 (T2) (rank 3, Q4), and Target 3 (T3) (rank 164, Q3) (Fig. 3.1A). The complete seed region of T1 aligns with single-strand target RNA (11-18 nts), while the first six nts of the seed region of T2 align with ssRNA (8-16 nts). T3 contains the most nts which align with ssRNA, including the entire seed region (5-20 nts). The off-targets against the *N. benthamiana* transcriptome and seed region of the gRNA were analysed for each target; where T1 contained two off-targets which complemented the seed region, but never the entire gRNA; T2 contained the most off-target possibilities (15), which complemented the seed region, but not the entire gRNA sequence; and T3 contained no off-targets complementing the seed region, nor the rest of the gRNA.

The vectors harbouring the CP gRNAs were constructed using Gibson and Golden Gate assembly. The intermediate constructs pJJB308 and pJJB296 were modified by Gibson assembly to contain the CasRx-gRNA promoter and scaffold sequence, and the *CasRx* gene, respectively. Following the successful assembly of the intermediate constructs pJJB308-CasRx and pJJB296-CasRx (Supplementary Fig. 2), the final binary pCasRx:CP vectors were constructed using Golden Gate assembly (Fig. 3.3B). The annealed gRNAs were cloned under the hU6 promoter, and upstream of the CasRx-gRNA scaffold. In addition, a vector not containing a gRNA (pCasRx-EMPTY) was assembled in parallel, using Golden Gate assembly (Fig. 3.3B). The sequences of the oligos for each target can be found in Supplementary Table 1.

Additionally, the CP gRNAs were cloned into the TRV-RNA2 (TRV2) genome of TRV. Subsequent to the confirmation of the TRV-RNA1 and TRV2 plasmids, the CP gRNAs and CasRx scaffold oligos were phosphorylated, annealed and ligated into the digested TRV2 vector. Sanger sequencing was used to confirm the successful assembled expression and delivery vectors pTRV2:CP-T1,

pTRV2:CP-T2, and pTRV2:CP-T3. A vector map representing all three constructs can be found in Supplementary Figure 6.

3.3.4 Transient experiment analysis with binary pCasRx vectors

As a preliminary analysis, transient assays were performed to assess the efficacy of the individual CP gRNAs. The assembled pCasRx constructs harbouring CP gRNAs were used for transient analysis to determine GVA interference. The expression of the *CasRx* gene was driven by the CaMV 35S promoter, while the gRNA was driven by the hU6 promoter. Transient assays consisted of co-infiltrations of the binary vectors pCasRx:CP_T1, pCasRx:CP_T2 and pCasRx:CP_T3 with the GVA clone (OD_{600} = 0.05), into wild-type *N. benthamiana*. As a control, co-infiltrations of the binary vector containing a non-specific (ns) gRNA (pCasRx-ns), along with the GVA clone, were performed. To reduce the possibility of variation caused by the empirical process of Agro-infiltration, the control and test samples were infiltrated into either side of the same leaf; the left side of the leaf was infiltrated with the control construct (pCasRx-ns), while the right side of the leaf was infiltrated with the test construct (pCasRx:CP). The resuspended cultures of the GVA infectious clone and pCasRx constructs were mixed in a 1:1 ratio prior to infiltration. Two to three leaves per plant were infiltrated with the control and test samples, and samples were harvested 5 dpi. The GVA titer in each half of the leaf was quantified with RT-qPCR, using the primers GVA_qPCR CP_F1/GVA_qPCR CP_R1 (Table 3.3), to assess the efficiency of the individual CP gRNAs (Fig. 3.4).

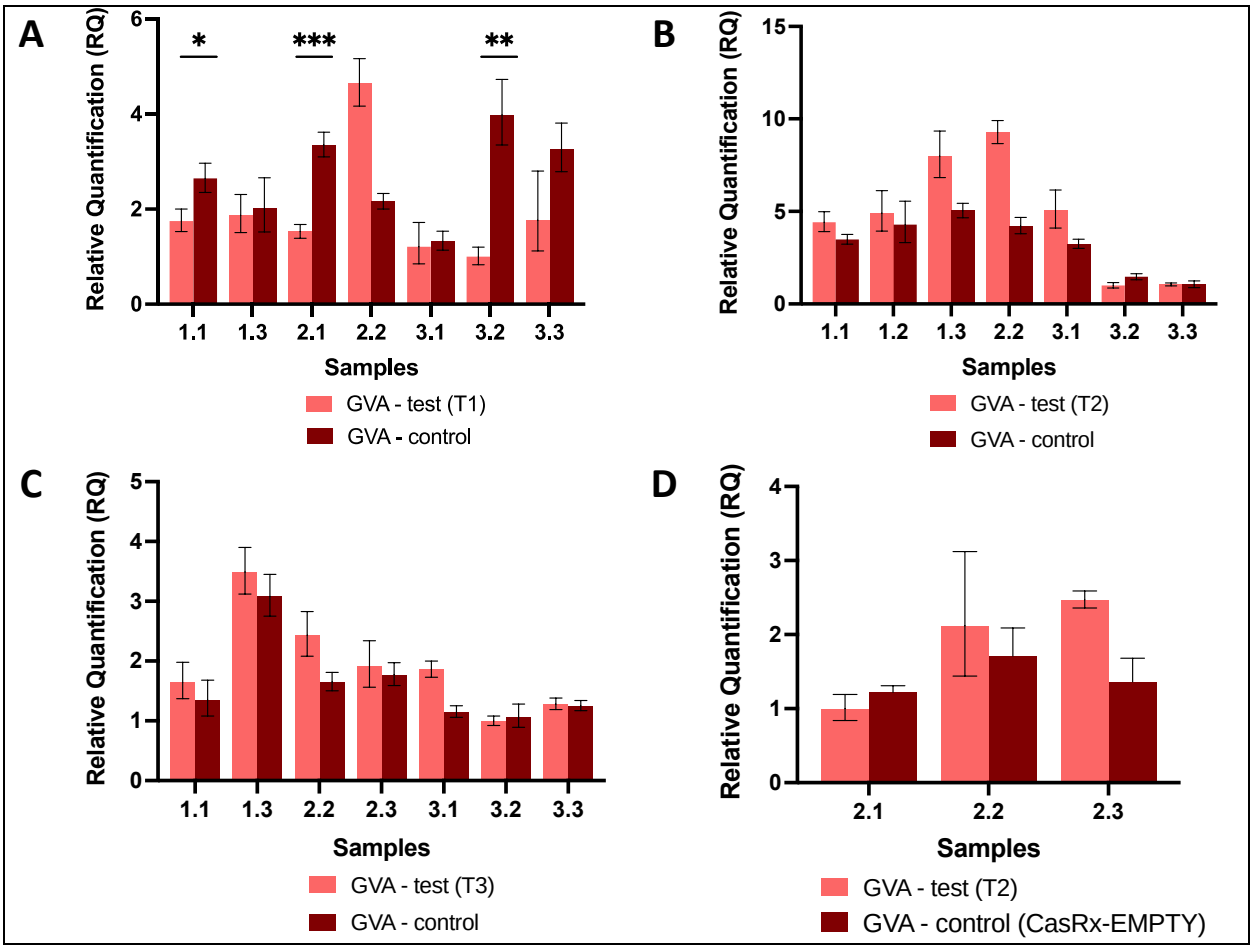

Figure 3.4. Relative quantification of GVA for transient experiment analysis. The control was infiltrated with the pCasRx-ns vector, while the test sample was infiltrated with: **A**) pCasRx:CP-T1, **B**) pCasRx:CP-T2, **C**) pCasRx:CP-T3. **D**). The control was infiltrated with the pCasRx-EMPTY vector, while the test sample was infiltrated pCasRx:CP-T2. The error bars represent the minimum and maximum values of n=3 technical replicates. Statistical analysis performed using a two-tailed unpaired Student's t-test; with the difference being significant at $p \leq 0.05$ with respect to the control group. * p=0.0163, ** p=0.0019, *** p=0.0004.

Fig. 3.4A represents the GVA quantification analysis when pCasRx:CP-T1 was infiltrated. Virus interference was suggested in three samples; sample 1.1, 2.1 and 3.2, as the relative quantification of GVA for the control sample was significantly higher than the test sample. Reductions in GVA quantification for sample 1.1, 2.1, and 3.2 are ~2-fold, ~4-fold, and ~1.5-fold, respectively. The other four samples did not indicate virus interference, and revealed GVA quantification in the test sample which showed similar or higher levels than the control sample. Fig. 3.4B presents the relative GVA quantification when the pCasRx:CP-T2 construct was infiltrated. No samples indicated GVA interference, as no test samples had reduced GVA quantification, when compared to the control sample. The same was observed when pCasRx:CP-T3 was infiltrated, where no samples indicate GVA interference (Fig. 3.4C). Contrary to what was expected, both Fig. 3.4B and Fig 3.4C showed higher GVA quantification in the test sample

infiltrated with a CP gRNA, rather than the control sample infiltrated with an ns gRNA (pCasRx-ns).

Due to the decrease in GVA quantification in the control samples infiltrated with pCasRx-ns, another control was tested for further clarity on this observation. A transient experiment was repeated using pCasRx:CP-T2, and pCasRx-EMPTY instead of pCasRx-ns, as a control (Fig. 3.4D). Relative GVA quantification in Fig. 3.4D did not show any reduction in GVA transcript quantification in the test samples, similarly to Fig. 3.4B and Fig. 3.4C. Interestingly, although the same leaf was infiltrated with the test and control sample, there was still a substantial amount of variation observed. Following transient experiments, stable experiments were performed to improve CRISPR/CasRx virus interference. CasRx-EMPTY plants were infiltrated with the GVA clone and TRV expression vectors harbouring the CP gRNAs.

3.3.5 CRISPR/CasRx interference of GVA

The study by Mahas and colleagues determined that CasRx resulted in the most robust virus interference, when compared to other Cas13 variants (Mahas, Aman and Mahfouz, 2019). In the current study, *N. benthamiana* plants constitutively expressing CasRx were utilised to determine the capability of the CRISPR/CasRx system to confer virus interference against GVA. Three gRNAs targeting the *CP* gene of GVA were assessed. The respective gRNAs were delivered individually by TRV delivery vectors, along with the GVA infectious clone, by means of Agro-infiltration. The pTRV-RNA1 and pTRV2-gRNA vectors were mixed in a 1:1 ratio (OD_{600}=1), prior to infiltration. The culture of the GVA clone (OD_{600}=0.05) was mixed with the TRV culture and infiltrated into three leaves of CasRx-EMPTY plants. Each pTRV2-gRNA vector was individually infiltrated into five CasRx-EMPTY plants. As the control, two wild-type *N. benthamiana* plants were infiltrated with pTRV2:CP-T1. Subsequent to the co-infiltration of the GVA clone and pTRV2 vector harbouring the respective gRNA, both the relative fold expression of GVA and the gRNA were analysed 5-dpi (Fig. 3.5).

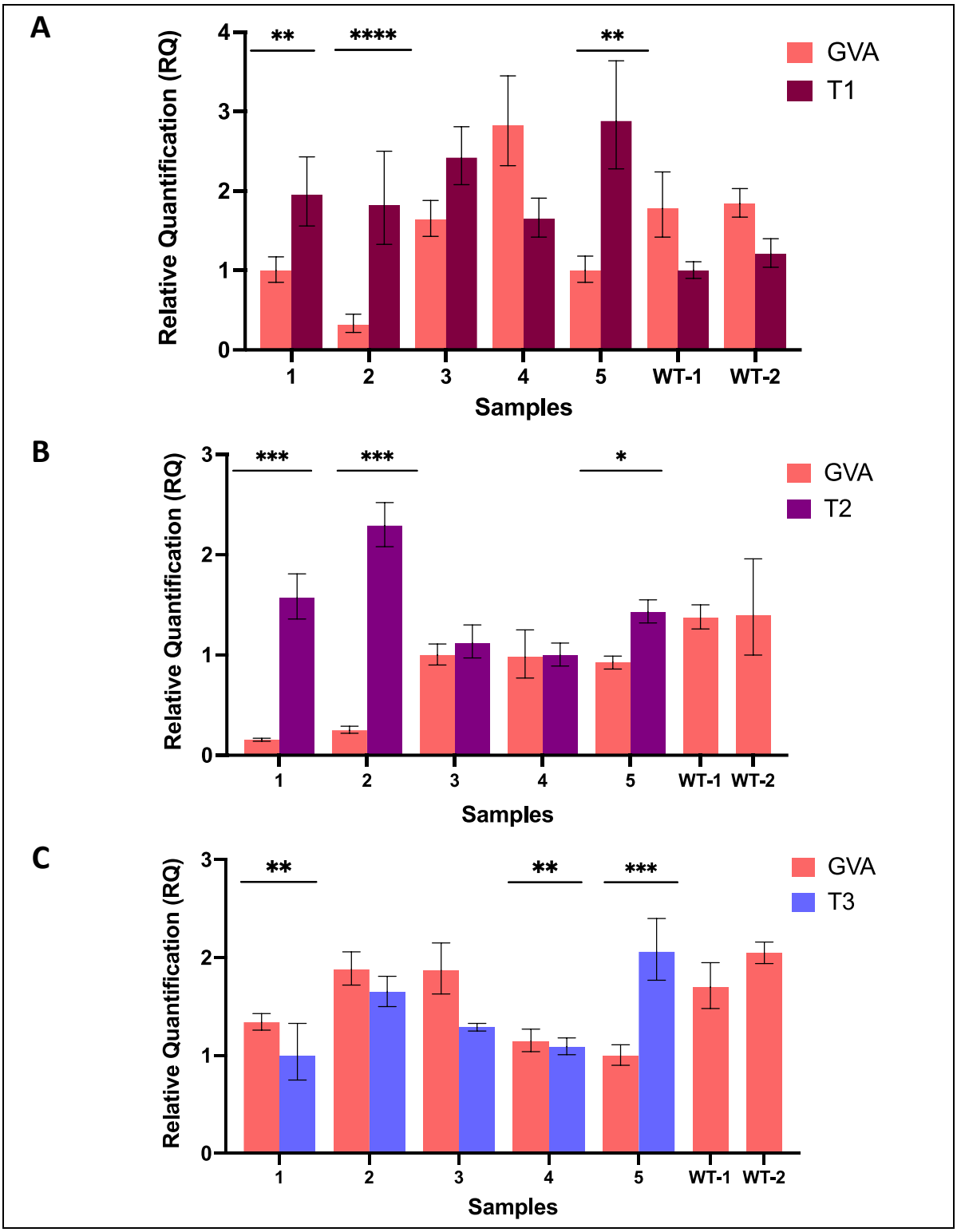

Figure 3.5. Gene expression analysis of stably-transformed *N. benthamiana* (CasRx-EMPTY plants). **A**) Relative fold expression of GVA (red) and T1 (maroon), subsequent to the GVA clone and pTRV2:CP-T1 co-infiltration into CasRx-EMPTY plants. ** p<0.0027, **** p<0.0001. **B**) Relative fold expression of GVA (red) and T2 (purple), subsequent to the GVA clone and pTRV2:CP-T2 co-infiltration in CasRx-EMPTY plants. * p=0.0038, *** p<0.0005. Correlation coefficient (r) is –0.7738 (p=0.024). **C**) Relative fold expression of GVA (red) and T3 (blue), subsequent to GVA and pTRV2:CP-T3 co-infiltration into CasRx-EMPTY plants. ** p<0.0095, *** p=0.0007. The error bars represent the minimum and maximum values of n=3 technical replicates. Statistical analysis performed using a two-tailed unpaired Student's t-test; with the difference

being significant at $p \leq 0.05$ with respect to the control group. Correlation analysis performed using the Pearson correlation coefficient (r); with the correlation being significant at $p \leq 0.05$.

When the GVA clone and pTRV2:CP-T1 were co-infiltrated into CasRx-EMPTY plants, RT-qPCR was used to quantify T1 gRNA and GVA transcripts. As controls, two wild-type (WT) *N. benthamiana* plants (WT1, WT2) were infiltrated with the GVA clone and pTRV2:CP-T1 (Fig. 3.5A). In Fig. 3.5A, GVA interference was observed in sample 1, 2 and 5, as there was a significant difference between GVA quantification in the sample compared to the WT controls. Of the three samples, sample 2 indicated the highest GVA reduction when compared to the control samples (~5-fold reduction, $p<0.0001$). Notably, sample 4 had no viral reduction whatsoever, as the relative quantification of GVA was greater than both control samples. No significant correlation existed between the T1 gRNA and GVA accumulation. When the GVA clone and pTRV2:CP-T2 were co-infiltrated, three samples (sample 1, 2 and 5) demonstrated GVA interference, when compared to the WT controls. The highest GVA interference was an ~8-fold reduction, observed in sample 1 and 2 ($p < 0.0005$), when compared to WT1. The relative T2 gRNA expression was negatively correlated with virus accumulation, at the $P \leq 0.05$ level. The Pearson correlation coefficient was –0.7738. Relative quantification analysis when pTRV2:CP-T3 was co-infiltrated with the GVA clone, similarly depicted three of the five samples which presented virus interference. Samples 1, 4 and 5 all had significantly lower GVA quantification compared to WT1 and WT2, with sample 5 demonstrating a ~1.7-fold reduction in GVA ($p=0.0007$). No significant correlation existed between T3 gRNA expression and GVA accumulation.

3.3.6 Guide-induced gene silencing of GVA

To analyse virus interference with a multi-guide system, as well as GIGS, the GVA infectious clone was infiltrated into CasRx-EMPTY plants, as well as into wild-type *N. benthamiana* plants, two days after the CP guides were infiltrated. A combination of all three pTRV2:CP vectors were mixed in a 1:1:1 ratio, which was then mixed in a 1:1 ratio with pTRV-RNA1. The TRV cultures were subsequently infiltrated two days before the GVA clone, to allow for the TRV vectors to express the gRNAs before viral infection. As controls, only the GVA clone was infiltrated into CasRx-EMPTY or wild-type plants, without TRV-gRNA mixtures. The TRV-gRNA mixture was infiltrated into wild-type *N. benthamiana* plants to assess the occurrence of possible GIGS (Sharma *et al.*, 2022). Five days post-infiltration of the GVA clone, three systemic leaves were harvested and pooled together, followed by RNA extraction and cDNA synthesis. Fig. 3.6 depicts the relative

quantification analysis of GVA, with primer pair GVA_qPCR CP_F1/GVA_qPCR CP_R1 (Table 3.3), in both CasRx-EMPTY plants (turquoise) and wild-type plants (green).

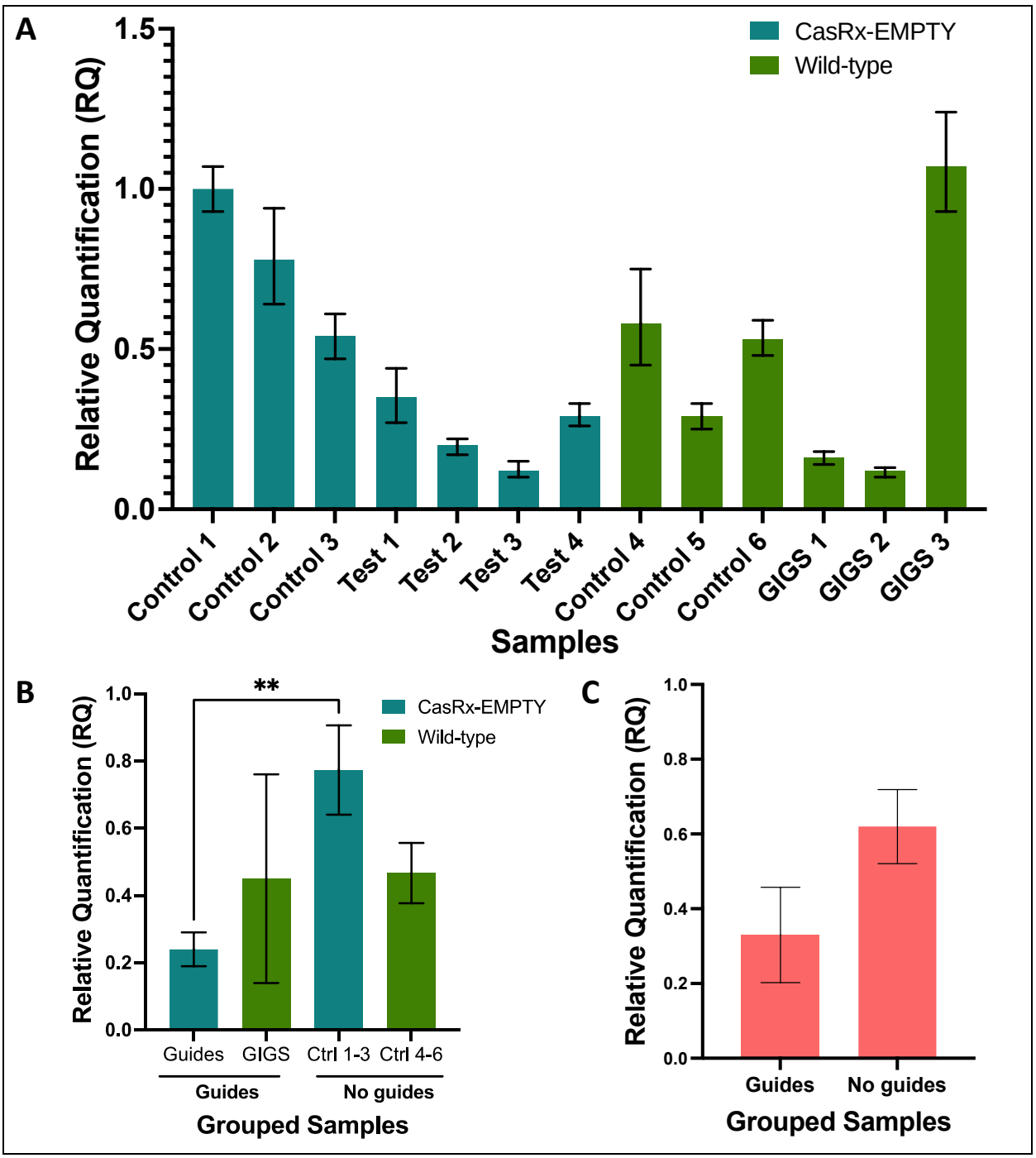

Figure 3.6. Relative quantification of GVA in the presence of CasRx, or without CasRx, to assess guide-induced gene silencing (GIGS). **A**) Relative fold expression of GVA, normalised to the reference sample 'control 1'. The error bars represent the minimum and maximum values of n=3 technical replicates. Samples 'control 1 to 3' represent CasRx-EMPTY plants infiltrated with the GVA clone only. Samples labelled 'guide 1 to 4' represent CasRx-EMPTY plants infiltrated with the three-guide TRV mixture, followed by the GVA clone two days later. Samples 'control 4 to 6' represent wild-type plants infiltrated with the GVA clone only. Samples labelled 'GIGS 1 to 3' represent wild-type plants infiltrated with the three-guide TRV mixture, followed by the GVA clone two days later. **B**) Relative quantification of GVA *CP* expression of

the samples grouped biologically. Data represents the mean relative gene expression, ± SEM of the biological replicates (n=3, n=4). **C**) Relative quantification of GVA *CP* expression of the samples grouped depending on whether they received the three-guide TRV mixture. Data represents the mean relative gene expression, ± SEM of the n=7 samples (Guides) and n=6 samples (No guides). Statistical analysis performed using a two-tailed unpaired Student's t-test; with the difference being significant at $p \leq 0.05$ with respect to the control group. ** p=0.0083.

Fig. 3.6A shows the test and control samples, when all three CP gRNAs were infiltrated. Of the test samples (Test 1 to 4), sample 'Test 3' showed the lowest GVA accumulation, with >3.5-fold reduction comparing to the samples 'control 1 to 3'. Notably, there was significant variation observed between the three CasRx-EMPTY control samples. Samples GIGS 1 and 2 both showed similar GVA quantities, which demonstrated a >2-fold reduction. Conversely, sample GIGS 3 showed the highest relative quantification of GVA among all the samples. When the samples are grouped biologically, there was a 3-fold reduction of GVA in the samples which received three gRNAs when CasRx was present (Fig. 3.6B), compared to the CasRx samples without the three gRNAs. In the GIGS samples, the large error bar represents the amount of variation observed among the three samples (Fig. 3.6A), which was due to outlying sample 'GIGS 3'. No clear difference in GVA accumulation was observed, when compared to the wild-type control samples which did not receive gRNAs. Fig. 3.6C represents the GVA relative quantification of the plants grouped by whether they were infiltrated with gRNAs compared to the control plants which did not receive gRNAs. Although the 'Guides' column presents a ~2-fold reduction in GVA when compared to the 'No guides' group, the reduction was not significant when $p \leq 0.05$.

The controls in the above experiment (Fig. 3.6) were only infiltrated with the GVA clone. In the next experiment, the control samples were infiltrated with a pTRV2 construct harbouring no gRNA (hereafter referred to as pTRV2-EMPTY). This was performed to assess the possibility of viral competition in Fig 3.6, which may have been the cause of GVA inhibition. As a control, wild-type *N. benthamiana* plants were Agro-infiltrated with pTRV1 and pTRV2-EMPTY constructs, to mimic "wild-type" TRV virus infection, and to assess competition between GVA and TRV *in planta*. Fig. 3.7 depicted the RT-qPCR analysis of GVA quantification with primers GVA_qPCR CP_F1/GVA_qPCR CP_R1 (Table 3.3), in the second GIGS experiment, when three gRNAs were co-infiltrated.

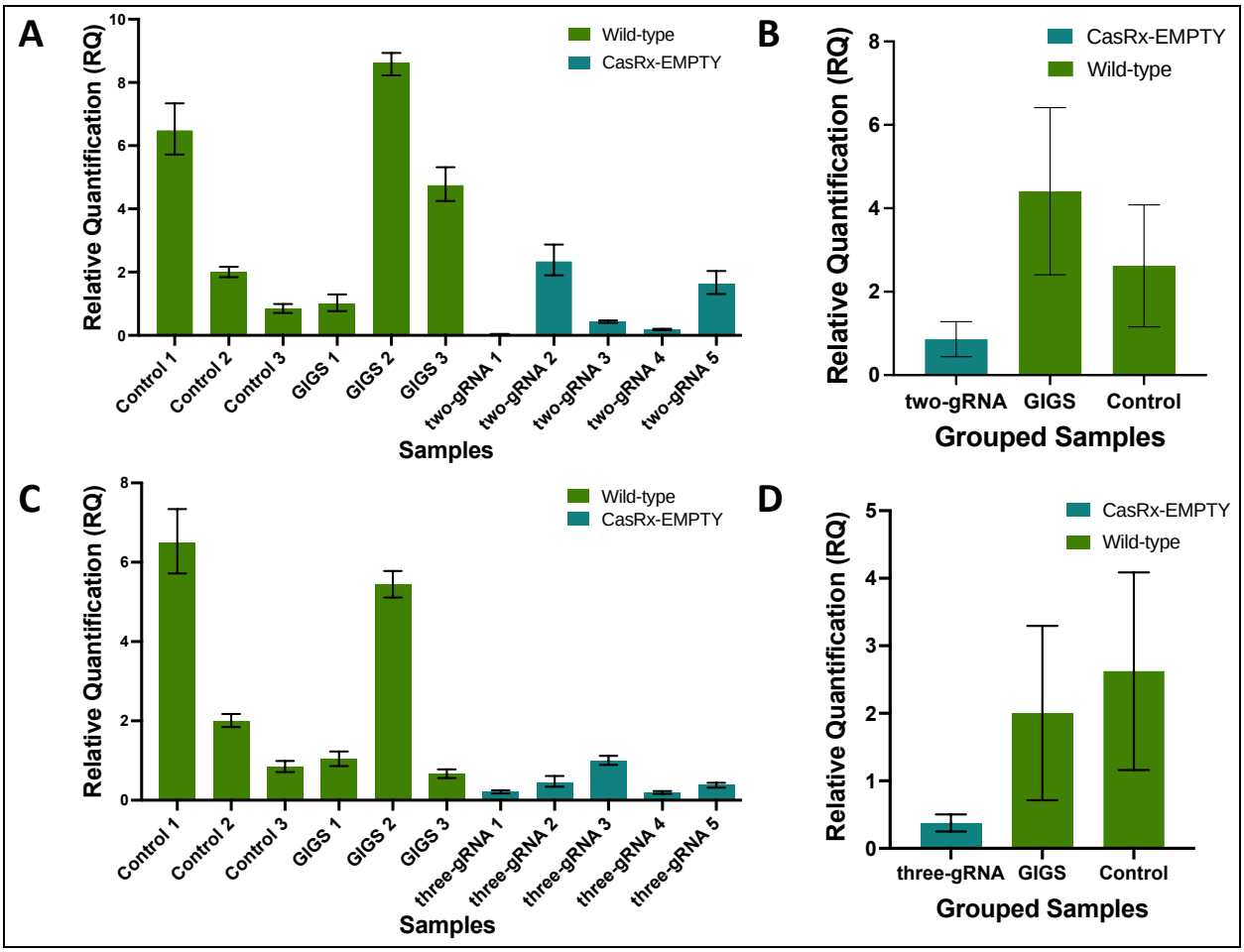

Figure 3.7. Relative quantification of GVA in the presence of CasRx, or without CasRx, to assess multi-guide virus inhibition, and guide-induced gene silencing (GIGS). **A**) Relative fold expression of GVA, normalised to the reference sample 'control 3'. The error bars represent the minimum and maximum values of n=3 technical replicates. Samples 'control 1 to 3' represent wild-type plants infiltrated with the TRV-EMPTY construct, and the GVA clone two days later. Samples labelled 'GIGS 1 to 3' represent wild-type plants (green) infiltrated with the T1 and T2 two-guide TRV mixture, followed by the GVA clone two days later. Samples labelled 'two-gRNA 1 to 5' represent CasRx-EMPTY plants (turquoise) infiltrated with the T1 and T2 two-guide TRV mixture, followed by infection with the GVA clone two days later. **B**) Relative quantification of GVA *CP* expression of the 'two-gRNA' samples grouped biologically. Data represents the mean relative gene expression, ± SEM of the n=3 samples (controls), n=3 samples (GIGS) and n=5 samples (two-gRNA). **C**) Relative fold expression of GVA, normalised to the reference sample 'control 3'. Samples 'control 1 to 3' represent wild-type plants infiltrated with TRV-EMPTY, and GVA two days later. Samples labelled 'GIGS 1 to 3' represent wild-type plants (green) infiltrated with the T1, T2 and T3 three-guide TRV mixture, followed by the GVA clone two days later. Samples labelled 'three-gRNA 1 to 5' represent CasRx-EMPTY plants (turquoise) infiltrated with the T1, T2 and T3 three-guide TRV mixture, followed by the GVA clone two days later. **D**) Relative quantification of GVA *CP* expression of the 'three-gRNA' samples grouped biologically. Data represents the mean relative gene expression, ± SEM of the n=3 samples (controls), n=3 samples (GIGS) and n=5 samples (three-gRNA). Statistical analysis performed using a two-tailed unpaired Student's t-test; with the difference being significant at $p \leq 0.05$ with respect to the control.

Viral reduction by GIGS was compared to viral reduction with the CasRx:gRNA system, in Fig. 3.7. Once again, significant variation was observed among the control samples, with a ~6-fold

difference observed between sample 'control 1' and 'control 3' (Fig. 3.7A and C). The use of pTRV2-EMPTY in the control samples seemed to indicate that no viral competition between GVA and TRV seemed to have taken place, although the variation in the control samples compromised the significance of the result (Fig. 3.7). The possible occurrence of GIGS was assessed, when wild-type plants were infiltrated with three gRNAs. The samples 'GIGS 1 to 3' in Fig. 3.7A represent three biological repeats of GIGS samples, with significant variation among the three samples. Notably, sample GIGS 2 presented the highest GVA accumulation, of all the samples analysed. When CasRx was present, three samples demonstrate GVA interference, when the two-guide system was infiltrated into CasRx-EMPTY plants (Fig. 3.7A). Sample 'two-gRNA 1' showed the lowest GVA accumulation, followed by 'two-gRNA 4' and 'two-gRNA 3', respectively. Samples 'two-gRNA 2 and 5' did not show reduced GVA accumulation, when compared to the control samples. A ~6-fold difference in GVA relative quantification was observed among the CasRx:gRNA samples (Fig. 3.7A). When the samples were grouped biologically, GIGS samples showed no reduction in GVA quantification, compared to the controls (Fig. 3.7B). The 'two-gRNA' group presented a ~3-fold reduction in GVA, when compared to the control group, although the reduction was not significant (Fig. 3.7B).

Fig. 3.7C depicts the relative quantification of GVA when all three CP gRNAs were co-infiltrated. Similarly, GVA quantification exhibited large variation among the three GIGS samples, with sample 'GIGS 2' presenting a ~7-fold difference in GVA expression, compared to 'GIGS 3'. When CasRx-EMPTY plants were infiltrated with all three CP gRNAs, followed by GVA two days later, GVA interference was observed among three of the five samples. Sample 'three-gRNA 4' showed the lowest GVA relative quantification, followed by samples 'three-gRNA 1 and 5', respectively. Among all five three-gRNA samples, a ~3-fold variation in GVA quantification was observed, demonstrating a more consistent GVA quantification, unlike the ~6-fold variation observed in Fig. 3.7A. When the samples were grouped biologically, 'three-gRNA' showed a ~5-fold reduction in GVA accumulation, when compared to the control group (Fig. 3.7D). The GIGS group also showed lower GVA quantification (~>1-fold reduction), compared to the control group. Although a reduction in GVA for both GIGS and 'three-gRNA' samples was observed, the reduction was not significant, when $p \leq 0.05$.

Efficient gRNA expression is necessary to achieve CRISPR/CasRx or GIGS RNA interference (Wessels *et al.*, 2020; Sharma *et al.*, 2022). In order to assess the efficiency of a TRV vector at delivering and expressing the CP gRNA transiently and systemically, RT-qPCR was performed with primers CasRx_gRNA-scaf_F/CP_T2_qPCR_R (Table 3.3), to compare the relative expression of the T2 gRNA, expressed either under the hU6 promoter from the binary pCasRx vector, or under the PEBV promoter, from the TRV2 vector (Fig. 3.8A).

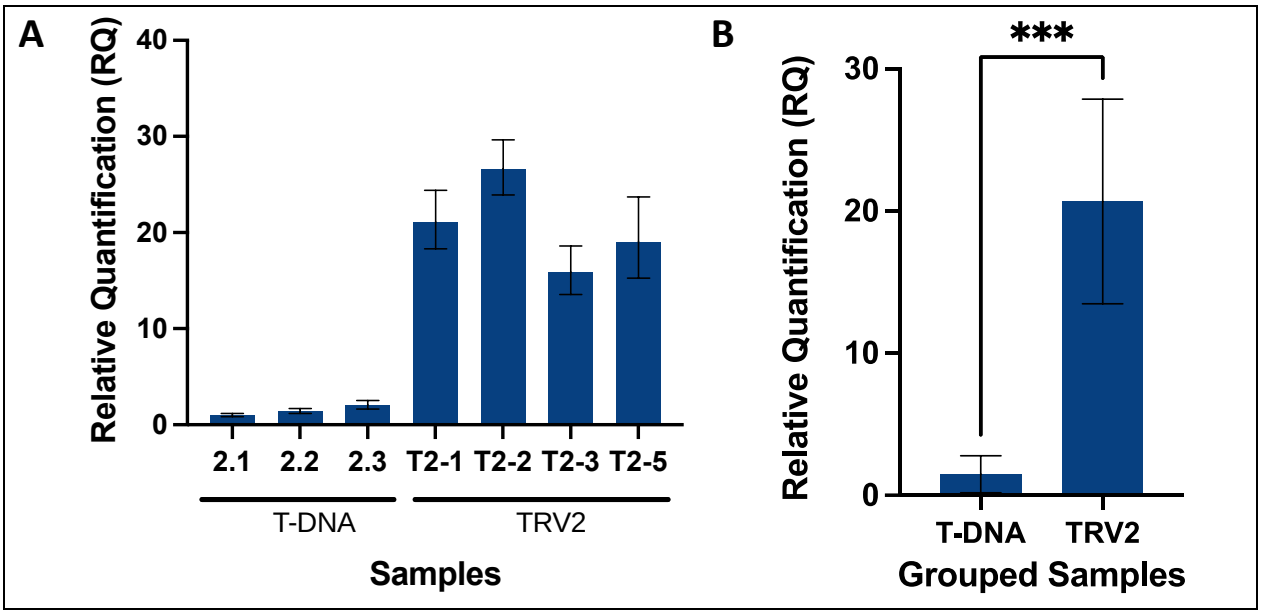

Figure 3.8. Relative expression levels of the T2 gRNA from a regular T-DNA binary vector and a TRV viral vector. **A**) Relative fold expression of T2 gRNA expressed under the hU6 promoter, from the T-DNA of the pCasRx:CP-T2 vector, compared to the expression of T2 gRNA under the PEBV promoter, from the pTRV2:CP-T2 vector. The error bars represent the minimum and maximum values of n=3 technical replicates. **B**) Relative quantification of T2 gRNA expression of the T-DNA samples and TRV2 samples grouped biologically. Data represents the mean relative gene expression, ± SEM of the three and four biological replicates, respectively (n=3, n=4). Statistical analysis performed using a two-tailed unpaired Student's t-test; with the difference being significant at $p \leq 0.05$ with respect to the TRV2 group. *** p=0.0008.

The expression of gRNA T2 from the two different vectors was compared. The relative fold increase in gRNA expression from the TRV2 vector, was >15-fold, when compared to T-DNA sample 2.1. The samples were grouped biologically, and a ~13-fold increase was observed when gRNA T2 was expressed from TRV2, compared to regular T-DNA (Fig. 3.8B).

3.4 DISCUSSION

Plant viruses are responsible for causing agricultural devastation and great economic losses worldwide. The majority of these viruses possess RNA genomes, and in an attempt to control

plant viruses, researchers have utilised the RNA-targeting CRISPR/Cas13 system to confer virus resistance in plants. While this method provides a means of controlling viruses, the efficient delivery of CRISPR components in plant cells has proved a bottleneck to scientists. To overcome this, some viruses have been harnessed and manipulated to deliver genome editing components *in planta*. Specifically, the bipartite virus, TRV, has been harnessed for the efficient expression of gRNAs in numerous studies (Aman, Ali, *et al.*, 2018; Mahas, Aman and Mahfouz, 2019). In the current study, the CRISPR/CasRx system was used for targeting of the RNA grapevine virus, GVA, by employing the conventional T-DNA expression system, and TRV-gRNA expression system in transgenic *N. benthamiana*.

The initial gene expression analysis experiment aimed to assess GVA interference of stably-transformed *N. benthamiana* plants harbouring the pCasRx:Rep constructs. The gRNA was designed to target the replicase gene of GVA; an essential gene responsible for the replication of the virus. One study found that when targeting the replicase gene, efficient RNA interference was observed when CasRx-NES was utilised, although variation among gRNAs was observed (Mahas, Aman and Mahfouz, 2019). In the current study, a significant level of variation was observed among biological repeat samples. The significant variation may be explained by the intrinsic nature of Agro-infiltration, and the variation observed among leaves, when quantitative assays are performed (Bashandy, Jalkanen and Teeri, 2015). To address this variation, biological repeats from the same line were grouped together, in order to simplify analysis. RT-qPCR analysis showed one line, Line 2-T2, which seemed to demonstrate robust GVA interference, when compared to the wild-type and Cas13a-EMPTY control samples. Additionally, Line 2-T2 showed the highest *CasRx* gene expression, seemingly inverse-correlating to the reduced GVA titre. However, when a Pearson correlation coefficient was determined for *CasRx* expression and GVA quantification, no significant correlation was found between the two variables. This result contrasts what the study by Jiao and colleagues found, where RNA targeting was positively correlated with *Cas13a* expression (Jiao *et al.*, 2022). Line 1-T2 and line 7-T2 showed higher GVA titre than both control samples, inferring no GVA interference occurred. It has been shown that the expression of both *CasRx* and the respective gRNA determine the interference efficiency of the CRISPR/Cas13 system (Jiao *et al.*, 2022). However, no correlation between *CasRx* expression and GVA quantification was found in this experiment, while the gRNA expression was not assessed. A study found that the limiting factor of the CRISPR/CasRx system was gRNA expression (Yu *et al.*, 2022). Not only is the

efficient expression of the gRNA necessary for virus interference, but recent literature has revealed the necessity of the target RNA to be accessible (Aman, Ali, *et al.*, 2018; Wessels *et al.*, 2020). When the respective replicase targets were designed, the target RNA folding and secondary structure was not analysed in depth, and this may also be a contributor to the varying results shown in Fig. 3.3. Indeed, when these were analysed, gRNA T2 was found to target a more accessible RNA region than T1, albeit both gRNAs not targeting completely accessible RNA regions.

Due to the ambiguous results discussed above, three new gRNAs were designed which targeted the *CP* gene of GVA, a common gene targeted in literature (Aman, Ali, *et al.*, 2018; Aman, Mahas, *et al.*, 2018). The activity of the CRISPR/Cas13 system is dependent on the target RNA secondary structure (Abudayyeh *et al.*, 2017; Mahas, Aman and Mahfouz, 2019; Bandaru *et al.*, 2020; Wessels *et al.*, 2020), and a study found that the most effective gRNAs with the strongest interference were clustered together, indicating gRNAs in more accessible regions resulted in better Cas13 activity (Abudayyeh *et al.*, 2016). Importantly, the central seed region of the gRNA should target single-strand RNA regions for efficient RNA interference (Bandaru *et al.*, 2020). Therefore, the CP gRNAs for this experiment were clustered together, within a more accessible region of ORF4, and the accessibility of the central seed region was emphasised during the selection process.

Transient assays to assess the virus interference efficiencies of the newly-designed gRNAs were performed as preliminary tests. Of the three gRNAs assayed transiently, T1 demonstrated GVA interference, as three samples demonstrated significantly reduced GVA levels in the test sample, when compared to the control (Fig. 3.4A). One study by the Aman group found that when transient assays were performed, a 50% reduction in virus accumulation was observed (Aman, Ali, *et al.*, 2018). It is important to note that the binary vector used in the Aman group study harboured the *Cas13a* gene, while the gRNAs targeting TuMV-GFP were expressed by the TRV delivery system, and successful TuMV-GFP targeting was observed 7-dpi in systemic leaves. A clear difference between the Aman group study, and the current study, is that the gRNA in this study was expressed from the binary vector, under the hU6 promoter, and not from TRV under the PEBV promoter. Similarly, another study found that when the expression of the CasRx gRNA was driven by the AtU6 promoter, no efficient RNA targeting was achieved, and when the

promoter was exchanged for the CmYLCV promoter, RNA interference was remarkably increased (Yu *et al.*, 2022). As mentioned previously, efficient gRNA expression is necessary for virus inhibition with CasRx (Yu *et al.*, 2022), and may explain why the transient assays gave negative results. Thus, utilisation of the TRV-expression system for gRNA delivery may provide more robust results.

By harnessing the constitutively expressed CasRx protein, and delivering the gRNAs transiently with TRV, multiple gRNAs could be assayed in parallel. For CRISPR/CasRx expression analysis, the CP-targeting gRNAs were delivered into transgenic CasRx-EMPTY plants. Fig. 3.5A depicted three samples which show reduced GVA quantification. For this experiment, the wild-type control samples infiltrated with T1 gRNA were used as control. Importantly, prior to this experiment, there had not been sufficient literature regarding the occurrence of GIGS (Sharma *et al.*, 2022). GIGS functions in the absence of Cas13, where the gRNA alone can elicit reductions in viral RNA (Sharma *et al.*, 2022). Considering the possibility of GIGS, our control may not have been accurate, as GIGS may have influenced the virus accumulation. Ultimately, the results for T1 did not show much consistency, with some samples indicating more GVA quantification than the control samples. The results of T2 presented more consistent GVA quantifications, and virus interference seemed to have taken place. The correlation which exists between the gRNA expression levels and the GVA quantification (–0.7738) indicated that GVA quantification was dependent on gRNA expression, which was corroborated by previous literature (Yu *et al.*, 2022).

Each CP gRNA demonstrated different levels of GVA interference, with T2 resulting in the lowest GVA accumulation in one sample (~8-fold reduction). The varying efficiencies of gRNAs has been observed previously in literature, and may be explained by the formation of secondary structures within the RNA target region, or the presence of RNA binding proteins which can affect the accessibility of the Cas13 nuclease with the target RNA (Aman, Ali, *et al.*, 2018). Therefore, the RNA target accessibility is an important factor which governs the activity of Cas13 (Aman, Ali, *et al.*, 2018). The difference in efficiency of T1, T2 and T3 may be as a result of the accessibility of the target RNA. A study found that the efficiency of the gRNA can be diminished if the seed region of the target RNA is not entirely accessible (Wessels *et al.*, 2020). In contrast to this, all 8 nts of the seed region of T1 and T3 are supposedly accessible, while only 6 nts of the T2 seed region are accessible. The study by Wessels *et al*. (2020) determined that gRNAs ranked within the top two

quartiles (Q4 and Q3) resulted in more efficient RNA interference than gRNAs ranked in the bottom two quartiles (Q2 and Q1). Interestingly, T2 was ranked the 3rd gRNA (Q4), while T1 was ranked 90th (Q3), and T3 was ranked 164th (Q3), which supports the finding in this study, that T2 seemed to result in the highest virus interference. Another important factor which can determine targeting efficiency is the secondary structure formation within the CasRx-gRNA-scaffold, as this determines binding of the CasRx:gRNA complex and target localisation (C. Zhang *et al.*, 2018). Of the three CP gRNAs, T2 showed the most precise folding with the scaffold sequence (C. Zhang *et al.*, 2018; Mahas, Aman and Mahfouz, 2019), while T3 had the least precise folding (Supplementary Fig. 5C), also supporting the finding that T2 was the more efficient gRNA.

As mentioned before, the control samples in the experiment discussed above, may not have been accurate due to the possible occurrence of GIGS. Therefore, subsequent experiments were performed to investigate this. It was shown from literature that a multi-guide system resulted in more robust RNA interference, compared to single gRNA systems (Sharma *et al.*, 2022). Thus, CasRx-EMPTY plants were infiltrated with multiple gRNAs simultaneously, to assess interference compared to a single gRNA system. In parallel, wild-type *N. benthamiana* plants were infiltrated with the same multi-guide suspensions, to assess the occurrence of GIGS. GVA quantification was lowest in the CasRx:three-guide samples, while the GIGS samples did not indicate decreased GVA accumulation when the samples were grouped biologically (Fig. 3.6B). This result was corroborated by literature, which described that RNA interference was most efficient when the Cas13 nuclease was present, although interference was possible without Cas13 (Sharma *et al.*, 2022). The lack of interference by GIGS may be explained by the fact that the CP gRNAs designed in this study were only 23 nts in length. The efficiency of RNA interference by GIGS increases with increased gRNA length, and guides below 20 nts in length did not result in GIGS (Sharma *et al.*, 2022). For GIGS to result in viral interference, the gRNA length should be between 24 to 28 nts in length (Sharma *et al.*, 2022). An interesting observation from Fig. 3.6C, was the lower GVA accumulation when three gRNAs were present and expressed from TRV, compared to the control samples which were not infiltrated with gRNAs. To understand if the reduction in GVA was due to viral competition between TRV and GVA, a control to investigate this was included in the next experiment, and no viral competition between GVA and TRV was suggested, although the variation among the control samples compromised the significance of the results.

The constructs pTRV1 and pTRV2-EMPTY were infiltrated together as a negative control. A two- and three-guide approach was utilised, and CasRx:gRNA samples in Fig. 3.7B and Fig. 3.7D both showed lower GVA accumulation when compared to the GIGS and control samples, although the reduction was not significant. This result was supported by a study which found that a multi-guide approach, in the presence of Cas13, results in increased RNA interference (Sharma *et al.*, 2022). When the two-guide system was compared to the three-guide system, the latter system seemed to cause more efficient virus interference (Fig. 3.7D). Once again, GIGS did not seem to result in much GVA interference, most likely due to the length of the gRNAs (Sharma *et al.*, 2022). It is important to note that in this study, the CasRx localisation signal was a nuclear localisation signal (NLS). However, one study found that the CasRx nuclease fused to a nuclear export signal (NES) resulted in the highest RNA interference when targeting RNA viruses, while CasRx-NLS also demonstrated RNA virus interference, albeit at a lower efficiency (Mahas, Aman and Mahfouz, 2019). This observation was most likely explained by the simultaneous localisation of CasRx and the RNA virus, which replicates in the cytoplasm (Mahas, Aman and Mahfouz, 2019). Additionally, the significant variation observed among samples may be due to the Agro-infiltration process. A study found high within-leaf variation, as well as between-leaf variation, existed when quantitative assays were performed in *N. benthamiana* (Bashandy, Jalkanen and Teeri, 2015). This variation may play a part in the ambiguous results obtained, and by increasing the number of biological repeats, more comprehensive results may be obtained.

Due to the lack of targeting efficiency with the transient assays (Fig. 3.4), gene expression analysis was performed to assess the gRNA expression under the hU6 promoter, and compare it to the TRV-based gRNA expression under the PEBV promoter (Fig. 3.8). The analysis clearly demonstrated the difference in expression levels (~13-fold) and confirmed that gRNA delivery and expression from the TRV-PEBV system is more efficient. This possibly explains the observation that no GVA inhibition was observed with the transient assays when the gRNA was expressed from T-DNA, but only with the stable experiments when expressed under PEBV from TRV2. As mentioned previously, one study found that expression of the gRNA under the AtU6 promoter did not result in efficient RNA targeting, and by replacing AtU6 with CmYLCV, more efficient interference was observed (Yu *et al.*, 2022). The study also concluded that efficient gRNA expression was essential for virus interference (Yu *et al.*, 2022), and may explain why no GVA interference was observed in the transient assays of the current study.

In conclusion, when the replicase gene was targeted, one line seemed to result in GVA interference. However, the inconsistencies of GVA targeting with the replicase gRNAs led to the design of CP gRNAs. More efficient and consistent targeting was observed with the CP gRNAs, specifically T2, when *CasRx*-expressing plants were infiltrated with the TRV-delivered gRNAs. The multi-guide infiltrations proved to result in lower GVA accumulation, specifically when all three CP gRNAs were co-infiltrated. Additionally, it was found that GIGS did not result in RNA interference in this case. Future considerations to improve GVA targeting might include using the CasRx-NES variant, as replication of GVA occurs in the cytoplasm, and CasRx-NES may prove more efficient, by synchronising the localisation of CasRx and viral replication. Although TRV-gRNA expression was relatively efficient in this study, the use of viral RNA silencing suppressors co-expressed with TRV can further improve expression of the system (Chiong, Cody and Scholthof, 2021). Importantly, the design of efficient gRNAs is essential to achieve RNA targeting, taking into consideration the use of multiple gRNAs and secondary structure formation.

Chapter 4: The implementation of a geminivirus-based pRIC vector for the delivery of CRISPR/Cas9 components

4.1 INTRODUCTION

The small geminivirus, bean yellow dwarf virus (BeYDV), from the family *Geminiviridae*, possesses the ability to infect a number of plant species, including major crops (Rey *et al.*, 2012). Several features make geminiviruses attractive for genome editing; their wide host range, replication initiation with the Rep protein alone, and replication by rolling circle amplification which results in high amounts of replicons (Hanley-Bowdoin *et al.*, 2013). The deconstruction of the geminivirus into an efficient expression vector has allowed for the convenient delivery of genome editing components in plant cells. The commonly-employed BeYDV vector has been harnessed for genome editing technology in a multitude of studies (Table 2.1) and has proven effective in the delivery of template DNA and genome editing components. BeYDV has been successfully used in both knockout and knock-in modifications *in planta*.

In one example, a study by Olivares and colleagues employed a BeYDV-based vector to express the key components of the CRISPR/Cas9 system, to cause large deletions within putative susceptibility genes in order to induce fungal tolerance in grapevine (Olivares *et al.*, 2021). Another example employed a geminivirus replicon (GVR) to deliver single-strand nucleases (SSNs) and repair templates in plants, with the aim of increasing herbicide resistance in potato plants, using knock-in modifications (Butler *et al.*, 2016). Similarly, a knock-in modification was made when anthocyanin biosynthesis was enhanced in tomato plants, by the insertion of a strong promoter, resulting in precise and heritable mutations (Čermák *et al.*, 2015).

The pRIC vector employed in the current study is similarly based on the BeYDV vector, and has been shown to produce high yields of recombinant proteins *in planta* (Regnard *et al.*, 2010). Convenient characteristics of pRIC are the *cis*-acting *REP* gene, which encodes the replication-associated proteins (Rep and RepA), while the transgene to be expressed replaces the *MP* and *CP* genes, rendering the vector unable to move systemically (Regnard *et al.*, 2010). After Agro-infiltration and expression, the Rep proteins are responsible for replicational release and re-circularisation of the replicon, as well as rolling-circle replication, resulting in high transgene copy numbers.

The employment of transient assays in *Nicotiana benthamiana* allowed for the confirmation of the pRIC vector's ability to successfully express the genome editing components of the CRISPR/Cas9 system. The large *Cas9* gene and the specific guide RNA (gRNA) were both individually expressed in *N. benthamiana*, by pRIC. The expressed CRISPR/Cas9 components were programmed to target both exogenous and endogenous DNA, to assess the effectiveness of the system following subsequent delivery and expression by pRIC. Additionally, the expression of *Cas9* was quantified, in order to determine the expression levels of the large *Cas9* gene from pRIC. Subsequent gene editing by CRISPR/Cas9 was analysed to elucidate the efficiency of the system for DNA targeting.

4.2 MATERIALS AND METHODS

4.2.1 Design of gRNA targets

To assess the ability of pRIC-Cas9 to target endogenous *N. benthamiana* DNA, one gRNA target was designed against the *N. benthamiana* phytoene desaturase (*PDS*) gene and two gRNAs were designed against the constitutively expressed green fluorescent protein (*GFP*) gene of the transgenic *N. benthamiana* 16c line (hereafter referred to as 16c). The software CRISPR-P 2.0 (http://crispr.hzau.edu.cn/CRISPR2/) and RGEN-Tools Cas-Designer (http://www.rgenome.net/cas-designer/) were used to design the gRNAs. gRNA candidates were selected based on the software-specific score, GC content and number of putative off-targets in the *N. benthamiana* genome. The software RGEN-Tools Cas-OFFinder (http://www.rgenome.net/cas-offinder/), and BLASTN (https://blast.ncbi.nlm.nih.gov/Blast.cgi) was used to detect putative off-target matches for candidate target sequences in *N. benthamiana*. High-scoring candidate targets were selected with the sequence 5'-A/TN_{19}GG-3', a GC content >40%, and no off-target matches when 0-, 1- or 2-mismatches were permitted between the target sequence and the gRNA. The secondary structure of the gRNA and scaffold sequence [(20nt target) GTTTTAGAGCTAGAAATAGCAAGTTAAAATAAGGCTAGTCCGTTATCAACTT GAAAAAGTGGCACCGAGTCGGTGCTTTTTTT] were assessed using the programs mFold (http://www.unafold.org/mfold/applications/rna-folding-form.php) and RNAfold (http://rna.tbi.univie.ac.at/cgi-bin/RNAWebSuite/RNAfold.cgi). The gRNA targets were designed to contain BsaI-overhangs on their 5'-ends (Table 4.1)

Table 4.1. Primers used for gRNA expression cassette preparation and cloning, Sanger sequencing and RT-qPCR expression analysis.

Primer name	Sequence 5'-3'	Tm (°C)	Amplicon (bp)
UF	CTCCGTTTTACCTGTGGAATCG	55.7	N/A
gR-R	CGGAGGAAAATTCCATCCAC	53.6	
Pps-R	TTCAGAACCTGGTATGGAATCGGCAGCAAAGG	64.5	486
Pps-L (SacI)	AGCGTGGAGCTCATCCATCCACTCCAAGCTC	67.2	
NbPDS_guide_F	gtcaTCACAAACCGATATTGCTGG	56.3	N/A
NbPDS_guide_R	aaacCCAGCAATATCGGTTTGTGA	57.2	
16c-gfp_guide_F1	GTCATTCGGCCGAGGATAATGAT	56.9	N/A
16c-gfp_guide_R1	AAACATCATTATCCTCGGCCGAA	56.6	
16c-gfp_guide_F2	GTCATTCGTTGGGATCTTTCGAAA	55.6	N/A
16c-gfp_guide_R2	AAACTTTCGAAAGATCCCAACGAA	55.2	
pRIC_sequeincing_F	TTAATATTACCGGCGTGGCC	54.6	776
pRIC_sequeincing_R	TCAACACATGAGCGAAACCCT	56.4	
Exon_4_NbPDS_seq_F	AACTTGTTCTTCAACTTGGCTTG	54.2	~520
Exon_4_NbPDS_seq_R	AAAGCTGGAAATTTTTAGGACAGA	53.0	
Exon_4_NbPDS(b)_R	AGCCTTCCTGAACAGGGACT	58.2	
mgfp5ER_Fw	AGGAGATATAACAATGAAGACTAAT	49.1	805
mgfp5ER_R	TTAAAGCTCATCATGTTTGT	47.4	
16c2_gRNA_seq_F	CAAGACACGTGCTGAAGTCAA	55.5	N/A
16c1_gRNA_seq_R	CCGTCGTCCTTGAAGAAGAT	54.4	
gfp_pRIC_qPCR_F	AGCTGACCCTGAAGTTCATCTG	56.1	127
gfp_pRIC_qPCR_R	AAGTCGTGCTGCTTCATGTG	55.6	
Cas9qPCR_F	TTTCGTTGAGCAGCACAAGC	56.5	88
Cas9qPCR_R	GTTTGCATCAGCGAGGATCAC	56.3	

4.2.2 Construction of pRIC-gRNA vectors

The targets were ordered and synthesised as single strand DNA (ssDNA) oligonucleotides (oligos), from IDT (Integrated DNA Technologies, USA). Adapter preparation consisted of annealing the ssDNA oligos in a reaction containing 1µL forward oligo (100µM), 1µL reverse oligo (100µM), 4µL 1xTE buffer, and dH_2O to a final volume of 10µL. The reactions were incubated as described in

Chapter 3. Cloning of the gRNA expression cassette into pRIC 3.0 was adapted from Ma and Liu (2016). The annealed target adapters were ligated into the intermediate vector pYLsgRNA-AtU3d/LacZ (Addgene; plasmid #66201) in a BsaI-digestion/ligation reaction (Fig 4.1A).

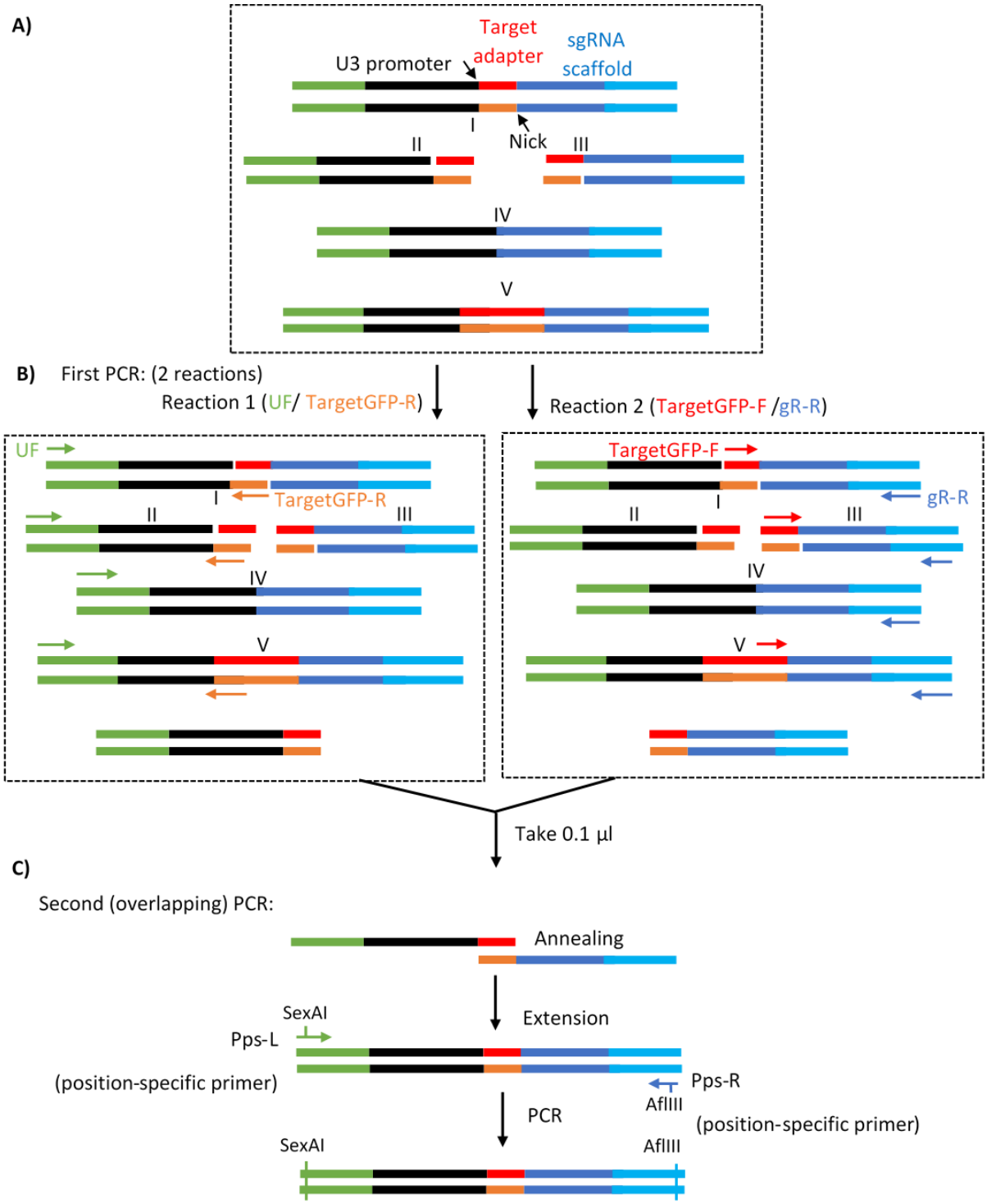

Figure 4.1. Adopted strategy for the construction of the gRNA expression cassette. **A**) BsaI-digestion/ligation reaction with the gRNA intermediate plasmid (pYLsgRNA-AtU3d/LacZ) and the annealed target adapter, resulting in various products (I-V), where abnormal IV and V products contain no target adapter or a doubled target adapter respectively. **B**) First PCR step containing two PCRs using the primer

sets UF/Target-R and Target-F/gR-R for PCR 1 and 2 respectively. Target-F and Target-R are the forward and reverse adapter oligos (Table 4.1). Product IV is not amplified in either PCR, while type V is amplified and produces the correct type II (PCR 1) and III (PCR 2) products. **C**) The (overlapping) nested PCR using position-specific primers (Table 4.1) to amplify the final gRNA expression cassette, containing the SexAI and SacI restriction sites for cloning into pRIC 3.0. This figure was adapted from (Duxbury, 2020) and (Ma and Liu, 2016).

The reaction was set up as follows: 20ng pYLsgRNA-AtU3d/LacZ, 0.4µL annealed adapters, 1µL 10x CutSmart Buffer (NEB, USA), 4U BsaI (NEB, USA), 2.5U T4 DNA Ligase (Thermo Fisher Scientific, USA), 0.5µL 10x T4 DNA Ligase buffer (Thermo Fisher Scientific, USA), and dH_2O to a final volume of 10µL. The thermocycler parameters were set to: 5 x (37°C/5mins + 20°C/5mins). The digestion/ligation reaction was diluted 10-fold, prior to PCR amplification. The diluted ligation product was PCR amplified with two PCR reactions: PCR 1) primer set UF/Target-R; PCR 2) primer set Target-F/gR-R (Table 4.1) (Fig 4.1B), to a final volume of 40µL. PCR cycle conditions were set to: 98°C/30sec + 28 x (98°C/10sec + 60°C/15 sec + 72°C/20sec) + 72°C/5mins + 4°C hold. PCR products from PCR 1 and 2 were visualised on a 1% (w/v) agarose gel by loading 3µL of the PCR product to confirm the successful amplification of bands 143 bp and 364 bp, respectively. Subsequently, a nested (overlapping) PCR was set up for each gRNA cassette using 1µL of product from PCR 1 and PCR 2 as the template, with position-specific primer set Pps-R/Pps-L (SacI) (Table 4.1). Thermocycler conditions were set to: 98°C/30sec + 22 x (98°C/10sec + 58°C/15sec + 72°C/20sec) + 72°C/5mins + 4°C hold. The PCR product containing the SexAI and SacI recognition sites was visualised on a 1% (w/v) agarose gel to confirm the correct gRNA expression cassette (Fig. 4.1C) with a band length of 486 bp. The 486 bp band was excised from the agarose gel and purified using the Zymoclean Gel DNA Recovery Kit (Zymo Research, USA), following the manufacturer's instructions, followed by DNA concentration and purity evaluation using spectrophotometry (Nanodrop 2000; Thermo Fisher Scientific, USA).

The purified expression cassette and binary vector pRIC 3.0 were both digested with SexAI and SacI. The reactions were set up using 1µg of DNA, 5µL of 10x CutSmart Buffer (NEB, USA), 5U of SexAI (Fermentas, USA), 20U of SacI-HF (NEB, USA), and dH_2O to a final volume of 50µL. The reactions were incubated at 37°C for 3 hours. Digestion reactions were resolved on a 1% (w/v) agarose gel, after which the pRIC 3.0 band of 5135 bp and the gRNA cassette bands of roughly 480 bp, were excised, gel purified and quantified as described previously. A ligation reaction was set up using a 4:1 (insert:backbone) ratio, 2µL 10X T4 DNA Ligase Buffer (Thermo Fisher Scientific,

USA), 5U T4 DNA Ligase (Thermo Fisher Scientific, USA), and dH_2O to a final volume of 20µL, and incubated overnight at 4°C. The ligation reaction was transformed into DH5α chemically competent *E. coli* cells using 5µL of the reaction by heat-shock transformation, and the cells were plated on selection plates containing 100µg/mL ampicillin. An end-point PCR using the primers Pps-R/Pps-L (SacI) (Table 4.1) was used to screen for positive colonies, and the thermocycler conditions were set as described previously. Positive colonies were inoculated in 5mL liquid Luria-Bertani (LB) containing 100µg/mL ampicillin, and incubated at 37°C overnight, shaking at 180 revolutions per minute (rpm). A plasmid isolation was performed using the GeneJet Plasmid Miniprep Kit (Thermo Fisher Scientific, USA), following the manufacturer's instructions. Plasmid concentration was assessed with spectrophotometry as previously described. The final plasmids harbouring the respective gRNA cassettes (pRIC-gRNA) were confirmed by Sanger sequencing using the primers pRIC_sequencing_F/pRIC_sequencing_R (Table 4.1) at the Central Analytical Facilities (CAF) (Stellenbosch University, Stellenbosch, SA).

4.2.3 Agro-infiltration of *N. benthamiana* plant material

The binary pRIC-gRNA constructs harbouring the gRNAs targeting *PDS*, *GFP* Target-1 or *GFP* Target-2, were individually electroporated into *A. tumefaciens* strain GV3101::pMP90RK electrocompetent cells using 400ng of DNA, under these conditions: 1.8kV, 25µF, and 200Ω. Transformed cells were grown on selected plates containing 50µg/mL carbenicillin, 30µg/mL kanamycin, and 50µg/mL rifampicin. Plates were incubated at 27°C for 72 hours. An end-point PCR with the primers Pps-R/Pps-L (SacI) (Table 4.1) were used to screen for positive colonies; and the thermocycler conditions were: 95°C/2min + 25 x (95°C/30sec + 58°C/30sec + 72°C/30sec) + 72°C/5mins + 4°C hold. Single colonies were grown in liquid cultures containing 10mM MES (pH 5.6), 20µM acetosyringone, and suitable antibiotics. Liquid cultures were incubated with agitation overnight (27°C, 150rmp). Overnight cultures were centrifuged at 1000rcf for 15 minutes at room temperature, and resuspended in infiltration buffer (10mM MES [pH 5.6], 10mM $MgCl_2$, 200µM acetosyringone) to a final OD_{600} of 0.25. The resuspended cultures were incubated in the dark at ambient room temperature for 2 hours. Cultures were mixed at a 1:1 ratio, and the desired mixtures were infiltrated by *Agrobacterium*-mediated infiltration. Mixed cultures were infiltrated into the underside of three fully expanded four-week old wild-type *N. benthamiana* or 16c leaves grown under long-day conditions (16-hour light, 8-hour dark at 25°C), using a needleless 2mL syringe (Fig. 4.2).

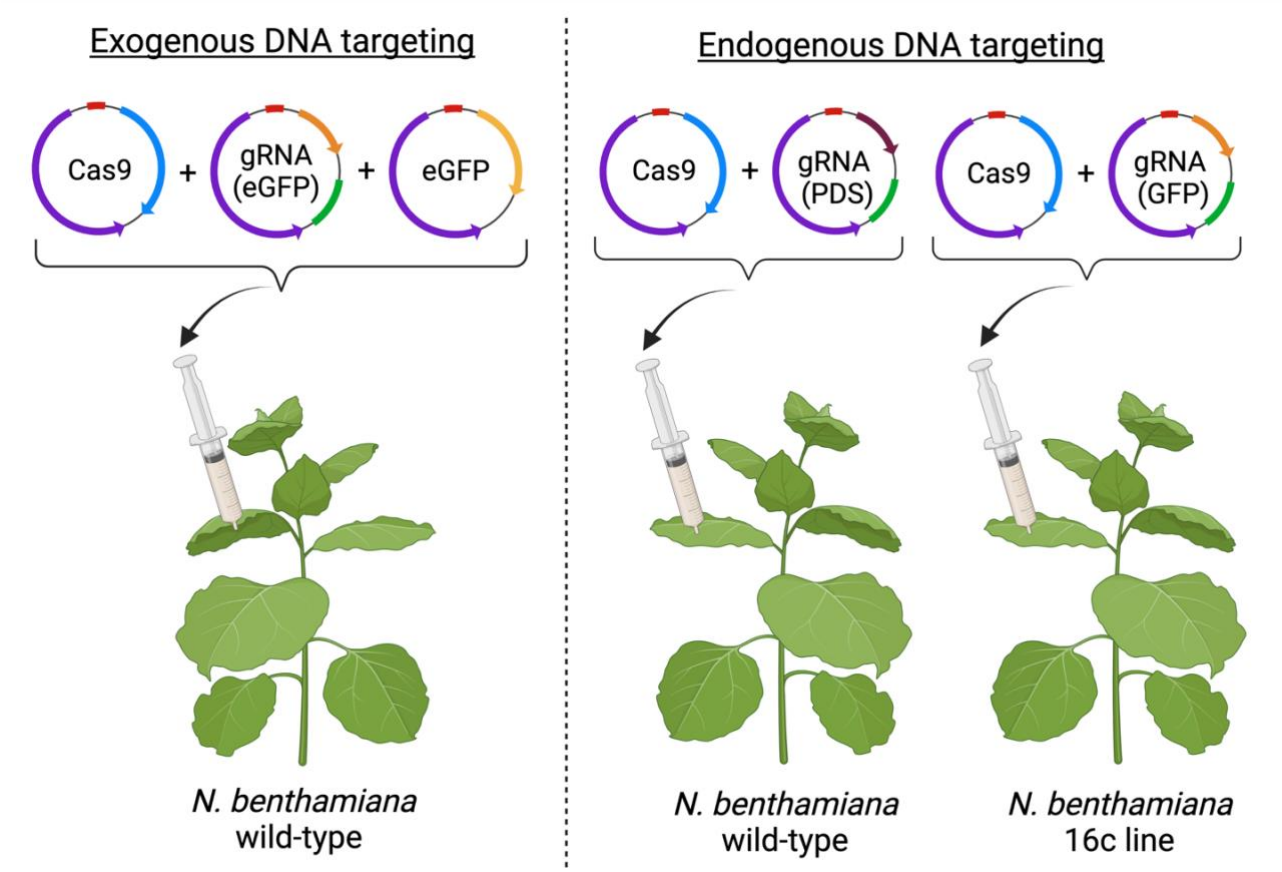

Figure 4.2. Schematic representing the Agro-infiltration experiment layout for the exogenous DNA targeting experiment and the endogenous DNA targeting experiment. *A. tumefaciens* cultures of respective constructs were at an OD_{600} of 0.25. Cultures were mixed at 1:1 ratio prior to infiltration into *N. benthamiana* lines.

4.2.4 GFP fluorescence imaging

The infiltrated plants were kept in a growth room (16-hour light, 8-hour dark, 25°C) and GFP fluorescence was monitored with a hand-held UV lamp. GFP fluorescence was monitored from 3-days post-infiltration (dpi), and photographed at 5-dpi.

4.2.5 DNA extraction and indel analysis

Infiltrated *N. benthamiana* wild-type and 16c leaf material were harvested 5-dpi and aliquoted (200mg) into 2mL Eppendorf tubes, and subsequently finely ground with an Eppendorf grinder. Ground leaf material was subjected to a DNA extraction following a standard Cetyltrimethylammonium bromide (CTAB) method (Murray and Thompson, 1980). DNA was resuspended in 40µL of dH_2O and quantified as previously described. Dilutions of the DNA

samples were made (50ng/µL) and used as the template for PCR amplification of the desired gene. A high-fidelity DNA polymerase (Phusion® High-Fidelity DNA Polymerase; NEB, USA) PCR was performed using the respective primers; Exon_4_NbPDS_seq_F/Exon_4_NbPDS_seq_R and mgfp5ER_Fw/mgfp5ER_R (Table 4.1). Thermocycler conditions were set to: 98°C/10sec + 35 x (98°C/30sec + 62°C/30sec + 72°C/20sec) + 72°C/5mins + 4°C hold and 98°C/10sec + 35 x (98°C/30sec + 57°C/30sec + 72°C/30sec) + 72°C/5mins + 4°C hold, respectively. The PCR products were visualised on a 1% agarose (w/v) gel, excised, purified and quantified as described previously. Purified products were analysed by Sanger sequencing using the primers Exon_4_NbPDS_seq_F/Exon_4_NbPDS_seq_R and 16c2_gRNA_seq_F/16c1_gRNA_seq_R, respectively (Table 4.1) at CAF (Stellenbosch University, Stellenbosch, SA). Sanger sequencing data files (.ab1) were analysed on the Inference of CRISPR Edits (ICE) v2 software (https://ice.synthego.com/#/), by inputting the respective gRNA sequence (excluding PAM sequence), the wild-type control file and the putatively edited sample file. Indel prediction was performed using two software; inDelphi (https://indelphi.giffordlab.mit.edu/) and FORECasT (https://partslab.sanger.ac.uk/FORECasT). A 50 bp flanking sequence on either side of the predicted cut site (3 bp upstream of PAM) was provided as the input for the inDelphi software, while a 50 bp sequence including the gRNA and PAM sequence was inputted into FORECasT, and the prediction outcomes were compared.

4.2.6 RNA extraction and cDNA synthesis

Infiltrated wild-type *N. benthamiana* leaf material was harvested 5-dpi, and the three infiltrated leaves per plant were pooled together and subsequently frozen in liquid nitrogen. The pooled material was then finely ground with liquid nitrogen in a mortar and pestle, and aliquots of 100mg were made in 2mL Eppendorf tubes. Total RNA was extracted from the 100mg aliquots as described in Chapter 3, and cDNA synthesis was performed as described in Chapter 3. RNA of stably-transformed *N. benthamiana* plants harbouring the *Cas9* gene (extracted previously) was subjected to a DNase treatment using RQ1 RNase-Free DNase (Promega, USA), following the manufacturer's instructions. cDNA synthesis of treated RNA was performed as previously described, using 9µL of treated RNA. cDNA synthesis was confirmed as previously described.

4.2.7 Reverse transcription quantitative-PCR (RT-qPCR) expression analysis

The cDNA dilution and RT-qPCR reaction were set up as described in Chapter 3. The housekeeping gene Adenine phosphoribosyltransferase like (*APR*) (Liu *et al.*, 2012) was chosen as the internal control (Table 3.3), and the desired RT-qPCR primer sets for gene expression analysis are listed in Table 4.1. The comparative C_T ($\Delta\Delta C_T$) method was selected, the cycle parameters were set for Standard cycling mode (Primer $T_m \geq$ 60°C): 50°C/2min + 95°C/2min + 40x (95°C/15sec + 60°C/1min), and the melt curve parameters were set as the default settings. The $2^{-\Delta\Delta CT}$ method was used to calculate the gene expression levels, relative to the reference sample, in the online Design and Analysis app (Thermo Fisher Scientific, USA). The error bars serve as an indication between the RQ minimum and RQ maximum for the sample. A confidence interval of 95% was used.

4.2.8 Statistical analysis

The relative gene expression of *eGFP* and *Cas9* were analysed statistically using a two-tailed unpaired Student's t-test. GraphPad Prism Version 9.1.1 (GraphPad Software, USA) software was used to compute the analysis, by comparing the test- or sample-group to the control- or sample-group. Data represents the mean ± standard error of the mean (SEM), and the significance determination was set at $p \leq 0.05$.

4.3 RESULTS

4.3.1 gRNA target design

In a previous study, targets were designed to target exogenous GFP, expressed from a pRIC vector. To compare exogenous DNA targeting to endogenous DNA targeting, gRNAs were designed which targeted the endogenous *PDS* gene of *N. benthamiana* (*NbPDS*), and the *GFP* gene of the transgenic *N. benthamiana* 16c line. *PDS* and *GFP* were selected as the target genes as both genes could potentially result in a detectable phenotype if successfully knocked-out. The *N. benthamiana* genome contains two *PDS* genes (Komatsu *et al.*, 2020). These are involved in the carotenoid biosynthetic pathway, and it has been demonstrated in literature that knockout of the genes results in reduced carotenoid accumulation and ultimately causes an albino phenotype (Naing *et al.*, 2019). 16c plants are constitutively expressing *GFP* which can be visualised under a UV light, and subsequent knockout of the gene should result in decreased GFP fluorescence.

The gRNAs consisted of 20 nucleotides (nts) (excluding the 3-nt PAM sequence), and their targets were located on either DNA strand. The AtU3 promoter was selected to drive gRNA expression and therefore target sequences which began with an A/T nt were selected, as AtU3 promoters require an A/T nt at the start of the target for initiating transcription. The gRNA targeting *NbPDS* was designed in exon 4 of the genes (Fig. 4.3A) and targets both *NbPDS* genes, while two gRNAs at the 5'- (*GFP* Target-1) and 3'-end (*GFP* Target-2) of *GFP* were designed for targeting (Fig. 4.3B).

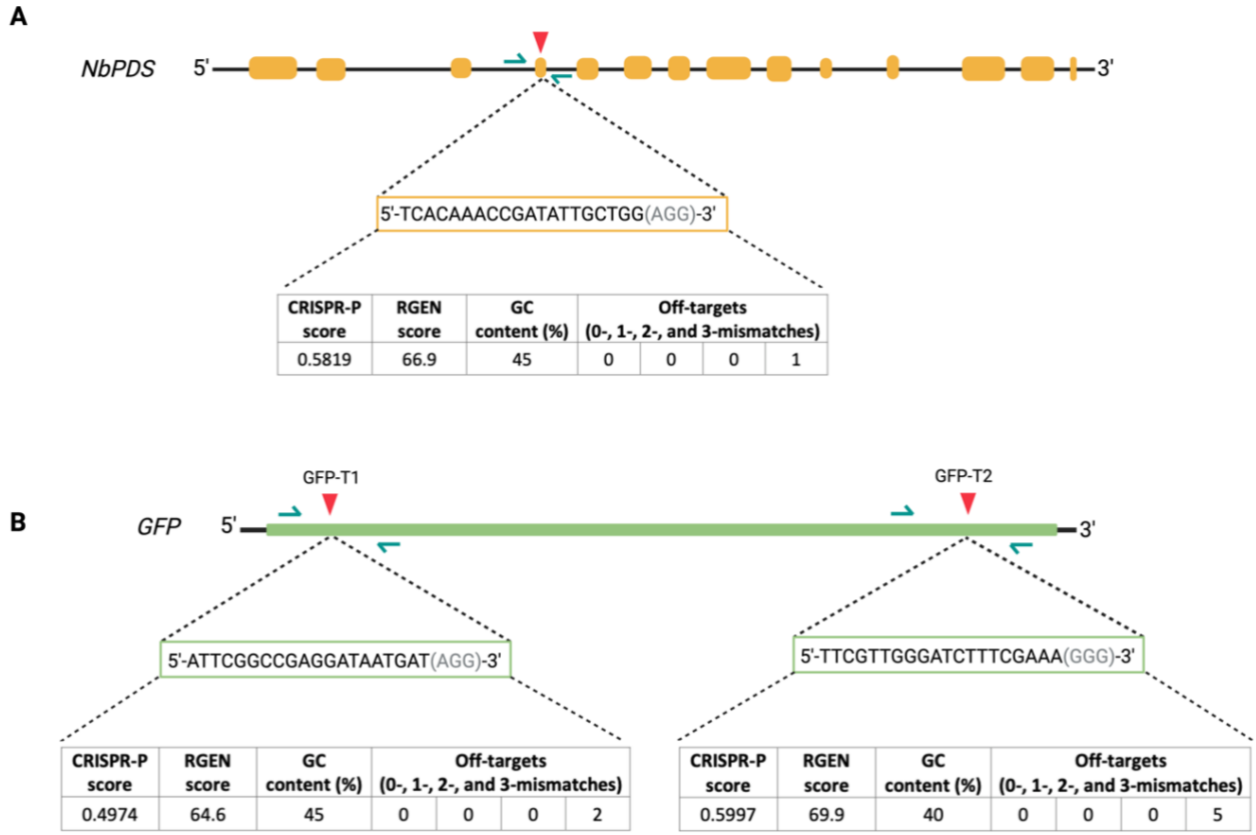

CRISPR-P score	RGEN score	GC content (%)	Off-targets (0-, 1-, 2-, and 3-mismatches)			
0.5819	66.9	45	0	0	0	1

CRISPR-P score	RGEN score	GC content (%)	Off-targets (0-, 1-, 2-, and 3-mismatches)			
0.4974	64.6	45	0	0	0	2

CRISPR-P score	RGEN score	GC content (%)	Off-targets (0-, 1-, 2-, and 3-mismatches)			
0.5997	69.9	40	0	0	0	5

Figure 4.3. gRNA target selection of endogenous gene sequences. **A**) The *NbPDS* gene representation portraying the exons (yellow), and the gRNA target site (red arrow) and 20nt sequence targeting exon 4. The PAM sequence is represented in grey. **B**) The 16c-*GFP* gene representation portraying the estimated gRNA target sites (red arrows) of *GFP* Target 1 at the 5'-end and *GFP* Target-2 at the 3'-end within the gene, and their respective 20nt sequences. PAM sequences are represented in grey. The blue arrows represent primer positions used for Sanger sequencing. Tables below each gRNA sequence depict the CRISPR-P and RGEN software score outputs for each gRNA sequence, as well as the respective GC content (%) and off-targets when 0-, 1-, 2-, or 3-mismatches were present within the gRNA sequence.

Off-target analysis was performed using RGEN-Tools Cas-OFFinder and BLASTN; the results are depicted below the gRNA sequences of Fig. 4.3. *GFP* Target-1 was found to have no off-targets

when 0-, 1-, or 2-mismatches were present, but identified two off-targets when 3-mismatches were present. *GFP* Target-2 was found to have no off-targets when 0-, 1-, or 2-mismatches were present, but identified five off-targets when 3-mismatches were present. The *NbPDS* target was designed to target both *NbPDS* genes, and no off-targets were identified when 0-, 1-, or 2-mismatches were present, but identified one off-target when 3-mismatches were present in the target sequence. Secondary structure formation of the candidate target-gRNA scaffold sequence was assessed (Supplementary Fig. 7). Subsequent to the selection and design of the respective gRNAs, construction of the gRNA:scaffold cassettes and vectors was performed.

4.3.2 pRIC-gRNA vector construction

Following synthesis and annealing of the gRNA oligos, an adapted protocol (Ma and Liu, 2016) was employed for the construction of the gRNA:scaffold cassettes. The gRNA adapters were cloned under the *A. thaliana* U3 (AtU3) promoter, commonly used to express gRNAs in dicot plants (Ren *et al.*, 2021), and adjacent to the Cas9 gRNA scaffold. Once the correct gRNA cassette was assembled (Fig. 4.1C), cloning into the pRIC 3.0 vector was performed using restriction enzyme digestion and ligation, for the construction of the final binary pRIC-gRNA vector (Fig. 4.4B), and confirmed using Sanger sequencing.

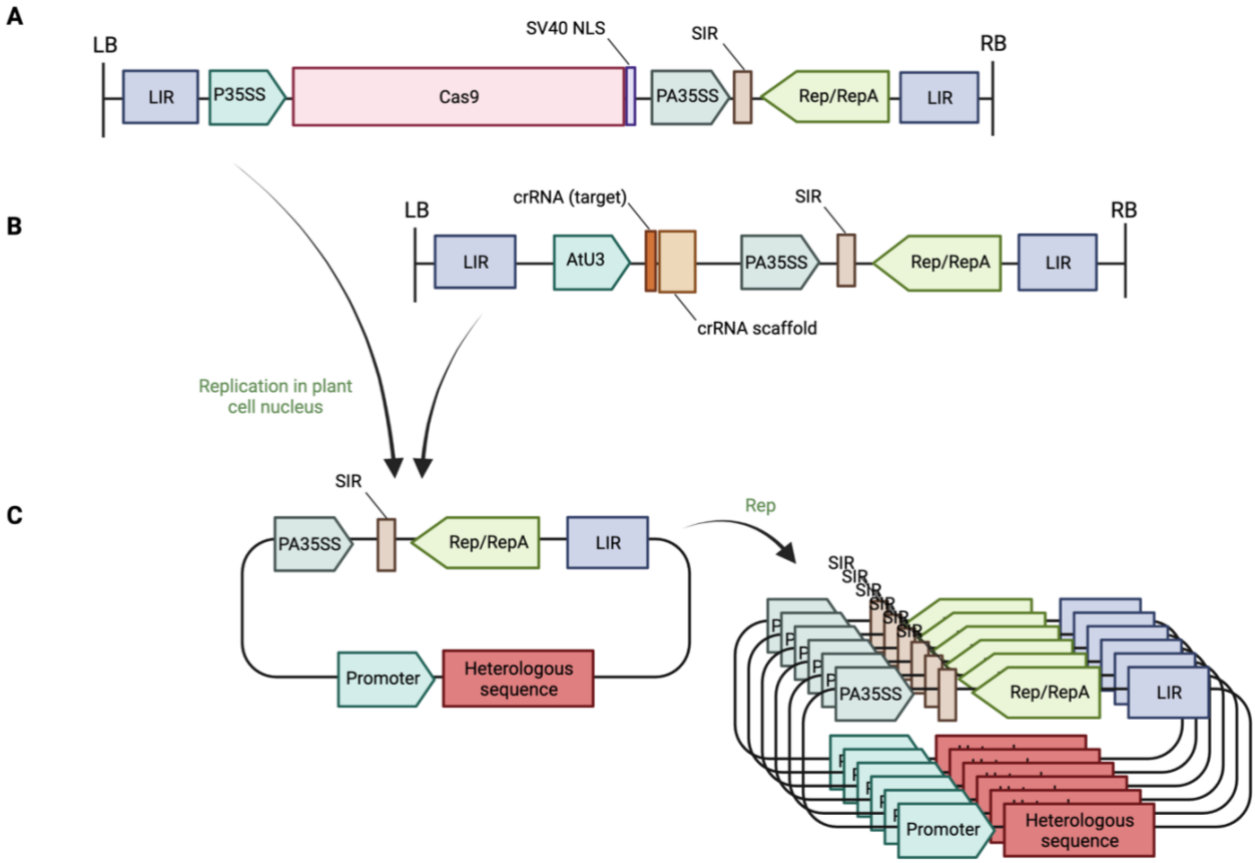

Figure 4.4. Schematic representation of the T-DNA region of the assembled binary pRIC vectors with their respective components. **A**) A schematic representing the pRIC-Cas9 T-DNA, assembled previously (Duxbury, 2020). The P35SS promoter is responsible for driving *Cas9* expression. **B**) The assembled pRIC-gRNA T-DNA schematic. The AtU3 promoter is responsible for driving expression of the gRNA and scaffold. **C**) Once the T-DNA from the binary vector is transformed into the plant cell nucleus, replication by Rep/RepA results in the formation of geminivirus-replicons (GVRs), producing high amounts of GVRs and ultimately yielding high recombinant protein expression. The LIR and SIR are necessary geminiviral-elements. LIR bounds the necessary elements to ensure release from the T-DNA into the plant cell, followed by rolling-circle replication by means of Rep/RepA. LIR, long-intergenic region; SIR, short intergenic region; SV40 NLS, Simian Vacuolating Virus 40 nuclear localisation signal; LB, left border; RB, right border.

4.3.3 Phenotypic and molecular analysis of exogenous DNA targeting

To assess the ability of the pRIC construct (Regnard *et al.*, 2010) to deliver and express the large *Cas9* gene, as well as target and cleave exogenously-delivered DNA, the enhanced green fluorescent protein (eGFP) visual reporter system was used. Individual pRIC constructs were used to deliver *eGFP*, *Cas9* and the necessary gRNA for eGFP targeting, into wild-type *N. benthamiana* leaves. The culture mixtures were delivered by Agro-infiltration, and after the delivery of the T-DNA from the binary vector into host plant cells, replicational release of the geminivirus-replicon (GVR) can occur. As a control, constructs either harbouring the Cas9 or the gRNA were excluded

from the co-infiltration. eGFP fluorescence was photographed 5-dpi. Subsequently, *eGFP* expression was molecularly analysed with RT-qPCR. When eGFP fluorescence was assessed at 5-dpi, a significant reduction was observed, when compared to the control (Fig. 4.5A).

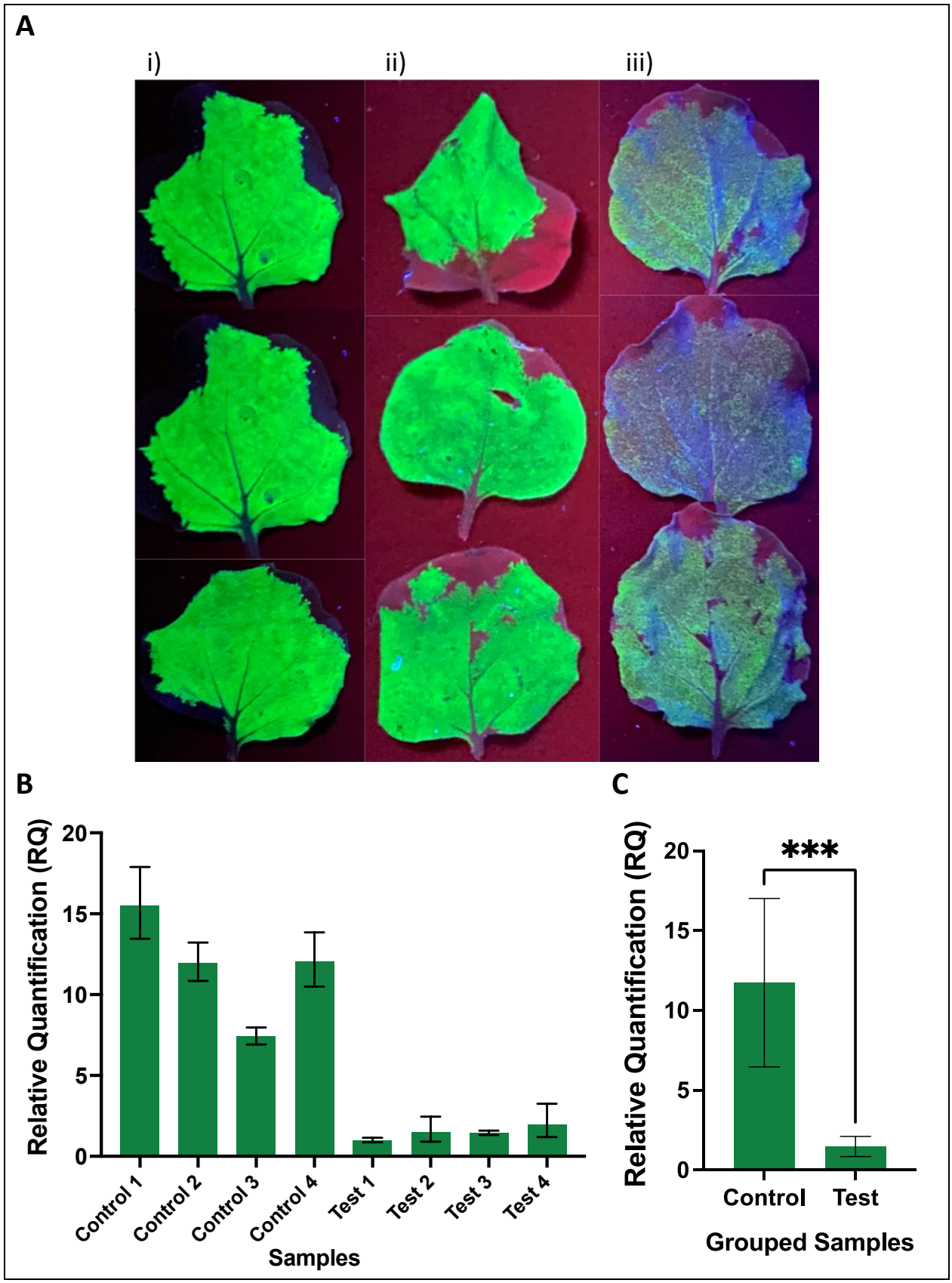

Figure 4.5. pRIC delivery and expression of *eGFP*, *Cas9* and gRNA(eGFP). (**A**) Phenotypic analysis of wild-type *N. benthamiana* leaves infiltrated with i) pRIC-eGFP, ii) pRIC-eGFP and pRIC-Cas9 (control), and iii) pRIC-eGFP, pRIC-Cas9 and pRIC-gRNA(eGFP) (test), photographed 5-dpi. (**B**) Relative fold expression of *eGFP*, normalised to the reference sample 'test 1'. The error bars represent the minimum and maximum

values of n=3 technical replicates. Samples labelled 'control 1 and 2' consisted of the co-delivery (1:1) of pRIC-eGFP and pRIC-Cas9, while 'control 3 and 4' consisted of the co-delivery (1:1) of pRIC-eGFP and pRIC-gRNA. Samples labelled 'test 1-4' represent the co-infiltration of all three constructs at a 1:1:1 ratio, into different plants. (**C**) Relative quantification of *eGFP* expression of the control samples and test samples grouped biologically. Data represents the mean relative gene expression, ± SEM of the four biological replicates (n=4). Statistical analysis performed using a two-tailed unpaired Student's t-test; with the difference being significant at $p \leq 0.05$ with respect to the control group. *** p=0.0008.

Infiltrated leaf material was subjected to RT-qPCR to molecularly quantify the eGFP reduction (Fig. 4.5B). Prior to RT-qPCR analysis, cDNA synthesis was confirmed by end-point PCR, with primers designed to span introns of the actin gene (Supplementary Fig. 8), that can differentiate between DNA and cDNA amplification (Table 4.1). Following successful cDNA amplification, *eGFP* expression was quantified using RT-qPCR (Fig. 4.5B), with four biological replicates for the control and test group (n=4) respectively. The housekeeping gene *APR* was used for normalisation. A distinct difference in *eGFP* expression was observed between the control and test group in Fig.4.5B, with a >3-fold reduction in *eGFP* relative quantification in the test samples. The samples were grouped biologically (Fig. 4.5C), and a ~5-fold reduction in *eGFP* expression was observed. Statistical analysis using a Student's t-test was performed, and the reduction in *eGFP* quantification was statistically significant (p=0.0008), when a significance value of $p \leq 0.05$ was used.

Putative editing of the *eGFP* gene was elucidated molecularly by amplifying the target region, following a DNA extraction, with primers gfp_pRIC_qPCR_F/ gfp_pRIC_qPCR_R (Table 4.1) and analysing the PCR-amplicon with Sanger sequencing. When the Sanger sequence data of the four eGFP samples was analysed with ICE v2.0, sample test-2 showed an altered sequence at the *eGFP* gene target site (Fig. 4.6), shown by untidy trace chromatogram readings following the predicted cut site (Fig. 4.6A).

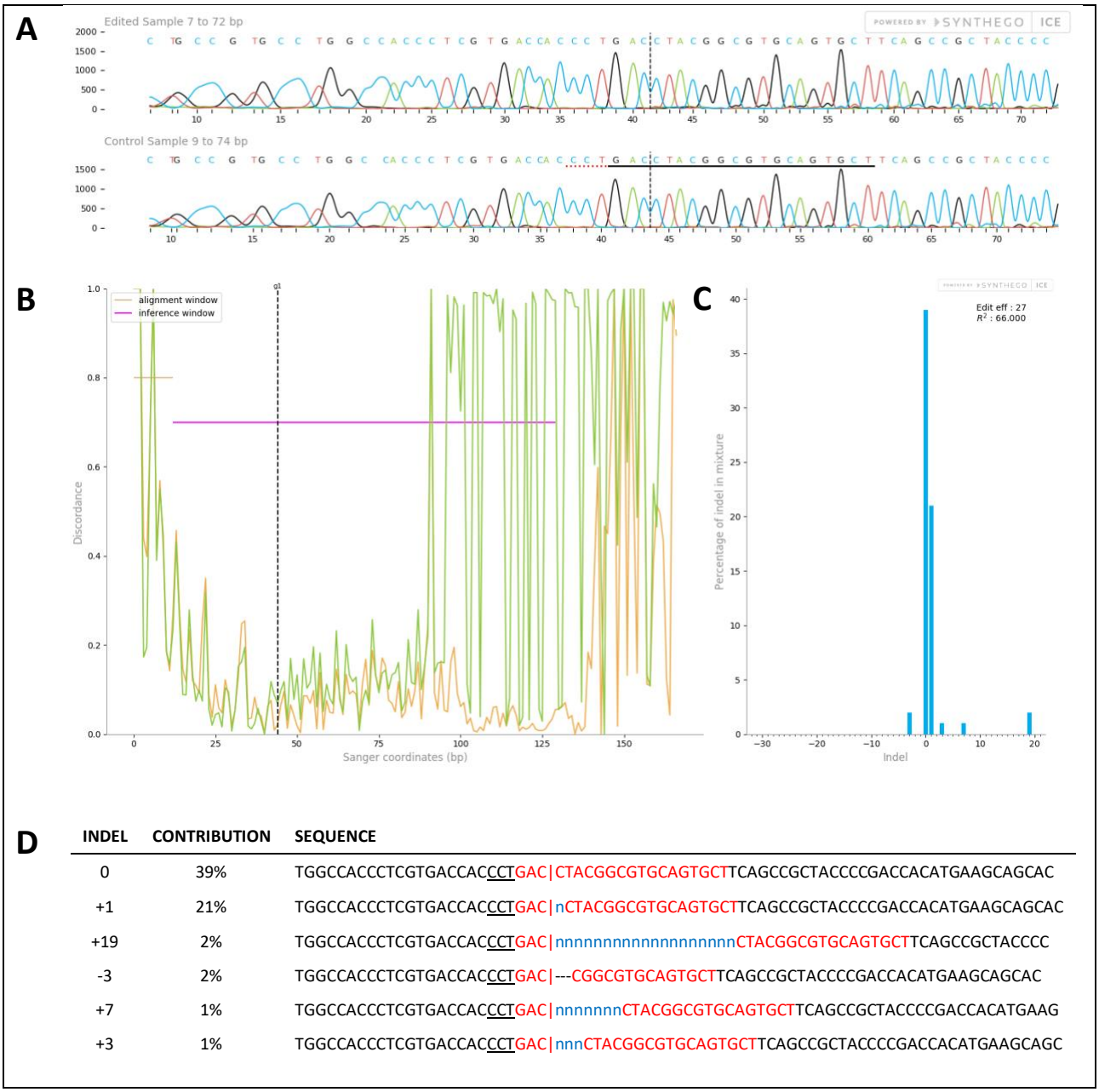

D

INDEL	CONTRIBUTION	SEQUENCE
0	39%	TGGCCACCCTCGTGACCAC<u>CCT</u>GAC|CTACGGCGTGCAGTGCTTCAGCCGCTACCCCGACCACATGAAGCAGCAC
+1	21%	TGGCCACCCTCGTGACCAC<u>CCT</u>GAC|nCTACGGCGTGCAGTGCTTCAGCCGCTACCCCGACCACATGAAGCAGCAC
+19	2%	TGGCCACCCTCGTGACCAC<u>CCT</u>GAC|nnnnnnnnnnnnnnnnnnnCTACGGCGTGCAGTGCTTCAGCCGCTACCCC
-3	2%	TGGCCACCCTCGTGACCAC<u>CCT</u>GAC|---CGGCGTGCAGTGCTTCAGCCGCTACCCCGACCACATGAAGCAGCAC
+7	1%	TGGCCACCCTCGTGACCAC<u>CCT</u>GAC|nnnnnnnCTACGGCGTGCAGTGCTTCAGCCGCTACCCCGACCACATGAAG
+3	1%	TGGCCACCCTCGTGACCAC<u>CCT</u>GAC|nnnCTACGGCGTGCAGTGCTTCAGCCGCTACCCCGACCACATGAAGCAGC

Figure 4.6. ICE v2.0 software outputs on the eGFP test-2 sample. **A**) Trace chromatograms showing the peaks of the edited and the control sequence files at the target site. The black underlined nucleotides represent the guide sequence. The PAM sequence is underlined with a horizontal red dotted underline. Vertical black dotted line represents the actual cut site. **B**) The discordance plot showing the alignment level per base between the control (orange) and edited (green) sample. The inference window represents the region around the cut site. The graph represents the signal disagreement between the control trace file and edited file. The orange and green line should remain close together before the cut site, followed by a jump in discordance after the cut site with a typical CRISPR edit. **C**) A plot representing the inferred distribution of indels within the edited genome population. **D**) Indel contributions and inferred sequences within the edited population. The PAM sequence is underlined in black, the *eGFP* target sequence is in red, and the short vertical red lines indicate the predicted cut site. Insertions and deletions are displayed in blue "n" and black "-''respectively.

The discordance plot (Fig. 4.6B) presents the green (edited) and orange (control) signal disagreement within the region surrounding the cut site (inference window), and Fig. 4.6C describes the inferred indels within the edited sequences. For sample test-2, the wild-type sequence contributed 39% of all sequence reads (Fig. 4.6D), while 1 bp insertions (+1) immediately following the cut-site contributed the second-most sequence reads (21%), and an indel range of -3 to +19 bp can be observed (Fig. 4.6C). ICE v2.0 computed the editing efficiency to be 27%, with a knockout-score of 24 (proportion of indels that indicate a frameshift). The model fit (R^2) value represents how well the proposed indel distribution fits the sequence of the edited sample. The R^2 value for the test-2 sample is 0.66. Additionally, ICE v2.0 produced a warning regarding the cut-site position being too close to the start of the sequence, impairing the quality of an accurate score. The other three samples; eGFP test-1, eGFP test-3 and eGFP test-4, contained too poor sequence quality to be analysed with ICE v2.0.

4.3.4 Analysis of *Cas9* expression

It has been found that the expression of the Cas9 protein is correlated with editing efficiency (Jiao *et al.*, 2022). Thus, we sought to quantify the expression of *Cas9* from pRIC, compared to the expression of a stably-integrated *Cas9* gene in transgenic *N. benthamiana*. The abovementioned pRIC-Cas9, pRIC-eGFP and pRIC-gRNA(eGFP) infiltration into *N. benthamiana* was used to assess the *Cas9* expression, and the extracted RNA was further utilised for RT-qPCR analysis, using the primer set Cas9qPCR_F/CasqPCR_R (Table 4.1). *Cas9* expression with the pRIC vector was compared to stably-transformed *N. benthamiana* plants harbouring the *Cas9* gene, which were produced previously (Robertson, 2018). The expression analysis indicated that pRIC-expressed *Cas9* was significantly greater than expression of stably-integrated *Cas9* (Fig. 4.7A).

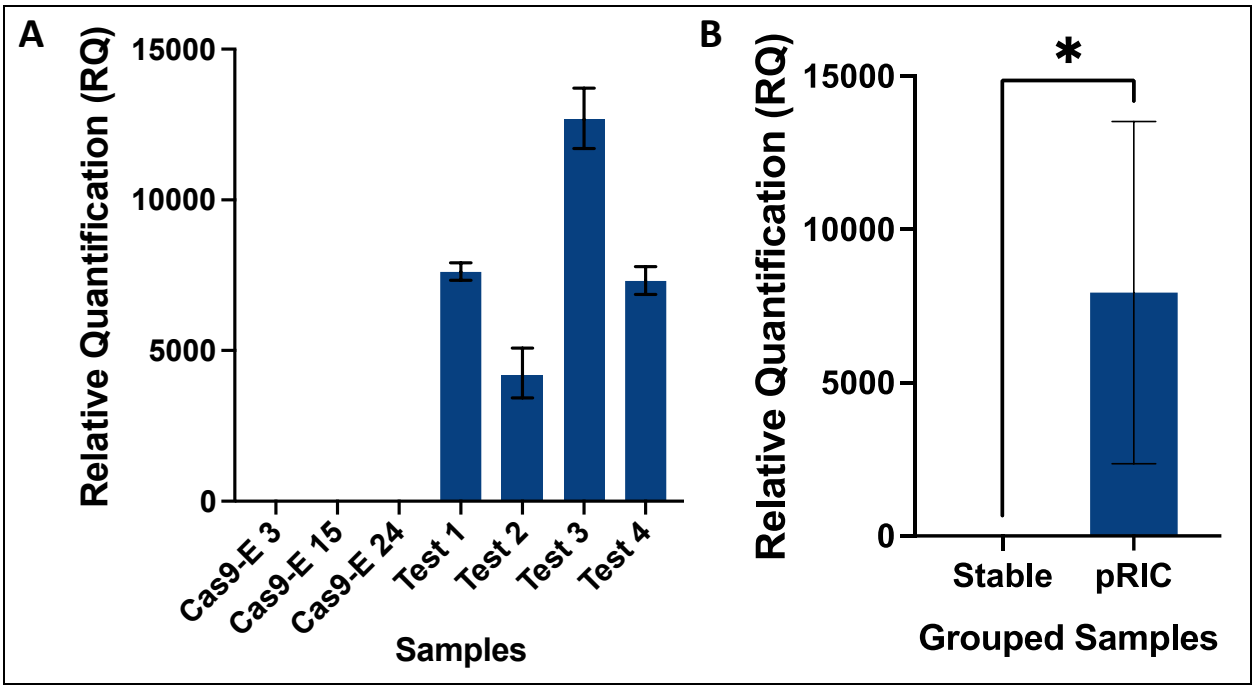

Figure 4.7. Relative gene expression of *Cas9* transiently expressed from the geminivirus-based pRIC vector and stably-transformed *N. benthamiana* harbouring *Cas9*. **A**) Relative quantification (RQ) of *Cas9* expression for Cas9-E (n=3) and test samples (n=4), in reference to Cas9-E 15 reference sample. The Cas9-E samples represent the stably-transformed *N. benthamiana* Cas9 plants, while the test samples represent the pRIC-infiltrated plants. The error bars represent the minimum and maximum values of n=3 technical replicates. **B**) Relative *Cas9* quantification when samples are grouped biologically. Data represents the mean relative gene expression, ± SEM of the n=3 biological replicates (Stable) and n=4 biological replicates (pRIC). Statistical analysis performed using a two-tailed unpaired Student's t-test; with the difference being significant at $p \leq 0.05$ with respect to the Stable group. * $p = 0.0123$.

Fig. 4.7A depicts the stably-transformed *N. benthamiana* plants constitutively expressing the *Cas9* gene (Cas9-E-) and the transient eGFP experiment where pRIC-Cas9, pRIC-eGFP and pRIC-gRNA(eGFP) were infiltrated into wild-type *N. benthamiana* (Test1-4). The *Cas9* gene was successfully expressed in all samples, albeit very low in the Cas9-E- samples (~3-fold) (Fig. 4.7A). Although there was considerable variation in the *Cas9* expression from pRIC (Test1-4), the relative quantification of Cas9 transcripts from pRIC demonstrated >1300-fold increase, when compared to the reference sample Cas9-E 15. When the samples were grouped biologically, a significant expression difference was observed between stably-integrated *Cas9* and pRIC-expressed *Cas9* (Fig. 4.7B). There was a ~2500-fold increase in *Cas9* expression when expressed using the BeYDV-based pRIC vector, compared to the stably-transformed group. Statistical analysis using a Student's t-test was performed, and the increase in Cas9 quantification was statistically significant ($p=0.0123$), when $p \leq 0.05$ (Fig. 4.7B).

4.3.5 Endogenous DNA targeting

To assess the ability of pRIC-Cas9 to cleave endogenous DNA, gRNAs were designed targeting the *NbPDS* and *GFP* genes. The cultures of pRIC-Cas9 and pRIC-gRNA(PDS) or pRIC-gRNA(GFP) were mixed at a 1:1 ratio, and Agro-infiltrations were performed which delivered the constructs into wild-type *N. benthamiana* leaves or into 16c leaves. As a control, a non-specific (ns) gRNA (pRIC-ns) was infiltrated along with pRIC-Cas9 at a 1:1 ratio. Prior to molecular analysis, the phenotype of infiltrated leaves was observed 5-dpi. No observable phenotype was detected for PDS-targeting in wild-type-infiltrated leaves, when compared to the control. Similarly, no distinguishable difference in *GFP* expression between the control (pRIC-ns) and the sample could be detected (Supplementary Fig. 9). Infiltrated leaf material of both the wild-type *N. benthamiana* and 16c plants were subjected to a DNA extraction and PCR-amplification (primers in Table 4.1) before being analysed with Sanger sequencing. To detect any possible editing, Sanger sequencing files were analysed using ICE v2.0.

Of the eight *NbPDS* samples analysed for putative editing, seven showed editing at the *PDS* target site. Fig. 4.8 depicts the ICE v2.0 output for one sample, NbPDS-1, as an example. The remaining outputs can be found in Supplementary Figure 10. Editing of both *NbPDSa* and *NbPDSb* was detected at the target site, represented by the untidy trace chromatogram after the predicted cut site (Fig. 4.8A).

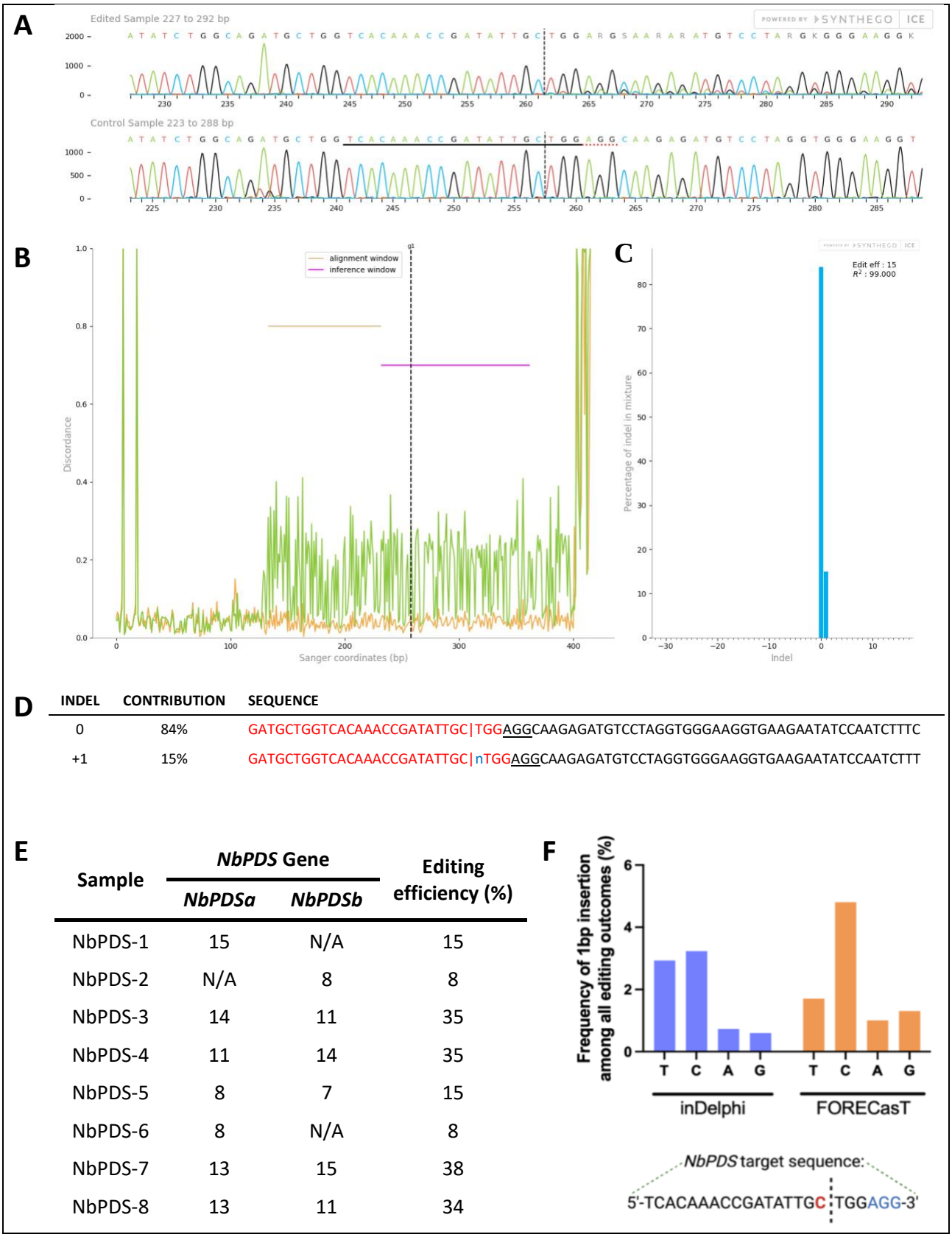

Sample	*NbPDS* Gene		Editing efficiency (%)
	NbPDSa	*NbPDSb*	
NbPDS-1	15	N/A	15
NbPDS-2	N/A	8	8
NbPDS-3	14	11	35
NbPDS-4	11	14	35
NbPDS-5	8	7	15
NbPDS-6	8	N/A	8
NbPDS-7	13	15	38
NbPDS-8	13	11	34

Figure 4.8. Example of the ICE v2.0 software outputs of *NbPDS* editing inference for sample NbPDS-1. **A**) Trace chromatograms portraying the peaks of the edited and the control sequence files at the target site of sample NbPDS-1. The black underlined nucleotides (nts) represent the guide sequence. The PAM sequence is underlined with a horizontal red dotted underline. Vertical black dotted line represents the

actual cut site. **B**) The discordance plot of NbPDS-1 showing the alignment level per base between the control (orange) and edited (green) sample. The inference window represents the region around the cut site. The graph represents the signal disagreement between the control trace file and edited file. The orange and green line should remain close together before the cut site, followed by a jump in discordance after the cut site with a typical CRISPR edit. **C**) A plot representing the inferred distribution of indels within the edited genome population. **D**) NbPDS-1 indel contributions and inferred sequences within the edited population. The PAM sequence is underlined in black, the *NbPDS* target sequence is in red, and the short vertical red lines indicate the predicted cut site. Insertions are displayed in blue "n". **E**) The different indel percentages (indel %) and knockout-scores for each sample and each *NbPDS* gene. In this case, the knockout-score and indel % are the same value. Samples with 'N/A' had inadequate Sanger sequence data for computation by ICE v2.0. The editing efficiency (%) represents the combination of the indel percentages for both edited genes. **F**) inDelphi and FORECasT model output for the +1 bp insertion prediction. The model output describing the frequency of 1 bp insertions for each nt, based on the sequence of the *NbPDS* gRNA sequence. Red nts represent the 4th bp upstream from the PAM; blue nts represent the PAM sequence; the dotted vertical line represents the predicted cut site.

The discordance plot corroborates the trace chromatogram data, with a signal disagreement between the edited (green) and control (orange) lines within the cut site region (Fig. 4.8B). All samples showed a +1 insertion at the predicted cut site, compared to the wild-type sequence (0 indels) (Fig. 4.8C and D). Both gene *NbPDSa* and gene *NbPDSb* revealed editing at the target site (Fig. 4.8E). For *NbPDSa*, the percentage of edited (indel) sequences in the edited population ranged from 8-15%, with sample NbPDS-2 having inadequate quality for ICE v2.0 to analyse it. Similarly, the edited sequences in *NbPDSb* also ranged from 8-15%, while samples NbPDS-1 and -6 were of inadequate quality for ICE v2.0 computation. It was noted that the same samples did not demonstrate the same indel percentages, but the editing efficiency for each sample was considered as the combination of the two editing events for each *NbPDS* gene (Fig. 4.8E). Hence, sample NbPDS7 demonstrated the highest editing efficiency, of 38%. Editing efficiency ranges from 8-38% for *NbPDS* collectively. ICE v2.0 computed the knockout-score to be equivalent to the editing efficiency of the sample (8 to 15%). The R^2 value was consistently ≥ 0.99 for all the samples analysed.

Subsequent to the mutation inference with ICE v2.0, the putative indels of the edited sequences were analysed using two predictor software generated for mammalian systems, but that have subsequently been utilised for indel prediction in plants (Fig. 4.8F) (Molla *et al.*, 2022). Fig. 4.8F describes the software outputs of inDelphi and FORECasT with the +1 bp identity prediction for each nt, as well as the respective target sequence highlighting the important –4 nt in red. Based

on the respective sequences of the gRNAs, the software predicted at what frequency each nt would be inserted into the edited sequence following cleavage and DSB repair. A single 'C' nt would be inserted at 3.2% (inDelphi) and 4.8% (FORECasT) among all editing outcomes, for 1 bp insertions. Insertion of a single T nt would occur at the second-highest frequency, followed by either A or G.

Molecular analysis by Sanger sequencing was performed, to detect putative editing of the *GFP* gene. Sanger sequence data was analysed with ICE v2.0, and three out of four samples for GFP Target-1 showed editing at the target site (Fig. 4.9).

A

Sample	Indel %	Model Fit (R^2)	Knockout-Score
GFP1.2	21	0.99	15

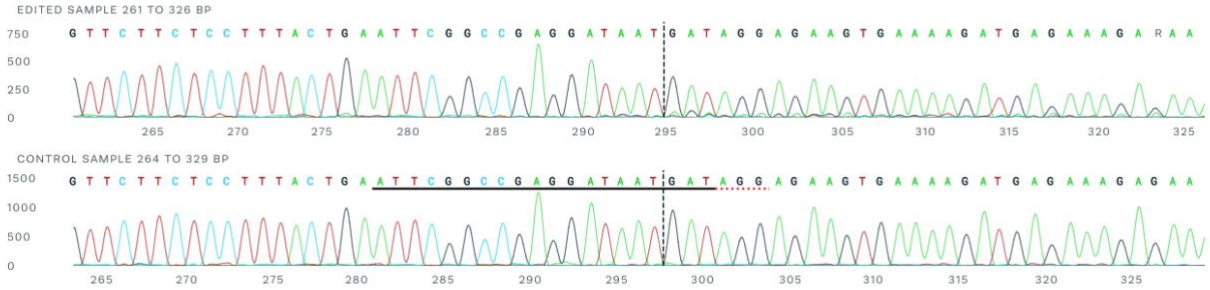

INDEL	CONTRIBUTION	SEQUENCE
0	78%	TTTACTGAATTCGGCCGAGGATAAT|GATAGGAGAAGTGAAAAGATGAGAAAGAGAAAAAGATTAGTCTTCATTGT
+1	7%	TTTACTGAATTCGGCCGAGGATAAT|nGATAGGAGAAGTGAAAAGATGAGAAAGAGAAAAAGATTAGTCTTCATTG
-6	4%	TTTACTGAATTCGGCCGAGGATAAT|------AGAAGTGAAAAGATGAGAAAGAGAAAAAGATTAGTCTTCATTGT
-5	2%	TTTACTGAATTCGGCCGAGGATAAT|-----GAGAAGTGAAAAGATGAGAAAGAGAAAAAGATTAGTCTTCATTGT
-4	2%	TTTACTGAATTCGGCCGAGGATAAT|----GGAGAAGTGAAAAGATGAGAAAGAGAAAAAGATTAGTCTTCATTGT
-7	1%	TTTACTGAATTCGGCCGAGGAT---|----GGAGAAGTGAAAAGATGAGAAAGAGAAAAAGATTAGTCTTCATTGT
-3	1%	TTTACTGAATTCGGCCGAGGAT---|GATAGGAGAAGTGAAAAGATGAGAAAGAGAAAAAGATTAGTCTTCATTGT
-2	1%	TTTACTGAATTCGGCCGAGGATA--|GATAGGAGAAGTGAAAAGATGAGAAAGAGAAAAAGATTAGTCTTCATTGT
-3	1%	TTTACTGAATTCGGCCGAGGATAA-|--TAGGAGAAGTGAAAAGATGAGAAAGAGAAAAAGATTAGTCTTCATTGT
-8	1%	TTTACTGAATTCGGCCGAGGATAAT|--------AAGTGAAAAGATGAGAAAGAGAAAAAGATTAGTCTTCATTGT
-7	1%	TTTACTGAATTCGGCCGAGGATAAT|-------GAAGTGAAAAGATGAGAAAGAGAAAAAGATTAGTCTTCATTGT

B

Sample	Indel %	Model Fit (R^2)	Knockout-Score
GFP1.3	12	0.99	6

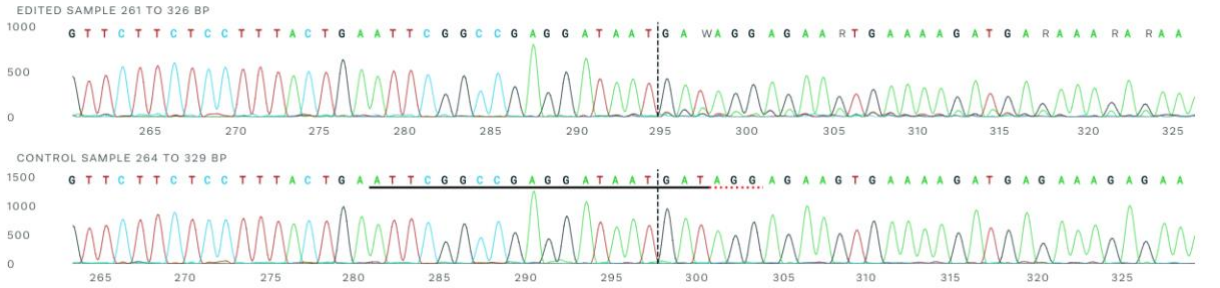

INDEL	CONTRIBUTION	SEQUENCE
0	87%	TTTACTGAATTCGGCCGAGGATAAT|GATAGGAGAAGTGAAAAGATGAGAAAGAGAAAAAGATTAGTCTTCATTGT
-3	6%	TTTACTGAATTCGGCCGAGGAT---|GATAGGAGAAGTGAAAAGATGAGAAAGAGAAAAAGATTAGTCTTCATTGT
+1	2%	TTTACTGAATTCGGCCGAGGATAAT|nGATAGGAGAAGTGAAAAGATGAGAAAGAGAAAAAGATTAGTCTTCATTG
-4	2%	TTTACTGAATTCGGCCGAGGATAAT|----GGAGAAGTGAAAAGATGAGAAAGAGAAAAAGATTAGTCTTCATTGT
-8	1%	TTTACTGAATTCGGCCGAGGATAAT|--------AAGTGAAAAGATGAGAAAGAGAAAAAGATTAGTCTTCATTGT
-5	1%	TTTACTGAATTCGGCCGAGGATAAT|-----GAGAAGTGAAAAGATGAGAAAGAGAAAAAGATTAGTCTTCATTGT

C

Sample	Indel %	Model Fit (R^2)	Knockout-Score
GFP1.4	27	0.95	17

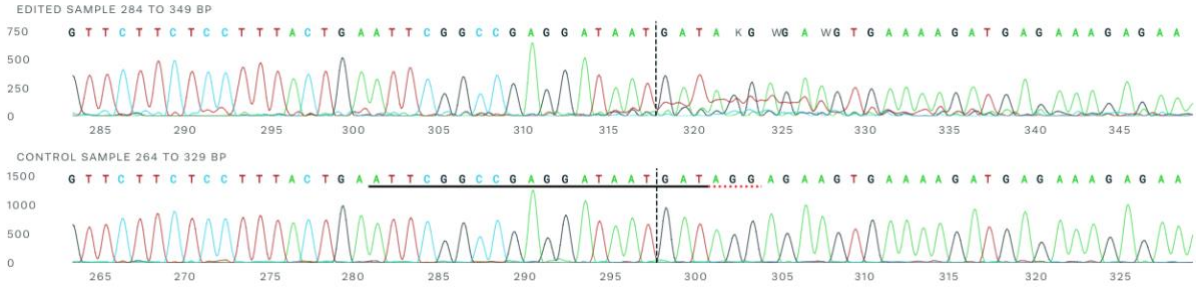

INDEL	CONTRIBUTION	SEQUENCE
0	68%	TTTACTGAATTCGGCCGAGGATAAT|GATAGGAGAAGTGAAAAGATGAGAAAGAGAAAAAGATTAGTCTTCATTGT
+13	4%	TTTACTGAATTCGGCCGAGGATAAT|nnnnnnnnnnnnnGATAGGAGAAGTGAAAAGATGAGAAAGAGAAAAAGAT
+7	4%	TTTACTGAATTCGGCCGAGGATAAT|nnnnnnnGATAGGAGAAGTGAAAAGATGAGAAAGAGAAAAAGATTAGTCT
+6	4%	TTTACTGAATTCGGCCGAGGATAAT|nnnnnnGATAGGAGAAGTGAAAAGATGAGAAAGAGAAAAAGATTAGTCTT
-3	3%	TTTACTGAATTCGGCCGAGGAT---|GATAGGAGAAGTGAAAAGATGAGAAAGAGAAAAAGATTAGTCTTCATTGT
+16	2%	TTTACTGAATTCGGCCGAGGATAAT|nnnnnnnnnnnnnnnnGATAGGAGAAGTGAAAAGATGAGAAAGAGAAAAA
+15	2%	TTTACTGAATTCGGCCGAGGATAAT|nnnnnnnnnnnnnnnGATAGGAGAAGTGAAAAGATGAGAAAGAGAAAAAG
-31	2%	TTTACTGAATTCGG----------|----------GAGAAAGAGAAAAAGATTAGTCTTCATTGT
-4	2%	TTTACTGAATTCGGCCGAGGATA--|--TAGGAGAAGTGAAAAGATGAGAAAGAGAAAAAGATTAGTCTTCATTGT
+8	1%	TTTACTGAATTCGGCCGAGGATAAT|nnnnnnnnGATAGGAGAAGTGAAAAGATGAGAAAGAGAAAAAGATTAGTC
-40	1%	TTTAC----------|----------GAGAAAGAGAAAAAGATTAGTCTTCATTGT
-7	1%	TTTACTGAATTCGGCCGAGGAT---|----GGAGAAGTGAAAAGATGAGAAAGAGAAAAAGATTAGTCTTCATTGT
-6	1%	TTTACTGAATTCGGCCGAGGATA--|----GGAGAAGTGAAAAGATGAGAAAGAGAAAAAGATTAGTCTTCATTGT

Figure 4.9. The ICE v2.0 output for GFP Target-1 editing of *GFP*. **A**) Sample GFP1.2 ICE v2.0 output, depicting the editing efficiency (top), trace chromatogram (middle) and indel contribution sequences (bottom). **B**) Sample GFP1.3 ICE v2.0 output, depicting the editing efficiency (top), trace chromatogram (middle) and indel contribution sequences (bottom). **C**) Sample GFP1.4 ICE v2.0 output, depicting the editing efficiency (top), trace chromatogram (middle) and indel contribution sequences (bottom). The PAM sequence is underlined in black, the eGFP target sequence is in red, and the short vertical red lines indicate the predicted cut site. Insertions and deletions are displayed in blue "n" and black "-"respectively.

Samples GFP1.2, GFP1.3 and GFP1.4 showed editing at the target site, at varying efficiencies (Fig. 4.9). Sample GFP1.4 showed the highest knockout-score (17) with the indel percentage at 27 (Fig. 4.9C). The most frequent edited sequence contained +13 insertions, at a 4% contribution. The type of mutations ranged from –40 to +13 nts. Sample GFP1.2 showed the second-highest knockout-score of 15, with an indel percentage of 21, and the most frequent edited sequence contained a single insertion (+1 bp) at 7%, with the range of mutations being –8 to +1 nts (Fig. 4.9A). Sample GFP1.3 showed the least editing in comparison to the other two samples, exhibiting a knockout-score of 6, with the indel percentage at 12%, and the most frequent edited sequences containing three deletions (-3 bp) at 6%, followed by a single insertion (+1 bp) at 2% (Fig. 4.9B). The mutation range of sample GFP1.3 was –8 to +1 nts. The model fit value was >0.95 for each sample. No editing was detected with the *GFP* Target-2 gRNA, which was designed to target the 3'-end of the *GFP* gene (Fig. 4.3B).

4.4 DISCUSSION

In this study, the pRIC vector (Regnard *et al.*, 2010) was adopted for the delivery and expression of CRISPR/Cas9 components *in planta*, with the aim of targeting exogenously-delivered DNA and endogenous plant genes. The necessary vectors were assembled, and subsequently infiltrated into either wild-type *N. benthamiana* or the 16c line plants (Fig. 4.2).

The initial experiment aimed to deliver Cas9 and to target the pRIC-delivered *eGFP* gene. The results indicated successful eGFP targeting, which can be observed in the decreased eGFP fluorescence, as well as reduced *eGFP* transcript quantification, when compared to the control samples. Following the successful targeting of exogenously-delivered *eGFP* with CRISPR/Cas9, targeting of endogenous genes was assessed. A single gRNA was designed to target exon 4 of both *NbPDSa* and *NbPDSb* genes simultaneously. Editing at the target sites of both genes was detected, albeit at different frequencies for the same samples. Collectively, the total editing efficiency of the pRIC-Cas9 system targeting *NbPDS* was the sum of the editing of *NbPDSa* and *NbPDSb*, resulting in efficient simultaneous targeting of two genes using a single gRNA. This result was supported by Komatsu *et al.* (2020), where the study similarly edited both *NbPDS* genes using a single gRNA.

When the GFP fluorescence of the 16c plants infiltrated with pRIC-Cas9 and pRIC-gRNA(GFP) was monitored using a UV light, no difference in fluorescence could be observed. This was not due to the unsuccessful targeting of the *GFP* gene, but rather because GFP fluorescence from 16c plants is relatively faint, and subsequent to Agro-infiltration, the infiltrated area seemed to become discoloured, impacting the GFP visualisation. Nonetheless, Sanger sequencing and ICE v2.0 were used to analyse putative editing of the *GFP* gene. Three out of four samples for GFP Target-1 exhibited editing at the target site. The study by Eini and colleagues supported this result, as a geminivirus replicon-based system was similarly used to target GFP in 16c plants (Eini *et al.*, 2022).

The genes *eGFP*, *NbPDS* and *GFP* were targeted with Cas9, whereby DSBs would be repaired by NHEJ. The repair and putative editing at the target sites of these genes were analysed with Sanger sequencing and the nature of the mutations were inferred with ICE v2.0. All three genes demonstrated editing at their respective target sites. Interestingly, the editing pattern of *eGFP*

and *NbPDS* genes both contained a single nt insertion as the most frequent indel, at 21% and 15% respectively. A study in *A. thaliana* supported this finding, where 1 bp insertions were the most common induced mutation (Feng *et al.*, 2014). Similarly, a study in cereal crops also found that 1 bp insertions were the most common mutation following Cas9 editing (Zhu *et al.*, 2017). When the editing of *NbPDS* and *GFP* genes were compared, drastically different editing patterns were observed. *NbPDS* targeting resulted in a single nt insertion consistently, while the mutations obtained following *GFP* editing were a range of mutations from multi-nt deletions to multi-nt insertions. A likely deduction explaining the different observed editing patterns may be the individual gRNA sequences and respective gRNA efficiencies, which play a large role in determining editing efficiency (Shojaei Baghini *et al.*, 2021). The transgenic 16c line was generated by stably-transforming *N. benthamiana* with the *GFP* gene (Ruiz, Voinnet and Baulcombe, 1998). Accordingly, *GFP* of the 16c line is obviously not a naturally occurring endogenous gene, but rather a transgene which has been stably-integrated into the plant genome. The editing of 16c-GFP was similar to editing of eGFP, while the endogenous *NbPDS* gene editing was considerably different, and did not contain multi-nt deletions or multi-nt insertions. Therefore, it may be speculated that the two editing events of 16c-*GFP* and *eGFP* were similar, as both are transgenes.

The software output of ICE v2.0 provides a model fit value (R^2) which measures the extent that the proposed edits can explain the observed edited sequence trace (Conant *et al.*, 2022). Results which are the most reliable will therefore have an R^2 value as close to 1.0 (100%) as possible. A low R^2 value signifies an experiment where the ICE v2.0 software was unable to find the indel contributions that appropriately explained the observed experimental trace, and are not reliable results (Conant *et al.*, 2022). The R^2 values for genes *eGFP*, *NbPDS* and *GFP* editing analysis were 0.66, >0.99 and >0.98 respectively. Genes *NbPDS* and *GFP* R^2 values were within the ideal range of being as close to 1.00 as possible, but the R^2 value for the *eGFP* gene was quite low. This low value may be attributed to the low sequence quality obtained from Sanger sequencing, as a result of a poor DNA extraction, or due to the position of the primers used for sequencing, which lie too close to the cut site and which may result in an inaccurate score (Conant *et al.*, 2022). In order to improve the low R^2 value in future studies, good quality Sanger sequencing data should be obtained. Primers which lie further away from the cut site may also improve the ICE v2.0 editing

inference. ICE v2.0 recommends primers flanking >100 bp on either side of the cut site (Conant *et al.*, 2022).

Although successful targeting of GFP was observed with Target-1, Target-2 did not demonstrate successful editing. Certain DNA sequences are not amenable to CRISPR/Cas9 cleavage (Riesenberg *et al.*, 2022), and the performance of the system is strongly dependent on the gRNA (Bruegmann, Deecke and Fladung, 2019). The GC content of the gRNA should range between 40-60%, and is optimal at 50% (Gagnon *et al.*, 2014; Bruegmann, Deecke and Fladung, 2019). The GFP Target-2 GC content was 40%, and was therefore on the fringe of the recommended range, where Target-1 had a GC content of 45%. The position of certain nts also determines the gRNA efficiency. For example, a study found that 'C' was rejected at position 3 and preferred at position 16 (Doench *et al.*, 2014). Target-2 contained a 'C' nt at position 3; while Target-1 did not. Another study identified that an 'A' nt at position 20 negatively impacted targeting efficiency (Liu *et al.*, 2016). In the current study, Target-1 contained a 'T' at position 20, while Target-2 possessed an 'A' at position 20. The combination of a 'C' and 'A' at positions 3 and 20 in Target-2 may explain the lack of editing. Additionally, Target 2 was located at the 3'-end of the *GFP* gene, and therefore this location may not be an efficient position for editing. The chromatin structure has also been identified as a major factor impacting the accessibility of the target region, and may also play a role in the cause of Target-2 not successfully targeting the region (Kuscu *et al.*, 2014; Wu *et al.*, 2014). Therefore, future studies should design multiple gRNAs, while adopting the abovementioned requirements and targeting different regions of a gene.

It has been observed that certain targets demonstrate distinct preferences for specific indel types (Chakrabarti *et al.*, 2019). Editing outcomes can be predicted on gRNA sequence-dependent rules, specifically depending on the fourth nt upstream of the PAM (Chakrabarti *et al.*, 2019). The software inDelphi and FORECasT have been utilised for indel prediction in plants (Molla *et al.*, 2022). In this study, both software tools were used to predict the inserted nt identify at the *NbPDS* target site, and the likeliest inserted nt was a 'C' nt, at 3.2 and 4.8% respectively. It is important to note that the predictability of the inserted base is dependent on the –4 nt position, but the accuracy of the prediction decreases in the order T > A > C > G (Molla *et al.*, 2020). Although the inserted nt was predicted to be a 'C', the prediction accuracy is low, and methods such as NGS would be required to determine the identity of the insertion (Zuo and Liu, 2016; Lemos *et al.*,

2018; Molla *et al.*, 2020). Future studies should consider basing the design of the gRNA on the –4 nt upstream from the PAM sequence, to allow for more predictable editing outcomes.

Literature has shown that editing efficiency of a CRISPR/Cas9 system was correlated with the *Cas9* and gRNA expression (Kalinina *et al.*, 2020). Therefore, this study sought to compare the expression of *Cas9* from the *eGFP*-targeting experiment, to the expression of a stably-integrated *Cas9* gene in *N. benthamiana* plants. The relative quantification of Cas9 from pRIC-infiltrated leaves was significantly higher when compared to the expression of *Cas9* from transgenic *N. benthamiana* plants. Supporting this result, a study showed that the use of a geminivirus replicon system for the expression of the CRISPR/Cas12a system resulted in *Cas12a* expression levels higher than regular T-DNA-based delivery (Eini *et al.*, 2022). Concurrently, another study demonstrated increased *Cas9* expression in *N. benthamiana* when expressing the *Cas9* gene from a sweet potato leaf curl virus (SPLCV)-replicon, compared to regular T-DNA (Yu *et al.*, 2020). These results, along with the results of the current study, confirm that the use of a geminivirus expression vector, such as pRIC, results in high yields of recombinant proteins.

In the current study, the editing efficiency of CRISPR/Cas9 demonstrated editing of up to 38% when NbPDS was targeted, and up to 27% when GFP was targeted. When tomato plants were edited by the Vu *et al.* group, that study detected up to 72% editing efficiency with the ICE software, using CRISPR/Cas12 components expressed from a GVR (Vu *et al.*, 2020). Other studies detected editing efficiencies of 18% in potato plants and up to 90% in tomato plants with GVRs, although these editing efficiencies were not computed using the ICE software (Butler *et al.*, 2016; Dahan-Meir *et al.*, 2018). Notably, the editing efficiencies obtained in this study were comparable to what had been observed in literature, but were not as efficient as some studies showed. The online ICE v2.0 software provides example data, where 18% editing efficiency is considered low, while 97% editing efficiency is high. Taking this into consideration, pRIC-expressed CRISPR/Cas9 components resulted in the lower range of editing events. The low editing may be as a result of the choice of gRNA, as gRNA efficiency considerably determines the robustness of the Cas9 system (Shojaei Baghini *et al.*, 2021). The possibility of delivering the gRNA and the Cas9 protein from a single pRIC vector may also improve editing efficiency, as shown in a study that obtained a 72% editing efficiency in tomato plants, by utilising a single vector for delivery (Vu *et al.*, 2020). The *Cas9* gene in this study was fused to a single 3'-NLS (Fig. 4.4A). However, studies have found

that a dual NLS system at the 5'- and 3'-end of the *Cas9* gene resulted in better Cas9 targeting (Grützner *et al.*, 2021). Alternatively, the most improved Cas9 targeting was observed when 13 introns were added to the *Cas9* coding sequence (Grützner *et al.*, 2021). To improve editing efficiency with the pRIC BeYDV vector, future studies should consider designing and implementing multiple gRNAs in the assay, as well as using a dual NLS system and a Cas9 coding sequence with additional introns.

In conclusion, the current study successfully modified the pRIC 3.0 vector to harbour the necessary gRNAs, targeting *NbPDS* and 16c-*GFP*. The pRIC-Cas9 vector was successful in delivering and expressing the large *Cas9* gene, and efficiently targeted both exogenously-delivered *eGFP* DNA and endogenous *N. benthamiana* DNA. These results contribute to the aim of utilising pRIC to deliver high amounts of genome editing components *in planta*, and may pose a method of achieving efficient gene editing in major crop plants, such as grapevine.

CHAPTER 5: General discussion and conclusion

5.1 SUMMARY OF FINDINGS

Genome editing in plants has been revolutionised by the harnessing of the Clustered Regularly Interspaced Short Palindromic Repeat (CRISPR) immune system of bacterial and archaeal species. The optimisation and implementation of the system as a defense mechanism against plant viruses has become a popular method among scientists. Specifically, the CRISPR/Cas13 RNA-targeting system has been used as a direct method to cleave RNA virus genomes. However, the efficient delivery of CRISPR/Cas components in plants has proved a bottleneck to scientists. To overcome this, plant virus-derived vectors have become an alternative fast and efficient delivery system for genome editing components in plants, due to the genome amplification and systemic movement of the virus. The purpose of this study was to target grapevine virus A (GVA) using the CRISPR/Cas13d (CasRx) system in a model plant, and to deliver and express CRISPR/Cas9 components *in planta*, using a bean yellow dwarf virus (BeYDV) vector.

Chapter 3, the first research chapter of this thesis, sought to target GVA with the RNA-targeting CRISPR/CasRx system, in *N. benthamiana*. Initially, the replicase gene of GVA was targeted, and suggested virus inhibition was observed in one transgenic line. However, due to the significant variation observed among transgenic lines, new guide RNAs (gRNAs) targeting the coat protein (*CP*) gene of GVA were designed, in an attempt to achieve more consistent GVA interference. Virus interference was observed in stable experiments, when transgenic *N. benthamiana* plants constitutively expressing the *CasRx* gene (hereafter referred to as CasRx-EMPTY plants) were infiltrated with gRNAs and the GVA infectious clone (pBINSN_GVA118_NbPDS). Tobacco rattle virus (TRV) vectors harbouring individual CP gRNAs were infiltrated into CasRx-EMPTY plants, and GVA interference in three of the five samples was shown, for each gRNA. Specifically, gRNA T2 demonstrated a significant negative correlation between gRNA expression and GVA accumulation. Subsequent experiments aimed to investigate the presence of guide-induced gene silencing (GIGS), when multiple gRNAs were infiltrated simultaneously. No viral interference by GIGS was observed, while CRISPR/CasRx samples resulted in decreased GVA accumulation.

The second research chapter, Chapter 4, sought to use a BeYDV vector, pRIC (Regnard *et al.*, 2010), to deliver and express CRISPR/Cas9 components *in planta*, with the aim of targeting

exogenously-delivered DNA and endogenous plant genes. Exogenously-delivered enhanced green fluorescence protein (eGFP) was successfully targeted with pRIC-expressed Cas9. When the endogenous genes *N. benthamiana* phytoene desaturase (*NbPDS*) and green fluorescence protein (*GFP*) of the 16c transgenic *N. benthamiana* line were targeted, both genes exhibited editing at the target site. The editing patterns of genes e*GFP* and *NbPDS* both featured a single nucleotide (nt) insertion as the most frequent indel. Moreover, both *eGFP* and *GFP* genes demonstrated editing at the target locus of multi-nt insertions and deletions, while NbPDS showed a single nt insertion only. The expression levels of *Cas9* from pRIC, and transgenic Cas9 *N. benthamiana* were compared, and results showed that the pRIC vector expressed *Cas9* at a significantly higher level. Although the editing efficiency of pRIC-expressed CRISPR/Cas9 components was lower than what has been observed in literature, the system still demonstrated successful editing of all target genes.

5.2 FUTURE CONSIDERATIONS

The gRNA design of CRISPR systems has been found to be an essential element for efficient DNA and RNA knockdown. Several factors can be considered when designing gRNAs for future studies, to improve targeting efficiencies. 1) The 'Genome-editing Optimized Lock Design' (GOLD)-gRNA for improved DNA cleavage: The occurrence of unintended secondary structures in gRNAs result in decreased interference (Riesenberg *et al.*, 2022). Structures such as hairpin loops in the spacer region or interactions between the gRNA backbone and spacer region result in inactive gRNAs (Thyme *et al.*, 2016). One study identified a solution to unintended intramolecular gRNA interactions, which described modifying the constant tracrRNA of the gRNA by elongation of the first hairpin with a stable loop motif, resulting in a 'locked' or 'superstable' tracrRNA (Riesenberg *et al.*, 2022). This GOLD-gRNA resulted in increased editing efficiencies of up to 1000-fold, even at otherwise non-editable loci, and prevents the need to screen multiple gRNAs to identify eligible ones. 2) Chemically modified crRNAs for RNA targeting: A study by the Méndez-Mancilla *et al.* group identified a subset of optimal modifications to the crRNA for RNA targeting (Méndez-Mancilla *et al.*, 2022). Modified crRNAs containing 2'-O-methylation at the 3'-end bases resulted in improved RNA knockdown, which also persisted longer than RNA knockdown with unmodified crRNAs. 3) "Polyvalent" gRNAs: Significant efforts are made in genome editing applications to minimise "off-targets" with CRISPR effectors, which occur when effectors have a tolerance for imperfect complementarity to their gRNA. One study exploited this natural tolerance of CRISPR

effectors, by designing gRNAs targeting multiple viral target sites simultaneously. The study demonstrated that single "polyvalent" gRNAs (pgRNAs), along with the Cas13 protein, efficiently degraded viral target pairs with sequence divergence of up to 40%, and that pgRNAs resulted in more robust plant virus suppression than a "monovalent" gRNA (Bagchi *et al.*, 2021). By designing a pgRNA to target multiple sites of GVA, future studies could improve virus interference with CRISPR/Cas13 systems. 4) Combining CRISPR/Cas13d and GIGS for RNA targeting: Although the current study did not identify GIGS, future studies might consider combining CRISPR/Cas13d targeting and GIGS, as a means to increase the possibility of successful RNA interference. The Sharma *et al.* group demonstrated that GIGS resulted in RNA silencing using a guide sequence that was shorter than conventional antisense constructs and hairpins used in plants (Sharma *et al.*, 2022). Therefore, by using a gRNA between 24-28 nts when employing the CRISPR/Cas13 system, the possibility of GIGS is increased, in addition to Cas13 RNA-targeting. The gRNA recommendations stated above could all possibly improve future DNA and RNA targeting with CRISPR systems.

Studies with CRISPR/Cas9 have shown that low gRNA expression levels resulted in inefficient genome editing in plants (Chiong, Cody and Scholthof, 2021), and that increased Cas9 protein accumulation contributed to higher editing efficiency (Cody, Scholthof and Mirkov, 2017). Furthermore, decreased gene editing efficiency could be caused by possible gRNA silencing in transgenic plants (Ma and Liu, 2016). The tomato bushy stunt virus (TBSV) P19 protein has been found to be a strong suppressor of RNA interference (RNAi), and has since been implemented in studies to increase the expression of recombinant proteins in plants (Chiong, Cody and Scholthof, 2021). A study by Chiong and colleagues showed that by separately adding the P19 protein had a significant additive effect on *Cas9* expression, and the addition of an RNA-silencing suppressor to CRISPR/Cas9 and CRISPR/Cas13 studies may ultimately result in increased targeting efficiency (Chiong, Cody and Scholthof, 2021). Additionally, the same group also showed evidence for a single delivery platform, to express both a gRNA and Cas9 protein from a single virus vector. By delivering both CRISPR/Cas9 components with the pRIC BeYDV vector, future studies could streamline delivery and possibly improve gene editing efficiencies. Importantly, studies have shown that RNA interference is correlated with *Cas13* expression and accumulation (Jiao *et al.*, 2022). The current study achieved virus interference when CasRx was expressed from stably-

transformed *N. benthamiana* plants. Therefore, by delivering CasRx with a viral vector that results in high expression levels, such as pRIC, future studies could improve virus targeting in plants.

5.3 CONCLUSION

CRISPR/Cas systems offer unprecedented opportunities for gene engineering, and continuous advancements in the field of CRISPR editing are expanding the possibilities available to scientists. The agricultural sector is afflicted by plant viruses and the diseases they cause, and thus sustainable solutions are necessary to control these viruses. The use of CRISPR/Cas systems has become a popular method to combat plant viruses, while plant virus vectors have simultaneously become a means of delivering CRISPR components. This study achieved moderate virus interference with an RNA-targeting CRISPR/CasRx system in a model plant, and showed that the pRIC geminivirus vector delivered CRISPR/Cas9 components *in planta*, and Cas9 successfully edited target loci. Ultimately, both research chapters of this thesis covered topics which contribute to finding a solution for controlling plant viruses. The recommendations mentioned above may significantly improve virus targeting in plants in future studies, and help find a solution to controlling plant viruses which plague economically important crops, such as grapevine.

REFERENCES

Abudayyeh, O.O., Gootenberg, J.S., Konermann, S., Joung, J., Slaymaker, I.M., Cox, D.B.T., Shmakov, S., Makarova, K.S., Semenova, E., Minakhin, L., Severinov, K., Regev, A., Lander, E.S., Koonin, E. V. and Zhang, F. (2016) 'C2c2 is a single-component programmable RNA-guided RNA-targeting CRISPR effector.', *Science (New York, N.Y.)*, 353(6299), p. aaf5573. Available at: https://doi.org/10.1126/science.aaf5573.

Abudayyeh, O.O., Gootenberg, J.S., Essletzbichler, P., Han, S., Joung, J., Belanto, J.J., Verdine, V., Cox, D.B.T., Kellner, M.J., Regev, A., Lander, E.S., Voytas, D.F., Ting, A.Y. and Zhang, F. (2017) 'RNA targeting with CRISPR-Cas13', *Nature*, 550(7675), pp. 280–284. Available at: https://doi.org/10.1038/nature24049.

Ahmar, S., Gill, R.A., Jung, K.-H., Faheem, A., Qasim, M.U., Mubeen, M. and Zhou, W. (2020) 'Conventional and Molecular Techniques from Simple Breeding to Speed Breeding in Crop Plants: Recent Advances and Future Outlook', *International Journal of Molecular Sciences*, 21(7), p. 2590. Available at: https://doi.org/10.3390/ijms21072590.

Akbar, S., Wei, Y. and Zhang, M.-Q. (2022) 'RNA Interference: Promising Approach to Combat Plant Viruses', *International Journal of Molecular Sciences*, 23(10), p. 5312. Available at: https://doi.org/10.3390/ijms23105312.

Alabi, O.J., Casassa, L.F., Gutha, L.R., Larsen, R.C., Henick-Kling, T., Harbertson, J.F. and Naidu, R.A. (2016) 'Impacts of Grapevine Leafroll Disease on Fruit Yield and Grape and Wine Chemistry in a Wine Grape (Vitis vinifera L.) Cultivar', *PLOS ONE*. Edited by H. Gerós, 11(2), p. e0149666. Available at: https://doi.org/10.1371/journal.pone.0149666.

Ali, Z., Abulfaraj, A., Idris, A., Ali, S., Tashkandi, M. and Mahfouz, M.M. (2015) 'CRISPR/Cas9-mediated viral interference in plants', *Genome Biology*, 16(1), pp. 1–11. Available at: https://doi.org/10.1186/s13059-015-0799-6.

Ali, Z., Abul-Faraj, A., Li, L., Ghosh, N., Piatek, M., Mahjoub, A., Aouida, M., Piatek, A., Baltes, N.J., Voytas, D.F., Dinesh-Kumar, S. and Mahfouz, M.M. (2015) 'Efficient Virus-Mediated Genome Editing in Plants Using the CRISPR/Cas9 System', *Molecular Plant*, 8(8), pp. 1288–1291. Available at: https://doi.org/10.1016/j.molp.2015.02.011.

Ali, Z., Ali, S., Tashkandi, M., Zaidi, S.S.E.A. and Mahfouz, M.M. (2016) 'CRISPR/Cas9-Mediated Immunity to Geminiviruses: Differential Interference and Evasion', *Scientific Reports*, 6(1), pp. 1–13. Available at: https://doi.org/10.1038/srep26912.

Aman, R., Mahas, A., Butt, H., Aljedaani, F. and Mahfouz, M. (2018) 'Engineering RNA Virus Interference via the CRISPR/Cas13 Machinery in Arabidopsis', *Viruses*, 10(12), p. 732. Available at: https://doi.org/10.3390/v10120732.

Aman, R., Ali, Z., Butt, H., Mahas, A., Aljedaani, F., Khan, M.Z., Ding, S. and Mahfouz, M. (2018)

'RNA virus interference via CRISPR/Cas13a system in plants', *Genome Biology*, 19(1), p. 1. Available at: https://doi.org/10.1186/s13059-017-1381-1.

Amitai, G. and Sorek, R. (2016) 'CRISPR–Cas adaptation: insights into the mechanism of action', *Nature Reviews Microbiology 2016 14:2*, 14(2), pp. 67–76. Available at: https://doi.org/10.1038/nrmicro.2015.14.

Anderson, P.K., Cunningham, A.A., Patel, N.G., Morales, F.J., Epstein, P.R. and Daszak, P. (2004) 'Emerging infectious diseases of plants: pathogen pollution, climate change and agrotechnology drivers', *Trends in Ecology & Evolution*, 19(10), pp. 535–544. Available at: https://doi.org/10.1016/J.TREE.2004.07.021.

Bagchi, R., Tinker-Kulberg, R., Supakar, T., Chamberlain, S., Ligaba-Osena, A. and Josephs, E.A. (2021) 'Polyvalent Guide RNAs for CRISPR Antivirals', *bioRxiv*, p. 2021.02.25.430352. Available at: https://doi.org/10.1101/2021.02.25.430352.

Baltes, N.J., Gil-Humanes, J., Cermak, T., Atkins, P.A. and Voytas, D.F. (2014) 'DNA Replicons for Plant Genome Engineering', *The Plant Cell*, 26(1), pp. 151–163. Available at: https://doi.org/10.1105/tpc.113.119792.

Baltes, N.J., Hummel, A.W., Konecna, E., Cegan, R., Bruns, A.N., Bisaro, D.M. and Voytas, D.F. (2015) 'Conferring resistance to geminiviruses with the CRISPR–Cas prokaryotic immune system', *Nature Plants 2015 1:10*, 1(10), pp. 1–4. Available at: https://doi.org/10.1038/nplants.2015.145.

Bandaru, S., Tsuji, M.H., Shimizu, Y., Usami, K., Lee, S., Takei, N.K., Yoshitome, K., Nishimura, Y., Otsuki, T. and Ito, T. (2020) 'Structure-based design of gRNA for Cas13', *Scientific Reports*, 10(1), p. 11610. Available at: https://doi.org/10.1038/s41598-020-68459-4.

Bashandy, H., Jalkanen, S. and Teeri, T.H. (2015) 'Within leaf variation is the largest source of variation in agroinfiltration of Nicotiana benthamiana', *Plant Methods*, 11(1), pp. 1–7. Available at: https://doi.org/10.1186/S13007-015-0091-5/FIGURES/3.

Bednarek, R., David, M., Fuentes, S., Kreuze, J. and Fei, Z. (2021) 'Transcriptome analysis provides insights into the responses of sweet potato to sweet potato virus disease (SPVD)', *Virus Research*, 295, p. 198293. Available at: https://doi.org/10.1016/j.virusres.2020.198293.

Belhaj, K., Chaparro-Garcia, A., Kamoun, S. and Nekrasov, V. (2013) 'Plant genome editing made easy: targeted mutagenesis in model and crop plants using the CRISPR/Cas system', *Plant Methods*, 9(1), p. 39. Available at: https://doi.org/10.1186/1746-4811-9-39.

Bernstein, E., Caudy, A.A., Hammond, S.M. and Hannon, G.J. (2001) 'Role for a bidentate ribonuclease in the initiation step of RNA interference', *Nature 2001 409:6818*, 409(6818), pp. 363–366. Available at: https://doi.org/10.1038/35053110.

Bertani, G. (1951) 'STUDIES ON LYSOGENESIS I', *Journal of Bacteriology*, 62(3), pp. 293–300. Available at: https://doi.org/10.1128/jb.62.3.293-300.1951.

Bhaya, D., Davison, M. and Barrangou, R. (2011) 'CRISPR-cas systems in bacteria and archaea: Versatile small RNAs for adaptive defense and regulation', *Annual Review of Genetics*, 45, pp. 273–297. Available at: https://doi.org/10.1146/annurev-genet-110410-132430.

Bloh, K., Kanchana, R., Bialk, P., Banas, K., Zhang, Z., Yoo, B.C. and Kmiec, E.B. (2021) 'Deconvolution of Complex DNA Repair (DECODR): Establishing a Novel Deconvolution Algorithm for Comprehensive Analysis of CRISPR-Edited Sanger Sequencing Data', *The CRISPR journal*, 4(1), pp. 120–131. Available at: https://doi.org/10.1089/CRISPR.2020.0022.

Boch, J., Scholze, H., Schornack, S., Landgraf, A., Hahn, S., Kay, S., Lahaye, T., Nickstadt, A. and Bonas, U. (2009) 'Breaking the code of DNA binding specificity of TAL-type III effectors', *Science*, 326(5959), pp. 1509–1512. Available at: https://doi.org/10.1126/science.1178811.

Bortesi, L. and Fischer, R. (2015) 'The CRISPR/Cas9 system for plant genome editing and beyond', *Biotechnology Advances*, 33(1), pp. 41–52. Available at: https://doi.org/10.1016/j.biotechadv.2014.12.006.

Boualem, A., Dogimont, C. and Bendahmane, A. (2016) 'The battle for survival between viruses and their host plants', *Current Opinion in Virology*, 17, pp. 32–38. Available at: https://doi.org/10.1016/j.coviro.2015.12.001.

Brinkman, E.K., Chen, T., Amendola, M. and Van Steensel, B. (2014) 'Easy quantitative assessment of genome editing by sequence trace decomposition', *Nucleic Acids Research*, 42(22), pp. e168–e168. Available at: https://doi.org/10.1093/nar/gku936.

Brouns, S.J.J., Jore, M.M., Lundgren, M., Westra, E.R., Slijkhuis, R.J.H., Snijders, A.P.L., Dickman, M.J., Makarova, K.S., Koonin, E. V. and Van Der Oost, J. (2008) 'Small CRISPR RNAs guide antiviral defense in prokaryotes', *Science*, 321(5891), pp. 960–964. Available at: https://doi.org/10.1126/science.1159689.

Bruegmann, T., Deecke, K. and Fladung, M. (2019) 'Evaluating the Efficiency of gRNAs in CRISPR/Cas9 Mediated Genome Editing in Poplars', *International Journal of Molecular Sciences*, 20(15), p. 3623. Available at: https://doi.org/10.3390/ijms20153623.

Burgyán, J. and Havelda, Z. (2011) 'Viral suppressors of RNA silencing', *Trends in Plant Science*, 16(5), pp. 265–272. Available at: https://doi.org/10.1016/J.TPLANTS.2011.02.010.

Butler, N.M., Atkins, P.A., Voytas, D.F. and Douches, D.S. (2015) 'Generation and Inheritance of Targeted Mutations in Potato (Solanum tuberosum L.) Using the CRISPR/Cas System', *PLOS ONE*. Edited by H. Fujii, 10(12), p. e0144591. Available at: https://doi.org/10.1371/journal.pone.0144591.

Butler, N.M., Baltes, N.J., Voytas, D.F. and Douches, D.S. (2016) 'Geminivirus-mediated genome editing in potato (Solanum tuberosum l.) using sequence-specific nucleases', *Frontiers in Plant Science*, 7, p. 1045. Available at: https://doi.org/10.3389/fpls.2016.01045.

Cao, Y., Zhou, H., Zhou, X. and Li, F. (2021) 'Conferring Resistance to Plant RNA Viruses with the CRISPR/CasRx System', *Virologica Sinica*, 36(4), pp. 814–817. Available at: https://doi.org/10.1007/s12250-020-00338-8.

Čermák, T., Baltes, N.J., Čegan, R., Zhang, Y. and Voytas, D.F. (2015) 'High-frequency, precise modification of the tomato genome', *Genome Biology*, 16(1), p. 232. Available at: https://doi.org/10.1186/s13059-015-0796-9.

Čermák, T., Curtin, S.J., Gil-Humanes, J., Čegan, R., Kono, T.J.Y., Konečná, E., Belanto, J.J., Starker, C.G., Mathre, J.W., Greenstein, R.L. and Voytas, D.F. (2017) 'A multipurpose toolkit to enable advanced genome engineering in plants', *Plant Cell*, 29(6), pp. 1196–1217. Available at: https://doi.org/10.1105/tpc.16.00922.

Chakrabarti, A.M., Henser-Brownhill, T., Monserrat, J., Poetsch, A.R., Luscombe, N.M. and Scaffidi, P. (2019) 'Target-Specific Precision of CRISPR-Mediated Genome Editing', *Molecular Cell*, 73(4), pp. 699-713.e6. Available at: https://doi.org/10.1016/j.molcel.2018.11.031.

Chaudhary, K. (2018) 'CRISPR/Cas13a targeting of RNA virus in plants', *Plant Cell Reports*, 37(12), pp. 1707–1712. Available at: https://doi.org/10.1007/s00299-018-2297-2.

Chen, J.S., Ma, E., Harrington, L.B., Da Costa, M., Tian, X., Palefsky, J.M. and Doudna, J.A. (2018) 'CRISPR-Cas12a target binding unleashes indiscriminate single-stranded DNase activity', *Science*, 360(6387), pp. 436–439. Available at: https://doi.org/10.1126/science.aar6245.

Chen, W., Qian, Y., Wu, Xiaoyun, Sun, Y., Wu, Xiaoxia and Cheng, X. (2014) 'Inhibiting replication of begomoviruses using artificial zinc finger nucleases that target viral-conserved nucleotide motif', *Virus Genes*, 48(3), pp. 494–501. Available at: https://doi.org/10.1007/s11262-014-1041-4.

Cheng, X., Li, F., Cai, J., Chen, W., Zhao, N., Sun, Y., Guo, Y., Yang, X. and Wu, X. (2015) 'Artificial TALE as a convenient protein platform for engineering broad-spectrum resistance to begomoviruses', *Viruses*, 7(8), pp. 4772–4782. Available at: https://doi.org/10.3390/v7082843.

Chiba, M., Reed, J.C., Prokhnevsky, A.I., Chapman, E.J., Mawassi, M., Koonin, E. V., Carrington, J.C. and Dolja, V. V. (2006) 'Diverse suppressors of RNA silencing enhance agroinfection by a viral replicon', *Virology*, 346(1), pp. 7–14. Available at: https://doi.org/10.1016/j.virol.2005.09.068.

Chiong, K.T., Cody, W.B. and Scholthof, H.B. (2021) 'RNA silencing suppressor-influenced performance of a virus vector delivering both guide RNA and Cas9 for CRISPR gene editing', *Scientific Reports*, 11(1), pp. 1–13. Available at: https://doi.org/10.1038/s41598-021-85366-4.

Clement, K., Rees, H., Canver, M.C., Gehrke, J.M., Farouni, R., Hsu, J.Y., Cole, M.A., Liu, D.R., Joung, J.K., Bauer, D.E. and Pinello, L. (2019) 'CRISPResso2 provides accurate and rapid genome editing sequence analysis', *Nature Biotechnology 2019 37:3*, 37(3), pp. 224–226. Available at: https://doi.org/10.1038/s41587-019-0032-3.

Clemente, T. (2006) '*Nicotiana* (*Nicotiana tobaccum, Nicotiana benthamiana*)', in *Agrobacterium Protocols*. New Jersey: Humana Press, pp. 143–154. Available at: https://doi.org/10.1385/1-59745-130-4:143.

Cody, W.B. and Scholthof, H.B. (2019) 'Plant Virus Vectors 3.0: Transitioning into Synthetic Genomics', *Annual Review of Phytopathology*, 57(1), pp. 211–230. Available at: https://doi.org/10.1146/annurev-phyto-082718-100301.

Cody, W.B., Scholthof, H.B. and Mirkov, T.E. (2017) 'Multiplexed Gene Editing and Protein Overexpression Using a Tobacco mosaic virus Viral Vector', *Plant Physiology*, 175(1), p. 23. Available at: https://doi.org/10.1104/PP.17.00411.

Coetzee, B., Freeborough, M.-J., Maree, H.J., Celton, J.-M., Rees, D.J.G. and Burger, J.T. (2010) 'Deep sequencing analysis of viruses infecting grapevines: Virome of a vineyard', *Virology*, 400(2), pp. 157–163. Available at: https://doi.org/10.1016/j.virol.2010.01.023.

Conant, D., Hsiau, T., Rossi, N., Oki, J., Maures, T., Waite, K., Yang, J., Joshi, S., Kelso, R., Holden, K., Enzmann, B.L. and Stoner, R. (2022) 'Inference of CRISPR Edits from Sanger Trace Data', *The CRISPR Journal*, 5(1), pp. 1–8. Available at: https://doi.org/10.1089/crispr.2021.0113.

Cong, L., Ran, F.A., Cox, D., Lin, S., Barretto, R., Habib, N., Hsu, P.D., Wu, X., Jiang, W., Marraffini, L.A. and Zhang, F. (2013) 'Multiplex genome engineering using CRISPR/Cas systems', *Science*, 339(6121), pp. 819–823. Available at: https://doi.org/10.1126/science.1231143.

Cox, D.B.T., Gootenberg, J.S., Abudayyeh, O.O., Franklin, B., Kellner, M.J., Joung, J. and Zhang, F. (2017) 'RNA editing with CRISPR-Cas13', *Science*, 358(6366), pp. 1019–1027. Available at: https://doi.org/10.1126/science.aaq0180.

Dahan-Meir, T., Filler-Hayut, S., Melamed-Bessudo, C., Bocobza, S., Czosnek, H., Aharoni, A. and Levy, A.A. (2018) 'Efficient in planta gene targeting in tomato using geminiviral replicons and the CRISPR/Cas9 system', *The Plant Journal*, 95(1), pp. 5–16. Available at: https://doi.org/10.1111/TPJ.13932.

Deltcheva, E., Chylinski, K., Sharma, C.M., Gonzales, K., Chao, Y., Pirzada, Z.A., Eckert, M.R., Vogel, J. and Charpentier, E. (2011) 'CRISPR RNA maturation by trans-encoded small RNA and host factor RNase III', *Nature*, 471(7340), pp. 602–607. Available at: https://doi.org/10.1038/nature09886.

Doench, J.G., Hartenian, E., Graham, D.B., Tothova, Z., Hegde, M., Smith, I., Sullender, M., Ebert, B.L., Xavier, R.J. and Root, D.E. (2014) 'Rational design of highly active sgRNAs for CRISPR-Cas9-

mediated gene inactivation', *Nature Biotechnology*, 32(12), pp. 1262–1267. Available at: https://doi.org/10.1038/nbt.3026.

Dong, D., Ren, K., Qiu, X., Zheng, J., Guo, M., Guan, X., Liu, H., Li, N., Zhang, B., Yang, D., Ma, C., Wang, S., Wu, D., Ma, Y., Fan, S., Wang, J., Gao, N. and Huang, Z. (2016) 'The crystal structure of Cpf1 in complex with CRISPR RNA', *Nature*, 532(7600), pp. 522–526. Available at: https://doi.org/10.1038/nature17944.

Doudna, J.A. and Charpentier, E. (2014) 'The new frontier of genome engineering with CRISPR-Cas9', *Science*, 346(6213), p. 1258096. Available at: https://doi.org/10.1126/science.1258096.

Duxbury, P. (2020) *Proof-of-concept : Geminivirus expression vector for testing the efficacy of CRISPR / Cas components on heterologous sequences in Nicotiana benthamiana*. Stellenbosch University.

East-Seletsky, A., O'Connell, M.R., Knight, S.C., Burstein, D., Cate, J.H.D., Tjian, R. and Doudna, J.A. (2016) 'Two distinct RNase activities of CRISPR-C2c2 enable guide-RNA processing and RNA detection', *Nature*, 538(7624), pp. 270–273. Available at: https://doi.org/10.1038/nature19802.

Eini, O., Schumann, N., Niessen, M. and Varrelmann, M. (2022) 'Targeted mutagenesis in plants using Beet curly top virus for efficient delivery of CRISPR/Cas12a components', *New Biotechnology*, 67, pp. 1–11. Available at: https://doi.org/10.1016/j.nbt.2021.12.002.

Elbashir, S.M., Lendeckel, W. and Tuschl, T. (2001) 'RNA interference is mediated by 21- and 22-nucleotide RNAs', *Genes and Development*, 15(2), pp. 188–200. Available at: https://doi.org/10.1101/gad.862301.

Elena, S.F., Fraile, A. and García-Arenal, F. (2014) 'Evolution and Emergence of Plant Viruses', in *Advances in Virus Research*. Academic Press, pp. 161–191. Available at: https://doi.org/10.1016/B978-0-12-800098-4.00003-9.

Fargette, D., Konaté, G., Fauquet, C., Muller, E., Peterschmitt, M. and Thresh, J.M. (2006) 'Molecular Ecology and Emergence of Tropical Plant Viruses', *Annual Review of Phytopathology*, 44(1), pp. 235–260. Available at: https://doi.org/10.1146/annurev.phyto.44.120705.104644.

Feng, Z., Zhang, B., Ding, W., Liu, X., Yang, D.-L., Wei, P., Cao, F., Zhu, S., Zhang, F., Mao, Y. and Zhu, J.-K. (2013) 'Efficient genome editing in plants using a CRISPR/Cas system', *Cell Research*, 23(10), pp. 1229–1232. Available at: https://doi.org/10.1038/cr.2013.114.

Feng, Z., Mao, Y., Xu, N., Zhang, B., Wei, P., Yang, D.L., Wang, Z., Zhang, Z., Zheng, R., Yang, L., Zeng, L., Liu, X. and Zhu, J.K. (2014) 'Multigeneration analysis reveals the inheritance, specificity, and patterns of CRISPR/Cas-induced gene modifications in Arabidopsis', *Proceedings of the National Academy of Sciences of the United States of America*, 111(12), pp. 4632–4637. Available at: https://doi.org/10.1073/PNAS.1400822111/SUPPL_FILE/SAPP.PDF.

Freije, C.A., Myhrvold, C., Boehm, C.K., Lin, A.E., Welch, N.L., Carter, A., Metsky, H.C., Luo, C.Y., Abudayyeh, O.O., Gootenberg, J.S., Yozwiak, N.L., Zhang, F. and Sabeti, P.C. (2019) 'Programmable Inhibition and Detection of RNA Viruses Using Cas13', *Molecular Cell*, 76(5), pp. 826-837.e11. Available at: https://doi.org/10.1016/j.molcel.2019.09.013.

Fuchs, M. (2020) 'Grapevine viruses: a multitude of diverse species with simple but overall poorly adopted management solutions in the vineyard', *Journal of Plant Pathology*. Springer, pp. 643–653. Available at: https://doi.org/10.1007/s42161-020-00579-2.

Gagnon, J.A., Valen, E., Thyme, S.B., Huang, P., Ahkmetova, L., Pauli, A., Montague, T.G., Zimmerman, S., Richter, C. and Schier, A.F. (2014) 'Efficient mutagenesis by Cas9 protein-mediated oligonucleotide insertion and large-scale assessment of single-guide RNAs', *PLoS ONE*, 9(5), p. e98186. Available at: https://doi.org/10.1371/journal.pone.0098186.

Gaj, T., Gersbach, C.A. and Barbas, C.F. (2013) 'ZFN, TALEN, and CRISPR/Cas-based methods for genome engineering', *Trends in Biotechnology*, 31(7), pp. 397–405. Available at: https://doi.org/10.1016/j.tibtech.2013.04.004.

Galiakparov, N., Tanne, E., Sela, I. and Gafny, R. (2003) 'Functional analysis of the grapevine virus A genome', *Virology*, 306(1), pp. 42–50. Available at: https://doi.org/10.1016/S0042-6822(02)00019-3.

Galiakparov, Nurbol, Tanne, E., Mawassi, M., Gafny, R. and Sela, I. (2003) 'ORF 5 of Grapevine Virus A Encodes a Nucleic Acid-Binding Protein and Affects Pathogenesis', *Virus Genes*, 27(3), pp. 257–262. Available at: https://doi.org/10.1023/A:1026395815980.

Gil-Humanes, J., Wang, Y., Liang, Z., Shan, Q., Ozuna, C. V., Sánchez-León, S., Baltes, N.J., Starker, C., Barro, F., Gao, C. and Voytas, D.F. (2017) 'High-efficiency gene targeting in hexaploid wheat using DNA replicons and CRISPR/Cas9', *The Plant Journal*, 89(6), pp. 1251–1262. Available at: https://doi.org/10.1111/TPJ.13446.

Goszczynski, D.E. and Jooste, A.E.C. (2003) 'Identification of grapevines infected with divergent variants of Grapevine virus A using variant-specific RT-PCR', *Journal of Virological Methods*, 112(1–2), pp. 157–164. Available at: https://doi.org/10.1016/S0166-0934(03)00198-8.

Goszczynski, D.E., du Preez, J. and Burger, J.T. (2008) 'Molecular divergence of Grapevine virus A (GVA) variants associated with Shiraz disease in South Africa', *Virus Research*, 138(1–2), pp. 105–110. Available at: https://doi.org/10.1016/j.virusres.2008.08.014.

Grützner, R., Martin, P., Horn, C., Mortensen, S., Cram, E.J., Lee-Parsons, C.W.T., Stuttmann, J. and Marillonnet, S. (2021) 'High-efficiency genome editing in plants mediated by a Cas9 gene containing multiple introns', *Plant Communications*, 2(2), p. 100135. Available at: https://doi.org/10.1016/j.xplc.2020.100135.

Guo, X., Rahman, J.A., Wessels, H.-H., Méndez-Mancilla, A., Haro, D., Chen, X. and Sanjana, N.E.

(2021) 'Transcriptome-wide Cas13 guide RNA design for model organisms and viral RNA pathogens', *Cell Genomics*, 1(1), p. 100001. Available at: https://doi.org/10.1016/j.xgen.2021.100001.

Halley-Stott, R.P., Tanzer, F., Martin, D.P. and Rybicki, E.P. (2007) 'The complete nucleotide sequence of a mild strain of Bean yellow dwarf virus', *Archives of Virology*, 152(6), pp. 1237–1240. Available at: https://doi.org/10.1007/s00705-006-0933-6.

Hanley-Bowdoin, L., Bejarano, E.R., Robertson, D. and Mansoor, S. (2013) 'Geminiviruses: masters at redirecting and reprogramming plant processes', *Nature Reviews Microbiology 2013 11:11*, 11(11), pp. 777–788. Available at: https://doi.org/10.1038/nrmicro3117.

Hashimoto, M., Neriya, Y., Yamaji, Y. and Namba, S. (2016) 'Recessive resistance to plant viruses: Potential resistance genes beyond translation initiation factors', *Frontiers in Microbiology*, p. 1695. Available at: https://doi.org/10.3389/fmicb.2016.01695.

Haurwitz, R.E., Jinek, M., Wiedenheft, B., Zhou, K. and Doudna, J.A. (2010) 'Sequence- and structure-specific RNA processing by a CRISPR endonuclease', *Science*, 329(5997), pp. 1355–1358. Available at: https://doi.org/10.1126/science.1192272.

Haviv, S., Iddan, Y., Goszczynski, D.E. and Mawassi, M. (2012) 'The ORF5 of Grapevine virus A is involved in symptoms expression in Nicotiana benthamiana plants', *Annals of Applied Biology*, 160(2), pp. 181–190. Available at: https://doi.org/10.1111/j.1744-7348.2012.00531.x.

Hefferon, K.L. and Dugdale, B. (2003) 'Independent expression of Rep and RepA and their roles in regulating bean yellow dwarf virus replication', *Journal of General Virology*, 84(12), pp. 3465–3472. Available at: https://doi.org/10.1099/vir.0.19494-0.

Hirano, H., Gootenberg, J.S., Horii, T., Abudayyeh, O.O., Kimura, M., Hsu, P.D., Nakane, T., Ishitani, R., Hatada, I., Zhang, F., Nishimasu, H. and Nureki, O. (2016) 'Structure and Engineering of Francisella novicida Cas9', *Cell*, 164(5), pp. 950–961. Available at: https://doi.org/10.1016/J.CELL.2016.01.039.

Hummel, A.W., Chauhan, R.D., Cermak, T., Mutka, A.M., Vijayaraghavan, A., Boyher, A., Starker, C.G., Bart, R., Voytas, D.F. and Taylor, N.J. (2018) 'Allele exchange at the EPSPS locus confers glyphosate tolerance in cassava', *Plant biotechnology journal*, 16(7), pp. 1275–1282. Available at: https://doi.org/10.1111/PBI.12868.

Jackson, A.L., Bartz, S.R., Schelter, J., Kobayashi, S. V, Burchard, J., Mao, M., Li, B., Cavet, G. and Linsley, P.S. (2003) 'Expression profiling reveals off-target gene regulation by RNAi', *Nature Biotechnology 2003 21:6*, 21(6), pp. 635–637. Available at: https://doi.org/10.1038/nbt831.

Jacquier, A. and Dujon, B. (1985) 'An intron-encoded protein is active in a gene conversion process that spreads an intron into a mitochondrial gene', *Cell*, 41(2), pp. 383–394. Available at: https://doi.org/10.1016/S0092-8674(85)80011-8.

Ji, X., Zhang, H., Zhang, Y., Wang, Y. and Gao, C. (2015) 'Establishing a CRISPR–Cas-like immune system conferring DNA virus resistance in plants', *Nature Plants*, 1(10), pp. 1–4. Available at: https://doi.org/10.1038/nplants.2015.144.

Ji, X., Si, X., Zhang, Y., Zhang, H., Zhang, F. and Gao, C. (2018) 'Conferring DNA virus resistance with high specificity in plants using virus-inducible genome-editing system', *Genome Biology*, 19(1), p. 197. Available at: https://doi.org/10.1186/s13059-018-1580-4.

Jiang, F. and Doudna, J.A. (2017) 'CRISPR–Cas9 Structures and Mechanisms', *Annual Review of Biophysics*, 46(1), pp. 505–529. Available at: https://doi.org/10.1146/annurev-biophys-062215-010822.

Jiang, W., Samai, P. and Marraffini, L.A. (2016) 'Degradation of Phage Transcripts by CRISPR-Associated RNases Enables Type III CRISPR-Cas Immunity', *Cell*, 164(4), pp. 710–721. Available at: https://doi.org/10.1016/j.cell.2015.12.053.

Jiao, B., Hao, X., Liu, Z., Liu, M., Wang, J., Liu, L., Liu, N., Song, R., Zhang, J., Fang, Y. and Xu, Y. (2022) 'Engineering CRISPR immune systems conferring GLRaV-3 resistance in grapevine', *Horticulture Research*, 9. Available at: https://doi.org/10.1093/hr/uhab023.

Jinek, M., Chylinski, K., Fonfara, I., Hauer, M., Doudna, J.A. and Charpentier, E. (2012) 'A programmable dual-RNA-guided DNA endonuclease in adaptive bacterial immunity', *Science*, 337(6096), pp. 816–821. Available at: https://doi.org/10.1126/science.1225829.

Jones, R.A.C. (2009) 'Plant virus emergence and evolution: Origins, new encounter scenarios, factors driving emergence, effects of changing world conditions, and prospects for control', *Virus Research*, 141(2), pp. 113–130. Available at: https://doi.org/10.1016/J.VIRUSRES.2008.07.028.

Kalinina, N.O., Khromov, A., Love, A.J. and Taliansky, M.E. (2020) 'CRISPR applications in plant virology: Virus resistance and beyond', *Phytopathology*, 110(1), pp. 18–28. Available at: https://doi.org/10.1094/PHYTO-07-19-0267-IA.

Kamburova, V.S., Nikitina, E. V, Shermatov, S.E., Buriev, Z.T., Kumpatla, S.P., Emani, C. and Abdurakhmonov, I.Y. (2017) 'Genome Editing in Plants: An Overview of Tools and Applications', *International Journal of Agronomy*, 2017, pp. 1–15. Available at: https://doi.org/10.1155/2017/7315351.

Karyeija, R.F., Gibson, R.W. and Valkonen, J.P.T. (1998) 'The Significance of Sweet Potato Feathery Mottle Virus in Subsistence Sweet Potato Production in Africa', *Plant disease*, 82(1), pp. 4–15. Available at: https://doi.org/10.1094/PDIS.1998.82.1.4.

Knott, G.J., East-Seletsky, A., Cofsky, J.C., Holton, J.M., Charles, E., O'Connell, M.R. and Doudna, J.A. (2017) 'Guide-bound structures of an RNA-targeting A-cleaving CRISPR–Cas13a enzyme', *Nature Structural & Molecular Biology 2017 24:10*, 24(10), pp. 825–833. Available at:

https://doi.org/10.1038/nsmb.3466.

Komatsu, H., Abdellatif, I.M.Y., Yuan, S., Ono, M., Nonaka, S., Ezura, H., Ariizumi, T. and Miura, K. (2020) 'Genome editing in *PDS* genes of tomatoes by non-selection method and of *Nicotiana benthamiana* by one single guide RNA to edit two orthologs', *Plant Biotechnology*, 37(2), pp. 213–221. Available at: https://doi.org/10.5511/plantbiotechnology.20.0527b.

Konermann, S., Lotfy, P., Brideau, N.J., Oki, J., Shokhirev, M.N. and Hsu, P.D. (2018) 'Transcriptome Engineering with RNA-Targeting Type VI-D CRISPR Effectors', *Cell*, 173(3), pp. 665-676.e14. Available at: https://doi.org/10.1016/j.cell.2018.02.033.

Koonin, E. V, Makarova, K.S. and Zhang, F. (2017) 'Diversity, classification and evolution of CRISPR-Cas systems.', *Current opinion in microbiology*, 37, pp. 67–78. Available at: https://doi.org/10.1016/j.mib.2017.05.008.

Kordyś, M., Sen, R. and Warkocki, Z. (2022) 'Applications of the versatile <scp>CRISPR-Cas13 RNA</scp> targeting system', *WIREs RNA*, 13(3), p. e1694. Available at: https://doi.org/10.1002/wrna.1694.

Kuluev, B.R., Gumerova, G.R., Mikhaylova, E. V., Gerashchenkov, G.A., Rozhnova, N.A., Vershinina, Z.R., Khyazev, A. V., Matniyazov, R.T., Baymiev, An. Kh, Baymiev, Al Kh and Chemeris, A. V. (2019) 'Delivery of CRISPR/Cas Components into Higher Plant Cells for Genome Editing', *Russian Journal of Plant Physiology*, 66(5), pp. 694–706. Available at: https://doi.org/10.1134/S102144371905011X.

Kuscu, C., Arslan, S., Singh, R., Thorpe, J. and Adli, M. (2014) 'Genome-wide analysis reveals characteristics of off-target sites bound by the Cas9 endonuclease', *Nature Biotechnology*, 32(7), pp. 677–683. Available at: https://doi.org/10.1038/nbt.2916.

Lawrenson, T., Shorinola, O., Stacey, N., Li, C., Østergaard, L., Patron, N., Uauy, C. and Harwood, W. (2015) 'Induction of targeted, heritable mutations in barley and Brassica oleracea using RNA-guided Cas9 nuclease', *Genome Biology*, 16(1), p. 258. Available at: https://doi.org/10.1186/s13059-015-0826-7.

Lemos, B.R., Kaplan, A.C., Bae, J.E., Ferrazzoli, A.E., Kuo, J., Anand, R.P., Waterman, D.P. and Haber, J.E. (2018) 'CRISPR/Cas9 cleavages in budding yeast reveal templated insertions and strand-specific insertion/deletion profiles', *Proceedings of the National Academy of Sciences*, 115(9), pp. E2010–E2047. Available at: https://doi.org/10.1073/pnas.1716855115.

Lewis, K.M. and Ke, A. (2017) 'Building the Class 2 CRISPR-Cas Arsenal', *Molecular Cell*, 65(3), pp. 377–379. Available at: https://doi.org/10.1016/j.molcel.2017.01.024.

Li, F. and Wang, A. (2019) 'RNA-Targeted Antiviral Immunity: More Than Just RNA Silencing', *Trends in Microbiology*, 27(9), pp. 792–805. Available at: https://doi.org/10.1016/j.tim.2019.05.007.

Li, J.-F., Norville, J.E., Aach, J., McCormack, M., Zhang, D., Bush, J., Church, G.M. and Sheen, J. (2013) 'Multiplex and homologous recombination–mediated genome editing in Arabidopsis and Nicotiana benthamiana using guide RNA and Cas9', *Nature Biotechnology*, 31(8), pp. 688–691. Available at: https://doi.org/10.1038/nbt.2654.

Li, T., Liu, B., Spalding, M.H., Weeks, D.P. and Yang, B. (2012) 'High-efficiency TALEN-based gene editing produces disease-resistant rice', *Nature Biotechnology*, 30(5), pp. 390–392. Available at: https://doi.org/10.1038/nbt.2199.

Li, Y. and Peng, N. (2019) 'Endogenous CRISPR-cas system-based genome editing and antimicrobials: Review and prospects', *Frontiers in Microbiology*. Frontiers Media S.A., p. 2471. Available at: https://doi.org/10.3389/fmicb.2019.02471.

Liang, Z., Chen, K., Zhang, Y., Liu, J., Yin, K., Qiu, J.L. and Gao, C. (2018) 'Genome editing of bread wheat using biolistic delivery of CRISPR/Cas9 in vitro transcripts or ribonucleoproteins', *Nature Protocols*, 13(3), pp. 413–430. Available at: https://doi.org/10.1038/nprot.2017.145.

Liu, D., Shi, L., Han, C., Yu, J., Li, D. and Zhang, Y. (2012) 'Validation of Reference Genes for Gene Expression Studies in Virus-Infected Nicotiana benthamiana Using Quantitative Real-Time PCR', *PLoS ONE*, 7(9). Available at: https://doi.org/10.1371/journal.pone.0046451.

Liu, J., Carmell, M.A., Rivas, F. V., Marsden, C.G., Thomson, J.M., Song, J.-J., Hammond, S.M., Joshua-Tor, L. and Hannon, G.J. (2004) 'Argonaute2 Is the Catalytic Engine of Mammalian RNAi', *Science*, 305(5689), pp. 1437–1441. Available at: https://doi.org/10.1126/science.1102513.

Liu, L., Chen, P., Wang, M., Li, X., Wang, J., Yin, M. and Wang, Y. (2017) 'C2c1-sgRNA Complex Structure Reveals RNA-Guided DNA Cleavage Mechanism', *Molecular Cell*, 65(2), pp. 310–322. Available at: https://doi.org/10.1016/j.molcel.2016.11.040.

Liu, L., Li, X., Ma, J., Li, Z., You, L., Wang, J., Wang, M., Zhang, X. and Wang, Y. (2017) 'The Molecular Architecture for RNA-Guided RNA Cleavage by Cas13a', *Cell*, 170(4), pp. 714-726.e10. Available at: https://doi.org/10.1016/j.cell.2017.06.050.

Liu, L., Li, X., Wang, J., Wang, M., Chen, P., Yin, M., Li, J., Sheng, G. and Wang, Y. (2017) 'Two Distant Catalytic Sites Are Responsible for C2c2 RNase Activities', *Cell*, 168(1–2), pp. 121-134.e12. Available at: https://doi.org/10.1016/j.cell.2016.12.031.

Liu, X., Homma, A., Sayadi, J., Yang, S., Ohashi, J. and Takumi, T. (2016) 'Sequence features associated with the cleavage efficiency of CRISPR/Cas9 system', *Scientific Reports*, 6(1), p. 19675. Available at: https://doi.org/10.1038/srep19675.

Loriato, V.A.P., Martins, L.G.C., Euclydes, N.C., Reis, P.A.B., Duarte, C.E.M. and Fontes, E.P.B. (2020) 'Engineering resistance against geminiviruses: A review of suppressed natural defenses and the use of RNAi and the CRISPR/Cas system', *Plant Science*, 292(November 2019), p. 110410. Available at: https://doi.org/10.1016/j.plantsci.2020.110410.

Lowder, L.G., Zhang, D., Baltes, N.J., Paul, J.W., Tang, X., Zheng, X., Voytas, D.F., Hsieh, T.F., Zhang, Y. and Qi, Y. (2015) 'A CRISPR/Cas9 toolbox for multiplexed plant genome editing and transcriptional regulation', *Plant Physiology*, 169(2), pp. 971–985. Available at: https://doi.org/10.1104/pp.15.00636.

Ma, X. *et al.* (2015) 'A Robust CRISPR/Cas9 System for Convenient, High-Efficiency Multiplex Genome Editing in Monocot and Dicot Plants', *Molecular Plant*, 8(8), pp. 1274–1284. Available at: https://doi.org/10.1016/j.molp.2015.04.007.

Ma, X. and Liu, Y. (2016) 'CRISPR/Cas9-Based Multiplex Genome Editing in Monocot and Dicot Plants', *Current Protocols in Molecular Biology*, 115(1), pp. 1–21. Available at: https://doi.org/10.1002/cpmb.10.

Maclean, J., Koekemoer, M., Olivier, A.J., Stewart, D., Hitzeroth, I.I., Rademacher, T., Fischer, R., Williamson, A.L. and Rybicki, E.P. (2007) 'Optimization of human papillomavirus type 16 (HPV-16) L1 expression in plants: comparison of the suitability of different HPV-16 L1 gene variants and different cell-compartment localization', *The Journal of general virology*, 88(Pt 5), pp. 1460–1469. Available at: https://doi.org/10.1099/VIR.0.82718-0.

Le Maguet, J., Beuve, M., Herrbach, E. and Lemaire, O. (2012) 'Transmission of Six Ampeloviruses and Two Vitiviruses to Grapevine by Phenacoccus aceris', *http://dx.doi.org/10.1094/PHYTO-10-11-0289*, 102(7), pp. 717–723. Available at: https://doi.org/10.1094/PHYTO-10-11-0289.

Mahas, A., Aman, R. and Mahfouz, M. (2019) 'CRISPR-Cas13d mediates robust RNA virus interference in plants', *Genome Biology*, 20(1), pp. 1–16. Available at: https://doi.org/10.1186/s13059-019-1881-2.

Makarova, K.S., Haft, D.H., Barrangou, R., Brouns, S.J.J., Charpentier, E., Horvath, P., Moineau, S., Mojica, F.J.M., Wolf, Y.I., Yakunin, A.F., van der Oost, J. and Koonin, E. V. (2011) 'Evolution and classification of the CRISPR–Cas systems', *Nature Reviews Microbiology*, 9(6), pp. 467–477. Available at: https://doi.org/10.1038/nrmicro2577.

Makarova, K.S. *et al.* (2015) 'An updated evolutionary classification of CRISPR-Cas systems', *Nature Reviews Microbiology*, 13(11), pp. 722–736. Available at: https://doi.org/10.1038/nrmicro3569.

Makarova, K.S. *et al.* (2020) 'Evolutionary classification of CRISPR–Cas systems: a burst of class 2 and derived variants', *Nature Reviews Microbiology*, 18(2), pp. 67–83. Available at: https://doi.org/10.1038/s41579-019-0299-x.

Mäkinen, K. (2020) 'Plant susceptibility genes as a source for potyvirus resistance', *Annals of Applied Biology*, 176(2), pp. 122–129. Available at: https://doi.org/10.1111/aab.12562.

Malzahn, A., Lowder, L. and Qi, Y. (2017) 'Plant genome editing with TALEN and CRISPR', *Cell &*

Bioscience, 7(1), p. 21. Available at: https://doi.org/10.1186/s13578-017-0148-4.

Mao, Y., Zhang, H., Xu, N., Zhang, B., Gou, F. and Zhu, J.-K. (2013) 'Application of the CRISPR–Cas System for Efficient Genome Engineering in Plants', *Molecular Plant*, 6(6), pp. 2008–2011. Available at: https://doi.org/10.1093/mp/sst121.

Mao, Y., Botella, J.R., Liu, Y. and Zhu, J.-K. (2019) 'Gene editing in plants: progress and challenges', *National Science Review*, 6(3), pp. 421–437. Available at: https://doi.org/10.1093/nsr/nwz005.

Maree, H.J., Almeida, R.P.P., Bester, R., Chooi, K.M., Cohen, D., Dolja, V. V., Fuchs, M.F., Golino, D.A., Jooste, A.E.C., Martelli, G.P., Naidu, R.A., Rowhani, A., Saldarelli, P. and Burger, J.T. (2013) 'Grapevine leafroll-associated virus 3', *Frontiers in Microbiology*, 4(APR), p. 82. Available at: https://doi.org/10.3389/fmicb.2013.00082.

Martelli, G.P., Adams, M.J., Kreuze, J.F. and Dolja, V. V. (2007) ' Family Flexiviridae : A Case Study in Virion and Genome Plasticity ', *Annual Review of Phytopathology*, 45(1), pp. 73–100. Available at: https://doi.org/10.1146/annurev.phyto.45.062806.094401.

Martinez, J., Patkaniowska, A., Urlaub, H., Lührmann, R. and Tuschl, T. (2002) 'Single-stranded antisense siRNAs guide target RNA cleavage in RNAi', *Cell*, 110(5), pp. 563–574. Available at: https://doi.org/10.1016/S0092-8674(02)00908-X.

Marwal, A. and Gaur, R.K. (2020) 'Host Plant Strategies to Combat Against Viruses Effector Proteins', *Current Genomics*, 21(6), pp. 401–410. Available at: https://doi.org/10.2174/1389202921999200712135131.

Méndez-Mancilla, A., Wessels, H.H., Legut, M., Kadina, A., Mabuchi, M., Walker, J., Robb, G.B., Holden, K. and Sanjana, N.E. (2022) 'Chemically modified guide RNAs enhance CRISPR-Cas13 knockdown in human cells', *Cell Chemical Biology*, 29(2), pp. 321-327.e4. Available at: https://doi.org/10.1016/j.chembiol.2021.07.011.

Miao, J., Guo, D., Zhang, J., Huang, Q., Qin, G., Zhang, X., Wan, J., Gu, H. and Qu, L.-J. (2013) 'Targeted mutagenesis in rice using CRISPR-Cas system', *Cell Research*, 23(10), pp. 1233–1236. Available at: https://doi.org/10.1038/cr.2013.123.

Minafra, A., Saldarelli, P. and Martelli, G.P. (1997) 'Grapevine virus A: Nucleotide sequence, genome organization, and relationship in the Trichovirus genus', *Archives of Virology*, 142(2), pp. 417–423. Available at: https://doi.org/10.1007/s007050050088.

Mohanraju, P., Makarova, K.S., Zetsche, B., Zhang, F., Koonin, E. V. and van der Oost, J. (2016) 'Diverse evolutionary roots and mechanistic variations of the CRISPR-Cas systems', *Science*, 353(6299). Available at: https://doi.org/10.1126/science.aad5147.

Mojica, F.J.M., Díez-Villaseñor, C., García-Martínez, J. and Almendros, C. (2009) 'Short motif

sequences determine the targets of the prokaryotic CRISPR defence system', *Microbiology*, 155(3), pp. 733–740. Available at: https://doi.org/10.1099/mic.0.023960-0.

Molla, K.A., Qi, Y., Karmakar, S. and Baig, M.J. (2020) 'Base Editing Landscape Extends to Perform Transversion Mutation', *Trends in Genetics*, 36(12), pp. 899–901. Available at: https://doi.org/10.1016/j.tig.2020.09.001.

Molla, K.A., Shih, J., Wheatley, M.S. and Yang, Y. (2022) 'Predictable NHEJ Insertion and Assessment of HDR Editing Strategies in Plants', *Frontiers in Genome Editing*, 4(March), pp. 1–11. Available at: https://doi.org/10.3389/fgeed.2022.825236.

Molla, K.A. and Yang, Y. (2020) 'Predicting CRISPR/Cas9-Induced Mutations for Precise Genome Editing', *Trends in Biotechnology*, 38(2), pp. 136–141. Available at: https://doi.org/10.1016/j.tibtech.2019.08.002.

Moriondo, M., Bindi, M., Fagarazzi, C., Ferrise, R. and Trombi, G. (2011) 'Framework for high-resolution climate change impact assessment on grapevines at a regional scale', *Regional Environmental Change*, 11(3), pp. 553–567. Available at: https://doi.org/10.1007/s10113-010-0171-z.

Moscou, M.J. and Bogdanove, A.J. (2009) 'A simple cipher governs DNA recognition by TAL effectors', *Science*, 326(5959), p. 1501. Available at: https://doi.org/10.1126/science.1178817.

Murray, M.G. and Thompson, W.F. (1980) 'Rapid isolation of high molecular weight plant DNA', *Nucleic Acids Research*, 8(19), pp. 4321–4326. Available at: https://doi.org/10.1093/NAR/8.19.4321.

Muruganantham, M., Moskovitz, Y., Haviv, S., Horesh, T., Fenigstein, A., Preez, J. du, Stephan, D., Burger, J.T. and Mawassi, M. (2009) 'Grapevine virus A-mediated gene silencing in Nicotiana benthamiana and Vitis vinifera', *Journal of Virological Methods*, 155(2), pp. 167–174. Available at: https://doi.org/10.1016/j.jviromet.2008.10.010.

Naidu, R., Rowhani, A., Fuchs, M., Golino, D. and Martelli, G.P. (2014) 'Grapevine Leafroll: A complex viral disease affecting a high-value fruit crop', *Plant Disease*, 98(9), pp. 1172–1185. Available at: https://doi.org/10.1094/PDIS-08-13-0880-FE.

Naing, A.H., Kyu, S.Y., Pe, P.P.W., Park, K. Il, Lee, J.M., Lim, K.B. and Kim, C.K. (2019) 'Silencing of the phytoene desaturase (PDS) gene affects the expression of fruit-ripening genes in tomatoes', *Plant Methods*, 15(1), pp. 1–10. Available at: https://doi.org/10.1186/S13007-019-0491-Z/FIGURES/5.

Nekrasov, V., Staskawicz, B., Weigel, D., Jones, J.D.G. and Kamoun, S. (2013) 'Targeted mutagenesis in the model plant Nicotiana benthamiana using Cas9 RNA-guided endonuclease', *Nature Biotechnology*, 31(8), pp. 691–693. Available at: https://doi.org/10.1038/nbt.2655.

Nemudryi, A.A., Valetdinova, K.R., Medvedev, S.P. and Zakian, S.M. (2014) 'TALEN and CRISPR/Cas Genome Editing Systems: Tools of Discovery', *Acta Naturae*, 6(3), pp. 19–40. Available at: https://doi.org/10.32607/20758251-2014-6-3-19-40.

Nicaise, V. (2014) 'Crop immunity against viruses: outcomes and future challenges', *Frontiers in Plant Science*, 5, p. 660. Available at: https://doi.org/10.3389/fpls.2014.00660.

Nishimasu, H., Ran, F.A., Hsu, P.D., Konermann, S., Shehata, S.I., Dohmae, N., Ishitani, R., Zhang, F. and Nureki, O. (2014) 'Crystal Structure of Cas9 in Complex with Guide RNA and Target DNA', *Cell*, 156(5), pp. 935–949. Available at: https://doi.org/10.1016/j.cell.2014.02.001.

Nishimasu, H., Cong, L., Yan, W.X., Ran, F.A., Zetsche, B., Li, Y., Kurabayashi, A., Ishitani, R., Zhang, F. and Nureki, O. (2015) 'Crystal Structure of Staphylococcus aureus Cas9', *Cell*, 162(5), pp. 1113–1126. Available at: https://doi.org/10.1016/j.cell.2015.08.007.

Olivares, F., Loyola, R., Olmedo, B., Miccono, M. de los Á., Aguirre, C., Vergara, R., Riquelme, D., Madrid, G., Plantat, P., Mora, R., Espinoza, D. and Prieto, H. (2021) 'CRISPR/Cas9 Targeted Editing of Genes Associated With Fungal Susceptibility in Vitis vinifera L. cv. Thompson Seedless Using Geminivirus-Derived Replicons', *Frontiers in Plant Science*, 12(December), pp. 1–15. Available at: https://doi.org/10.3389/fpls.2021.791030.

Orthwein, A., Noordermeer, S.M., Wilson, M.D., Landry, S., Enchev, R.I., Sherker, A., Munro, M., Pinder, J., Salsman, J., Dellaire, G., Xia, B., Peter, M. and Durocher, D. (2015) 'A mechanism for the suppression of homologous recombination in G1 cells', *Nature 2015 528:7582*, 528(7582), pp. 422–426. Available at: https://doi.org/10.1038/nature16142.

Pattanayak, V., Lin, S., Guilinger, J.P., Ma, E., Doudna, J.A. and Liu, D.R. (2013) 'High-throughput profiling of off-target DNA cleavage reveals RNA-programmed Cas9 nuclease specificity', *Nature Biotechnology*, 31(9), pp. 839–843. Available at: https://doi.org/10.1038/nbt.2673.

Petolino, J.F. (2015) 'Genome editing in plants via designed zinc finger nucleases', *In Vitro Cellular & Developmental Biology - Plant*, 51(1), pp. 1–8. Available at: https://doi.org/10.1007/s11627-015-9663-3.

Pietersen, G., Liu, L., Davies, J.W., Stanley, J. and van Tonder, T. (1997) 'Molecular characterization of a subgroup I geminivirus from a legume in South Africa.', *Journal of General Virology*, 78(8), pp. 2113–2117. Available at: https://doi.org/10.1099/0022-1317-78-8-2113.

Du Preez, J. (2005) *The construction of an infectious clone of grapevine virus A (GVA)*. Stellenbosch University. Available at: https://scholar.sun.ac.za/handle/10019.1/2650.

Price, A.A., Sampson, T.R., Ratner, H.K., Grakoui, A. and Weiss, D.S. (2015) 'Cas9-mediated targeting of viral RNA in eukaryotic cells', *Proceedings of the National Academy of Sciences of the United States of America*, 112(19), pp. 6164–6169. Available at: https://doi.org/10.1073/pnas.1422340112.

Rampersad, S. and Tennant, P. (2018) 'Replication and Expression Strategies of Viruses', in *Viruses*. Elsevier, pp. 55–82. Available at: https://doi.org/10.1016/B978-0-12-811257-1.00003-6.

Ran, Y., Liang, Z. and Gao, C. (2017) 'Current and future editing reagent delivery systems for plant genome editing', *Science China. Life sciences*, 60(5), pp. 490–505. Available at: https://doi.org/10.1007/S11427-017-9022-1.

Regnard, G.L., Halley-Stott, R.P., Tanzer, F.L., Hitzeroth, I.I. and Rybicki, E.P. (2010) 'High level protein expression in plants through the use of a novel autonomously replicating geminivirus shuttle vector', *Plant Biotechnology Journal*, 8(1), pp. 38–46. Available at: https://doi.org/10.1111/j.1467-7652.2009.00462.x.

Ren, C., Liu, Y., Guo, Y., Duan, W., Fan, P., Li, S. and Liang, Z. (2021) 'Optimizing the CRISPR/Cas9 system for genome editing in grape by using grape promoters', *Horticulture Research 2021 8:1*, 8(1), pp. 1–12. Available at: https://doi.org/10.1038/s41438-021-00489-z.

Rey, M.E.C., Ndunguru, J., Berrie, L.C., Paximadis, M., Berry, S., Cossa, N., Nuaila, V.N., Mabasa, K.G., Abraham, N., Rybicki, E.P., Martin, D., Pietersen, G. and Esterhuizen, L.L. (2012) 'Diversity of Dicotyledenous-Infecting Geminiviruses and Their Associated DNA Molecules in Southern Africa, Including the South-West Indian Ocean Islands', *Viruses 2012, Vol. 4, Pages 1753-1791*, 4(9), pp. 1753–1791. Available at: https://doi.org/10.3390/V4091753.

Richter, K.S., Serra, H., White, C.I. and Jeske, H. (2016) 'The recombination mediator RAD51D promotes geminiviral infection', *Virology*, 493, pp. 113–127. Available at: https://doi.org/10.1016/j.virol.2016.03.014.

Riesenberg, S., Helmbrecht, N., Kanis, P., Maricic, T. and Pääbo, S. (2022) 'Improved gRNA secondary structures allow editing of target sites resistant to CRISPR-Cas9 cleavage', *Nature Communications*, 13(1), pp. 1–8. Available at: https://doi.org/10.1038/s41467-022-28137-7.

Robertson, G. (2018) *CRISPR / Cas9-mediated genome editing in Vitis vinifera*. Stellenbosch University.

Robertson, G. (2021) *Establishing the CRISPR / Cas13a genome editing system in Nicotiana benthamiana for RNA targeting applications*. Stellenbosch University.

Rubio, L., Galipienso, L. and Ferriol, I. (2020) 'Detection of Plant Viruses and Disease Management: Relevance of Genetic Diversity and Evolution', *Frontiers in Plant Science*, 11(July), pp. 1–23. Available at: https://doi.org/10.3389/fpls.2020.01092.

Ruiz, M.T., Voinnet, O. and Baulcombe, D.C. (1998) 'Initiation and Maintenance of Virus-Induced Gene Silencing', *The Plant Cell*, 10(6), pp. 937–946. Available at: https://doi.org/10.1105/tpc.10.6.937.

Saldarelli, P., Dell'Orco, M. and Minafra, A. (2000) 'Infectious cDNA clones of two grapevine

viruses', *Archives of Virology*, 145(2), pp. 397–405. Available at: https://doi.org/10.1007/s007050050031.

Sandhya, D., Jogam, P., Allini, V.R., Abbagani, S. and Alok, A. (2020) 'The present and potential future methods for delivering CRISPR/Cas9 components in plants', *Journal of Genetic Engineering and Biotechnology*, 18(1), p. 25. Available at: https://doi.org/10.1186/s43141-020-00036-8.

Schindele, P., Wolter, F. and Puchta, H. (2018) 'Transforming plant biology and breeding with CRISPR/Cas9, Cas12 and Cas13', *FEBS Letters*, 592(12), pp. 1954–1967. Available at: https://doi.org/10.1002/1873-3468.13073.

Schmidt, S.M., Belisle, M. and Frommer, W.B. (2020) 'The evolving landscape around genome editing in agriculture', *EMBO reports*, 21(6), p. e50680. Available at: https://doi.org/10.15252/embr.202050680.

Semenova, E., Jore, M.M., Datsenko, K.A., Semenova, A., Westra, E.R., Wanner, B., Van Der Oost, J., Brouns, S.J.J. and Severinov, K. (2011) 'Interference by clustered regularly interspaced short palindromic repeat (CRISPR) RNA is governed by a seed sequence', *Proceedings of the National Academy of Sciences of the United States of America*, 108(25), pp. 10098–10103. Available at: https://doi.org/10.1073/pnas.1104144108.

Sentmanat, M.F., Peters, S.T., Florian, C.P., Connelly, J.P. and Pruett-Miller, S.M. (2018) 'A Survey of Validation Strategies for CRISPR-Cas9 Editing', *Scientific reports*, 8(1). Available at: https://doi.org/10.1038/S41598-018-19441-8.

Shan-E-Ali Zaidi, S. and Mansoor, S. (2017) 'Viral vectors for plant genome engineering', *Frontiers in Plant Science*. Frontiers Research Foundation, p. 539. Available at: https://doi.org/10.3389/fpls.2017.00539.

Shan, Q., Wang, Y., Li, J., Zhang, Y., Chen, K., Liang, Z., Zhang, K., Liu, J., Xi, J.J., Qiu, J.L. and Gao, C. (2013) 'Targeted genome modification of crop plants using a CRISPR-Cas system', *Nature Biotechnology*. Nature Publishing Group, pp. 686–688. Available at: https://doi.org/10.1038/nbt.2650.

Sharma, V.K., Marla, S., Zheng, W., Mishra, D., Huang, J., Zhang, W., Morris, G.P. and Cook, D.E. (2022) 'CRISPR guides induce gene silencing in plants in the absence of Cas', *Genome Biology*, 23(1), pp. 1–24. Available at: https://doi.org/10.1186/s13059-021-02586-7.

Shmakov, S., Abudayyeh, O.O., Makarova, K.S., Wolf, Y.I., Gootenberg, J.S., Semenova, E., Minakhin, L., Joung, J., Konermann, S., Severinov, K., Zhang, F. and Koonin, E. V. (2015) 'Discovery and functional characterization of diverse Class 2 CRISPR-Cas systems', *Molecular cell*, 60(3), p. 385. Available at: https://doi.org/10.1016/J.MOLCEL.2015.10.008.

Shmakov, S., Smargon, A., Scott, D., Cox, D., Pyzocha, N., Yan, W., Abudayyeh, O.O.,

Gootenberg, J.S., Makarova, K.S., Wolf, Y.I., Severinov, K., Zhang, F. and Koonin, E. V. (2017) 'Diversity and evolution of class 2 CRISPR-Cas systems', *Nature Reviews Microbiology*, 15(3), pp. 169–182. Available at: https://doi.org/10.1038/nrmicro.2016.184.

Shojaei Baghini, S., Gardanova, Z.R., Zekiy, A.O., Shomali, N., Tosan, F. and Jarahian, M. (2021) 'Optimizing sgRNA to Improve CRISPR/Cas9 Knockout Efficiency: Special Focus on Human and Animal Cell', *Frontiers in Bioengineering and Biotechnology*, 9, p. 1106. Available at: https://doi.org/10.3389/fbioe.2021.775309.

Silva, G., Poirot, L., Galetto, R., Smith, J., Montoya, G., Duchateau, P. and Paques, F. (2011) 'Meganucleases and Other Tools for Targeted Genome Engineering: Perspectives and Challenges for Gene Therapy', *Current Gene Therapy*, 11(1), pp. 11–27. Available at: https://doi.org/10.2174/156652311794520111.

Smargon, A.A., Cox, D.B.T., Pyzocha, N.K., Zheng, K., Slaymaker, I.M., Gootenberg, J.S., Abudayyeh, O.A., Essletzbichler, P., Shmakov, S., Makarova, K.S., Koonin, E. V. and Zhang, F. (2017) 'Cas13b Is a Type VI-B CRISPR-Associated RNA-Guided RNase Differentially Regulated by Accessory Proteins Csx27 and Csx28', *Molecular Cell*, 65(4), pp. 618-630.e7. Available at: https://doi.org/10.1016/j.molcel.2016.12.023.

Smargon, A.A., Shi, Y.J. and Yeo, G.W. (2020) 'RNA-targeting CRISPR systems from metagenomic discovery to transcriptomic engineering', *Nature Cell Biology*, 22(2), pp. 143–150. Available at: https://doi.org/10.1038/s41556-019-0454-7.

Spencer, K. (2019) *CRISPR-Cas13a-mediated viral resistance induction in Nicotiana benthamiana*. Stellenbosch University.

Sternberg, S.H., Redding, S., Jinek, M., Greene, E.C. and Doudna, J.A. (2014) 'DNA interrogation by the CRISPR RNA-guided endonuclease Cas9', *Nature*, 507(7490), pp. 62–67. Available at: https://doi.org/10.1038/nature13011.

Sun, S., Hu, Y., Jiang, G., Tian, Y., Ding, M., Yu, C., Zhou, X. and Qian, Y. (2020) 'Molecular Characterization and Genomic Function of Grapevine Geminivirus A', *Frontiers in Microbiology*, 11, p. 555194. Available at: https://doi.org/10.3389/fmicb.2020.555194.

Svitashev, S., Schwartz, C., Lenderts, B., Young, J.K. and Mark Cigan, A. (2016) 'Genome editing in maize directed by CRISPR–Cas9 ribonucleoprotein complexes', *Nature Communications 2016 7:1*, 7(1), pp. 1–7. Available at: https://doi.org/10.1038/ncomms13274.

Swarts, D.C. and Jinek, M. (2019) 'Mechanistic Insights into the cis- and trans-Acting DNase Activities of Cas12a', *Molecular cell*, 73(3), pp. 589-600.e4. Available at: https://doi.org/10.1016/J.MOLCEL.2018.11.021.

Taliansky, M., Samarskaya, V., Zavriev, S.K., Fesenko, I., Kalinina, N.O. and Love, A.J. (2021) 'RNA-Based Technologies for Engineering Plant Virus Resistance', *Plants*, 10(1), p. 82. Available

at: https://doi.org/10.3390/plants10010082.

Tang, Y. and Fu, Y. (2018) 'Class 2 CRISPR/Cas: an expanding biotechnology toolbox for and beyond genome editing', *Cell & Bioscience*, 8(1), p. 59. Available at: https://doi.org/10.1186/s13578-018-0255-x.

Terns, M.P. and Terns, R.M. (2011) 'CRISPR-based adaptive immune systems', *Current Opinion in Microbiology*. Elsevier Current Trends, pp. 321–327. Available at: https://doi.org/10.1016/j.mib.2011.03.005.

Thyme, S.B., Akhmetova, L., Montague, T.G., Valen, E. and Schier, A.F. (2016) 'Internal guide RNA interactions interfere with Cas9-mediated cleavage', *Nature Communications 2016 7:1*, 7(1), pp. 1–7. Available at: https://doi.org/10.1038/ncomms11750.

Tröder, S.E. and Zevnik, B. (2022) 'History of genome editing: From meganucleases to CRISPR', *Laboratory Animals*, 56(1), pp. 60–68. Available at: https://doi.org/10.1177/0023677221994613.

Tsai, C.-W., Rowhani, A., Golino, D.A., Daane, K.M. and Almeida, R.P.P. (2010) 'Mealybug Transmission of Grapevine Leafroll Viruses: An Analysis of Virus–Vector Specificity', *Phytopathology®*, 100(8), pp. 830–834. Available at: https://doi.org/10.1094/PHYTO-100-8-0830.

Varanda, C.M.R., Félix, M.D.R., Campos, M.D., Patanita, M. and Materatski, P. (2021) 'Plant Viruses: From Targets to Tools for CRISPR', *Viruses*, 13(1), p. 141. Available at: https://doi.org/10.3390/v13010141.

Voinnet, O. (2005) 'Induction and suppression of RNA silencing: insights from viral infections', *Nature Reviews Genetics 2005 6:3*, 6(3), pp. 206–220. Available at: https://doi.org/10.1038/nrg1555.

Voytas, D.F. (2013) 'Plant Genome Engineering with Sequence-Specific Nucleases', *Annual Review of Plant Biology*, 64(1), pp. 327–350. Available at: https://doi.org/10.1146/annurev-arplant-042811-105552.

Vu, T. Van, Sivankalyani, V., Kim, E.J., Doan, D.T.H., Tran, M.T., Kim, J., Sung, Y.W., Park, M., Kang, Y.J. and Kim, J.Y. (2020) 'Highly efficient homology-directed repair using CRISPR/Cpf1-geminiviral replicon in tomato', *Plant biotechnology journal*, 18(10), pp. 2133–2143. Available at: https://doi.org/10.1111/PBI.13373.

Wang, F., Wang, L., Zou, X., Duan, S., Li, Z., Deng, Z., Luo, J., Lee, S.Y. and Chen, S. (2019) 'Advances in CRISPR-Cas systems for RNA targeting, tracking and editing', *Biotechnology Advances*, 37(5), pp. 708–729. Available at: https://doi.org/10.1016/j.biotechadv.2019.03.016.

Wang, J., Zhang, C. and Feng, B. (2020) 'The rapidly advancing Class 2 CRISPR-Cas technologies:

A customizable toolbox for molecular manipulations', *Journal of Cellular and Molecular Medicine*. Wiley-Blackwell, pp. 3256–3270. Available at: https://doi.org/10.1111/jcmm.15039.

Wang, M., Lu, Y., Botella, J.R., Mao, Y., Hua, K. and Zhu, J. (2017) 'Gene Targeting by Homology-Directed Repair in Rice Using a Geminivirus-Based CRISPR/Cas9 System', *Molecular Plant*, 10(7), pp. 1007–1010. Available at: https://doi.org/10.1016/j.molp.2017.03.002.

Weeks, D.P., Spalding, M.H. and Yang, B. (2016) 'Use of designer nucleases for targeted gene and genome editing in plants', *Plant Biotechnology Journal*, 14(2), pp. 483–495. Available at: https://doi.org/10.1111/pbi.12448.

Wessels, H.-H., Méndez-Mancilla, A., Guo, X., Legut, M., Daniloski, Z. and Sanjana, N.E. (2020) 'Massively parallel Cas13 screens reveal principles for guide RNA design', *Nature Biotechnology*, 38(6), pp. 722–727. Available at: https://doi.org/10.1038/s41587-020-0456-9.

Wiedenheft, B., Sternberg, S.H. and Doudna, J.A. (2012) 'RNA-guided genetic silencing systems in bacteria and archaea', *Nature*, 482(7385), pp. 331–338. Available at: https://doi.org/10.1038/nature10886.

Wolter, F. and Puchta, H. (2018) 'The CRISPR/Cas revolution reaches the RNA world: Cas13, a new Swiss Army knife for plant biologists', *Plant Journal*, 94(5), pp. 767–775. Available at: https://doi.org/10.1111/tpj.13899.

Wu, X., Scott, D.A., Kriz, A.J., Chiu, A.C., Hsu, P.D., Dadon, D.B., Cheng, A.W., Trevino, A.E., Konermann, S., Chen, S., Jaenisch, R., Zhang, F. and Sharp, P.A. (2014) 'Genome-wide binding of the CRISPR endonuclease Cas9 in mammalian cells', *Nature Biotechnology 2014 32:7*, 32(7), pp. 670–676. Available at: https://doi.org/10.1038/nbt.2889.

Xie, K. and Yang, Y. (2013) 'RNA-Guided genome editing in plants using a CRISPR-Cas system', *Molecular Plant*, 6(6), pp. 1975–1983. Available at: https://doi.org/10.1093/mp/sst119.

Xu, C., Zhou, Y., Xiao, Q., He, B., Geng, G., Wang, Z., Cao, B., Dong, X., Bai, W., Wang, Y., Wang, X., Zhou, D., Yuan, T., Huo, X., Lai, J. and Yang, H. (2021) 'Programmable RNA editing with compact CRISPR–Cas13 systems from uncultivated microbes', *Nature Methods 2021 18:5*, 18(5), pp. 499–506. Available at: https://doi.org/10.1038/s41592-021-01124-4.

Yamada, M., Watanabe, Y., Gootenberg, J.S., Hirano, H., Ran, F.A., Nakane, T., Ishitani, R., Zhang, F., Nishimasu, H. and Nureki, O. (2017) 'Crystal Structure of the Minimal Cas9 from Campylobacter jejuni Reveals the Molecular Diversity in the CRISPR-Cas9 Systems', *Molecular cell*, 65(6), pp. 1109-1121.e3. Available at: https://doi.org/10.1016/J.MOLCEL.2017.02.007.

Yan, W.X., Chong, S., Zhang, H., Makarova, K.S., Koonin, E. V., Cheng, D.R. and Scott, D.A. (2018) 'Cas13d Is a Compact RNA-Targeting Type VI CRISPR Effector Positively Modulated by a WYL-Domain-Containing Accessory Protein', *Molecular Cell*, 70(2), pp. 327-339.e5. Available at: https://doi.org/10.1016/j.molcel.2018.02.028.

Yang, H., Wu, J.-J., Tang, T., Liu, K.-D. and Dai, C. (2017) 'CRISPR/Cas9-mediated genome editing efficiently creates specific mutations at multiple loci using one sgRNA in Brassica napus', *Scientific Reports*, 7(1), p. 7489. Available at: https://doi.org/10.1038/s41598-017-07871-9.

Yang, X., Caro, M., Hutton, S.F., Scott, J.W., Guo, Y., Wang, X., Rashid, M.H., Szinay, D., de Jong, H., Visser, R.G.F., Bai, Y. and Du, Y. (2014) 'Fine mapping of the tomato yellow leaf curl virus resistance gene Ty-2 on chromosome 11 of tomato', *Molecular Breeding*, 34(2), pp. 749–760. Available at: https://doi.org/10.1007/s11032-014-0072-9.

Yin, K., Han, T., Liu, G., Chen, T., Wang, Y., Yu, A.Y.L. and Liu, Y. (2015) 'A geminivirus-based guide RNA delivery system for CRISPR/Cas9 mediated plant genome editing', *Scientific Reports*, 5(1), p. 14926. Available at: https://doi.org/10.1038/srep14926.

Yu, Y., Wang, X., Sun, H., Liang, Q., Wang, W., Zhang, C., Bian, X., Cao, Q., Li, Q., Xie, Y., Ma, D., Li, Z. and Sun, J. (2020) 'Improving CRISPR-Cas-mediated RNA targeting and gene editing using SPLCV replicon-based expression vectors in Nicotiana benthamiana', *Plant Biotechnology Journal*, 18(10), pp. 1993–1995. Available at: https://doi.org/10.1111/pbi.13384.

Yu, Y., Pan, Z., Wang, X., Bian, X., Wang, W., Liang, Q., Kou, M., Ji, H., Li, Y., Ma, D., Li, Z. and Sun, J. (2022) 'Targeting of SPCSV- RNase3 via CRISPR-Cas13 confers resistance against sweet potato virus disease', *Molecular Plant Pathology*, 23(1), pp. 104–117. Available at: https://doi.org/10.1111/mpp.13146.

Zaidi, S.S. e. A., Tashkandi, M., Mansoor, S. and Mahfouz, M.M. (2016) 'Engineering plant immunity: Using CRISPR/Cas9 to generate virus resistance', *Frontiers in Plant Science*, 7(November 2016), p. 1673. Available at: https://doi.org/10.3389/fpls.2016.01673.

Zetsche, B., Gootenberg, J.S., Abudayyeh, O.O., Slaymaker, I.M., Makarova, K.S., Essletzbichler, P., Volz, S.E., Joung, J., Van Der Oost, J., Regev, A., Koonin, E. V. and Zhang, F. (2015) 'Cpf1 Is a Single RNA-Guided Endonuclease of a Class 2 CRISPR-Cas System', *Cell*, 163(3), pp. 759–771. Available at: https://doi.org/10.1016/j.cell.2015.09.038.

Zhang, B., Ye, Y., Ye, W., Perčulija, V., Jiang, H., Chen, Y., Li, Y., Chen, J., Lin, J., Wang, S., Chen, Q., Han, Y.-S. and Ouyang, S. (2019) 'Two HEPN domains dictate CRISPR RNA maturation and target cleavage in Cas13d', *Nature Communications*, 10(1), p. 2544. Available at: https://doi.org/10.1038/s41467-019-10507-3.

Zhang, C., Konermann, S., Brideau, N.J., Lotfy, P., Wu, X., Novick, S.J., Strutzenberg, T., Griffin, P.R., Hsu, P.D. and Lyumkis, D. (2018) 'Structural Basis for the RNA-Guided Ribonuclease Activity of CRISPR-Cas13d', *Cell*, 175(1), pp. 212-223.e17. Available at: https://doi.org/10.1016/j.cell.2018.09.001.

Zhang, Hui, Zhang, J., Wei, P., Zhang, B., Gou, F., Feng, Z., Mao, Y., Yang, L., Zhang, Heng, Xu, N. and Zhu, J.K. (2014) 'The CRISPR/Cas9 system produces specific and homozygous targeted gene editing in rice in one generation', *Plant biotechnology journal*, 12(6), pp. 797–807. Available at: https://doi.org/10.1111/PBI.12200.

Zhang, T., Zheng, Q., Yi, X., An, H., Zhao, Y., Ma, S. and Zhou, G. (2018) 'Establishing RNA virus resistance in plants by harnessing CRISPR immune system', *Plant Biotechnology Journal*, 16(8), pp. 1415–1423. Available at: https://doi.org/10.1111/pbi.12881.

Zhang, T., Zhao, Y., Ye, J., Cao, X., Xu, C., Chen, B., An, H., Jiao, Y., Zhang, F., Yang, X. and Zhou, G. (2019) 'Establishing CRISPR/Cas13a immune system conferring RNA virus resistance in both dicot and monocot plants', *Plant Biotechnology Journal*, 17(7), pp. 1185–1187. Available at: https://doi.org/10.1111/PBI.13095.

Zhao, Y., Yang, X., Zhou, G. and Zhang, T. (2020) 'Engineering plant virus resistance: from RNA silencing to genome editing strategies', *Plant Biotechnology Journal*, 18(2), pp. 328–336. Available at: https://doi.org/10.1111/pbi.13278.

Zherdev, A., Vinogradova, S., Byzova, N., Porotikova, E., Kamionskaya, A. and Dzantiev, B. (2018) 'Methods for the Diagnosis of Grapevine Viral Infections: A Review', *Agriculture*, 8(12), p. 195. Available at: https://doi.org/10.3390/agriculture8120195.

Zhou, Z.S., Dell'Orco, M., Saldarelli, P., Turturo, C., Minafra, A. and Martelli, G.P. (2006) 'Identification of an RNA-silencing suppressor in the genome of Grapevine virus A', *Journal of General Virology*, 87(8), pp. 2387–2395. Available at: https://doi.org/10.1099/vir.0.81893-0.

Zhu, C., Bortesi, L., Baysal, C., Twyman, R.M., Fischer, R., Capell, T., Schillberg, S. and Christou, P. (2017) 'Characteristics of Genome Editing Mutations in Cereal Crops', *Trends in Plant Science*, 22(1), pp. 38–52. Available at: https://doi.org/10.1016/J.TPLANTS.2016.08.009.

Zhu, H., Li, C. and Gao, C. (2020) 'Applications of CRISPR–Cas in agriculture and plant biotechnology', *Nature Reviews Molecular Cell Biology*, 21(11), pp. 661–677. Available at: https://doi.org/10.1038/S41580-020-00288-9.

Zuo, Z. and Liu, J. (2016) 'Cas9-catalyzed DNA Cleavage Generates Staggered Ends: Evidence from Molecular Dynamics Simulations', *Scientific Reports 2016 6:1*, 6(1), pp. 1–9. Available at: https://doi.org/10.1038/srep37584.

SUPPLEMENTARY DATA

Supplementary Table 1. gRNA Oligonucleotides used in Chapter 3, for GVA targeting.

Oligo name	Sequence (5'-3')	Target gene
GVA_Rep_T1_F	AAACGTACTGGAGTCTAGACGAGATGCAAAGGT	Replicase
GVA_Rep_T1_R	AAAAACCTTTGAATCTCGTCTAGACTCCAGTAC	
GVA_Rep_T2_F	AAACGCGCTACTTTTGAGGTGAAAGAGAATCAA	Replicase
GVA_Rep_T2_R	AAAATTGATTCTCTTTCACCTCAAAAGTAGCGC	
GVA_CP_T1_F	AAACGAACCAACTTTCCGCGCGGGTCTA	Coat protein
GVA_CP_T1_R	AAAATAGACCCGCGCGGAAAGTTGGTTC	
GVA_CP_T2_F	AAACGTCTCATCCTTCCCACCAGCTCAG	Coat protein
GVA_CP_T2_R	AAAAACTGAGCTGGTGGGAAGGATGAGA	
GVA_CP_T3_F	AAACGCCCCTTTCACGGGTCCCTCGCTA	Coat protein
GVA_CP_T3_R	AAAATAGCGAGGGACCCGTGAAAGGGGC	
CP_T1_gRNA_F	ctagaaccctaccaactggtcggggtttgaaacgAACCAACTTTCCGCGCGGGTCTATTTTTTTTT	Coat protein
CP_T1_gRNA_R	tcgaAAAAAAAAATAGACCCGCGCGGAAAGTTGGTTcgtttcaaaccccgaccagttggtaggggtt	
CP_T2_gRNA_F	ctagaaccctaccaactggtcggggtttgaaacgTCTCATCCTTCCCACCAGCTCAGTTTTTTTTT	Coat protein
CP_T2_gRNA_R	tcgaAAAAAAAAACTGAGCTGGTGGGAAGGATGAGAcgtttcaaaccccgaccagttggtaggggtt	
CP_T3_gRNA_F	ctagaaccctaccaactggtcggggtttgaaacgCCCCTTTCACGGGTCCCTCGCTATTTTTTTTT	Coat protein
CP_T3_gRNA_R	tcgaAAAAAAAAATAGCGAGGGACCCGTGAAAGGGGcgtttcaaaccccgaccagttggtaggggtt	

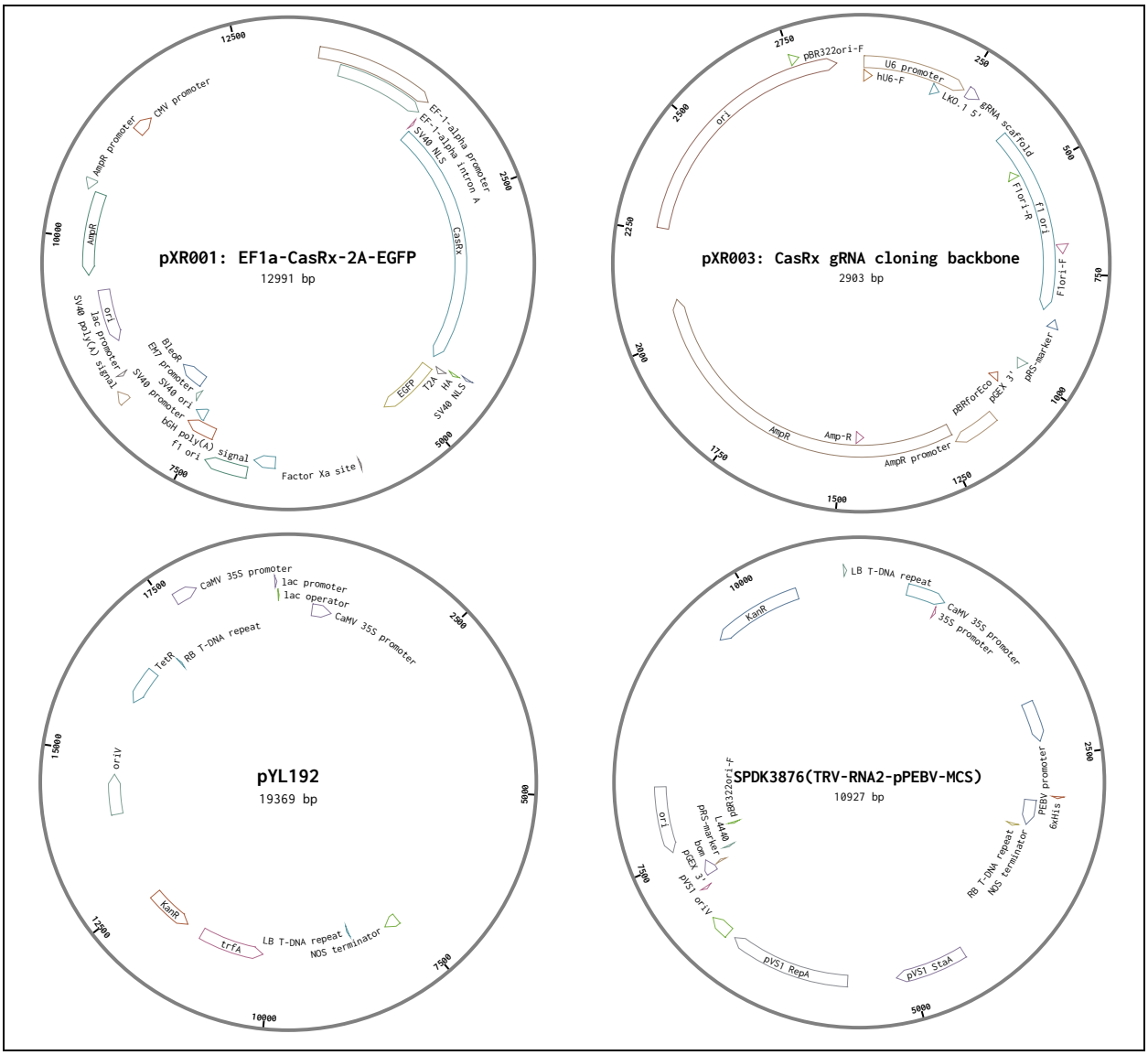

Supplementary Figure 1. Vector maps of plasmids in Table 3.1.

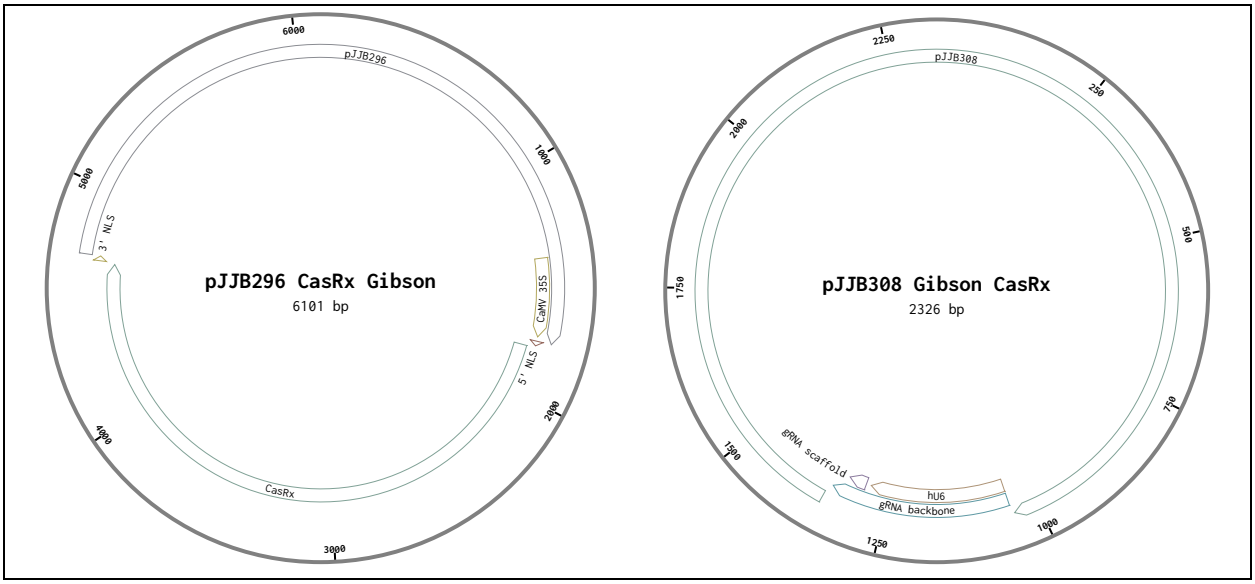

Supplementary Figure 2. Intermediate vector maps of plasmids modified by Gibson assembly.

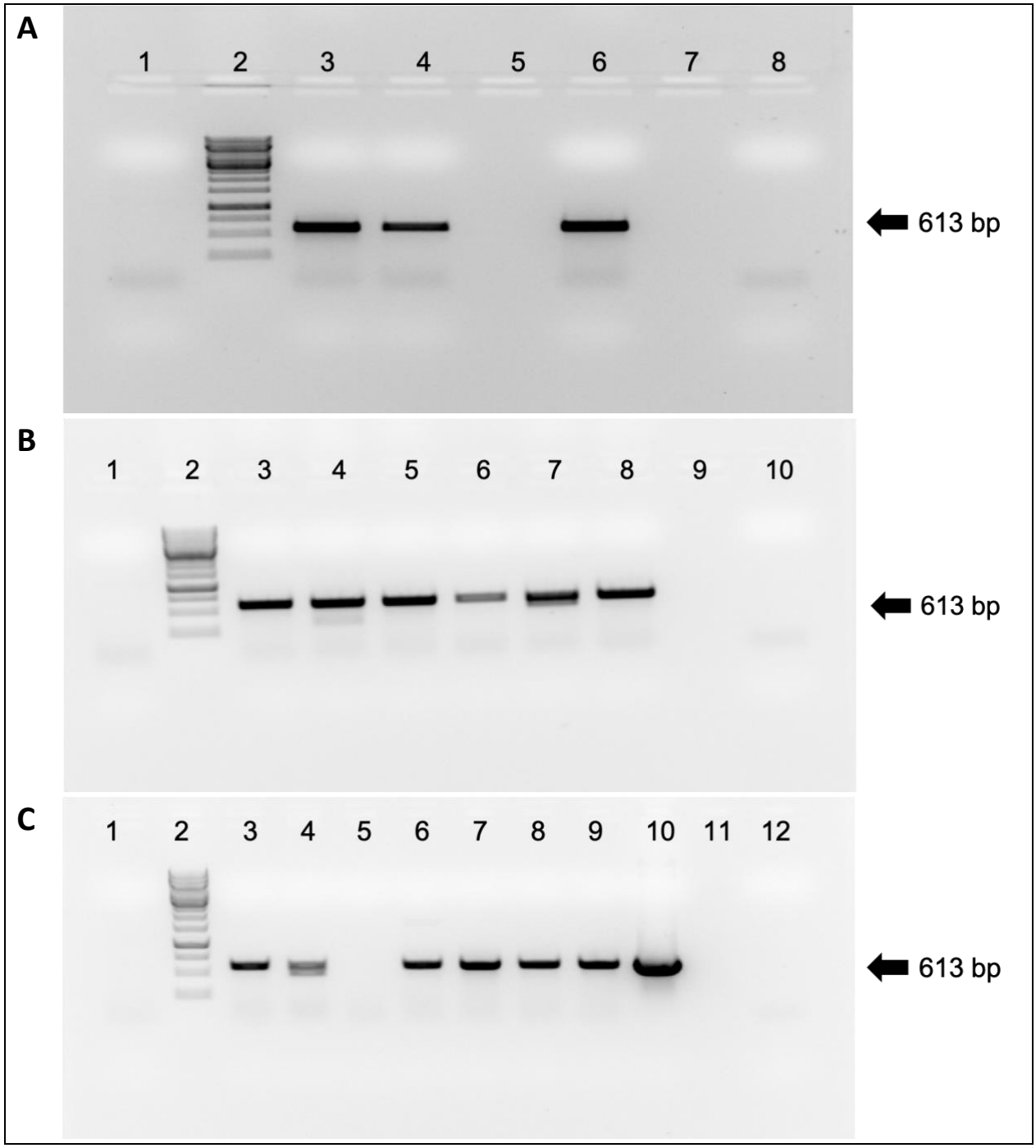

Supplementary Figure 3. End-point PCR products to confirm transgenic events. Visualised with agarose gel electrophoresis 2% (w/v), representing screened regenerated plantlets following *Agrobacterium*-mediated stable transformation of *N. benthamiana*, with the anticipated band length of 613 base pairs (bp). **A**) Screened plantlets transformed with constructs pCasRx-EMPTY. Lane 1: Wild-type (WT), Lane 2: GeneRuler 1 kb ladder (Thermo Fisher Scientific, USA), Lane 3,4: pCasRx-EMPTY samples, Lane 6: Positive control, Lane 8: no template control (NTC). **B**) pCasRx:Rep-T1. Lane 1: WT, Lane 2: GeneRuler 1 kb ladder (Thermo Fisher Scientific, USA), Lane 3-8: pCasRx:Rep-T1 samples, Lane 10: NTC. **C**) pCasRx:Rep-T2. pCasRx:Rep-T1. Lane 1: WT, Lane 2: GeneRuler 1 kb ladder (Thermo Fisher Scientific, USA), Lane 3-9: pCasRx:Rep-T2 samples, Lane 10: Positive control, Lane 12: NTC.

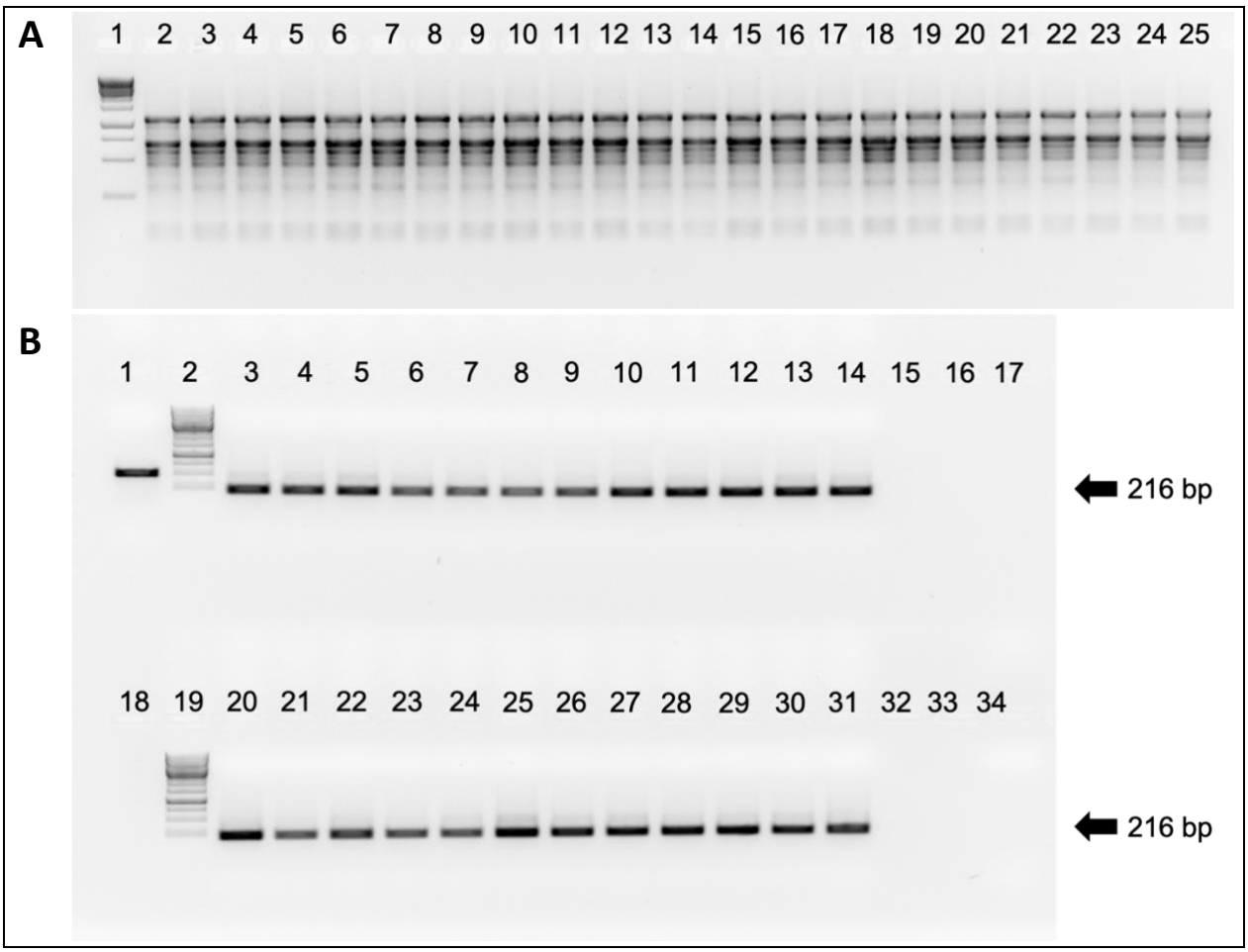

Supplementary Figure 4. Agarose gel electrophoresis confirmation prior to RT-qPCR analysis. **A**) Total RNA integrity gel (2% w/v). Lane 1: GeneRuler 1 kb ladder (Thermo Fisher Scientific, USA), Lane 2-25: Total RNA samples extracted. **B**) cDNA synthesis confirmation gel (1% w/v), with anticipated 216 bp band for cDNA amplification. Lane 1: Genomic DNA, Lane 2/19: GeneRuler 1 kb ladder (Thermo Fisher Scientific, USA), Lane 3-14, 20-31: cDNA samples, Lane 34: No Template Control (NTC).

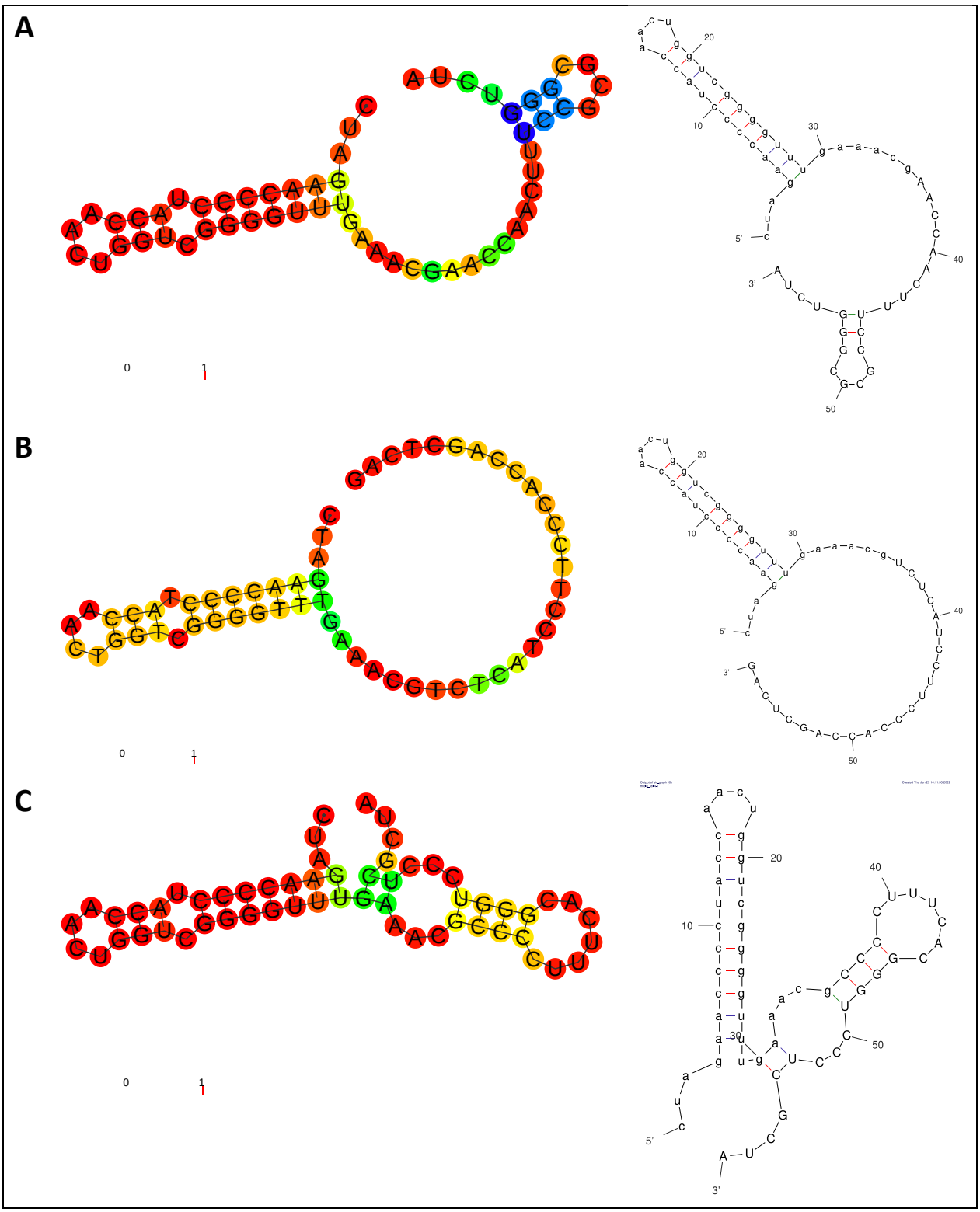

Supplementary Figure 5. Predicted RNA folding of coat protein (CP) guide RNA (gRNA) and CasRx-gRNA-scaffold sequences, with RNAfold software. **A**) CP gRNA Target 1 and scaffold folding. **B**) CP gRNA Target 2 and scaffold folding. **C**) CP gRNA Target 3 and scaffold folding. The structure is colored by base-pairing probabilities, for unpaired regions the color denotes the probability of being unpaired.

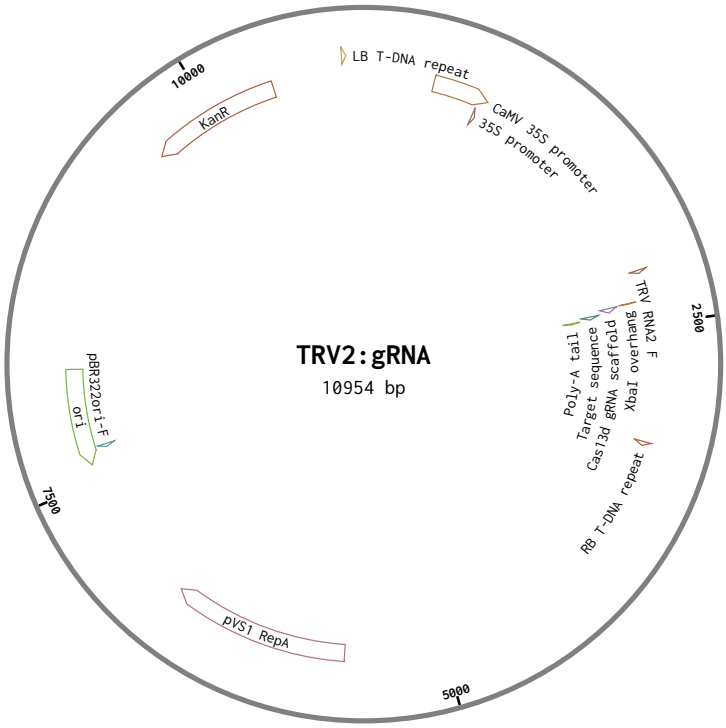

Supplementary Figure 6. Vector map representing all three tobacco rattle virus (TRV-RNA2) vectors harbouring the specific coat protein (CP) guide RNAs (gRNAs).

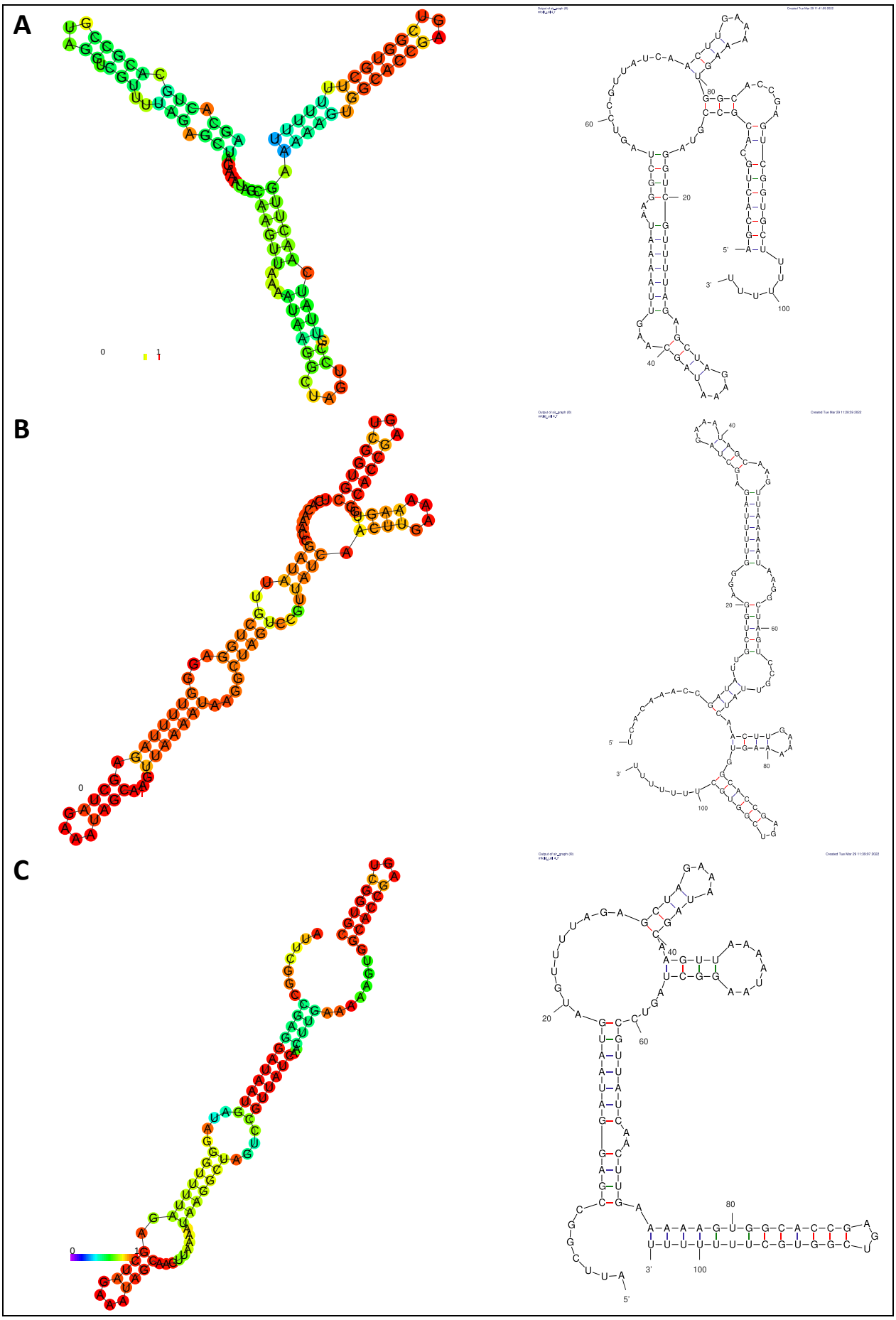

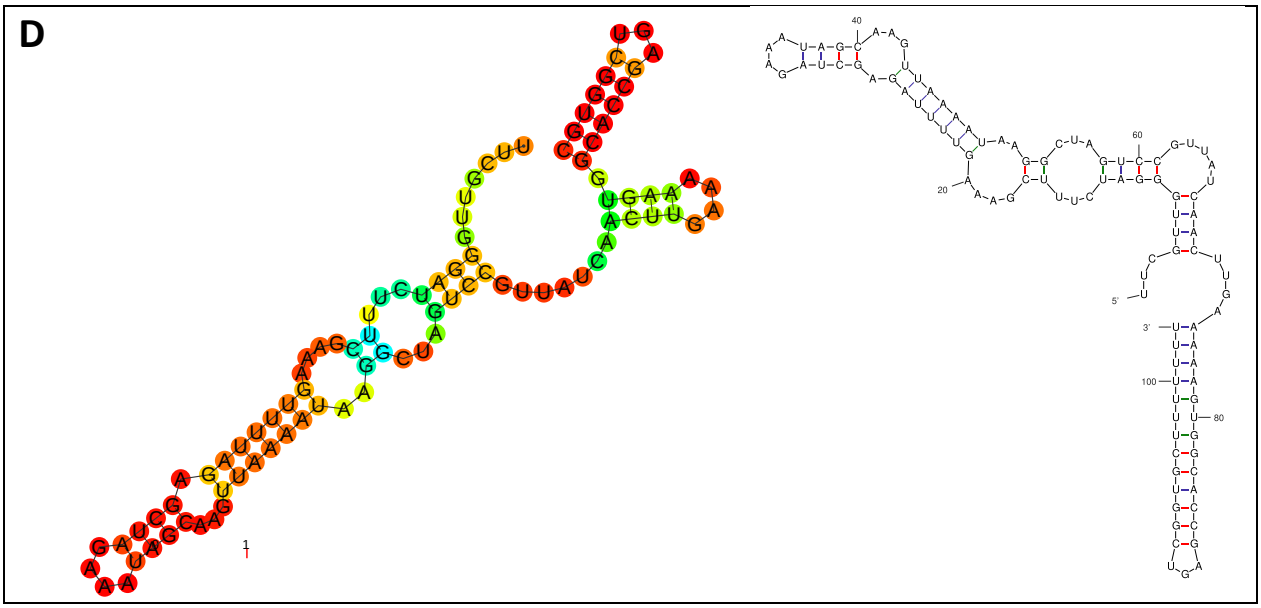

Supplementary Figure 7. Predicted RNA folding structures for guide RNA (gRNA) and Cas9-scaffold sequence, predicted using the mfold (left) and RNAfold (right) software. **A**) eGFP gRNA and scaffold folding**.** **B**) PDS gRNA and scaffold folding. **C**) 16c-GFP Target 1 and scaffold folding. **D**) 16c-GFP Target 2 and scaffold folding. The structures on the left are colored by base-pairing probabilities, for unpaired regions the color denotes the probability of being unpaired.

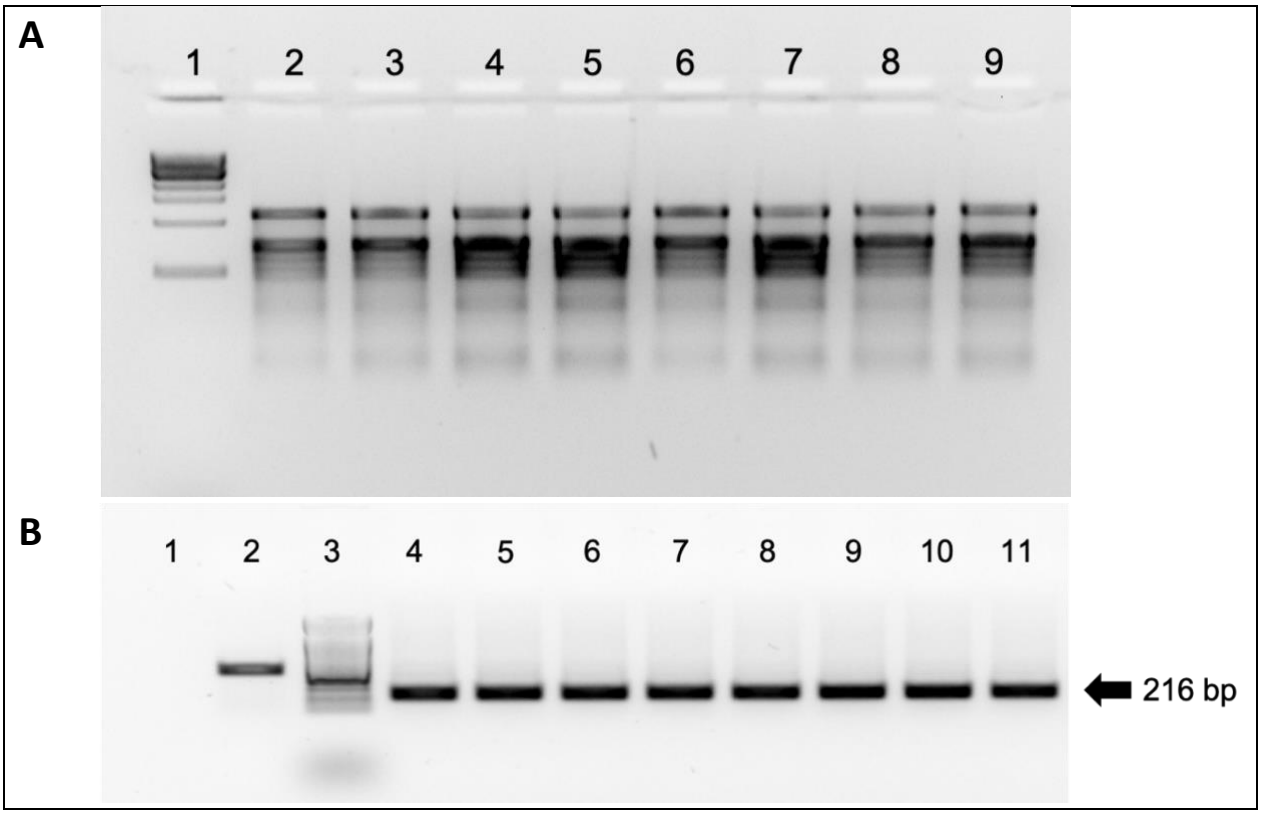

Supplementary Figure 8. Agarose gel electrophoresis confirmation prior to RT-qPCR analysis. **A**) Total RNA integrity gel (2% w/v). Lane 1: GeneRuler 1 kb ladder (Thermo Fisher Scientific, USA), Lane 2-9: Total RNA samples extracted. **B**) cDNA synthesis confirmation gel (1% w/v), with anticipated 216 bp band for cDNA amplification. Lane 1: no template control (NTC), Lane 2: Genomic DNA, Lane 3: GeneRuler 1 kb ladder (Thermo Fisher Scientific, USA), Lane 4-11: cDNA samples.

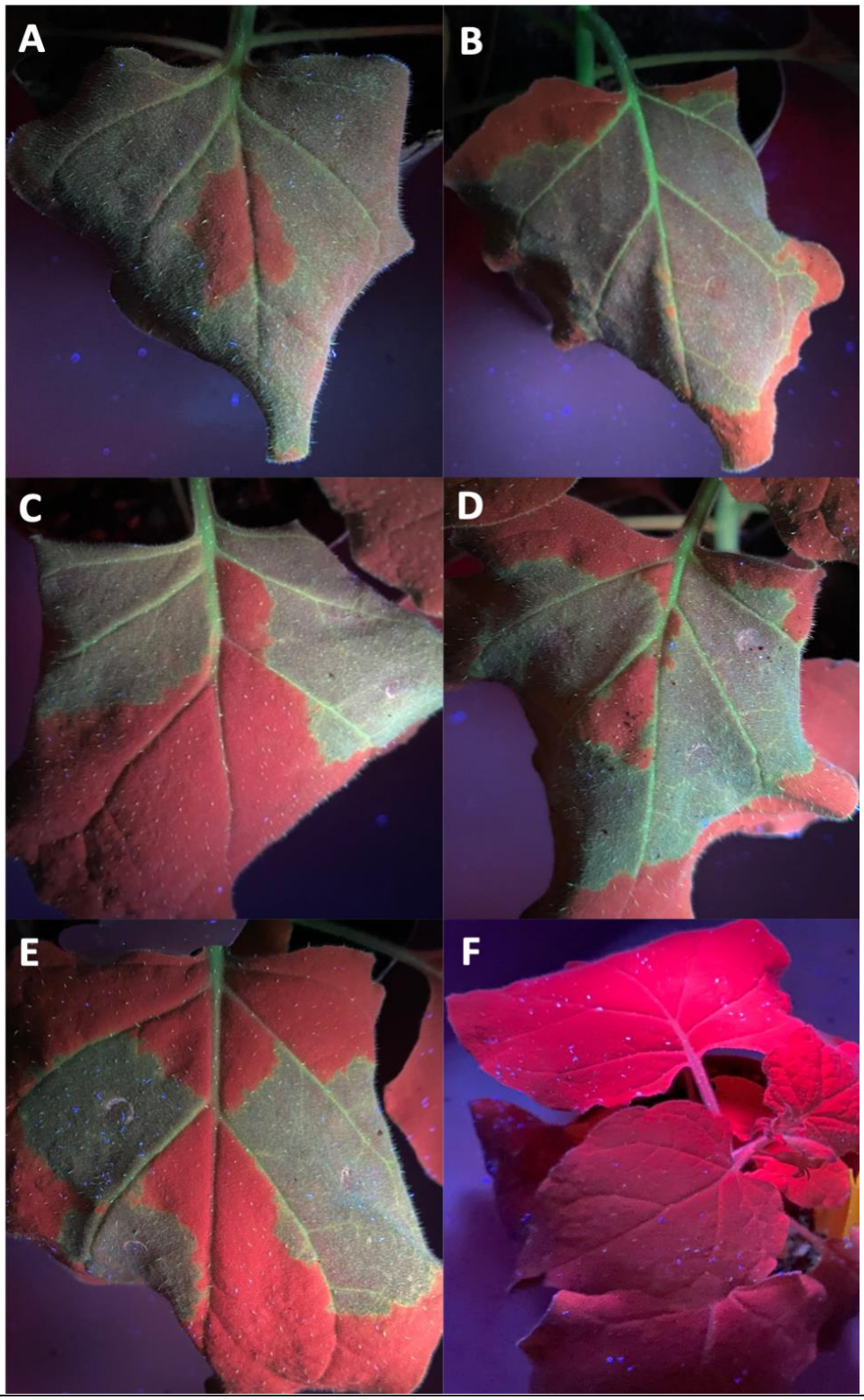

Supplementary Figure 9. *N. benthamiana* 16c line infiltrated with pRIC-Cas9 and pRIC-gRNA constructs targeting 16c-*GFP*. **A**) Sample infiltrated with pRIC-gRNA(GFP-T1) and pRIC-Cas9. **B**) Control sample infiltrated with pRIC-gRNA-ns and pRIC-Cas9. **C**) Sample infiltrated with pRIC-gRNA(GFP-T2) and pRIC-Cas9. **D**) Control sample infiltrated with pRIC-gRNA-ns andpRIC-Cas9. **E**) Half-leaf assay to distinguish the control and sample infiltrated on the same leaf; control (pRIC-gRNA-ns) on the left of the leaf, sample (pRIC-gRNA-GFP-T1) on the right of the leaf. **F**) Wild-type *N. benthamiana* plant for reference, to distinguish the 16c line from wild-type plants.

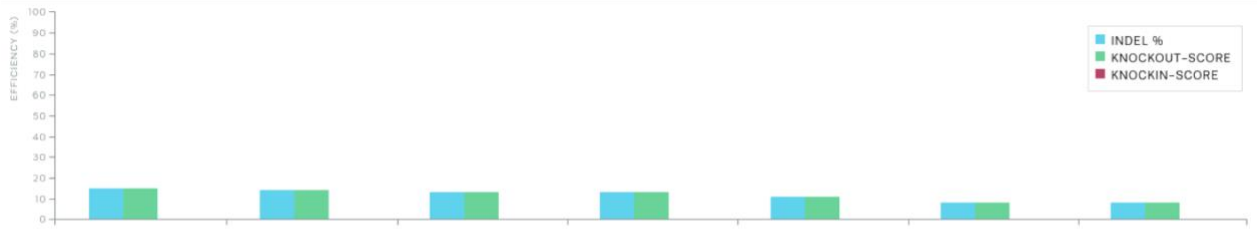

SUCCESSFULLY ANALYZED SAMPLES

SAMPLE	GUIDE TARGET	PAM SEQUENCE	INDEL %	MODEL FIT (R^2)	KNOCKOUT-SCORE
NbPDSa 1	TCACAAACCGATATTGCTGG	AGG	15	0.99	15
NbPDSa 3	TCACAAACCGATATTGCTGG	AGG	14	0.99	14
NbPDSa 8	TCACAAACCGATATTGCTGG	AGG	13	0.99	13
NbPDSa 7	TCACAAACCGATATTGCTGG	AGG	13	0.99	13
NbPDSa 4	TCACAAACCGATATTGCTGG	AGG	11	0.99	11
NbPDSa 5	TCACAAACCGATATTGCTGG	AGG	8	1	8
NbPDSa 6	TCACAAACCGATATTGCTGG	AGG	8	1	8

Supplementary Figure 10. ICE output summary of *NbPDS* Sanger sequencing samples, analysed after CRISPR/Cas9 cleavage.